Part 5 of 19 of Appendices for Resource Report No. 13 LNG

I.3 - Seismic Categorization List

Document Number:	Description:	Revision:	Appendix:
USAL-CB-MLMEL-00-000001-000	Seismic Categorization List (this information is found in the Master Equipment List)	Rev 0	Public

APPENDIX 13J – SITE INVESTIGATION AND CONDITIONS, AND FOUNDATION DESIGN

J.1 - Geotechnical Hazard Report

Document Number:	Description:	Revision:	Appendix:
USAL-FG-GRHAZ-00-002015-002	LNG Facilities Geologic Hazard Report	Rev 0	Public

Confidential

LNG FACILITIES
GEOLOGIC HAZARD REPORT

USAL-FG-GRHAZ-00-002015-002

Rev	Date	Revision Description	Originator	Reviewer	Response Code	Approver
A	19-Feb-2016	Issued for Review	J. Sowers	P. Wong	2	P. Hogan
0	21-Jun-2016	Issued for Use	J. Sowers			

Document Control No.	Country	Facility	Originator	Discipline	Type	Sub-Type	Location	Sequence	Identifier
	US	AL	FG	G	R	HAZ	00	002015	002

FUGRO CONSULTANTS, INC.

LNG FACILITIES GEOLOGIC HAZARD REPORT ALASKA LNG PROJECT NIKISKI, ALASKA

AKLNG DOCUMENT NO. USAL-FG-GRHAZ-00-002015-002

REPORT NO. 04.10140334-10
EXXONMOBIL ALASKA LNG LLC (EMALL)
HOUSTON, TEXAS

Rev	Date	Revision Description	Originator	Reviewer	Approver
A	19-Feb-2016	Issued for Review	J. Sowers	P. Hogan	
0	20-Jun-2016	Issued for Use	J. Sowers	P. Hogan	

6100 Hillcroft (77081)
Houston, Texas 77274
Tel: (713) 369-5400
P.O Box 740010

Fax: (713) 369-5518

AKLNG Document No. USAL-FG-GRHAZ-00-002015-002
Fugro Report No. 04.101400334-10
June 21, 2016

ExxonMobil Alaska LNG LLC (EMALL)
10613 W. Sam Houston Pkwy N, Suite 500
Houston, TX, 77064

Attention: Patrick Wong
Geotechnical Engineer/Technical POC

Geologic Hazard Report LNG Facilities
Alaska LNG Project
Nikiski, Alaska

Fugro Consultants, Inc. (Fugro) is pleased to present this draft geologic hazard report for the onshore and marine LNG facilities of the Alaska LNG Project (AKLNG) located in Nikiski, Alaska. Our services were authorized under Service Work Order No. AKLNG-FUG-US-003 Rev 0, dated August 8, 2014 in accordance with the Service Agreement No. A2275592 between Fugro and ExxonMobil Global Services Company, dated October 29, 2012. Fugro has been performing geophysical and geotechnical site investigation (G&G) for the proposed AKLNG Project since August 2014.

This report presents the results of the geologic hazard assessments performed for the 2015 G&G program. This comprehensive report covers both the onshore and marine LNG facilities areas, and incorporates the geologic hazard assessments performed for the 2014 G&G program.

We appreciate the opportunity to be of service to EMALL. Please call us at (713) 369-5400 if you have any questions or comments concerning this report, or when we may be of further assistance.

Sincerely,
FUGRO CONSULTANTS, INC.
TBPG Firm Registration No. 50337

Janet Sowers, Ph. D, P. G.
Associate Geologist

Phillip Hogan, Ph. D.
Senior Principal Geologist

Copies Submitted: E-mail

TABLE OF CONTENTS

TABLES

ILLUSTRATIONS

APPENDICES

EXECUTIVE SUMMARY

This report provides a Pre-FEED assessment of geologic hazards at the proposed Nikiski, Alaska LNG site, for both the onshore and marine facilities. The assessment is based on review of published literature and available datasets, and on analysis of the 2014 and 2015 geologic, geotechnical, and geophysical investigations conducted by Fugro for the AKLNG project. This geologic hazard report is a complement to the probabilistic seismic hazards assessment (Fugro report no. 14.10140334-6) which assesses the hazard from earthquake-induced ground motion.

The Nikiski LNG site is located within the active convergent margin between the North American Plate and the subducting Pacific Plate. The region is characterized by high rates of seismicity and relatively frequent moderate to great (≥**M**8) earthquakes. The subducting Pacific Plate underlies the site and is the primary source for great earthquakes in the region. The LNG site is located in the center of the Cook Inlet Basin, a forearc basin filled with over 20,000 feet of Tertiary sediments. These sediments are unconformably overlain by several hundred feet of Quaternary glacial deposits. East-west compression has caused folding and blind thrust faulting of these deposits.

Seismic reflection data from the oil and gas industry as well as marine and onshore seismic reflection data collected during the 2015 Geotechnical and Geophysical Program were used to interpret the geometry and locations of fold and faults closest to the site. The LNG site is located in a synclinal flat between the Middle Ground Shoal Anticline to the west, and the Kenai-Cannery Loop monocline to the east. Each of these folds is cored by a blind thrust fault, located 4 to 5 miles in opposite directions from the LNG site center. Based on interpretation of 2015 seismic reflection data, no tectonic fault is present beneath the onshore or the marine LNG facilities areas.

Onshore and marine LNG sites are underlain by Quaternary glacial and glacially derived deposits, consisting of sand, silt, gravel, boulders, and clay. Onshore, sandy glacial outwash deposits 40 to 60 feet thick from the Killey glacial advance (17,500 to 18,500 years ago) overlie finer grained subestuarine deposits of the Moosehorn glacial advance (27,000 to 32,000 years ago). In the marine area, the Killey and upper Moosehorn deposits have been eroded away, and the sea floor is underlain by earlier Quaternary glacial deposits.

Geologic hazards assessed include surface faulting, folding and tilting, effects of earthquake-related strong ground motions, tsunami inundation, coastal erosion, volcanic hazards, seafloor erosion and sedimentation, slope failure, fluid expulsion features, sea level change, and anthropogenic hazards.

Surface faulting hazard was evaluated through lineament analysis, review of information regarding known surface faults, mapping of stratigraphic contacts in coastal bluff exposures, and analysis of shallow and deep geophysical data. The surface faulting hazard to the LNG facilities is considered low. There is very low hazard of tectonic fault rupture, as seismic reflection data show no tectonic faults are present beneath the site. The hazard of non-tectonic surface faulting, specifically lateral spreading from strong ground shaking, is low but cannot be ruled out. Surface faults are documented in the Nikiski area outside the LNG facilities area. These structures displace Quaternary deposits

only, and could be either the result of strong ground shaking, or may have formed by glacial processes. These faults show no geomorphic evidence of late Holocene displacement.

The hazard of tectonic tilting and folding is considered very low. Geomorphic evidence for rates of tilting was evaluated through examination of paleo-shorelines along kettle lakes, profiles of the glacial outwash plain, and evaluation of the slope of the Tertiary unconformity from marine seismic reflection data. Observed geologic rates of tilting are very low and do not pose a hazard to the site.

Strong ground motions are considered a potential ground deformation hazard to the site. Strong ground motion from the 1964 **M**9.2 Great Alaskan Earthquake caused ground fissuring, liquefaction, and slope failure throughout the Kenai Lowland. Geotechnical studies underway will assess liquefaction potential and slope stability on a site specific basis, and will be reported in the Site Response Report LNG Facilities (Fugro Report No. 04.10140334-12), and the Integrated Site Characterization and Engineering Report Onshore LNG Facilities (Fugro Report No. 04.10140334-13).

Tsunami inundation hazard is considered to be low for the onshore facilities, and high for marine facilities. Tsunamis at the site could be generated by a great earthquake like the 1964 event, by a flank collapse of Augustine volcano, or by a submarine landslide in the Cook Inlet. Tsunami modeling shows a maximum wave height of 33 feet at the highest astronomical tide from the landslide source, with lower heights from the other two sources. This wave would not reach the onshore LNG facilities, located on the bluff at approximately 120 feet elevation. The wave would, however, potentially affect the marine facilities.

Coastal erosion is a potential hazard to the facilities. The coastal bluffs in the onshore LNG facilities study area are 100 to 125 feet in elevation, and slope 35 to 40 degrees up from the beach to the crest of the bluff. The bluffs erode as a result of waves undercutting of the base of the bluff, followed by shallow land sliding, raveling, and gullying of the bluff face. Long term rates of bluff retreat are estimated at approximately two feet per year, with as much as 50 feet occurring during a powerful storm event.

Volcanic ash fall is a potential hazard to the onshore and marine facilities. The Nikiski site is located across Cook Inlet from the Aleutian Range, a chain of active volcanoes. Five historical eruptions have deposited ash in the Nikiski area since 1976. Ash fall thickness may vary from a fraction of an inch to several inches, based on historical events and thicknesses of post-17,500 yr ash observed in soils during geologic field mapping. Ash-fall events can hamper plant operations, damage machinery, slow or halt vehicle transportation, ship traffic, and aviation, and impact human health.

Erosion and sedimentation resulting from strong tidal currents in Cook Inlet is a hazard to the marine facilities. The tidal range is 24 to 28 feet, and currents range from 3 to 8 knots. Erosion could undermine the pier foundations, and sand and gravel carried as bedload may abrade the piers or foundations.

Additional investigations that may reduce uncertainty include evaluation of the potential effects of a tsunami on coastal bluff erosion, field sampling, and geochronologic sediment age dating to constrain the age and activity of the Salamatof Road faults.

Hazard mitigation recommendations include addressing the potential for liquefaction-related ground deformation through geotechnical analysis, developing alternatives to protect the coastal bluffs from erosion and/or slope failure, monitoring the bluff face, designing marine foundations appropriately to withstand the wave, current, and tidal conditions, monitoring the sea floor to detect erosion or sedimentation problems around marine facilities, and address the potential for volcanic ash fall with appropriate facility design and development of emergency procedures.

1.0 INTRODUCTION

1.1 Project Description

The Alaska Gasline Development Corporation, BP Alaska LNG LLC, ConocoPhillips Alaska LNG Company, and ExxonMobil Alaska LNG LLC (Applicants and also referred as AKLNG in this report) plan to construct one integrated liquefied natural gas (LNG) Project (Project) with interdependent facilities for the purpose of liquefying supplies of natural gas from Alaska, in particular from the Point Thomson Unit (PTU) and Prudhoe Bay Unit (PBU) production fields on the Alaska North Slope (North Slope), for export in foreign commerce and opportunities for in-state deliveries of natural gas.

The Natural Gas Act (NGA), 15 U.S.C. § 717a(11) (2006), and Federal Energy Regulatory Commission (FERC) regulations, 18 C.F.R. § 153.2(d) (2014), define "LNG terminal" to include "all natural gas facilities located onshore or in State waters that are used to receive, unload, load, store, transport, gasify, liquefy, or process natural gas that is exported to a foreign country from the United States." With respect to this Project, the "LNG Terminal" includes the following: a liquefaction facility (Liquefaction Facility) in Southcentral Alaska; an approximately 804-mile gas pipeline (Mainline); a gas treatment plant (GTP) on the North Slope; an approximately 62-mile gas transmission line connecting the GTP to the PTU gas production facility (PTU Gas Transmission Line or PTTL); and an approximately 1-mile gas transmission line connecting the GTP to the PBU gas production facility (PBU Gas Transmission Line or PBTL). All of these facilities are essential to export natural gas in foreign commerce.

These components are shown in Resource Report No. 1, Figure 1.1 - 1, as well as the maps found in Appendices A and B of Resource Report No. 1. Their current basis for design is described as follows.

The new Liquefaction Facility would be constructed on the eastern shore of Cook Inlet just south of the existing Agrium fertilizer plant on the Kenai Peninsula, approximately 3 miles southwest of Nikiski and 8.5 miles north of Kenai (Plate 1). The Liquefaction Facility would include the structures, equipment, underlying access rights, and all other associated systems for final processing and liquefaction of natural gas, as well as storage and loading of LNG, including terminal facilities and auxiliary marine vessels used to support Marine Terminal operations (excluding LNG carriers [LNGCs]). The Liquefaction Facility would include three liquefaction trains combining to process up to approximately 20 million metric tons per annum (MMTPA) of LNG. Two 240,000-cubic-meter tanks would be constructed to store the LNG. The Liquefaction Facility would be capable of accommodating two LNG carriers. The size of LNGCs that the Liquefaction Facility would accommodate range between 125,000 – 216,000-cubic-meter vessels. In addition to the Liquefaction Facility, the LNG Terminal would include the following interdependent facilities:

- Mainline: A new 42-inch-diameter natural gas pipeline approximately 804 miles in length would extend from the Liquefaction Facility to the GTP on the North Slope, including the structures, equipment, and all other associated systems. The Mainline would include up to eight compressor stations; one standalone heater station, one heater station co-located with a compressor station, and six cooling stations associated with six of the compressor stations; four meter stations; 53 mainline block valves; one pig launcher facility at the GTP meter station, one pig receiver facility at the Nikiski meter station, and eight combined pig launcher and receiver facilities at each of the compressor stations; and associated infrastructure facilities. Associated infrastructure facilities would include additional temporary work spaces, access roads, helipads, construction camps, pipe storage areas, material extraction sites, and material disposal sites. Along the Mainline route, there would be at least five gas interconnection points to allow for future in-state deliveries of natural gas. The approximate locations of three of the gas interconnection points have been tentatively identified by the State of Alaska as follows: MP 475 to serve Fairbanks, MP 763 to serve the Matanuska-Susitna Valley and Anchorage, and MP 804 to serve the Kenai Peninsula. The size and location of the remainder of interconnection points are unknown at this time. None of the potential third-party facilities used to condition, if required, or move natural gas away from these off-take interconnection points are part of the Project. Potential third-party facilities will be addressed in the Cumulative Impacts analysis found in Appendix L of Resource Report No. 1.

- GTP: A new GTP and associated facilities in the Prudhoe Bay area would receive natural gas from the PBU Gas Transmission Line and the PTU Gas Transmission Line. The GTP would treat/process the natural gas for delivery into the Mainline. There would be custody transfer, verification, and process metering between the GTP and PBU for fuel gas, propane make-up, and byproducts. All of these would be on the GTP or PBU pads.

- PBU Gas Transmission Line: A new 60-inch natural gas transmission line would extend approximately 1 mile from the outlet flange of the PBU gas production facility to the inlet flange of the GTP. The PBU Gas Transmission Line would include one-meter station on the GTP pad.

- PTU Gas Transmission Line: A new 32-inch natural gas transmission line would extend approximately 62 miles from the outlet flange of the PTU gas production facility to the inlet flange of the GTP. The PTU Gas Transmission Line would include one-meter station on the GTP pad, four MLBVs, and two pig launcher and receiver facilities—one each at the PTU and GTP pads.

Existing State of Alaska transportation infrastructure would be used during the construction of these new facilities including ports, airports, roads, railroads, and airstrips (potentially including previously abandoned airstrips). A preliminary assessment of potential new infrastructure and modifications or additions to these existing in-state facilities will be provided in Appendix L of Resource Report No.1. The Liquefaction Facility, Mainline, and GTP would require the construction of modules that may or may not take place at existing or new manufacturing facilities in the United States. EMALL's Draft Resource Report No. 1, Appendix A, contains maps of the Project footprint. Appendices B and E of Resource Report No. 1 depict the footprint, plot plans of the aboveground facilities, and typical layout of above-ground facilities.

AKLNG contracted Fugro to investigate the site conditions of the onshore LNG facilities, marine LNG Terminal, and marine pipeline corridors. Plate 1 and Plate 2 show the overview of overall project facilities described above and the proposed location of the onshore facilities, marine terminal area, and the pipeline corridors of the proposed LNG plant. More details regarding the project can be found in document USAKE-PT-SRREG-00-0001 released by AKLNG.

The summary of the reports developed as a part of site investigation are listed in Table 1.1. This report is indicated in **boldface** type.

Table 1.1: Summary of Reports

Report Title	AKLNG Document Number	Fugro Report Number
Project Execution Plan for 2015 Onshore and Marine G&G Program	USAL-FG-GRZZZ-00-002015-002	04.10140334-1
LNG Facilities Onshore Geologic Field Mapping Report	USAL-FG-GRZZZ-00-002015-004	04.10140334-2
Pipeline Marine Geophysical Survey Report - Route 1	USAP-FG-GRZZZ-10-002015-013	04.10140334-3
Pipeline Marine Geophysical Survey Report - Route 2	USAP-FG-GRZZZ-10-002015-014	04.10140334-4
LNG Facilities Marine Geophysical Survey Report	USAL-FG-GRZZZ-90-002015-010	04.10140334-5
LNG Facilities Probabilistic Seismic Hazard Analysis (PSHA) Report	USAL-FG-GRHAZ-00-002015-001	04.10140334-6
LNG Facilities Onshore Geophysical Survey Report	USAL-FG-GRZZZ-00-002015-005	04.10140334-7
LNG Facilities Onshore Geotechnical Data Report	USAL-FG-GRZZZ-00-002015-006	04.10140334-8
LNG Facilities Marine Geotechnical Data Report	USAL-FG-GRZZZ-90-002015-011	04.10140334-9

Report Title	AKLNG Document Number	Fugro Report Number
LNG Facilities Geologic Hazard Report	USAL-FG-GRHAZ-00-002015-002	04.10140334-10
LNG Facilities Onshore Groundwater Monitoring Well Installation Report	USAL-FG-GRZZZ-00-002015-007	04.10140334-11
LNG Facilities Onshore Hydrogeologic Report	USAL-FG-GRZZZ-00-002015-008	04.10140334-12
LNG Facilities Seismic Engineering Report	USAL-FG-GRZZZ-00-002015-003	04.10140334-13
LNG Facilities Onshore Integrated Site Characterization and Geotechnical Engineering	USAL-FG-GRZZZ-00-002015-009	04.10140334-14
LNG Facilities Marine Integrated Site Characterization and Geotechnical Engineering	USAL-FG-GRZZZ-90-002015-012	04.10140334-15

1.2 Purpose and Scope

The purpose of this geologic hazard report is to provide a comprehensive assessment of geologic hazards at the proposed Nikiski, Alaska LNG site, onshore and marine facilities based on information available at the close of 2015. The report specifically addresses whether any geologic hazards are present that may significantly impact the siting or design of the proposed facility. Emphasis is placed on hazards most likely to affect the site, This report addresses the Federal Energy Resources Commission (FERC) (2007) guidelines for LNG facilities.

The scope of work specified in EMALL Work Order No. AKLNG-FUG-US-003 Rev 0, dated August 8, 2014 includes the preparation of a report which documents the findings of the 2014 and 2015 geologic field mapping and hazards investigations and provides a comprehensive assessment of the geologic hazards at the onshore and marine LNG facilities sites. This comprehensive geologic hazard report builds on the 2014 report and includes analysis of the 2015 geologic, geophysical, and geotechnical data. The report is to include discussion of all hazards evaluated in the 2014 onshore geologic hazards report (Fugro report No. 04.10140094-9), adding specific additional items as follows:

- Presentation and discussion of a structural geologic model for the northern Cook Inlet basin that includes a map of faults and folds and a structural cross section,
- Assessment of marine geologic hazards, LNG terminal area facilities, including sediment transport and erosional processes, and
- Development of a revised seismic source model for the northern Cook Inlet Basin.

In addition to these items, this report includes expanded evaluations of surface faulting hazard, and an evaluation of volcanic hazards.

The revised seismic source model for the North Cook Inlet Basin is presented in the probabilistic seismic hazard assessment report (Fugro report no. 04.10140334-6), and is based on the structural geologic model for the northern Cook Inlet basin, presented in the geologic hazard report. Another companion report, the seismic engineering (Fugro report no. 04.10140334-11), includes site response analysis, seismic slope stability, and liquefaction susceptibility.

1.3 Approach

Fugro conducted the assessment of geologic hazards presented within this report based on the analysis and interpretation of existing data for the region and local area, and on the analysis of site-specific data collected during the 2014 and 2015 geologic, geotechnical, and geophysical field investigations.

The geologic hazards assessment process began with a review of existing data. The extensive published literature on the geologic history, tectonic setting, structural geology, and seismology of southern Alaska formed the basis for our understanding of this region. Individual publications are cited throughout the text, and full citations are provided in Section 6. In addition, geologic information on the Nikiski LNG site and seven other candidate LNG sites had been collected and presented in earlier reports by Fugro-McClelland Marine Geosciences, Inc. (FMMG, 2012a, and 2012b). These reports included a screening-level assessment of geologic hazards at each site.

An important element of the existing data was geospatial data, including topographic, bathymetric, geologic, and soil maps as listed in Table 1.2. These data were assembled in an ArcGIS database for use in the hazard analysis and for presentation as illustrations in this report. The data were available either as digital datasets or printed maps, which were then scanned and georectified for use in ArcGIS.

The geologic hazard report was prepared by Janet Sowers, Mike Buga, Josh Goodman, Jeff Hoeft, David Trench, Robert Turner, and James Turner. GIS and graphic illustrations were prepared by Marco Ticci and Jason Holmberg. Fugro internal technical review was provided by Dr. Phillip Hogan. All data and analyses in this report are in compliance with Fugro's quality assurance program.

1.4 Regulatory Guidelines

The geologic hazards report was prepared to address portions of the Federal Energy Resources Commission (FERC) (2007) draft guidelines for the assessment of geologic and seismic hazards for LNG facilities. The guidelines suggest that a geotechnical report and a site-specific seismic hazard report be prepared. The sample report content from FERC (2007) is outlined below. Items fully addressed in this geologic hazards report are shown in **boldface** type; those partially addressed are <u>underlined</u>. The remainder of the items are addressed in other reports listed in Table 1.1.

The FERC (2007) Geotechnical Report requirements include:

1. Project Description
2. Exploration
3. Laboratory Testing
4. **Geologic and Seismic Setting**
5. Site Conditions
6. Seismic Hazards,
7. Poor Soil Conditions,
8. Foundation Recommendations,
9. Corrosion
10. Pavement Design

The FERC (2007) Seismic Ground Motion Hazard evaluation requirements include:

1. General,
2. **Geology: regional and site geology**
3. **Faulting: Quaternary fault investigation, determination of active faults, fault rupture investigation**
4. **Tsunami and Seiche**
5. Ground Motions: Historic seismicity, **geologic structures and tectonic activity**, maximum earthquake potential, near-fault effects, site class, deterministic seismic hazards analysis, probabilistic hazard analysis, code values of ground motions.

FERC (2007) guidelines for the geology chapter specify the detail and content. The chapter begins with a review of the regional geologic and tectonic setting within a 100-mile radius of the site, providing context for more local information. Detailed mapping and description of the geology, stratigraphy, and tectonic features within the 5-mile radius of the site follows. Finally, a thorough assessment of all potential geologic hazards within the site proper is performed. A list of hazards to be evaluated is provided in the guidelines (FERC, 2007).

For the evaluation of surface fault rupture, the FERC (2007) guidelines specify investigation of all faults within the 5-mile radius to determine potential of each for surface rupture. The relationship of the faults to the regional tectonic setting should be discussed, including their association with historical seismicity. Age of most recent movement, fault geometry, magnitude of vertical and horizontal deformation, and probability of occurrence should be evaluated. Any lineaments should be discussed.

1.5 Unit Conversion and Datums

The data and analyses presented herein are based on the Imperial Unit System. Table 1.2 provides a quick reference for conversion from Imperial Units to SI.

Table 1.2: Conversion Units

From Imperial System	To SI System	Divide by
Kips – k	Kilo Newtons – kN	0.224809
Kips – k	Mega Newtons – MN	224.809
Pounds/foot^2 - psf	Kilo Newtons/meter^2 – kN/m^2 (kPa)	20.885
Pounds/foot^3 - pcf	Kilo Newtons/meter^3 – kN/m^3	6.3659
Feet – ft	Meters – m	3.2808
Inches – in.	Millimeters – mm	0.03937

All coordinates are reported in Zones AK3 AK4 AK5 North, NAD83 (NSRS 2007), and are in feet. Topographic elevations for onshore areas are referenced to NAVD88. It should be noted that the marine geophysical survey is referenced to Mean Low Lower Water (MLLW). The following formula is used to convert the elevations from MLLW to NAVD88:

- Elevation, in feet (NAVD88) = Elevation, in ft (MLLW) – 7.32 ft

Elevations presented in this report, and the corresponding illustrations and plates are all referenced to the NAVD88 datum, unless noted otherwise.

1.6 Report Organization

This report is organized in five sections. Section 1, the Introduction, describes the purpose, scope, and approach of the geologic hazards assessment. Section 2 provides an overview of the regional (100-mile radius) and local (5-mile radius) geologic and tectonic setting, and presents the 5-mile geologic map prepared for the project. Sections 3 and 4 evaluate geologic hazards in the onshore and marine sites, respectively. These sections evaluate hazards including surface fault rupture, folding and tilting, effects of strong ground shaking, tsunami inundation, and coastal erosion. Conclusions and recommendations are presented in Section 5, and Section 6 provides a list of references. Illustrations are provided as plates, numbered sequentially and referenced in the text. Two oversized charts are included, presenting geologic mapping of the 5-mile site radius for the onshore and marine areas.

Table 1.2: Existing Geospatial Data

Date	Description	Scale/ Resolution
1950	Aerial photography, black and white, scanned and georectified by the U.S. Fish and Wildlife Service in Soldotna, AK.	Horizontal resolution = 9.8 feet
1980	Aerial photography, U.S. Geological Survey, Color Infrared	1:32,000
2005	Soil survey of the western Kenai Peninsula area, Alaska, USDA and Natural Resources Conservation Service (NRCS)	1:25,000
2008	U.S. Geological Survey 1/9-arcsecond National Elevation Dataset digital elevation model, from LiDAR data collected in 2008 covering the Kenai Peninsula Borough	Horizontal resolution = 8.2 feet; vertical accuracy = 0.5 feet
2009	Preliminary Geologic Map of the Cook Inlet Region, Alaska, Wilson et al., U.S. Geological Survey	1:350,000
2009	Southern Alaska Coastal Relief Model, Bathymetric data, National Oceanic Atmospheric Administration (NOAA)	Horizontal resolution = 2300 feet
2012	Aerial imagery, Kenai Peninsula Borough, RGB and NIR (four-band)	Horizontal resolution = 2.5 feet
2014	AFSC/RACE: Cook Inlet Shoreline, Alaska Fisheries Science Center, NOAA	Horizontal resolution = 160 feet
2015	Wilson, F.H., Hults, C.P., Mull, C.G, and Karl, S.M, comps., 2015, Geologic map of Alaska: U.S. Geological Survey Scientific Investigations Map 3340, pamphlet 196 p., 2 sheets, scale 1:1,584,000, http://dx.doi.org/10.3133/sim3340.	1:1,584,000

The assessment of geologic hazards incorporated data collected during the 2014 and 2015 field investigations. These data are presented and documented in the Fugro Consultants, Inc. reports listed in Table 1.3. Relevant geospatial data from these reports were added to the ArcGIS database for use in the geologic hazards analysis.

Table 1.3: Relevant Data, 2014 and 2015 Site Investigations

Report No.	Report Title and Date	Relevant Data
04.10140094-2 04.10140334-2	Geologic Mapping Report, Onshore LNG Facilities, Rev. 0, November 18, 2014 Geologic Mapping Report, Onshore LNG Facilities, Rev 0, August 21, 2015	Field observations of geologic materials, stratigraphic relationships, geomorphic processes and features
04.10140094-5 04.10140334-5	Marine Survey Report, Nearshore LNG Facilities & Approach Channel, Rev. 0 April 29, 2015. Marine Survey Report, Nearshore LNG Facilities & Approach Channel, Rev A, December 2015	LiDAR topographic data for coastal bluff MBES bathymetry, seafloor features, seismic reflection, and boomer data for LNG marine terminal
04.10140094-6	Probabilistic Seismic Hazard Analysis Report, Onshore LNG Facilities, Rev. 0, September 1, 2015	Review of regional tectonic setting and characterization of active faults
04.10140094-7 04.10140334-7	Geophysical Survey Report, Onshore LNG Facilities, Rev. 0, April 20, 2015 Geophysical Survey Report, Onshore LNG Facilities, Rev. A, December 7, 2015	Seismic refraction profiles of subsurface strata Seismic reflection, ERT, and IMASW profiles of deep and shallow strata.
04.10140094-8 04.10140334-8	Geotechnical Data Report, Onshore LNG Facilities, Rev 0, May 8, 2015 LNG Facilities Onshore Geotechnical Data Report, Rev. A, November 3, 2015	Onshore borehole logs and laboratory data collected in 2014. Onshore borehole logs and laboratory data collected in 2015

2.0 GEOLOGIC SETTING

This section describes the regional and local geologic setting providing background for the assessment of geologic hazards at the Nikiski LNG site. Section 2.1 reviews the regional geologic setting. The region is tectonically active, and is characterized by multiple seismogenic structures including the Aleutian megathrust, the master fault of the Aleutian subduction zone. The information in this section helped to characterize the seismic sources that were input to the Probabilistic Seismic Hazard Assessment (PSHA), presented in Fugro report No. 04.10140334-6.

The subsequent section, 2.2, focusses on the local geologic setting, within 5-miles of the site and at the LNG facilities area itself. Section 2.2.1 describes the geology and structure of the Cook Inlet, and presents a geologic model and cross section of the folds and blind thrust faults nearest the site. This geologic model includes some local seismogenic sources included in the 2015 PSHA.

Sections, 2.2.2 and 2.2.3 focus on description of the local Quaternary geology and geomorphology in the onshore and marine areas. Onshore geomorphology resulted from Quaternary glacial processes and the deposits are primarily glacially-derived sediments. Marine geomorphology is dominated by the erosional and depositional effects of the strong tidal currents in the Cook Inlet, and surficial sediments are primarily reworked glacially-derived silts, sands, gravels, and boulders. Geologic maps of both the onshore and marine portions of the 5-mile radius are presented. These are based on review of the literature and interpretation of 2014-2015 project-generated LiDAR topographic data, bathymetric data, geophysical data, and geologic field mapping.

2.1 Regional Geologic Setting

Centered on the northwest shore of the Kenai Peninsula, the study region includes the Cook Inlet-Susitna Basin and surrounding mountains of the Alaska Range, the Aleutian Range, the Kenai Mountains, Talkeetna Mountains, and the Chugach Range (Plate 3). The geology of the region is diverse, with rock formations dating from the Paleozoic to the Quaternary (Plate 4 and 5).

The study region is located at the active convergent margin between the North American Plate (Southern Alaska block) and the subducting Pacific Plate (Plate 6). The study region (Plate 7), is characterized by high rates of seismicity and relatively frequent moderate to great earthquakes (Plates 8 and 9). This includes the 1964 moment magnitude (Mw, or **M**) 9.2 Great Alaskan, or Good Friday earthquake, the largest recorded event in Alaska.

2.1.1 Regional Tectonics

North- to northwest-directed oblique convergence between the oceanic Pacific Plate and the western edge of the Southern Alaska block along the Aleutian megathrust, at a rate of 51 mm/yr (LePain et al., 2013) to 55 mm/yr (Bruhn and Haeussler, 2006), drives active tectonism in the region (Plates 6 and 10). To the north of the Alaska-Aleutian megathrust, in the interior of south-central Alaska, the plate boundary strain changes from predominantly convergent to predominantly oblique strike-slip (i.e., it becomes transpressional). Transpressional deformation is accommodated by dextral slip along the Denali and Castle Mountain faults (Plates 6 and 7), with a component of horizontal crustal shortening north of the Denali fault.

The transition from subduction-dominated tectonics to transform-dominated tectonics is complicated by northwest motion of the allochthonous Yakutat microplate terrane (Plate 6), which underthrusts southern Alaska at a rate of 44 mm/yr (Perry et al., 2009). The collision of the Yakutat microplate has substantial influence on the deformation and counterclockwise rotation in the interior of south-central Alaska, as well as contributing to Cook Inlet dextral transpression and lateral escape of the forearc to the southwest (Haeussler et al., 2000; Haeussler, 2008).

The Nikiski site lies within a highly active tectonic region (Plates 7, 8, and 9). Earthquakes with accompanying fault displacement, ground deformation, and secondary effects such as earthquake-induced liquefaction and tsunami are among the known geologic hazards of the region. Paleoseismic investigations indicate seven to ten great earthquakes took place on the Prince William Sound segment of the Aleutian megathrust in the last 4,000 to 6,000 years (Carver and Plafker, 2008; Shennan et al., 2014). The 1964 **M** 9.2 Great Alaskan earthquake caused extensive damage and surface deformation throughout the Cook Inlet (Plate 11), including 0.9 feet of subsidence recorded at a standard U.S. Coast and Geodetic Survey tide-gage station near Nikiski (Foster and Karlstrom, 1967). Great earthquakes such as the 1964 event typically occur at depth along the subducting slab. The seismicity cross section in Plate 12 shows a cluster of subduction zone earthquakes delineating the arc of the downgoing slab. Included in this group of earthquakes is the 2016 Mw7.1 Iniskin earthquake, whose epicenter was located approximately 70 miles southwest from the site.

The Cook Inlet basin (Plates 7 and 10) is a Tertiary forearc basin bounded to the north and west by the Alaska Range and Aleutian volcanic arc, and to the southeast by the Chugach and Kenai Mountains (Haeussler et al., 2000). The depth to the top of the subducting Pacific slab beneath Cook Inlet rapidly increases from 35 km near Anchorage to 50-60 km beneath the basin’s center to the north (Page et al., 1991; Wesson et al., 2007). Four fault zones define the basin margins: the Border Range fault and Bruin Bay fault, both of which are pre-Quaternary, and the Quaternary-active Castle Mountain fault and Lake Clark fault (Plates 7 and 10).

Cook Inlet Tertiary basin fill (Haeussler et al., 2000) noncomformably overlies the Mesozoic basement terranes bounding the inlet (Hartman et al., 1972; Haeussler et al., 2000). The Tertiary basin fill and overlying Quaternary deposits, known as the Kenai Group, have a combined thickness of over 20,000 feet in the center of the basin (Hartman et al., 1972; Shellenbaum et al., 2010) (Plate 13). Formations include (from older to younger) the West Foreland Formation, Hemlock Conglomerate, Tyonek Formation, Beluga Formation, and Sterling Formation (Hartman et al., 1972) (Plate 14). The Pliocene and younger Sterling Formation and the overlying early Quaternary sediments constitute up to 10,000 feet of sediment in the central and eastern Cook Inlet Basin. They are glacial and alluvial materials sourced from the Alaska and Chugach ranges and consist of massive sandstones, conglomeratic sandstones, and interbedded claystones (Hartman et al., 1974; Calderwood and Fackler, 1972).

Cook Inlet Folds

Cook Inlet basin sediments exhibit multiple north to northeast-trending folds, subparallel to the basin margins (Kirschner and Lyon, 1973; Fisher et al., 1987; Magoon et al., 1976; Alaska Oil and Gas Conservation Commission, 1994; Haeussler et al., 2000; Koehler et al., 2012). Folding of Cook Inlet forearc basin materials provides the structural traps for the inlet's numerous oil and gas fields and these folds have been described in the geologic literature from the early 1960s (Kelly, 1961, 1963; Kirschner and Lyon, 1973, Boss et al., 1976, Shellenbaum, 2013) (Plate 15). Since that time, understanding of the structural relationships between folds, buried faults, and earthquakes has grown substantially. Events such as the 1995 Kobe **M** 6.9 earthquake, sourced in a transpressional forearc setting, have provided valuable understanding of the seismic hazard potential in forearc settings above Benioff zones (Sugiyama, 1995; Wesnousky and Scholz, 1982). Additionally, Bucknam et al. (1992) and Johnson, S.Y., et al. (1996) show that events with magnitudes larger than 8.0 have likely occurred as a result of transpression within the Cascadia forearc basin overlying the subduction zone (Haeussler et al., 2000). The Alaska Quaternary Fault and Fold database (QFF) (Koehler et al., 2012) identifies 19 potential Quaternary active tectonic structures in the Cook Inlet basin based on the correlation of magnetic and gravity lineaments with available oil and gas industry seismic reflection data (Plate 7).

Mapped structures in Cook Inlet are characterized as fault-cored anticlines (Fisher and Magoon, 1976; Haeussler et al., 2000; Bruhn and Haeussler, 2006; Haeussler and Saltus, 2011). Steeply dipping master faults accommodate predominantly reverse (thrust) motion, with faults extending from the Mesozoic basement up into the Tertiary basin fill (Bruhn and Haeussler, 2006). Cross sections generated from industry seismic data indicate variable directions of structural vergence (Plate 16). Blind thrust faults may dip to the northwest or to the southeast (Bruhn and Haeussler, 2006).

Haeussler et al. (2000) used existing public and private-sector data to evaluate evidence for Quaternary activity associated with these structures, and assess the timing and rates of deformation. The data support onset of deformation as early as the late Miocene, but suggest that most occurred in the late Pliocene and Quaternary, and many structures are probably still active in the contemporary stress regime (Haeussler et al., 2000). Observations of depositional patterns within the Miocene Beluga Formation by Hartman et al. (1974) suggest that Cook Inlet deformation may have begun post- late Miocene time. The thickness of the Beluga Formation does not change across mapped fold axes, consistent with post-depositional folding. Therefore, the majority of deformation would be post-Miocene (Haeussler et al., 2000).

Haeussler et al. (2000) place the majority of deformation as beginning in the late Pliocene and continuing throughout the Quaternary. Several observations support this conclusion. First, the Castle Mountain fault that bounds the Cook Inlet Basin is known to be active, as is the associated anticline. Second, virtually all the strata above the base of the Pliocene Sterling Formation maintain thickness across the crests of anticlinal folds, indicating post-Pliocene deformation. Third, growth wedges of younger sediments filling the troughs between anticlines are shallow, suggesting Quaternary fold growth, and the growth wedge margins are folded, indicating continuing deformation. Finally, the seafloor above the North Cook Inlet structural axis is uplifted and folded concordantly with the deeper fold structure.

Historical Seismicity in the Cook Inlet Basin

Historical seismicity patterns in the Cook Inlet basin (Plate 8) bolster the case for ongoing forearc basin deformation. Frequent **M** ≤ 3.0 earthquakes with depths of 15 to 35 km, clustered at 20 to 30 km depth (Stephens et al., 1995), occur above the Benioff zone of the subducting Pacific slab (Page et al., 1991; Stephens et al., 1995; Ratchkovski et al., 1998) (Plate 12). An examination of focal mechanisms for 21 of these earthquakes by Ratchkovski et al. (1998) determined that two-thirds of these events were consistent with thrust motion on northeast-striking nodal planes, and the remaining one-third of events were consistent with strike-slip motion on northeast- and northwest-striking nodal planes. Haeussler et al. (2000) do not correlate any **M** ≤ 3.0 earthquakes to a known structure within the Cook Inlet basin, but the depths and focal mechanisms of these earthquakes are consistent with structures resulting from Upper Cook Inlet forearc basin deformation.

A Ms 6.9 earthquake in 1933 with an epicenter location 16±50 km south of the Castle Mountain fault trace was widely felt in southern Alaska (Abe, 1984). Modified Mercalli intensity (MMI) maxima of the 1933 event were greatest on the northwest margin of Upper Cook Inlet. Haeussler et al. (2000) indicate that this intensity pattern is inconsistent with a subduction zone earthquake at this epicenter location, which would produce MMI maxima on the southeast side of Cook Inlet (Anchorage area). Instead, Haeussler et al. (2000) interpret the observed MMI from the 1933 event to indicate a seismic source within the Cook Inlet forearc basin. Historical seismicity in Alaska and the Cook Inlet region is discussed in greater detail in the project PSHA (Fugro, 2016).

2.1.2 Regional Geology and Physiography

Geology and physiography in southern Alaska are a result of the tectonic history described above. Southern Alaska consists of many accreted terranes and tectonic elements associated with a long history of subduction.

Within the site region, the two primary terranes are the Peninsular and Chugach terranes (Plafker and Berg, 1994; LePain et al., 2013). In map view, these define a nested, arch-shaped pattern that is convex to the north, which is visible in the regional topographic fabric (Plate 1 and 3). Each tectonic terrane has its own suite of rock types, which are a function of the geologic makeup of the original terrane before accretion, and subsequent metamorphism that occurred during the accretion process.

The site lies within the Peninsular terrane, which is separated from the Chugach Terrane to the east-southeast by the Border Ranges fault (Plate 10). Rocks within the Peninsular Terrane formed largely within the ancestral (Mesozoic) oceanic magmatic arc and consist of: Upper Triassic interbedded tuff, limestone and shale; andesite of the Lower Jurassic Talkeetna Formation (the volcanic carapace); Triassic to Tertiary diorite and granite (plutonic rocks that define the plutonic roots of the volcanic arc); and an overlying succession of Middle Jurassic to Upper Cretaceous marine sedimentary rocks (LePain et al., 2013).

The Chugach Terrane represents the remains of the Triassic to Upper Cretaceous subduction complex and consists of: blueschist of the Kodiak-Seldovia schist belt; ophiolite of the McHugh and Uyak Complexes and the Kelp Bay Group; and phyllitic trench-fill turbidites that record progressive growth of the subduction complex due to shallow (depth of 4 to 7 miles) underplating during the Cretaceous to early Paleocene.

Superimposed onto the older bedrock terranes are the Aleutian Range volcanic arc and Cook Inlet Basin. Both features are physiographic and tectonic elements formed in response to Neogene to present-day plate subduction along the Aleutian megathrust. The Aleutian volcanic arc partially bounds Cook Inlet Basin on the west. Active volcanoes near the site such as Augustine, Redoubt, Iliamna, and Mt. Spur have erupted in historical times.

Cook Inlet Basin trends north-northeast and forms a contiguous structural and physiographic trough with the Susitna Basin to the north of the Castle Mountain fault (Plate 3). This trough defines the ancestral forearc basin, which formed as a result of warping and down-faulting between the Aleutian Arc and the Kenai Mountains (Haeussler et al., 2000). The forearc basin is actively closing due to compressional forces driven by east-west convergence between the Kenai Mountains and the Aleutian-Alaska Ranges.

Cook Inlet Basin is filled with over 20,000 feet of Triassic through Tertiary strata. Formations include (from older to younger) the West Foreland Formation, Hemlock Conglomerate, Tyonek Formation, Beluga Formation, and Sterling Formation (Hartman et al., 1972) (Plate 14). The Pliocene and younger Sterling Formation and the overlying early Quaternary sediments constitute up to 10,000 feet of sediment in the central and eastern Cook Inlet Basin. They are glacial and alluvial materials sourced from the Alaska and Chugach ranges and consist of massive sandstones, conglomeratic sandstones, and interbedded claystones (Hartman et al., 1974; Calderwood and Fackler, 1972).

During the Pleistocene, repeated glaciations covered the mountain valleys and lowlands with blankets of glacial till and glacio-fluvial deposits (Wilson et al., 2009). These deposits covered the Cook Inlet-Susitna Basin including the Kenai Lowland (Plate 3). At the close of the Pleistocene, glaciers retreated, and sea level rose to fill the Cook Inlet. Holocene streams and rivers now drain the mountain valleys and their much smaller glaciers, and bring large volumes of reworked glacial sediment to Cook Inlet.

2.2 Site Area Geologic Setting (5-Mile Radius)

The Nikiski LNG 5-mile site radius or *site area* straddles onshore and marine environments, due to the location of the LNG facilities on the coast of the Kenai Peninsula (Plate 17). The site area boundary shown on the plate encompasses 5-mile site radius circles for both the onshore LNG site center (yellow star) and the marine LNG terminal site center (green star). The combined site area is divided almost evenly between onshore and marine areas.

Both marine and onshore areas share a common geologic setting with respect to the Tertiary and older bedrock strata and structure. Their common geologic history, stratigraphy, and tectonic structure is detailed in subsection, 2.2.1.

Quaternary geology and geomorphology differ markedly between the marine and onshore environments, primarily due to differing geomorphic processes active in the Holocene. The onshore geomorphology is dominated by glacial landforms formed in the Pleistocene with little Holocene modification, whereas the marine seafloor geomorphology is dominated by tidal current erosion and sedimentation processes. Thus the Quaternary history, stratigraphy, structure, and landscape evolution will be described separately for each setting. Onshore Quaternary geology and geomorphology is described in section 2.2.2, and marine Quaternary geology and geomorphology is discussed in section 2.2.3.

2.2.1 Bedrock Geology and Structure of the Site Area

The site area lies approximately at the center of the Cook Inlet Basin, a forearc basin formed in the crust above the subducting slab of the Pacific Plate. Beneath a veneer of Quaternary sediments, the Tertiary sediments in the center of the basin attain a thickness of 20,000 to 25,000 feet (Plate 13) (Shellenbaum et al., 2010). These sediments were gradually deposited in the subsiding basin by streams draining the rising mountains. Continual compression by tectonic forces warped them into folds which are cored by blind thrust-faults (Plate 16). The Tertiary sediments unconformably overlie a basement of Mesozoic sedimentary rocks through which the faults also extend. Though restricted to the crust of the upper plate, these fault are seismogenic sources.

This section describes the pre-Quaternary bedrock geologic history, stratigraphy, and structure of the site area. The emphasis is on the Tertiary stratigraphy and tectonic structure, as it is relevant to the assessment of present-day seismic hazards.

2.2.1.1 Site Area Tertiary Stratigraphy

A generalized stratigraphic column for the Cook Inlet is shown in Plate 14. Major late Tertiary stratigraphic units occurring within the site area include the Sterling Formation, the Beluga Formation and the Tyonek Formation. Three early Tertiary formations (West Foreland, Hemlock, and Chickaloon Formations), are local in extent are not of significant thicknesses within the site area. The lithologies of the Tertiary units are documented primarily from oil and gas exploration wells (LePain et al., 2013), though some outcrops can be found around the margins of the Cook Inlet. The three major late Tertiary units are described below.

The late Miocene to Pliocene age Sterling Formation is characterized by thick fluvial sandstone beds deposited by meandering rivers (LePain et al., 2013). The rivers flowed south and southeast from the Aleutian and Alaska ranges along the axis of the Cook Inlet Basin, depositing layers of point-bar sands and flood-plain silts, muds, and coal. The lithology of the sand is primarily quartz, feldspar, biotite, and volcanic rock fragments, reflecting the strong component of detritus from the Aleutian Arc volcanic terrane. The Sterling sandstone is friable, with little cementation.

The thickness of the Sterling Formation in the site area is at least 4,500 feet (Hartman et al, 1972, 1974) based on wells drilled near the Swanson River gas field located about 20 miles east of the site (Plate 15) on the basin slope. However, based on the location of the LNG site in the deepest part of the basin (Plate 13), the thickness of the Sterling Formation beneath the site area may reach 10,000 feet (Hartman et al., 1972). Interpretation of industry seismic reflection data performed as part of the structural analysis presented in section 2.2.1.3, supports a thickness of the Sterling Formation beneath the site of approximately 9,000 feet (Plate 18).

The middle to late Miocene age Beluga Formation consists of floodplain and channel deposits, and differs from the Sterling Formation in both provenance and bedding characteristics (Lepain et al., 2013). The Beluga Formation has a strong component of detritus from the Chugach terrane metamorphic rocks, in contrast to the volcanic detritus of the Sterling Formation. The Beluga Formation is described as interbedded claystone, siltstone, sandstone, and coal. Individual sandstone beds are thinner than in the Sterling. The thickness of the Beluga Formation in the site area is approximately 2,500 feet based on wells drilled at the Kenai gas field, located approximately 10 miles south of the site (Enos and Maier, 2013) (Plate 15).

The late Oligocene to middle Miocene age Tyonek Formation is comprised of a succession of sandstone, conglomeratic sandstone, siltstone, claystone, and thick coal beds. The Tyonek Formation reaches a maximum thickness of about 7,000 feet in the central part of the basin (LePain et al., 2013). In the site area, the Tyonek is the oldest of the Tertiary strata and rests unconformably on Mesozoic marine sedimentary rocks (cite reference here).

2.2.1.2 Site Area Geologic Structure and Tectonics

The site area lies within a broad, approximately 10-mile-wide (16 kilometers) synclinal flat formed between the Middle Ground Shoal anticline on the west and an unnamed monocline on the east (Plates 19 and 18). Deformation of these structures involves the entire 20,000-foot-thick sequence of Tertiary forearc basin strata as well as the underlying Mesozoic basement (Bruhn et al., 2000; Shellenbaum et al., 2010). Contraction within the forearc basin is attributed to movement on blind reverse and/or reverse-oblique faults that lie at considerable depths below upper Cook Inlet (Kirschner and Lyon, 1973; Haeussler et al., 2000; Bruhn and Haeussler, 2006).

Our understanding of the subsurface structure within the site area, as shown in Plates 19 and 18, was developed through review of published and unpublished technical literature and maps, and interpretation of different suites of seismic reflection data. Locations of the seismic reflection profile lines examined for this study are shown on Plate 20. Some of these seismic reflection data were acquired in 2014 and 2015 for the AKLNG project and provide both shallow and deep imaging exclusively within the 5-mile radius of the site (including onshore and marine). Remaining datasets consisted of older 2D time-domain seismic reflection profiles that were collected for oil and gas exploration in upper Cook Inlet. These data cover both onshore and offshore areas and extend beyond the site radius. For commercial reasons, Fugro was granted the opportunity to view and take raster images of the proprietary seismic reflection data in the ConocoPhillips data room in Anchorage, Alaska. As discussed in detail in the 2016 Probabilistic Seismic Hazard Analysis (PSHA) (Fugro report #04.10140334-6), raster images of the exploration data were georeferenced in ArcGIS to locate key structural features such as fault tip-lines and fold hinges.

Seismic reflection data collected during the 2015 field season show details of the geologic structure beneath the LNG onshore and marine facilities. Plate 21 shows the onshore data collection lines. Individual seismic reflection profiles are presented in Plates 22, 23, and 24. Oblique 3D views of these data are shown in Plate 25. The onshore data show planar, horizontal to gently dipping reflectors (beds) within the Tertiary strata, consistent with their position in the synclinal flat between anticlines. Marine seismic reflection line SL203 (Plate 26) shows the gradual transition from the synclinal flat to the east, to the flank of the Middle Ground Shoal anticline to the west. Neither the onshore nor the marine 2015 seismic reflection data show vertical separation of reflections consistent with faulting. These data constitute positive evidence for the absence of tectonic faulting beneath the proposed LNG facilities.

Bounding the site area on the west, the offshore Middle Ground Shoal anticline (Plate 20, 19) is a west-vergent fold that is described in the literature as the largest and tightest fold in Cook Inlet (Boss et al., 1976; Bishop, 1982; Haeussler and Saltus, 2011). Geometric properties of the fold change continually along strike. For example, south of the site area, folding is expressed by a kinked monocline with sharp, angular hinges. Within the site area, the geometry defines a broad, concentrically-folded anticline. To the north, it is expressed as a tight anticline superimposed onto the upper hinge of a larger-scale monoclinal warp.

Relationships described in the literature (Haeussler et al., 2000) as well as interpretations of the deep seismic reflection profiles indicate that the Middle Ground Shoal anticline overlies a blind, west-dipping (i.e., east vergent) master fault (Plates 27 and 28). The asymmetry of the fold—the west limb is subvertical (Bishop, 1982), while the east limb has a moderate dip—is caused by an east-dipping backthrust that roots into the main thrust at a depth of approximately five seconds (TWTT) (Plate 28). Structural relief on the top of the Mesozoic basement across the master fault is approximately 10,000 feet (3 kilometers). By using the amount of structural relief and a fault dip of 55 degrees, Haeussler et al. (2000) applied simple trigonometric relationships to estimate a net dip-slip displacement of 13,500 feet (4.9 kilometers) on the master fault.

While there is uncertainty regarding when contraction began within upper Cook Inlet, Haeussler et al. (2000) favor an age of onset beginning around 1.6 million years ago (Ma). This is based on the assumption that (1) most of the regional deformation post-dates the base of the Sterling Formation (~5.2 Ma), and (2) the oldest strata within the growth wedges lie at relatively shallow depths and at elevations well above the base of the Sterling Formation. Using the net displacement reported above for the Middle Ground Shoal master fault, they calculate a preferred slip rate of 2.72 mm/year, but allow rates as low as 0.39 to 0.82 mm/year. These later slip rates assume that the onset of contraction began at 11.2 Ma and 5.2 Ma, respectively.

Both the down-to-the-east step in basement and presence of a west-vergent fault-propagation fold can be traced in the seismic reflection data continuously to the north into the Granite Point anticline. Along-strike continuity of these features indicates that the underlying master fault ramp is approximately 67 kilometers in length.

On the other side of Cook Inlet, bounding the site area on the east, the unnamed monocline defines a left *en echelon* step with respect to the Kenai-Cannery Loop anticline to the south (Plate 28). Although there is no seismic reflection coverage within the zone of overlap, a structural link is inferred because both folds are west-vergent and overlie a down-to-the-west step in basement. Geometrically, this relationship is identical to the Middle Ground Shoal fault-fold system on the other side of Cook Inlet. The main difference is that the vergence, or transport direction, of the master fault is in the opposite direction.

Because of the subsurface continuity of the master fault, we informally refer to this northern extent of the structure as the Kenai-Cannery Loop monocline. Interpretation of the seismic reflection data indicates that, collectively, the Kenai-Cannery Loop fault-fold system has a length of over 48 kilometers. Location of the fault tip-line below the monocline is only loosely constrained because the fault tip lies at an elevation below the imaging depth of the reflection data (Plate 28). However, the tip-line location can be inferred generally by the position of the axial hinge that separates the monocline from the synclinal flat (e.g., Suppe and Medwedeff, 1990). East of the monocline, the amplitude of the fold begins to increase due to the presence of a second east-dipping fault that lies structurally above (i.e., in the hanging wall of) the master fault. This fault breaches the core of the Beaver Creek anticline (Plate 28). Based on the elevation of the top of Mesozoic basement, there is a total of approximately 10,000 feet (3 kilometers) of structural relief between the Beaver Creek anticline and the synclinal flat below the site. There are no published slip rate estimates for this structure.

In terms of relative timing, preliminary analyses of the industry seismic reflection data suggest that fold growth and concomitant slip on the underlying thrust ramp is considerably younger on the east side of the basin (i.e., Kenai-Cannery Loop fault-fold system) than it is on the west (i.e., Middle Ground Shoal). The two uppermost dashed lines shown on Plate 28 are structural form lines, which were created by manually tracing arbitrary reflectors across the seismic data. As these lines pass from the synclinal flat onto the eastern flank of the Middle Ground Shoal anticline, they converge, which indicates active fold growth during deposition of the corresponding strata. In contrast, as these seismic-stratigraphic horizons are traced to the east onto the Kenai-Cannery Loop monocline, they stay evenly spaced, indicating that fold growth necessarily post-dates deposition of the corresponding strata.

2.2.2 Onshore Quaternary Geology and Geomorphology of the Site Area

The onshore portion of the 5-mile site radius is underlain entirely by deposits of Quaternary age. These deposits consist of Pleistocene glacial till and glacially derived fluvial, deltaic, and subestuarine deposits, with a veneer of Holocene eolian, lacustrine, and fluvial deposits. Based on deep seismic reflection data collected in 2015, the Quaternary deposits within the onshore site area range from 200 to 800 feet in thickness, and overlie a generally planar unconformity eroded into gently folded strata of the Pliocene Sterling Formation. Locations of the deep seismic reflection lines are shown in Plate 21, and interpreted profiles are shown in Plates 22, 23 and 24.

Quaternary geologic deposits and landforms can serve as key strain gauges to help detect and assess neotectonic activity, a topic that will be explored in Section 3.1.2. In addition, an understanding of their origin, type, and distribution also establishes a framework for characterizing the subsurface geologic deposits on which the onshore LNG facilities are sited.

Geologic mapping of the onshore portion of the 5-mile site radius is presented in Plates 17 and Chart 1. These maps are referred to throughout the discussion. Plate 17 shows the geology of the entire 5-mile site radius including marine and onshore portions. Chart 1 is a detailed geologic map of the onshore portion of the site area at 1:15,000 scale. The onshore mapping is based on interpretation of LiDAR topographic data (USGS, 2008), field geologic mapping and geotechnical exploration, and review of existing literature.

Field geologic mapping was conducted in September of 2014 and June of 2015. Photographs taken during the field mapping are used as illustrations throughout this report; their locations are shown on Plate 29. Complete documentation of the field mapping is presented in Fugro reports 04.10140094-2, and 04.10140334-2 (Table 1.3).

2.2.2.1 Topography and Geomorphology

The Alaska LNG Nikiski site lies on the north-central coast of the Kenai Peninsula on a low relief plain of glacial and glaciofluvial deposits referred to as the Kenai Lowland (Karlstrom, 1964). Elevation within the 5-mile site radius ranges from approximately 120 feet below sea level to 310 feet above sea level, with the center point of the proposed site at 125 feet (Plate 17, Chart 1). Topography is hilly in the northwest, where hummocky glacial moraine deposits of the Killey age (stade) ice advance are exposed, then becomes more gentle and planar toward the south, where the surface is covered with glacial outwash fans extending south and southwest from the moraine deposits. The LNG onshore facilities area sits on the glacial outwash deposits adjacent to the edge of the coastal bluff, which rises approximately 120 feet above the shore of the Cook Inlet. Beds of glacial outwash and sub-estuarine glacial deposits are exposed in the face of the bluff. The bluff itself is slowly retreating as wave erosion undercuts the toe of the slope (discussed further in Section 3.4).

Table 2.1: Summary of Glacial Chronology of Cook Inlet Area

Glaciation	Stade	Approximate Age and duration	Area affected/ description/ more information
Naptowne	Elemndorf	11 to 16 ka	Restricted to mountain valleys
	Skilak	16.0 to 17.5 ka	Restricted to mountain valleys
	Killey	17.5 ka to 18.5 ka	Till and outwash cover Nikiski area
	Moosehorn	27 ka to 32 ka	Till and subestuarine deposits cover Nikiski area

Source: Reger et al., 2007

Previous published studies on the late Quaternary glacial history of Cook Inlet (Karlstrom, 1964, Reger et al, 2007) document several glaciations as recorded by geomorphic features such as lateral and terminal moraines. Large glaciers flowing south from the Alaska Range covered most of the Cook Inlet during the last major glaciation, leaving deposits of glacial moraine and outwash across the Kenai Peninsula (Plate 30) (Karlstrom, 1964; Reger et al., 2007). The last major glacial advance to extend across the Cook Inlet was the Naptowne glaciation, which included four advances, or *stades*, named from oldest to youngest: Moosehorn, Killey, Skilak, and Elemndorf (Karlstrom, 1964, Reger et al., 2007) (Table 2.1). Mapping by Reger et al, (2007) shows that only the Late Moosehorn (at 27,000 to 32,000 years) and Killey (at 17,500 to 18,500 years) stades of the Naptowne glaciations extended across the 5-mile site radius (Plate 30). Deposits and landforms associated with these advances include ground and recessional moraines composed of glacial till, and outwash plains of gravelly sandy alluvial fan deposits that fine toward the south, away from the glacial front. Kettle holes, filled with small lakes and fens (marshes), dot the till and outwash plains between the moraine ridges.

Kettle lakes are prominent features of the site area. Blocks of ice left by the retreating Killey glacier were buried by outwash, and subsequently melted to form kettle holes (Reger et al., 2007) (Plate 31).). The deeper holes filled with groundwater to form lakes. Within the 5-mile site radius, the kettle lakes vary in their morphology with distance from the glacial source. Lakes in the northern portion of the 5-mile radius, such as Island Lake, are deep, sitting 30 to 50 feet below the surface of the Killey moraine and outwash deposits; paleoshoreline and shoreline slump features are prominent. By contrast, lakes in the southern portion of the 5-mile site radius are shallower, sitting 10 to 15 feet below the Killey outwash plain. Paleoshoreline and shoreline slump features are subtle to absent. Plate D-14 presents field photographs of typical kettle lakes.

2.2.2.2 Onshore Quaternary Stratigraphy

Stratigraphy in onshore portion of the 5-mile site radius is dominated by glacial and glaciofluvial deposits laid down during the late Pleistocene Naptowne glaciation (Karlstron, 1964; Reger et al., 2007). Relatively thin Holocene deposits form a discontinuous mantle over the Pleistocene deposits, occurring in mappable thicknesses (10 feet or greater) primarily in depressions (kettle holes) and stream valleys. Offshore, Pleistocene deposits are partially to completely removed by erosion and the sea floor covered by a discontinuous layer of sand and silt deposited by waves and tidal currents. Stratigraphic units are listed from youngest to oldest in Table 2.2. Plate 17 Chart 1 show the mapped distribution of stratigraphic units. Plate 33 illustrates an idealized schematic of the stratigraphic relationships of the mapped deposits across the site.

Table 2.2: Quaternary Stratigraphic Units, Onshore Site Area

Stratigraphic Unit	Description
af	Artificial fill, including engineered fill underlying coastal dock facilities, and large gravel piles.
Hp	Holocene peat and muck deposits. Deposits of peat and organic-rich silt accumulated in marshy areas along the margins of kettle lakes and in depressions and fens or *muskegs* (Plate 34). The soils of this unit are mapped by the USDA (2005) as the Salamatof peat soil series, described as very deep (≥ 5 feet) and very poorly drained, with a parent material of coarse sphagnum moss interlayered with sedge peat. The peat and muck may also include layers of diatomaceous earth (lacustrine), loess, and tephra. This unit is underlain by glacial outwash and moraine of the Killey glacial stade.
Hfp	Holocene alluvial fan and peat deposits. Deposits of peat interbedded with fluvial silt and sand on very gentle slopes at the distal end of the Killey glacial outwash fan. This unit forms a thin fan-shaped deposit derived from erosion of the Killey outwash. It overlies the toe of the Killey fan. High groundwater conditions have resulted in the accumulation of significant thicknesses of peat.
Pko	Pleistocene glacial outwash deposits of the Killey glacial stade (Plate 35). Exposures of the deposit in the coastal bluffs adjacent to the site and collected samples include: tan pebbly sand; laminated sand and silt; coarse sands and rounded gravel; and sandy silt. Reger et al. (2007) indicate a range of grain sizes and broadly indicate coarser grained deposits to the north in the Nikiski area proximal to the inferred Killey stade ice margins, and finer grain deposits to the south. Thickness of the deposit is approximately 50 to 90 feet, estimated from coastal bluff exposures near the site, and site borings (Plate 36).
Pkop	Pleistocene glacial outwash deposits of the Killey glacial stade, pitted with depressions and kettle lakes.
Pkm	Pleistocene glacial moraine deposits of the Killey stade. Boulders, gravel, sand, and silt deposited as terminal, recessional, and ground moraine. This unit underlies ridges and rolling hills in the northern part of the 5-mile site area.
Pko/Pkm	Undifferentiated Pleistocene glacial outwash deposits and moraine deposits of the Killey stade. Moraine deposits consist of glacial till, poorly sorted boulders, gravel, sand, and silt deposited in mounds and ridges as terminal, recessional, and ground moraines. Outwash sediments overlie the moraine and level the surface, leaving moraine crests protruding as low ridges. Outwash sediments consist of fluvial bedded gravels, sands, and silts. Grain size generally fines southward with increasing distance from ice margins. Kettle lakes and depressions pit the surface.
Pme	Pleistocene subeastuarine deposits of the Late Moosehorn glacial stade, exposed in the coastal bluffs adjacent to the site underlying the Killey age outwash deposits (Plate 36). Exposures observed consisted of compact silt with minor fine to medium sand, clay, and trace gravel. The unit also includes scattered boulders. These are interpreted to be ice-rafted glacial debris dropped into the estuarine waters from the melting glacier, termed "rain-out" deposits by Reger et al. (2007). Such boulders are strewn on the beach where erosion has left them as a lag.

2.2.2.3 Quaternary Geologic History

The geologic history presented below provides a framework for the stratigraphic units observed in the map area. As discussed in Section 2.2.1, the primary geologic deposits and geomorphic features in the 5-mile site radius are the result of the Moosehorn and Killey stades of the late Quaternary Naptowne glaciation (Table 2.1). The glacial history of the Kenai area was first detailed by Karlstrom (1964), who mapped the Kenai Lowland and identified and named the glacial stades. This work was followed by Reger et al. (2007) who refined the mapping and understanding of the glacial history and placed well-supported age constraints on several of the glacial stades.

Moosehorn Stade

The Moosehorn stade is the oldest and longest stade of the Naptowne glaciation extending from approximately 32 to 23 ka (Plate 30) (Reger et al., 2007). Glaciers formed in the valleys of the Kenai Mountains to the east and the Tordrillo and Aleutian Mountains to the west spreading out across the Cook Inlet and the lower Kenai Peninsula. Within the 5-mile radius, glacial advances associated with the Moosehorn stade resulted in a laterally extensive subestuarine fan rainout deposit that underlies Killey age moraine (map unit Pkm) and outwash deposits (map unit Pko) (Plates 17 and Chart 1). Reger et al. (2007) describe a subestuarine fan depositional environment where fine-grained sediment rained out from sand-charged plumes that discharged from beneath a calving tide-water glacier (Plate 37). Reger et al. (2007) assigns these deposits to the Late Moosehorn, dated at 23 ka to 27 ka.

The contact between the Killey and late Moosehorn deposits is visible in the coastal bluffs east and south of the site location, generally marked by orange discoloration of the underlying late Moosehorn deposits. The finer-grained and more compact (i.e., lower permeability) Moosehorn deposits act as an aquitard for iron-rich groundwater descending through the Killey sands (Plate 16). The water flows laterally along the contact and emerges at the bluff face as a seep, where the iron oxidizes and stains the face of the exposure. Based on field observations, the contact between the two deposits represents a prominent surface present throughout the Kenai-Nikiski area. Along the coastal bluffs, deposits of colluvium and beach gravels ranging in thickness from zero to five feet overlie the late Moosehorn deposits. Additionally, previous mapping by Reger et al. (2007) indicates that the contact between the Pleistocene Pme and Pko map unit deposits dips gently northward.

Killey Stade

The Killey stade followed the Moosehorn stade from 18.5 to 17.5 ka and left much of the Kenai lowlands ice free (Plate 30) (Reger et al., 2007). Three ice limits associated with the Killey stade are mapped in the 5-mile radius (Plate 17 and Chart 1). The Killey age glacial advances resulted in extensive outwash and moraine deposits overlying the late Moosehorn subestuarine deposits throughout the 5-mile site radius.

Evidence of the oldest advance of the Killey stade is apparent in the LiDAR as a diffuse boundary between Salamtof Lake, Upper Salamatof Lake, Douglas Lake and the outwash plain to the south (Plate 17). To the north, the southern margins of Bernice Lake and Island Lake delineate the limit of a younger glacial advance. The younger ice limit marks a more distinct transition in the landscape, characterized by geomorphic evidence of a modified terminal moraine at the eastern margin of the 5-mile radius. The discontinuous hummocky ridge at the northern margin of the site radius is the terminal moraine from the youngest Killey age glacial advance in the site area. Glaciofluvial processes and braided outwash plain deposits generated by subsequently younger glacial advances likely modified and reworked deposits associated with the older ice margins.

Killey age glaciations resulted in the formation of outwash plains across the 5-mile radius. Outwash plains formed at the terminal margin of Killey stade glaciers and extended across much of the 5-mile site radius. Material deposited in the outwash plains typically consist of stratified gravels, sands and silts. Roughly planar surfaces, with a braid-plain geomorphology consisting of multiple channels that divide and rejoin, braid bars, point bars, and shallow overlapping channels define the outwash plains in the LiDAR (Plate 17 and Chart 1). Orientations of the fluvial channel margins and point bars indicate the outwash plains flowed in a predominantly south-southeast direction.

Surficial Killey age deposits in the 5-mile site radius consist of the following: glacial moraine deposits (map unit Pkm); undifferentiated glacial outwash and moraine deposits (map unit Pko/Pkm); glacial outwash deposits pitted with depressions and kettle lakes (map unit Pkop); and glacial outwash deposits (map unit Pko).

Pleistocene moraine deposits (map unit Pkm) define a discontinuous hummocky ridge in the LiDAR at the northern margin of the 5-mile radius (Plates 17 and Chart 1). The slope break at the base of the ridge marks the contact with the undifferentiated Killey outwash and moraine deposits (map unit Pko/Pkm). To the north, the moraine deposits comprise the height of the coastal bluffs (approximately 130 feet). At the base of the bluffs, deposits of colluvium and beach gravels ranging in thickness from zero to five feet overlie the moraine deposits.

Undifferentiated Pleistocene Killey outwash and moraine deposits (map unit Pko/Pkm) (Plate 17 and Chart 1) comprise the surficial materials south of the moraine deposits. Outwash deposits are defined in the LiDAR data by shallow pits (less than approximately 15 feet deep) and aligned northeast trending kettle lakes. Modified moraine deposits are apparent as discontinuous, low arcuate ridges in the LiDAR, specifically at the eastern margin of the site radius. The base of the modified moraine at the eastern margin of the site as well as the southern margin of Bernice Lake, approximately define the southern extent of the deposits.

South of the undifferentiated outwash and moraine deposits (map unit Pko/Pkm), outwash deposits pitted with depressions (map unit Pkop) characterize the surficial materials. Variations in the surface expression of the outwash plains (e.g., planar versus pitted) define the deposits in the LiDAR data. The occurrence of the pitting and hummocky depressions generally decreases from north to south with increasing distance from the youngest Killey age glacial advance. The southern extent of the deposits is approximately defined by the southern margins of the depressions surrounding Salamatof Lake, Upper Salamatof Lake, and Douglas Lake (Plate 17).

Outwash deposits (map unit Pko) extend south from the contact of the outwash deposits with pitted depressions (map unit Pkop) to the southern margin of the 5-mile site radius. The absence of pitting or depressions in the surface of the outwash plain defines this mapping unit in the LiDAR data.

Holocene Deposits

Published literature (Reger et al., 2007) and geomorphic evidence indicates that the 5-mile site radius has remained ice free from the end of the Killey stade, about 17,500 years ago, to the present. The absence of ice allowed biogenic, fluvial, lacustrine, and eolian sediments to accumulate in the numerous pits and closed depressions across the site. The Holocene peat and muck (Hp) mapping unit includes peat, diatomaceous earth, silt, sand, and volcanic tephra from ash fall events (Plate 33). Criteria used to identify Holocene peat and muck deposits in the remote sensing data include the presence of shallow, hummocky depressions in the LiDAR data, and a preponderance of grasses versus adjacent tree-covered surfaces in satellite imagery,

Holocene peat and alluvial fan deposits (Hpf) occur as a veneer over the Pleistocene outwash fan (Pko) deposits at the southeastern margin of the 5-mile radius (Plate 17 and Chart 1). These deposits are derived from fluvial erosion of the Pleistocene outwash fan upslope. These deposits are very wet and marshy, and feature a distinct patterned ground appearance on aerial photography, reflecting seasonal freezing and thawing of the ground.

2.2.3 Marine Quaternary Geology and Geomorphology of the Site Area

The proposed marine LNG terminal site is located in Cook Inlet adjacent to the western shore of the Kenai Peninsula. The following description of the Quaternary geology and geomorphology is based on a review of the literature and available data, and on geophysical and geotechnical data collected during the 2014 and 2015 field seasons. Multi-beam bathymetry and side-scan sonar data were collected in 2014 and 2015. Seismic reflection data, air gun, boomer, and chirp data were collected in 2015, and nearshore geotechnical borings were made in 2015. A map of the 2014-2015 geophysical data collection program is presented in Plate 38.

In the marine LNG terminal area, erosion by waves and currents has removed the Killey deposits, resulting in a sea floor underlain primarily by Moosehorn and pre-Moosehorn Quaternary glacial deposits. These consist of fine-grained glacially-derived subestuarine sediments, sandy and gravelly glacial outwash deposits, and poorly sorted bouldery to gravelly glacial till deposits. Locally, currents have deposited waves and ridges of sand and silt, forming a mantle of very young sediment over the older deposits. Large boulders are scattered across the sea floor, likely a lag from erosion exposing large glacial drop-stones of the upper beds of the Moosehorn deposit.

The geologic map of the marine portion of the 5-mile radius site area (Chart 2 and Plate 17), shows the distribution of geologic materials and geomorphic features on the sea floor. The map is based on interpretation of 2014 and 2015 bathymetric, geotechnical, and seismic reflection data collected for the LNG facilities area, and publically available geologic and topographic data for the remainder of the site area.

The marine terminal site is located on the east limb of the Middle Ground Shoal anticline, one of the larger of the Cook Inlet folds (see section 2.2.1.2). Bedding in the Tertiary deposits beneath the site dips gently to the east-southeast on the limb of this fold. This anticline is considered to be active and its underlying blind-thrust a potential seismic source (Haeussler et al., 2000).

The Quaternary deposits overlie an erosional surface cut on gently folded Tertiary marine sediments, a surface referred to as the Quaternary/Tertiary unconformity. Immediately below the unconformity lies the Pliocene age Sterling Formation, the youngest in the sequence of Tertiary formations filling the Cook Inlet basin (Plate 14). The Sterling Formation sediments are described as well-sorted, fine to coarse-grained sands that are rich in volcanic lithic fragments, quartz, and feldspars (McElmoyl, 2013). They may include conglomerate beds, thin seams of coal, and clays.

2.2.3.1 Cook Inlet Quaternary Geology

The morphology and geologic units of the seafloor in Cook Inlet record the complex interplay between the effects of the Pleistocene glaciations, modern sedimentary contributions from the Susitna and Knik Rivers (Plate 3), and the strong tidal currents that flow within the inlet. An eroded surface of Pleistocene deposits with a discontinuous veneer of shifting Holocene sands and gravels characterizes almost the entire extent of the seafloor within the 5-mile radius. A small sliver of Pliocene age Sterling Formation is exposed at the northwest edge of the 5-mile radius (Plate 17 and Chart 2).

The Quaternary geologic history presented below provides a framework for the stratigraphic units observed in the map area (Chart 2). As discussed in Sections 2.2.1 and 2.2.2.3, the primary geologic deposits in the 5-mile site radius are the result of repeated Pleistocene glaciations during which glacial till, outwash, and glacially-derived sub-estuarine deposits accumulated on the floor of the Cook Inlet basin. After the retreat of the glaciers in the latest Pleistocene-early Holocene, sea level gradually rose in the Holocene to fill Cook Inlet. For the past approximately 10,000 years, the Holocene epoch, fluvial and tidal processes have eroded and removed the youngest of the Pleistocene deposits from the seafloor of Cook Inlet, leaving older Pleistocene deposits in place.

The Quaternary (Pleistocene) deposits overlie an erosional surface cut on gently folded Tertiary marine sediments, a surface referred to as the Tertiary unconformity. Immediately below the unconformity lies the Pliocene Sterling Formation, the youngest in the sequence of Tertiary formations filling the Cook Inlet basin. Borings drilled in the marine terminal area penetrate the overlying Quaternary deposits, and encounter the Sterling Formation at elevations of -180 +/- 20 feet. Plate 39, a cross section parallel to the shoreline, shows borehole data projected onto seismic reflection data, illustrating the Quaternary stratigraphy in the marine LNG terminal study area. The location of the cross section in Plate 39 is shown on Plate 40.

Four geologic units are identified in cross section B-B' (Plate 39). The contacts between the thicker units are evident in the seismic reflection data. The uppermost unit, unit 4, is a thin, discontinuous layer of Holocene sand and gravel that forms ridges, waves, and sheets over the underlying Pleistocene unit 3. Unit 4 is not evident on the air gun seismic reflection data, but it is present in the borehole data. Beneath the sea floor, unit 3 is relatively uniform on the seismic reflection profile, with relatively weak internal reflectors. Borehole data show this unit to consist of thick beds of lean clay with some interbeds of silty sand. The underlying deposit, unit 2, is characterized by strong parallel, planar to undulating reflectors, shown in the boreholes to consist of layered sediments of varying composition, including sand, gravel, silt, and clay. Units 2 and 3 are separated by an erosional unconformity.

The Pleistocene deposits of units 2 and 3 are underlain at about -180 ft. elevation (-150 to -200 ft.) by the Sterling Formation, a late Tertiary sandstone (marine unit 1). The Sterling Formation sediments are described as well-sorted, fine to coarse-grained sands that are rich in volcanic lithic fragments, quartz, and feldspars (LePain et al, 2013). Siltstone and coal are also present. This formation was penetrated by several of the 2015 marine boreholes (eg. MB-23 and MB-17 on Plate 39). The top of the Sterling Formation is a roughly planar erosional unconformity. Bedding in the Sterling Formation in the marine LNG area dips gently to the southeast, reflecting the area's position on the east limb of the Middle Ground Shoal anticline.

2.2.3.2 Top Tertiary Angular Unconformity

An erosional angular unconformity marks the top of the folded Tertiary deposits of the Cook Inlet basin. Within most of the 5-mile site radius this angular unconformity lies approximately 250 to 800 feet below sea level (Plate 22). The folded Pliocene Sterling Formation strata across most of the area are overlain by Quaternary glacial and glacially-derived deposits (Chart 2). Tertiary strata are exposed at the seafloor only at the far northwest ends of 2015 Fugro airgun seismic reflection lines SL200 and SL203 (Plate 38), where Quaternary deposits are eroded away near the crest of the Middle Ground Shoal anticline.

Long Array Airgun SL203 (Plate 26) shows dipping Tertiary strata delineated by magenta bedform lines. The dipping strata are truncated upwards against the angular unconformity mapped as a cyan blue horizon. Quaternary glacial deposits overlie the angular unconformity along the entire length of SL203. All of the long array air gun data acquired in 2015 were mapped, and Plate 41 provides a top Tertiary angular unconformity structure contour map, which shows the extent and shape of the angular unconformity, as well as approximate depth conversion values assuming a simplified uniform water and shallow sub-sea bottom velocity of 5,000 ft/second.

The thickness of the Quaternary deposits was calculated by comparing the elevations of the unconformity to the elevations of the sea floor. An isopach map of the Quaternary deposits is presented in Plate 42. Thickness of the Quaternary deposits is about 150 feet thick in the marine terminal area. It decreases in thickness to the west where erosion has removed much of these deposits. In the far southeast portion of the mapped area the thickness of the Quaternary deposits increases greatly where the deposits fill an erosional trough in the top of the Tertiary.

Plate 41 shows that the angular unconformity dips gently to the east. Presuming this unconformity was originally horizontal, it can be used as a strain marker useful for estimating long-term tilting associated with uplift on the eastern flank of the Middle Ground Shoal anticline. Plate 26 Line SL203 is an east-west transect across the angular unconformity. Measuring the two-way-time (TWT) to the unconformity from sea level, it is 0.05 seconds TWT at offset 500 ft on the west side of SL203, and 0.075 seconds TWT at offset 26,000 ft on the east side. The equation to convert TWT to depth is as follows:

$$D=(TWT/2)*V$$

Where D=depth (ft)

TWT = two way time (sec)

V = Seismic Velocity (ft/sec).

The approximate depth to the unconformity on the west side of SL203 is (0.05 sec/2)*5000 ft/sec = 125 ft, and on the east side (0.075/2)*5000 ft/sec = 187.5 ft. The resulting Δ depth is 62.5 feet over a distance of 25,500 feet, or (62.5 ft / 25,000 ft) = 0.0025% tilting since erosion of the top-of-Tertiary angular unconformity. The tilting may result from growth on the Middle Ground Shoal anticline, which lies just to the west.

Plate 43 shows sub-bottom profiler line SB129, an approximately north-south line. The top of the Tertiary angular unconformity is mapped as a cyan blue horizon overlying upward-truncating Tertiary strata shown in magenta. Overlying the angular unconformity, two distinct Quaternary units are mapped. An older Quaternary unit, unit 1, was deposited directly over the Tertiary angular unconformity, and was then partly eroded (Plates 44, 43). Quaternary unit 2 was then deposited. A bright green horizon marks the unconformity between Quaternary units 1 and 2. This Quaternary unconformity is restricted to the marine area and is not observed in the onshore seismic data. Within the LNG area marine seismic survey, this unconformity is laterally discontinuous.

An erosional channel, or trough, incises the Tertiary strata along the southern extent of offshore profile SB129 from offset 18,000 to the southern line end (Plate 43). This erosional trough is also delineated in several other marine reflection lines as shown in Plate 41 that shows the top Tertiary angular unconformity time structure contour map. The trough is shown in the southeast edge of seismic reflection line coverage. Onshore Vibroseis line NS-2 (Plate 22) shows that there are no reflector truncations associated with the onshore projection of this trough to the east.

Onshore high-resolution seismic reflection profile NS-0 (Plate 45) was acquired on the beach, over beach gravels deposited on top of the Moosehorn stade subestuarine deposits. The southern extent of line NS-0 is just north of the erosional trough identified in Plates 44 and 43. Line NS-0 shows very detailed shallow aggradational packages in the heterogeneous Quaternary glacial deposits underlying the Moosehorn deposits.

2.2.3.3 Geomorphic Processes

The seafloor environment of the Cook Inlet adjacent to the site area is best described as a tide-dominated shallow clastic seaway, as defined by Nichols (1999). The extreme tidal range and resultant currents in Cook Inlet play a major role in the reworking and distribution of sediments flooring the inlet. Cook Inlet has the largest average tidal range in the United States, with a mean of 27.0 feet, (NOAA, 2016a, 2016b). and the fourth highest in the world, behind Bay of Fundy (31.3 feet), Ungava Bay (29.0 feet), and Bristol Channel (28.9 feet) (NOAA, 2016b). In the vicinity of the site area, the tidal range is between 24 and 28 feet (NOAA, 2016a). Tidal currents average 3 to 6 knots (7 mph) for flood currents and can reach a peak of 6 to 8 knots (10 mph) or more for ebb currents (Schumacher, 2005).

These tidal currents can affect the seafloor to depths of 300 feet or more below sea level and are capable of mobilizing large quantities of sand and gravel in shallow marine environments (Nichols, 1999). The geomorphology of tidal deposits in shallow marine environments is a function of the tidal current velocity and sediment supply (Sharma and Burrell, 1970). In shallow seas with tidal current velocities above ~2 knots and sufficient sediment supply, sand ribbons form parallel to the direction of tidal currents. In the Bay of Fundy, these ribbons can be 3 feet thick, up to 650 feet wide and can stretch for 6 miles in the flow direction (Kenyon, 1970). Sand ribbons are typically separated by a substrate of gravel. In areas that experience very high velocity currents, only gravel may be left on the seafloor and scour pits or furrows may develop (Kenyon, 1970).

In high velocity tidal current conditions, areas that have a sparse supply of sand can develop isolated sand wave bedforms scattered over the substrate. Conversely, areas that have abundant sand supply may form large banks called tidal sand ridges. These sand ridges may be 30 to 100 feet high and stretch for more than 10 miles (Nichols, 1999).

Sediment input to Upper Cook Inlet varies seasonally. During the summer months, large quantities of glacially derived sediment are added to the upper reaches of the inlet by the Susitna and Knik Rivers. The strong tidal currents prevent early deposition of most of the silt and clay, transporting them south through the constriction between the East and West Forelands, near the site area (Plate 2) (Sharma and Burrell, 1970). The abundance of gravels and sands within the Forelands are a result of the water-movement patterns. Within the constriction, incoming and outgoing tides create turbulence near the seafloor which entrains sediments smaller than gravel size. The grain size distribution becomes a function of distance from the Forelands; the incoming tide controls sediment distribution north of the Forelands constriction while the ebb tide controls distribution south of it (Sharma and Burrell, 1970.) Aggradation on the seafloor within 5 miles from the site area does not appear to be occurring; active erosion by strong tidal currents is taking place in many areas. Some of the observed geomorphic features may be relict. Sediments consist predominately of cobbles, pebbles, and coarse sands with minor amounts of silt and clay (Sharma and Burrell, 1970).

2.2.3.4 Bathymetry and Sea Floor features – 5-mile geologic map 1:15,000

Seafloor surface geology in the offshore portion of the 5-mile site radius is dominated by eroded and reworked glacial and glaciofluvial deposits laid down during the Pleistocene, and by tidal-current Holocene deposits forming discontinuous localized geomorphic features laying atop the Pleistocene deposits. Stratigraphic units are listed from youngest to oldest in Table 2.3. Chart 2 and Plate 17 show the mapped distribution of stratigraphic units. These units are mapped based on multi-beam high resolution bathymetry data, shallow and deep seismic reflection line interpretation, local and regional mapping, and relating the observed tide-dominated shallow clastic seafloor morphology to descriptions and examples from published literature.

*2.2.3.4.1 Anthropogenic (**an**)*

Anthropogenic features include structures or items intentionally or unintentionally emplaced by man. The primary anthropogenic features observed include an arcuate, sinuous feature located approximately 3,500 feet southeast of the proposed facilities interpreted to be an abandoned salmon gill fishing net and a rectangular shaped object approximately 6,300 feet southeast of the proposed facilities. These features are recognized and mapped based on the high resolution bathymetric data. The dimensions of the rectangular object are 300 feet by 100 feet, with approximately 40 feet of relief.

*2.2.3.4.2 Sand Waves (**Hsw**)*

Several sand wave fields are observed and mapped within the multibeam bathymetric data (Plate 17, Chart 2). These bedforms exhibit heights of between 0.9 and 1.5 feet and wavelengths from 35 feet to 45 feet. The crests are straight to slightly sinuous and are oriented generally perpendicular to the prevalent tidal current directions. Many of these sand wave fields appear to be situated in gentle north-northwest trending troughs, which may be acting to stabilize the fields and prevent the erosion and removal of the sands by tidal currents. The sand waves were mapped based on their geomorphic expression and sonar signature in areas where high resolution bathymetrric and sidescan sonar data were collected.

*2.2.3.4.3 Sand Ribbons (**Hsr**)*

Sand ribbons are current-parallel ridges of sand common to tide-dominated environments. Multiple elongate features in the marine site area are interpreted to be sand ribbons (Plate 17, Chart 2). These north-northwest trending ridges are located approximately 1,100 to 3,800 feet from the coastline, and trend subparallel to the coast and the predominant tidal current direction. As discussed in section 2.2.3.3, sand ribbons typically form in shallow clastic seas where tidal currents dominate. In the site area the sand ribbons are approximately three feet high and 60 to 100 feet wide, with lengths ranging between 150 to 2,300 feet. The north-northwest trending sand ribbons are located in an area that experiences tidal currents ranging from 4 and 8 knots, and have dimensions consistent with sand ridges and ribbons reported elsewhere in the literature (Kenyon, 1970; Nichols, 1999).

The geomorphic expression of these features resembles outcropping tilted bedrock ridges. However, seismic data collected perpendicular to the ridges shows reflections from subhorizontal bedding unconformably overlying reflections from gently dipping bedding interpreted to consist of Pliocene age Sterling Formation strata.

*2.2.3.4.4 Sand Ridge (**Hs**)*

One significant sand ridge was interpreted within 5 miles of the site area (Plates 17 and Chart 2). This feature is approximately 21,000 ft long, 1,100 to 1,700 feet wide, and 20 to 40 feet high. It is located west of the area of high resolution bathymetric data coverage. The presence of the ridge is interpreted and mapped based on contours developed from NOAA bathymetric data. This ridge differs from the sand ribbons in its much larger scale, and its position in the inlet closer to the stream of sediment coming through the Forelands constriction. This ridge may be constructed of sand from the upper Cook Inlet.

*2.2.3.4.5 Lag Gravels (**Hg**)*

Large areas of the scoured sea floor are covered with sinuous, discontinuous, irregular patches of rough surficial deposits, as observed in the high resolution bathymetric data. These patches are interpreted to be of sheets of lag gravels and sands (Plate 17, Chart 2). These areas may experience turbulent current conditions precluding formation of regular continuous features, or the gravels may be sufficiently large enough in size that the currents do not have enough energy to remobilize them to either form more regular morphologic features or to allow transport.

In order to more precisely constrain the extents of these gravels, a binned slope gradient map was developed (Plate 46). These deposits are seen in this map as patches exhibiting slope gradients between 3 to 4 degrees.

*2.2.3.4.6 Pleistocene Glacial deposits (**Pg**)*

A significant portion of Cook Inlet seafloor bottom has been scoured and eroded down to semi-consolidated Pleistocene glacial deposits by the strong tidal currents. This scoured surface has a slope gradient typically less than 2 degrees (Plates 17 and 46). Seismic data show reflections interpreted as sub-horizontal bedded deposits overlying gently tilting Tertiary bedrock. If there is bedload on the seafloor it is too thin to be discernible in the high resolution seismic data. Scattered boulders (dropstones) are also locally present; tidal current-induced turbulence around the boulders has created erosional scour depressions.

*2.2.3.4.7 Undifferentiated Pleistocene and Holocene Deposits (**Hsg / Pg**)*

A significant portion of the seafloor within 5 miles of the site area lies outside of high resolution bathymetric and sidescan sonar data coverage. Seismic reflection data within this area exhibits reflections from subhorizontal bedding unconformably overlying seismic reflections from gently dipping bedding interpreted to consist of Pliocene Sterling Formation beds. The seafloor in this area is mapped as undifferentiated reworked Pleistocene glacial deposits and Holocene marine deposits (Plates 17 and Chart 2).

Table 2.3: Quaternary Stratigraphic Units, Marine Site Area

Stratigraphic Unit	Description
an	Anthropogenic detritus including structures or any items intentionally or unintentionally emplaced by man.
Hsw	Holocene sand waves. These bedforms are between 0.9 and 1.5 feet high with wavelengths ranging from 35 feet to 45 feet. The crests are straight to slightly sinuous and are oriented generally perpendicular to the prevalent tidal current directions. Many of these sand wave fields appear to be situated in gentle north-northwest trending troughs, which may act to stabilize the fields and prevent the erosion and removal of the sands by the tidal currents.
Hsr	Holocene Sand Ribbons. Deposits of sand about three feet high, 60 to 100 feet wide, and 150 to 2,300 feet long. These north-northwest trending ridges are subparallel to the coastline and the dominant tidal current directions. They are most common within 1,100 and 3,800 feet from the shore.
Hs	Sand Ridge. This large feature is approximately 21,000 ft long, 1,100 to 1,700 feet wide, and 20 to 40 feet high. It is identified from the NOAA bathymetric contours.
Hg	Holocene lag gravels. Irregular, laterally discontinuous deposits with rough surfaces interpreted to consist of lag gravels and coarse sands. These areas may experience turbulent current conditions precluding formation of regular continuous features, or the gravels may be large enough that the tidal currents lack the energy required to remobilize them. This unit also contains rare, scattered boulders (dropstones).
Pg	Pleistocene Glacial deposits. Semiconsolidated glacial outwash, subestuarine, and moraine deposits. These deposits have been scoured by tidal currents. The surface of this contains rare, scattered boulders (dropstones) and numerous scour pit depressions.
Hsg / Pg	Holocene silt, sand, and gravel deposited by tidal currents and waves, overlying undifferentiated Pleistocene glacial deposits.

3.0 ONSHORE GEOHAZARD ANALYSIS

The analysis of onshore geologic hazards includes those hazards most likely to affect the site and hazards listed in the FERC (2007) draft guidelines. Hazards that result in tectonic surface deformation include surface faulting (Section 3.1), tectonic tilting and folding (Section 3.2), and the effects of strong ground motion (Section 3.3). Other hazards addressed include tsunami inundation (Section 3.4) , coastal erosion (Section 3.5), and volcanic hazards (Section 3.6).

3.1 Onshore Surface Faulting Hazard

The potential for surface faulting was evaluated through geologic and geotechnical data, geomorphic analysis, and analysis of 2014-2015 geologic, geotechnical, and geophysical data. Surface faulting is defined as movement that displaces the ground along a fault plane. The movement may be rapid coseismic rupture, or slow aseismic creep.

The published literature shows no active surface faults mapped within the 5-mile site radius (Koehler et al., 2012). The site falls between the axes of a group of tectonically active north-trending fault-cored folds. As described in section 2.2.1, the faults are blind-thrust faults that core anticlinal folds. Seismic reflection imaging of these structures shows that the faults extend from the Mesozoic basement upward through much of the Tertiary basin sediments, but do not project shallower than a depth of about one kilometer (Haeussler et al., 2000) (Plate 16). Therefore, these faults do not pose a surface fault rupture hazard.

3.1.1 Lineament analysis

A screening for evidence of surface faulting within the 5-mile site radius was conducted based on examination of LiDAR topographic data and field reconnaissance. LiDAR topographic data collected in 2008 (USGS, 2008) show the topography at a resolution sufficient to detect elevation changes as small as one foot. The LiDAR data were viewed in ArcGIS alternately as a bare-earth hillshade image and a slope-shade image at a scale of 1:5,000, enabling detailed examination of geomorphic features. These topographic data are presented at a scale of 1:15,000 on Chart 1. In addition, high-precision topographic data collected during the 2015 on-the-ground survey of the LNG study area were reviewed to confirm their consistency with the LiDAR data.

Lineaments are natural linear features in the landscape that can have a tectonic or non-tectonic origin. Evidence of surface faulting is typically expressed as a linear scarp or set of en-echelon scarps marking the trace of the fault plane, but linear features are also formed as a result of fluvial, glacial, or other geological processes. A lineament identification and analysis was undertaken to identify and characterize linear geological or geomorphological features within the 5-mile site area to evaluate whether any of the lineaments are a result of surface faulting.

3.1.1.1 Lineament Mapping Methods

As a first pass, a slope-shade image with aspect coloration (coloration based on dip direction) and a hillshade image were used to identify linear features within the landscape. Linear features within the 5-mile site area were delineated in ArcGIS; the goal was to capture the full variability of feature orientations, regardless of length and feature morphology. The initial analysis resulted in numerous features with orientations in nearly every direction, and many of the features intersected each other. Several orientations and morphologies were recognized to be common among many lineaments, the most prominent of which is a northeast-southwest orientation.

Following initial feature identification, each feature was evaluated based on its length and morphology. Features that shared a particular alignment were either merged or grouped, and a length exclusion criteria was implemented. Features with lengths of 0.6 miles or shorter were excluded from further analysis. The result of the filtering and grouping was the identification of thirteen (13) features that were of sufficient length or prominence in the landscape to warrant further attention. Each of the lineaments exhibit one of two morphology types: 1) linear escarpments with abrupt changes in slope adjacent to otherwise relatively horizontal (and planar) surfaces, and 2) a series of aligned features (such as lakes or depressions). The result of the analysis is a lineament map shown on Plate 47.

The thirteen lineaments were further evaluated based on their geomorphology and genesis. The criteria listed in Table 3.1 were applied to the identified linear features to exclude those features from further analysis if they are interpreted to beof non-tectonic origin. None of the identified features met the criteria that would warrant additional investigation. All thirteen features are considered to be of non-tectonic origin. Table 3.2 provides a summary of the characteristics of the 13 lineaments identified within a 5-mile radius of the site. A discussion of each lineament follows.

Table 3.1: Criteria for Assessing Lineament Origin

	Criteria	Reasoning
Not Likely Tectonic	Lineament groups whose individual features are dominantly erosional and or depositional with no apparent association with previously mapped faults.	Such lineaments are not-tectonic in origin and not considered further.
	Lineament groups with inconsistent sense of displacement along strike.	Inconsistent, contrasting, or discrepant lineament kinematics indicates low likelihood as a potential seismic source.
	Lineaments that collectively aggregate to less than about 10 km (6 miles) in length.	Length criterion is based on an approximately minimal structural length for a seismogenic source capable of ground rupture.
Likely Tectonic	Lineaments that appear to represent potential extensions or continuation of known Quaternary faults.	These lineaments may contribute to additional fault source length in ground motion calculations.
	Lineaments with possible tectonic geomorphologic evidence that are spatially associated with previously mapped faults or lineaments.	Suggestive, but not conclusive, of tectonic origin. Association with previously mapped faults or lineaments supports inference of structure.
	Lineaments with possible tectonic geomorphologic evidence that are not spatially associated with previously mapped faults or lineaments.	Suggestive, but not conclusive, of tectonic origin.

Table 3.2: Lineament Descriptions

Lineament Number	Description	Length (Miles)	Origin
1	Southwest-northeast oriented, southeast-facing linear escarpment. Includes two gaps where escarpment is obscured by glacial deposits.	3.78	Non-tectonic
2	Southwest-northeast oriented, linear alignment of small lakes.	1.56	Non-tectonic
3	Southwest-northeast oriented, linear alignment of small lakes. Lineament separates the eastern and western outwash fans located at the southern end of the site 5-mile radius.	8.06	Non-tectonic
4	Southwest-northeast oriented, linear alignment of small depressions. Lineament cuts across contours.	0.76	Non-tectonic
5	Southwest-northeast oriented linear escarpment along south shore of lake.	0.66	Non-tectonic
6	Southwest-northeast oriented linear alignment of small lakes.	2.41	Non-tectonic
7	Southwest-northeast oriented, southeast facing linear escarpment. Lineament has a change in orientation	2.99	Non-tectonic
8	Southwest-northeast oriented linear escarpment along south shore of lake.	0.61	Non-tectonic
9	Southwest-northeast oriented lineament. Linear alignment of small lakes.	1.54	Non-tectonic
10a	North-south oriented, east facing linear escarpment. East facing paleo-channel margin	2.07	Non-tectonic
10b	North-south oriented, west facing linear escarpment. west facing paleo-channel margin	1.69	Non-tectonic
11	Southwest-northeast oriented linear alignment of small lakes.	2.31	Non-tectonic
12	East-west oriented, north facing linear escarpment. Lineament is slightly arcuate.	0.89	Non-tectonic
13	Southwest-northeast oriented linear alignment of small lakes.	3.39	Non-tectonic

3.1.1.2 Lineament Description and Evaluation

Lineament number 1 (Plate 47) is referred to as the Bernice Lake lineament. It extends northeast from the coastline, follows the shore of Bernice Lake, and continues northeastward for a total of 3.7 miles. It is characterized by a down-to-the-southeast escarpment up to 40 feet high. The slope of the escarpment is gentle and shows no fresh scarps that would suggest Holocene fault displacement. The lineament has consistent morphology along its mapped extent with the exception of two gaps where glacial deposits obscure the lineament (Plate 47). Three possibilities were considered as an origin for this lineament: (1) a tectonic fault, (2) a geologic contact between separate glacial deposits, and (3) a shallow fault that formed from glacial processes or ground shaking. The conclusion from the following discussion is that the lineament represents a geologic contact.

Chevron consultants interpreted a fault approximately coincident with the Bernice Lake lineament on the basis of borehole and well data. Chevron property straddles the lineament between Bernice Lake and the shoreline. Site of a former refinery, the property was the subject of several investigations of a hydrocarbon contamination groundwater plume, and is dotted with many borings (e.g. GeoMega, 2006; URS, 2007). Faults are mapped in the subsurface based on offset units and ground water flow contours. Here also, the inferred faults seem to act as hydrologic barriers. The shape of the plume appears to be influenced by the fault as it has an elongate boundary roughly coincident and/or parallel to the Bernice Lake lineament (URS, 2007). Strata and water levels are displaced across the interpreted fault.

Fugro onshore and marine seismic reflection data provide subsurface coverage of the Bernice Lake lineament. Onshore, deep geophysical Vibroseis line NS-2 clearly shows no reflector truncations or fold-related deformation in the vicinity of the Bernice Lake lineament (Plate 22). Similarly, marine air gun and boomer seismic reflection lines show no reflector displacements along the projection of the lineament. Thus, both onshore and offshore seismic data provide clear evidence for no tectonic faulting beneath this lineament.

Lineament 1, the Bernice Lake lineament, is assumed to be the result of glacial processes. The long length and linearity are not consistent with slope failure from strong ground shaking. The presence of two gaps obscured by glacial deposits show that the process created the lineament has not been active since the close of the Killey glacial advance (17,500 to 18,500 years ago (Reger et al, 2007). The lineament likely represents a geologic contact between glacial deposits laid down during different phases of Killey-age glacial retreat.

Lineaments 2, 6, 9, 11, and 13 are alignments of small lakes oriented northeast-southwest. The lineaments are of varying length but exemplify the dominant ‘fabric’ of the landscape. These alignments of lakes are interpreted to have formed as a result of glacial processes. The orientation of each lineament reflects successive positions of the margin of Killey glacier as it retreated across the landscape. At each position of the glacier, ice blocks broke off the margin and became submerged in sediment, eventually melting and forming lake depressions. The extent and direction of glacial motion is indicated in Plate 30 (Roger et al., 2007). Earlier Killey stade glacial advances included ice that extended to the southeast of the site, and the youngest and terminal moraine is located to the north of the site at the northern boundary of the 5-mile radius. Due to the short lengths of these lineaments, lack of association with any previously identified Quaternary faults, and strong correlation with glacial processes, this group of lineaments does not appear to be the result of tectonic processes and does not warrant additional analysis.

Lineament 3 is also an alignment of lakes, and is a total of about 8 miles in length. Two segments are mapped, separated by a slight change in orientation and a gap in geomorphic expression. The southwestern portion of Lineament 3 follows topographic low between the northwest and southeast outwash fans (Plate 47) and includes Salamatof Lake. Again, this lineament can be attributed to glacial processes.

Lineament 4 is an alignment of small depressions oriented nearly east-west. The lineament is located approximately at elevation 125 feet and shows evidence of water flowing from depression to depression crossing the channels of the outwash fan (i.e. not flowing in the current down slope direction). The alignment is curious, but because it is relatively short (0.76 miles) the feature does not warrant additional analysis.

Lineaments 5 and 8, oriented northeast-southwest, are north-facing linear escarpments along the southern margins of kettle lakes. The escarpments appear to be the result of subsidence during kettle formation as described above. Despite their clear origin, the escarpments have elevation changes of approximately 23 feet and 35 feet for lineaments 5 and 8 respectively. Given that lineaments 5 and 8 do not extend beyond the edge of the lake, and have relatively short lengths (about 0.6 miles) additional analysis is not warranted.

Lineament 7 is a southeast facing escarpment that is just to the north of the Bernice Lake Lineament (Feature 1). It is approximately 2.9 miles long and changes orientation and strike at its approximate midpoint. The feature appears to be related to glacial processes, and may represent a former terminal moraine from a glacial advance. The strong association with glacial processes, its lack of linearity, and its relatively short length support a non-tectonic origin for this lineament; it does warrant additional analysis.

Lineament 10 is a pair of north-south oriented escarpments facing toward each other. The feature is unique because of its abrupt break in slope and because it cuts across the northeast-southwest ‘fabric’ that is common to most of the lineaments. These lineaments are interpreted to delineate margins of a large paleo channel; likely the source for the large outwash plain located at the southern portion of the 5-mile site radius. The lineament is of non-tectonic glaciofluvial origin; it therefore does not warrant additional analysis.

Lineament 12 is an east-west oriented arcuate lineament defined by a north-facing escarpment. The feature has a length of about 0.8 miles, and height of the escarpment is approximately 54 feet. The break in slope appears as though it could be related to Lineament 6, corresponding with a former intermediate glacial moraine. The short length and likely glacial origin indicate lineament 12 does not need additional analysis.

3.1.1.3 Lineament Origins

No lineaments with characteristics consistent with a tectonic origin were observed within the 5-mile site radius. All identified lineaments have characteristics consistent with formation by glacial or glaciofluvial processes. Seismic refection data show continuous, un-faulted Tertiary sediments beneath the most prominent lineament, eliminating a tectonic origin.

3.1.2 Evaluation of the Salamatof Road faults

Geotechnical and environmental studies in the Nikiski area have noted evidence for faulting of the glacial sediments immediately north of the LNG Facilities area. Faults were identified primarily from borehole data and from patterns of groundwater flow. One set of faults, referred to in this report as the Salamatof Road faults, was mapped in a coastal bluff exposure. These are the only surface faults known to have been directly observed. The faults were mapped by hydrogeologist Clay Sullivan of Kent & Sullivan, Inc, in reports to Tesoro (Kent & Sullivan, 1997, 2000 and 2001). Sullivan had been working for Tesoro since the 1990s on site characterization and groundwater contaminant migration issues related to the Tesoro refinery in Nikiski. Fugro geologists interviewed Sullivan in May of 2015. Documentation of the interview is found in Fugro report #04.10140334-2, AKLNG document No. USAL-FG-GRZZZ-00-002015-004.

In a site characterization report prepared for Tesoro, Kent & Sullivan (1997) reported the presence of two faults immediately south of Salamatof Road and west of the Kenai Spur Highway. The faults were mapped in the coastal bluff in 1997 following a 1996 storm that eroded the bluff face and exposed the late Quaternary stratigraphy (Plate 48). The faults are steeply dipping to vertical, trending east-northeast about 1,100 feet apart. The South fault is a single fault, whereas the North fault is composed of a main fault and three nearby smaller faults. The stratigraphic units between the two main faults are displaced downward, defining a graben, and the beds in the down-dropped block are downwarped into a syncline. Stratified sediments of the Killey and the Moosehorn glacial stades are vertically displaced up to 30 feet on either side of each fault.), and deposits of peat and fine sand fill a depression in the center of the syncline. Surface topography roughly mimics the sense of displacement on the faults, showing a smooth swale between the two faults and no discernible fault scarps, although the original topography is partially obscured by grading on the Tesoro property. The filing of the graben and subtle nature of the surface expression suggest that the faulting is not recent.

Kent & Sullivan (1997) traced the two main faults east beneath the Tesoro PIRM area, trending in the east-northeast direction on the basis of borehole data (Plate 48). Cross-sections drawn from borehole data on the Tesoro PIRM property suggest that the beds are tilted and warped into arches, troughs, and monoclines. They noted that the faults constitute a groundwater barrier, and that groundwater head differed 15 to 17 feet on either side of the South fault. Groundwater flow directions also differed on either side of this fault. Kent & Sullivan made no conclusions as to the origin of the faults.

The Salamatof Road faults and are located beyond the north boundary of the LNG facilities area, thus pose no direct surface faulting hazard to the site. However, their presence is noted and the formative mechanism of these faults is evaluated. Four possible origins for these faults were considered:

1. Tectonic faults.
2. Glacial push faults.
3. Kettle subsidence.
4. Lateral spreading failure from strong ground shaking.

The 2015 geophysical program was designed to help evaluate the origin of these faults. Deep seismic reflection data were collected across the west and east projections of the faults to determine whether deep underlying strata are displaced, a requirement for a tectonic fault. Seismic reflection profiles for marine seismic line S-129 (Plate 43), beach line NS-0 (Plate 45) and onshore line NS-2 (Plate 22) show no evidence of displacement of Tertiary strata across this area. Tertiary reflectors can be followed continuously. Based on the seismic reflection data, the Salamatof Road faults are not tectonic faults because they do not displace the underlying Tertiary strata.

The faults are unlikely to be glacial push faults, as these are typically thrust faults that form at the front of an advancing glacier; the Salamatof Road faults are extensional faults.

Two other possible formative mechanisms remain, kettle subsidence, and a lateral spread failure from strong ground shaking. Neither of these formative processes can be ruled out on the basis of available evidence. The faults are located adjacent to a lowland interpreted to be a kettle. Lateral spreading toward the kettle could have occurred either during initial kettle formation, or afterwards when triggered by strong ground shaking.

Field relationships suggest the faulting likely occurred a short time after deposition of the displaced strata, perhaps in the late Pleistocene or early Holocene. As described above, the graben between the faults is filled with sediment including peat and diatomaceous earth (Plate 48), suggesting a wetland or lacustrine environment once occupied the depression. The surface expression of the faulting has been smoothed over by the filling of the graben, suggesting a relatively long time interval for the sediment to accumulate.

The presence of the Salamatof Road faults is judged to pose no ground motion hazard to the site. The faults are not tectonic in nature, thus pose no ground motion hazard. The faults affect only Quaternary age deposits. Field evidence suggests they are not recent features, and may have occurred in the latest Pleistocene as the ground moved laterally toward the kettle depression, either as a result of the loss of the ice, or from strong ground shaking. Obtaining geochronologic data on a sample of the interbedded peat within the graben fill could provide confirmation of the age of most recent fault movement.

3.1.3 Surface fault screening of Onshore LNG Facilities Area

Two methods were used to screen for surface faulting of the upper 200 feet of sediments through the LNG facilities area. First, a field precision survey of the elevations of stratigraphic markers in the coastal bluff was conducted. Second, shallow geophysical survey was conducted along approximately 70,000 linear feet of lines. This survey allowed the mapping of planar beds as imaged in the geophysical profiles.

3.1.3.1 Field Elevation Survey of Coastal Bluff Stratigraphic Contacts

Our approach to assessing the presence or absence of surface faulting through field mapping was to carefully document the location and geometry of stratigraphic contacts exposed in the coastal bluff face. Geologic deposits consist of the sandy and gravelly Killey age glacial outwash deposits overlying silty to bouldery late Moosehorn subestuarine fan-rainout deposits. The contact between the two units is generally marked by seeps and orange discoloration at the top of the late Moosehorn deposits due their lower permeability. The Moosehorn deposits act as an aquitard for perched iron-oxide-rich groundwater (Plate 36).

Mapping of the coastal bluff focused on describing the Killey-Moosehorn deposit contact and surveying precise points on the contact wherever it was exposed. Specific points along geologic contacts exposed in the bluff face were surveyed using a Trimble R10 RTK base and receiver with Trimble TSC3 controllers coupled with a TruPulse 360ºR laser range finder. The survey equipment was operated by a professional land surveyor from McLane. Detailed procedures are provided in the geologic mapping report (Fugro report no. 04-10140334-2, AKLNG document No. USAL-FG-GRZZZ-00-002015-004). In addition to the contact, other stratigraphic markers and locations of seeps and springs were surveyed.

Approximately 9,300 feet of coastal bluff were surveyed in detail in the LNG facilities area. Of this length, approximately two thirds were covered with colluvium and vegetation at the time of the survey such that no exposure of the underlying stratigraphy could be seen. The presence or absence of surface faulting could not be evaluated in these areas. Plate 49, 50, & 51 is a profile view of the surveyed contacts along the traverse.

Approximately 3,000 feet of the 9,300 feet of coastal bluff surveyed exhibited “reasonably continuous” exposure. To be considered continuous, individual exposures of the contact were either visibly continuous, or concealed for no more than 120 feet between exposures. The two longest reasonably continuous exposures measured 1,210 ft. and 1,110 ft., respectively.

Areas of continuous exposure within the LNG facilities area show the Killey/Moosehorn contact to possess two types of geometry: (1) planar and horizontal (elevations from 45 to 60 ft.), and (2) gently warped (elevations as low as 35 ft.). No positive evidence for surface faulting was observed in the portions of the coastal bluff where stratigraphic contacts were clearly exposed. Continuity of exposure also provides positive evidence for no surface faulting along the mapped transects.

3.1.3.2 IMASW Screening for Surface Faults

Shallow seismic survey data were collected within the onshore LNG facilities area in 2014 and 2015 (Plate 52), and were processed using the Interferometric Multi-channel Analysis of Surface Waves (IMASW) method. A total of fourteen geophysical lines were processed using the IMASW method to develop 2D tomography profiles. A full discussion of the IMASW processing and results can be found in the geophysical survey report (Fugro report No. 04.10140334-7, AKLNG document No. USAL-FG-GRZZZ-00-002015-005). Summary portions of that report are included below.

The IMASW method provides shear wave (Vs) tomography for depths up to 200 feet. This depth range of resolution is useful for recognizing and evaluating the presence or absence of faulting in shallow sediments. Abrupt shear wave velocity(Vs) contrasts observed in the profiles correlate well with bedding, such that individual continuous beds could be mapped on the Vs profiles. Only those beds having a strong contrast in Vs are detected. The IMASW profiles show the shear wave velocities of the subsurface materials, and illustrate the continuous or discontinuous nature of the strata.

Nine shallow seismic lines collected in 2015 were processed using the IMASW method, and five of the 2014 shallow refraction seismic lines were reprocessed for 2D IMASW profiles (Plate 52). The 2015 lines were processed for 2D IMASW by estimating 1D Vs-depth at every receiver position except along the 9 receivers at each end of the line segments. The 2015 seismic lines used a 1-m (3.3-ft) receiver spacing except for the northern segment of line NS-5 which used a 4-ft receiver spacing. The 2014 data had been collected with a 10-ft receiver spacing, approximately three times wider than the 1 m to 4 ft spacing used in 2015. As a result, the 2014 data exhibit somewhat lower resolution relative to the 2015 data. To ensure the highest-possible resolution of glacial stratigraphic structure, the IMASW processing parameters were optimized to image Vs in the 10- to 120-ft. depth interval. Consequently, details of Vs variations in the top 10 feet are generally not resolved in the 2D Vs-elevation profiles. An estimate of topsoil thickness was made by assigning materials having a Vs of 800 fps or less to the topsoil.

The 2D IMASW data shows planar features, such as sedimentary bedding, where rapid increases in Vs take place over short vertical distances, indicating a planar impedance contrast. Comparison with borehole data show these features correlate reasonably well with the tops of fine-grained beds. The planar impedance contrasts within each 2D IMASW profile were mapped to evaluate the continuity of the bedding. Two line types are shown on the interpreted IMASW plates: solid lines indicate higher confidence, and dashed lines indicate lower confidence. Solid lines delineate planar impedance contrasts that have a velocity increase of at least 200 feet per second (fps) over a vertical distance of less than approximately 5 feet and extend for a minimum of 30 linear feet. The dashed lines extend from the higher confidence solid lines to connect short line segments or to extend along planar features that do not meet the higher confidence criterion. The dashed lines extend along the planar feature until the feature is no longer traceable within approximately 50 to 75 feet, or until there is more than one planar feature that could match up with the delineated feature. It should be noted that additional planar features are recognizable in the data, but are not delineated as they do not meet the aforementioned criteria.

Planar impedance contrasts were identified within each of the IMASW profiles. A good example showing an un-interpreted and interpreted IMASW profile is presented on Plate 53 and Plate 54, and additional profiles are in the geophysical survey report (Fugro report No. 04.10140334-7, AKLNG document No. USAL-FG-GRZZZ-00-002015-005). The NS-1 north IMASW profile shows an abrupt increase in shear wave velocity at approximate 75 feet elevation; this velocity increase is coincident with the contact between the Killey and Moosehorn geologic units. As shown in this profile and others, the Killey-Moosehorn contact can be characterized by one to several planar impedance contrasts at approximate elevation 50 feet (plus or minus 30 feet). Each planar impedance contrast within this zone is presumed to represent a dense fine-grained bed near the top of the Moosehorn deposits or base of the Killey deposits. No single planar impedance contrast within any of the profiles could be traced laterally across the entire profile length; suggesting that the contact is transitional and best modeled as a zone of interfingering beds within a zone rather than a single discrete planar surface.

To provide an overview of how individual profiles compare with each other and the landscape, two summary maps are presented compiling all the east-west oriented IMASW profiles (Plate 55); and all the north-south oriented profiles (Plate 56). The summary figures illustrate how the individual profiles compare to adjacent profiles, and illustrate the correlation between surface morphology and the IMASW tomography.

Within the IMASW tomography profiles, higher velocities are indicated with warmer colors, and lower velocity materials indicated by cooler colors. The contact between the Killey and Moosehorn is generally observed to be at the transition between cooler and warmer colors (approximately 1200 fps) but this does not appear to always be the case. There are areas within each profile where the lower velocity materials appear to extend to the bottom of the profile. These zones of low velocity may be the result of poor data quality in some cases; but may represent real material properties in others. The top of the Moosehorn deposits may be locally weathered, or may have been eroded by streams prior to the deposition of the Killey deposits. Regardless of their origin, laterally extensive impedance contrasts do not appear to extend across these zones.

To further assess the low velocity zones and determine if there was as systematic pattern shared between profiles, areas of continuous bedding were compiled for each profile. The extent within each profile where at least one continuous bed was recognizable was determined. The extent from each profile was then compiled into a summary map on Plate 57. The compilation map highlights the portion of each profile where continuous bedding is absent (indicated by orange areas of each profile). The profiles generally have continuous horizontal to sub-horizontal bedding that extend across the majority of the profile lengths, however there are gaps of continuous bedding within each profile. The spatial distribution of gaps throughout the LNG facilities area was evaluated, and no linear patterns emerge that would suggest faulting.

The results of the mapping of the IMASW profiles show that approximately 44,727 feet of the 51,343 feet of survey lines, or 87%, show positive evidence of the lack of faulting. The remaining 13% is indeterminate, without positive evidence to support either the presence of faulting or the lack of faulting.

3.1.4 Assessment of Surface Faulting Hazard

The evaluation of surface faulting within the 5-mile site radius, shows that the hazard at the site is low. The major lines of evidence are summarized below.

Lineament analysis shows no evidence of lineaments or linear scarps consistent with a surface faulting origin. Natural geomorphic features are attributed to glacial, fluvial, or lacustrine processes, or to erosion and bluff retreat along the coast. Prominent northeast-trending lineaments are the result of glacial processes. They are aligned parallel to the margin of the Killey stade glacier, and mark the gradual retreat of this glacier across the Kenai Lowland.

The Bernice Lake lineament, the strongest and most linear of the northeast-trending lineaments, is also shown to be related to glacial processes rather than faulting. Deep seismic reflection data show no displacement of the underlying Tertiary deposits, providing positive evidence for no faulting. Shallow seismic reflection in the marine area show the projection of the lineament to correspond with a Quaternary unconformity, supporting a glacial origin for this lineament.

The Salamatof Road faults, surface faults mapped in 1997 immediately north of the site, are not tectonic faults based on their absence on deep seismic reflection profiles. They are attributed to either failure of a kettle margin during melting of the ice, or to lateral spread failure from strong ground shaking. Field relationships suggest these faults may be late Pleistocene in age.

Screening of the LNG facilities area using the IMASW shallow seismic method shows that 87% of the area is underlain by planar bedded, continuous strata, with no discernible displacement. The strata do exhibit some local gentle warping, which may be attributed to glacial processes. Portions of the IMASW profiles where planar bedding is not observed may be explained by erosion or weathering of the top of the Moosehorn unit, or low data quality.

As described in section 2.2.1.2, deep seismic reflection survey data show continuous unbroken planar reflectors in the underlying Tertiary strata. This constitutes positive evidence of the absence of tectonic faulting within the LNG facilities area.

3.2 Onshore Folding and Tilting Hazard

Folding or tilting may accompany major seismic events, including very large megathrust earthquakes, as well as smaller earthquakes on crustal faults, such as the Cook Inlet blind-thrust faults. Tectonic tilting at the site, therefore, is a potential geologic hazard. To evaluate the hazard to the LNG facilities from tectonic tilting, we begin by comparing the potential magnitude of tectonic tilting from these two primary tectonic sources to the magnitude of tilting acceptable under FERC guidelines (2007). We then present a geomorphic analysis of two landscape features-- paleolake shorelines and outwash plains--that may have the potential to record evidence of tectonic tilting.

As described in Sub-Section 1.3.1, the Aleutian subduction zone, or *megathrust*, which dips beneath the site, has historically generated very large earthquakes (Plate 2). The 1964 **M** 9.2 Great Alaskan earthquake caused extensive damage and surface deformation throughout the Cook Inlet, including 0.9 feet of subsidence recorded at a standard U.S. Coast and Geodetic Survey tide-gage station near Nikiski (Plate 18) (Foster and Karlstrom, 1967). Mapping by Pflaker (1969) shows contours of subsidence and uplift after this event (Plate 19). Subsidence at the site is part of a regional dip toward the southeast on the limb of a synclinal warp located in the hanging wall of the Aleutian megathrust.

At the proposed LNG site, ground tilt resulting from the 1964 earthquake is estimated at 0.0008 degrees east-southeast, based on the contours drawn by Pflaker (1969) (Plate 58). FERC (2007) guidelines (Part 1, Section 7.41) allow a maximum of 0.002 radians (0.1146 degrees) of planar tilt, two orders of magnitude greater than documented tilt from the 1964 earthquake. Assuming no more than one such event would occur in the 50-year lifespan of the plant (justified by the approximately 400 to 960 year return interval of the megathrust earthquake), tilting due to an Aleutian subduction zone event similar to the 1964 earthquake, the maximum ever recorded for the Aleutian subduction zone, does not pose a significant hazard to the site (Table 3.3).

A large earthquake on a Cook Inlet fold could also potentially cause tilting at the site. The site is located on the distal eastern limb of the Middle Ground Shoal Anticline. Co-seismic growth of this fold could result in gentle tilting of the site toward the east (Plate 18). The largest historical earthquake associated with the Cook Inlet faults was a Ms 6.9 earthquake in 1933 (Haeussler et al., 2000). Sufficient data do not exist to estimate the degree of tilt expected from an earthquake event on any of the Cook Inlet folds. However, based on the current gentle dip of the Tertiary strata beneath the site (Plate 16), lack of measureable tilting of the Quaternary strata, and relatively small historical earthquake magnitude, we qualitatively judge that tilt in an event on the Middle Ground Shoal Anticline will be no greater than tilt from the 1964 **M** 9.2 earthquake.

The potential for non-tectonic tilting due to differential settlement, liquefaction, or other failure of the geologic deposits is discussed in Section 3.3.2 (ground shaking effects). An evaluation of geotechnical site conditions identifying areas susceptible to these type failures, is presented in the integrated site characterization and engineering reports for this project (Fugro reports. 04.10140334-13 (AKLNG document no. USAL-FG-GRZZZ-00-002015-003), 04.10140334-14 (USAL-FG-GRZZZ-00-002015-009), and 04.10140334-15 (AKLNG document no. USAL-FG-GRZZZ-00-002015-0012).

Table 3.3: Relative Magnitudes of Tectonic Tilting

Description	Magnitude of Tilting
FERC (2007) guidelines for LNG tanks	Tilting tolerance = 0.002 radians (0.1146 degrees)
1964 **M** 9.2 Great Alaskan earthquake, on the Aleutian megathrust	Documented tectonic tilting at the site from this event = 0.0008 degrees
Hypothetical Cook-Inlet-style folding event at the site	Predicted max tilting at the site in an event is unknown, but likely $\leq$ than the 1964 earthquake

3.2.1 Paleoshoreline Analysis

The paleoshoreline analysis is the first of three analyses that evaluate the potential usefulness of geomorphic and stratigraphic features for assessing the presence and magnitude of tectonic deformation. Following this section, are Sections 3.1.2.3 and 3.1.2.4, which evaluate the surface of the glacial outwash plain and the contact between the Killey and Moosehorn stade deposits.

The banks of the many kettle lakes in the Nikiski area are characterized by shoreline-parallel benches and scarps (Plate 59). These benches sit 5 to 50 feet above the present lake levels. Some clearly mark earlier lakes levels and constitute paleoshoreline features, but others appear to have a different origin. Below, we review the geologic history of the lakes and origins for the shoreline benches and scarps, and then evaluate the potential of the paleoshoreline features to be used as horizontal strain gauges for the assessment of past tectonic deformation.

3.2.1.1 Origin of the Shoreline Benches

As described in Section 2.2, the kettle lakes on the Kenai Peninsula formed during the late Wisconsin-age Killey glacial stade (Reger et al, 2007). As the ice sheet covering the peninsula retreated northward at the end of the Killey stade, large blocks of ice calved off the front of the glacier. These ice blocks were subsequently covered with glacial outwash emanating from the front of the retreating glacier. When the ice blocks melted, the overlying veneer of outwash sank to form the depressions that now hold the kettle lakes (Reger et al, 2007). Lake levels since that time have reflected the balance among precipitation, infiltration, and evaporation, and generally coincide with the groundwater table.

Three different processes are envisioned for the formation of the shoreline benches, each resulting in a slightly different geomorphology (Plate 60). The benches may have formed as: (1) wave-cut shorelines that date from a time of higher lake levels, (2) ice-shoved ramparts, also associated with times of higher lake levels, or (3) slump features formed either by subsidence during the melting of the ice blocks, or from later earthquake ground shaking. *Wave-cut shorelines* form along a level plane at or slightly above the water line, and consist of a wave-cut platform or bench at the foot of a wave-cut scarp. The larger the lake the more distinct the shorelines may be due to the greater wave energy generated by longer fetch of the wind. The shoreline angle, or line that marks the intersection of the scarp and the platform, is level and at an equal elevation. *Ice-shoved ramparts* form when slabs of winter ice on the lake are blown shoreward by the wind (Plate 61). The leading edge of the ice bulldozes the sand and gravel into low ridges that parallel the shoreline and may add a bump to a wave-cut bench (Dionne, 1992) *Slump scarps* are characterized by a linear to arcuate scarp above a sloping, hummocky, or back-tilted bench. The base of the scarp need not be level, and typically slopes upward or downward following the slide plane.

To be useful as a strain gauge and therefore recorder of past tectonic deformation, a geomorphic feature must have a well-constrained original geometry. Of the features listed above, only wave-cut shorelines meet that criterion. Formed at lake level, the *shoreline angle*, or intersection of the wave-cut bench and the wave-cut scarp, would have been consistently level along the entire perimeter of the water body. If tectonic deformation took place after lake levels dropped, the shoreline angle would deform accordingly and this deformation could potentially be detected in detailed topographic data, such as the available LiDAR data.

To evaluate whether kettle lake shoreline angles are present, distinguishable from other features, and extensive enough to be mapped and analyzed to detect deformation, we conducted a pilot study of the shoreline of Island Lake. Island Lake is one of the larger lakes in the 5-mile radius site area (Plate 17 and Chart 1). With a longer fetch, waves in this lake would have had greater energy than waves in smaller lakes, and thus greater potential to erode scarps and benches.

3.2.1.2 Methodology and Map Results

The paleoshoreline analysis is based on the interpretation of LiDAR elevation data and digital imagery of the Island Lake area (USGS, 2008; KPB, and 2012). We created a base map in ArcGIS that displayed the LiDAR elevation data as a hillshade map, slope map, digital elevation model, and a topographic contour map. From the slope map, we mapped a line following the base of any scarp that met the following criteria: (1) a minimum of 200-feet long, (2) approximately parallel to the margin of a lake or depression, and (3) within 1,000 feet of a lake shoreline. The resulting map of shoreline features is shown as Plate 62.

Scarps were then classified as follows (Plate 62):

- *Paleoshoreline at 118 feet*: A set of linear scarps with adjacent benches having a relatively level shoreline angle at an elevation of 118 +/- 3 feet. This set of scarps closely parallels the modern wave-cut scarp and is found along most of the lake perimeter, including the island.
- *Present shoreline*: A continuous scarp adjacent to the present shoreline. The base of the scarp is at an elevation of 108 +/- 3 feet, slightly above the lake level of 105 feet recorded at the time of the 2008 LiDAR data collection.

- *Other scarp:* Scarp which approximately follows the lake shoreline, but varies in elevation and slope, and may be arcuate or branched in form. Most scarps in this category are interpreted as slump features. Wave erosion may have modified these scarps, but not enough to establish a level bench at a consistent elevation. The bench at the base of the scarp may be gently sloped, hummocky, or back-tilted.

3.2.1.3 Paleoshorelines for the Assessment of Tectonic Deformation

Paleoshorelines can provide a robust strain marker for the assessment of tectonic deformation given certain conditions. The shoreline must be clearly mapped based on its topographic expression, and must be a unique feature that is not confused with other similar features. It must also be present over an area commensurate with the scale of the possible deformation. The mapping uncertainty must be significantly less than the magnitude of the tectonic deformation being detected, given the age of the feature and possible rates of deformation.

These criteria are not met by the Island Lake setting. Although a clear paleoshoreline occurs in the Island Lake area, it is not likely that its analysis will yield meaningful results for the assessment of tectonic deformation for three main reasons.

First, the mapped uncertainty in the paleoshoreline of +/- 3 feet elevation may exceed the magnitude of the expected deformation. The latter can be estimated given the tectonic setting and likely age of the shoreline. The 1964 **M** 9.2 Good Friday earthquake was the largest historical earthquake in the region, and caused measureable tilting on the Kenai Peninsula (Plate 18). Post-earthquake mapping of the Cook Inlet show that the Nikiski area tilted to the southeast approximately 0.0008 degrees (Plafker, 1969) (Plate 19). Paleoseismic investigations indicate seven to ten great earthquakes took place on the Prince William Sound segment of the Aleutian megathrust in the last 4,000 to 6,000 years, an approximate recurrence interval of 400 to 960 years. If tilting similar to that documented from the 1964 earthquake took place with each event, tilting would amount to a maximum of 0.0309 to 0.00802 degrees over the past 10,000 to 17,000 years, respectively. The minimum age of 10,000 years is based on radiocarbon dating by Reger et al, (2007) and the maximum age of 17,000 years is based on the end of the Killey glaciation, also dated by Reger et al. (2007) The lake is about 3,400 feet across in the NW-SE direction, perpendicular to the direction of tilting. A tilt of 0.0309 degrees would amount to a difference of 0.5 to 2 feet in the shoreline elevation on either side of the lake, with the southeastern side down. This difference is not detectable given that the shoreline elevation is mapped with an uncertainty of plus or minus 3 feet.

Second, wave-cut shorelines may be confused with slump scarps, leading to larger uncertainties in mapping. Some portions of the paleoshoreline may consist of slump scarps that happen to fall within the same elevation range. At Island Lake (Plate 62), the rounded peninsula southeast of the island is an example of a complex of slump scarps (green lines) that has been modified by wave erosion (red lines).

Third, modification of the shoreline angle by colluviation, erosion, and ice-shoved ramparts may have taken place. This post-formation modification of the shoreline scarp obscures the shoreline angle and decreases the precision and confidence with which the paleoshoreline can be mapped.

To document the consistency in elevation of the shorelines at Island Lake, and quantitatively compare paleo-shoreline elevations across the expected axis of tilting to determine if measureable tilt is present, elevations of the mapped shorelines were tabulated at regular intervals along the shoreline, and plotted on Plate 63. The upper panel shows the distribution of elevations for the present shoreline and the paleoshoreline. The lower panel divides the shoreline into segments based on its location relative to arbitrary zones oriented parallel to a northeast axis of tilting. The plot of present shoreline elevations shows no significant difference in the elevations between zones A B, and C, as expected. The plot of paleoshorelines shows the northwest shoreline segment, zone A, to be one to three feet lower than the central (zone B) or southeastern (zone C) segments. This difference is within the mapping uncertainty of ± 3 feet, therefore no tilting could be detected.

In sum, the adequacy of paleoshorelines bordering the kettle lakes to act as strain markers for the assessment of tectonic deformation is limited. Limitations include the accuracy by which the shorelines can be identified given the presence of similar-appearing slump scarps and post-formation modification of the shorelines, the precision with which the shoreline angle can be mapped from the LiDAR data, and the small elevation differences across the lake that may be expected from tectonic tilting.

3.2.2 Outwash Plain Geomorphic Analysis

Two outwash plains of the Killey stade glaciations are clearly visible in LiDAR elevation data within the 5-mile site radius and extending south toward Kenai. They appear as broad fan-shaped surfaces, gently sloping to the south, with arcuate concentric contours that converge northward toward their paleo-source channels (Plate 64). The ground surface is characterized by a braid plain micromorphology typical of outwash plains, consisting of multiple channels that divide and re-join, braid bars, point bars, and shallow overlapping channels (Plate 65). Field investigations in the southeastern portion of the 5-mile radius confirm the subtle morphology of the braid plain surfaces identified in the LiDAR, confirming the interpretation of a broad braid plain extending southward and eastward from the site. Orientations of the point bars and shallow overlapping channels indicate outwash emanating from the glaciers flowed northwest to southeast (Plate 64).

To the north, upslope and closer to the ice front, the plains are typically pitted with kettle holes that now contain lakes and fens. Swaths of kettle holes outboard of the almost-buried recessional moraines impart a prominent northeast-trending fabric to the landscape. Fluvial channel features of the outwash plain are truncated at the margins of the kettle holes, indicating that ice blocks calving off the front of the glacier were first buried by outwash, then melted to form the kettle holes. The overlying outwash then subsided or collapsed into the holes.

The outwash plains provide a geomorphic datum of known geometry that may have the potential to assess regional tectonic deformation within the 5-mile site radius. A reconnaissance level assessment was undertaken to evaluate the suitability of these outwash plains as strain markers to detect regional tectonic tilting and deformation. In aggregate, the fluvial channels that traverse the outwash plains have a well-constrained geometry to potentially detect regional tilting and tectonic deformation. Fluvial channels in an alluvial fan setting have been shown to have a smooth, gently concave longitudinal profile (Bull, 1964). A significant deviation from this shape could indicate tectonic warping or tilting. An abrupt vertical step in the profile over short horizontal distances could indicate surface faulting.

The effect of tectonic deformation on the longitudinal profile does depend on the relative orientation of the deformation. Deformation oriented perpendicular to the channel profile would be most clearly expressed. Conversely, deformation parallel to the channel profile may not be expressed or may be minimally expressed. Vertical deformation is better expressed in fluvial profiles as compared to horizontal (i.e., strike-slip) deformation. Strike-slip deformation may be recorded as systematic lateral shifts in the drainages plan form orientation, should the deformation rate outpace the rate of fluvial erosion.

The orientation of regional deformation of the Kenai Peninsula measured from the 1964 **M** 9.2 Great Alaskan earthquake, and the orientations of mapped fault-cored folds were compared with the channel orientations to assess the viability of the braided outwash plains as a strain marker.

Post-earthquake mapping of the Cook Inlet region indicates that the Nikiski area tilted to the east-southeast approximately 0.002 degrees (Plafker, 1969) (Plate 58). The south to southwest orientations of the fluvial channels within the outwash plain are therefore almost parallel to the axis of tilting. The parallel to oblique intersection of the fluvial channels with the axis of regional tilting is unfavorable to record regional surface deformation from a 1964 type event. Therefore, regional tilting associated with events like the 1964 Great Alaskan earthquake are not expected to be measurable in longitudinal profiles of channels on the outwash plains (Plate 64).

Similarly, the orientations of the fluvial channels relative to the mapped fault-cored folds suggest that along-channel profiles would not record measurable surface deformation as a result of an event generated from one of the structures (Plate 64). The axes of the folds are oriented north to northeast, again almost parallel to the orientation of the stream channels. Although the braid plains are extensive and well-expressed geomorphically within the 5-mile site radius, the assessment suggests they are not likely to record measurable tectonic tilting and deformation associated with either a 1964-type seismic event, or an event generated from a nearby subsurface fault-cored fold.

As expected, representative longitudinal profiles of the two outwash plains in the 5-mile site radius exhibit normal gently concave upward profiles with no demonstrable irregularities that would suggest tectonic deformation (Plate 64). Based on the parallel to oblique orientation of the axes of deformation to the channels, this result provides little information on the magnitude of possible tectonic deformation.

3.2.3 Analysis of Stratigraphic Contacts

Stratigraphic contacts may also provide a known datum by which tectonic deformation can be assessed. The original geometry of the contact must be known in order for deviations to be detected; an ideal stratigraphic contact would be planar and horizontal (e.g., a lake bed). If the stratigraphic contact departs from this ideal geometry, the assessment of tectonically-related deformation will correspondingly decrease in reliability.

As exposed in the coastal bluffs adjacent to the Nikiski LNG site, the contact between the Moosehorn and Killey stade sediments appears generally planar and horizontal (Plate 36).The Yelllowish-brown Killey sands and gravels sit directly on gray compact silt of the Moosehorn deposits. However, exposures of the contact on the bluff face are discontinuously covered by colluvium. Therefore, the contact is not continuously exposed.

Analysis of 2015 IMASW geophysical data shows the contact to occur at a relatively consistent elevation throughout the LNG facilities area (Plates 55 and 56). Tectonic tilting of these late Pleistocene is not detectable in these data.

3.2.4 Assessment of Tilting and Folding Hazard

The potential for tectonic folding that could cause ground tilting in excess of FERC (2007) guidelines is judged to be very low. Tilting documented from the 1964 Great Alaskan earthquake was an order of magnitude lower than the guidelines allow. Three types of geologic and geomorphic features (paleoshorelines, outwash plains, and stratigraphic contacts) were assessed for their potential to record long-term tectonic deformation. As a group, these features exhibit no measureable tectonic tilting.

3.3 Effects of Strong Ground Motions

Strong ground shaking associated with large earthquakes can cause ground deformation, including settlement, liquefaction, cracking, and slope failure, particularly in weak or unconsolidated sediments. The 1964 **M** 9.2 earthquake resulted in extensive damage throughout Cook Inlet and the Kenai Peninsula, with documented ground failure within the 5-mile radius of the site (Plates 11 and 58). The occurrence of the earthquake in recent history, and the geologic data collected in the immediate aftermath of the earthquake, provide a valuable and relevant analog for potential hazards at the site relative to future strong ground shaking.

3.3.1 Ground Breakage and Liquefaction

Within the 5-mile radius of the site, two locations with ground cracks and pressure ridges were observed in muskeg deposits (Plate 11). In addition, published literature documented a zone of extensive ground breakage proximal to the site (Plate 11) (Foster and Karlstrom, 1967). Features observed within the zone included ground cracking, and ground cracking with associated eruptions of sand and water. Sand and water eruptions associated with ground cracking suggest sub-surface sediments liquefied as a result of strong ground shaking during the 1964 event, and were subsequently ejected through open fissures in the ground. Field observations (Foster and Karlstrom, 1967) provide estimates of the magnitude of surface deformation in the region, documenting a ground crack with up to three feet of displacement, interpreted by this study to have resulted from the liquefaction of sub-surface sediments (Plate 66). The surface deformation feature was observed approximately 15 miles to the east of the site (Plate 11).

No liquefaction features were documented within the 5-mile radius, but limited access, and the presence of dense vegetation, as well as a thick root mat (Haeussler et al., 2002) may have prevented observations of such features. Multiple liquefaction features were observed in two locations about 15 miles east of the site within glacial deposits similar to those within the 5-mile site radius. Photographs from one of these sites are presented in Plate 66. The occurrence of these features suggests that co-seismic liquefaction poses a potential hazard in the 5-mile radius. The observation of up to approximately three feet of displacement on a ground crack associated with liquefaction features provides an initial estimate for potential magnitude of ground breakage that may be produced by strong ground shaking (Plate 66) (Foster and Karlstrom, 1967).

Landsliding was also documented by Foster and Karlstrom (1967) along the shore of Lake Tustumena on the Kenai Peninsula. These were described as rotational slumps that occurred in delta, beach, and terrace deposits along the lake shoreline. It is possible that slump-like features observed along the shorelines of kettle lakes within the 5-mile site radius may also have a co-seismic origin (Plate 59).

3.3.2 Potential for Future Ground Shaking Effects

Given the seismically active nature of the region, the severity and extensive nature of the ground cracking, liquefaction, deformation and slope failure observed in the Kenai Lowland after the 1964 earthquake, it is likely that future events of this magnitude will cause similar effects. The lack of recorded features in the Nikiski area may be partly the result of lack of road access in 1964. Geotechnical studies underway for the project will assess the potential for liquefaction due to strong ground shaking on a site specific basis (Fugro report 04.10140334-13, AKLNG document no. USAL-FG-GRZZZ-00-002015-003)

3.4 Tsunami Hazard

A deterministic tsunami hazard assessment was conducted for the proposed liquefied natural gas (LNG) site in Nikiski, Alaska. The site is located on the eastern shore of central Cook Inlet (Plate 67), a region which has historically experienced large-magnitude tectonic events and significant tsunami (Lander, 1996). The primary facility and structures will be constructed on a coastal bluff at an elevation of approximately 125 feet above mean sea level (AMSL).

The scope of this analysis is to define a range in wave height for use in the design (e.g. excavation grade) by defining tsunami sources and modeling the wave propagation across the local bathymetry. The analysis includes an assessment of potential tsunamigenic sources and their potential impact on the site.

This document presents the methodology and results from the site-specific tsunami hazard analysis performed by Fugro and consulting tsunami hazard modeling specialists Dr. Roy Walters of Ocean-River Hydrodynamics and Clayton Hiles of Cascadia Coast Research, Ltd. A report submitted by Clayton Hiles and Dr. Walters to Fugro on April 23, 2015 describes the modeling approach, the tsunami sources, and the results of the numerical analysis. Their report is included as Appendix A.

Tsunami sources which could impact Cook Inlet include distal sources such as large-magnitude plate-boundary earthquakes around the Pacific Rim, and proximal sources such as earthquakes occurring on the Aleutian subduction zone, normal or reverse faulting near the site, volcanic flank collapse and submarine landslides. The effects of distal sources outside Alaska that generate “teletsunami,” were not evaluated. Historical records from 1737 to 1996 show that the hazard from teletsunami is minor in Alaska (Lander, 1996). Most have occurred in the western Aleutian Islands, and have not been recorded in south central Alaska. Also not evaluated were near-site faults. Active geologic structures in the Cook Inlet are characterized as fault-cored folds in which little to no surface fault rupture occurs, and the magnitudes of deformation from folding would be insufficient to generate significant tsunami.

For this study, three sources, judged to be the most likely to cause a significant tsunami at the site, were evaluated using a deterministic analysis (see Plate 67). They include:

- A submarine landslide in Cook Inlet,
- The 1964 Great Alaskan Earthquake, and
- Volcanic flank collapse and debris flow at Augustine Volcano.

The submarine landslide and the 1964 event were evaluated using numerical modeling. The Augustine volcano flank collapse scenario was evaluated based on published results from previous studies. The maximum wave height for each scenario was calculated, or estimated in the case of the Augustine volcano scenario, for three locations positioned along the Cook Inlet shoreline directly adjacent to the site (Plate 68). Water elevation as a function of time after the event, and maximum water elevation at these locations are used as a proxy for site-specific evaluation; the exact locations of structures and facilities for the planned LNG site were not available at the time of this analysis.

The tsunami hazard analysis included the following steps:

1. Comprehensive literature review,
2. Compilation of bathymetric and topographic data and creation of a “nested” digital elevation model (DEM),
3. Delineation of tsunami sources and characterization of tsunami source parameters; and
4. Numerical modeling of tsunami propagation and calculation of water elevation as a function of time after the tsunamigenic event at the site.

3.4.1 Bathymetry and Topography

The results of tsunami and hydrodynamic models are very sensitive to the quality, location, and resolution of the topographic and bathymetric data. The model area includes portions of the northern Gulf of Alaska and the southern and central portions of Cook Inlet. This area was represented with a "nested" grid of multi-scale digital elevation models (DEMs) constructed from bathymetric and topographic data primarily from publically available sources. A high-resolution bathymetry dataset collected specifically for this project (Fugro Report No. 04.10140094) was also incorporated into the DEMs. The data were compiled using GIS.

The largest-scale bathymetric data in the model is NOAA's Southern Alaska Coastal Relief Model (~720 meter spatial resolution) (Lim et al., 2011), which was used to provide bathymetric coverage for marine areas outside of the Cook Inlet. Within the Cook Inlet, NOAA's AFSC/RACE Cook Inlet Bathymetry data (50 meter spatial resolution) (Zimmerman and Prescott, 2014) provide the best continuous bathymetric coverage. Swaths of high-resolution multi-beam bathymetry collected as part of this project by Fugro Pelagos were incorporated into the model to provide high-resolution bathymetry for the area immediately offshore from the site. Topography was compiled from three sources. USGS NED 30-m data (USGS, 1999) provide elevations for shoreline and terrain for areas away from the site. Directly surrounding the site, ~2.5 meter resolution LiDAR (USGS, 2008), and ~1 meter LiDAR (FMMG, 2012a) is used to provide ground surface elevation.

The combined topography and bathymetry data were combined into a single terrain model as a triangulated irregular network built inside an ESRI ArcGIS geodatabase. The flexibility and scalability of the terrain model allows for the input of several different data sources that all share the same coordinate system. The terrain can be interrogated at any user-defined scale for raster (grid) bathymetric/topographic surface development using linear or natural neighbor interpolation methods, as well as at any requested cell resolution.

Data were selected for import into the model based on the extent of coverage and the density and accuracy of coverage. This selection process resulted in the creation of non-overlapping data selection areas by data source. All data were compiled into a terrain model in the project geodatabase. The data sources were converted, as necessary, to points in the project state plane coordinate system (AK State Plane Zone 4 NAD 1983/NSRS2007), with elevation values for input into the terrain model. Other data, such as the SRTM shoreline, were incorporated into the terrain as breaklines. This forces the model to incorporate the elevations along the entire extent of these lines.

For the Nikiski LNG tsunami hazard analysis terrain model, the best results for the size of the model area were achieved using a natural neighbors interpolation method. The interpolation method is well suited for data sources that have an irregular spatial distribution, which is characteristic of the data outside of the multibeam gridded data. The natural neighbors interpolation of an elevation value at any given point is weighted according to the Voronoi polygons of the source data points around it. Once the terrain was completed, we used the natural neighbors interpolation to export the triangulated surface to a raster grid at 50 m resolution, then converted from State Plane to geographic coordinates on the WGS84 datum for subsequent input to the modeling software.

3.4.2 Tsunami Sources

Three tsunami sources (Plate 67) were evaluated in this analysis: (1) a volcanic flank collapse of Augustine Volcano (Beget et al., 2008; Waythomas and Waitt, 1998; Waythomas, 2000), (2) a submarine landslide within Cook Inlet, and (3) the 1964 Great Alaskan Earthquake (Plafkar, 1969 and Johnson, J.M., et al., 1996).

The Augustine volcano is a stratovolcano island located in the southwestern Cook Inlet (Plate 67). The volcano has erupted explosively at least six times since the early 1800s (Waythomas and Waitt, 1998). In the last 2,000 years, at least 12-14 debris avalanches from Augustine have entered Cook Inlet, most recently in 1883 a debris avalanche on Augustine entered Cook Inlet and caused a tsunami (Waythomas et al., 2006). Historical accounts from English Bay (about 50 miles to the east) report that 20- to 30-foot (6- to 9-meter) waves were observed (Waythomas et al., 2006). Beget et al. (2008) provide evidence for multiple prehistoric debris avalanches and tsunami (450 and 1,600 years ago) based on correlations between volcanic eruptions, paleotsunami deposits, and cultural data. Through the comprehensive literature review portion of this analysis, six published reports (Kienle et al., 1987; Kienle et al., 1996; Waythomas, 2000; Waythomas and Waitt, 1998; Beget and Kowalik, 2006; Waythomas et al., 2006) were identified that modeled tsunami generated by Augustine volcano debris flows. None of the models provide detailed impact results for the Nikiski project site, and in fact the northern boundary for all of these models is located to the south of the site. However, the models are all in agreement that tsunami waves are attenuated to wave heights of about 1-meter or less during passage from Augustine into the central portion of the Cook Inlet. Because this scenario has already been modeled through numerical analysis in at least six published studies, it was not modeled during this analysis. Instead, the results from the preceding studies were analyzed and applied to this study. Our analysis indicates that maximum tsunami heights at the site from the Augustine source are likely to be in the 3- to 16-foot (1- to 5-meter) elevation range for highest astronomical tide conditions.

The second tsunami source considered in this analysis is a hypothetical submarine landslide scenario within the Cook Inlet. NOAA bathymetric data for Cook Inlet (Zimmerman and Prescott, 2014) depicts over-steepened slopes, and geomorphic expression indicative of prior submarine slope failure (Plate 67, and Plate A-16 in Appendix A). Submarine slopes can fail as a result of being over-steepened by scour from submarine currents, sediment loading, and tectonic shaking among other causes. The 1964 Great Alaskan Earthquake triggered at least 20 local submarine landslides that caused tsunamis, in addition to a major tectonic tsunami (Sokolowski, 2004). A deep submarine channel exists along the central axis of Cook Inlet about 7 km northwest of the site at the constriction between the West and East Foreland (Plate 67, and Plate A-16 in Appendix A). Along the western margin of the channel, a 3.3 mile long by ~0.6 mile wide east-facing segment of submarine slope was selected as the modeled landslide mass. The overall size of the modeled landslide mass is estimated as ~.03 mi^3 (0.12 km^3). The hypothetical submarine landslide was identified as an area with over-steepened landslide-prone slopes based on a geomorphic assessment of the NOAA bathymetric data (Zimmerman and Prescott, 2014). This scenario presents a plausible and relatively large event compared with other observed submarine landslide deposits in the area, which are on the order of 1/2 to ¾ of the areal size of the modeled mass. For this analysis, the entire landslide mass was modeled as three separate scenarios of slope failure: failure of the northern segment (~1/3 of the entire mass), failure of the southern segment (~2/3 of the entire mass), and failure of the entire mass (Appendix A).

The 1964 Great Alaskan Earthquake is the defining tsunamigenic event for the Cook Inlet region. This tsunami source was simulated to provide model validation. Fault rupture parameters for the 1964 event were applied from Ichinose et al. (2007). However, initial tests of these parameters produced results that poorly reproduced actual tsunami observations from the 1964 event at Yakutat, Seward, and Kodiak, Alaska. Three other models (Holdahl and Sauber, 1994; Johnson, J.M., et al., 1996; and Suito and Freymuller, 2009) were evaluated for accuracy with respect to observed wave heights from 1964. The Johnson, J.M., et al. (1996) model was chosen for the simulation because results best represented tsunami wave heights and arrival times observed in 1964 at Yakutat, Seward, and Kodiak, Alaska. A splay fault was added to the model to better match tsunami wave arrival times and the observed subsidence at Seward.

3.4.3 Excluded Sources

The scope of this project called for the above three tsunami source types to be evaluated in this analysis. To confirm that these sources were most likely to produce the largest tsunami at the site, we briefly examined other sources. These sources included: coseismic uplift along the Middle Ground Shoal and Granite Point fold in Cook Inlet (Haeusler et al., 2000), alternative submarine landslides, and flank collapse of Redoubt volcano (Beget and Nye, 1994; and Waythomas and Waitt, 1998).

The Middle Ground Shoal and Granite Point fold is a fault-cored anticline underlying the Cook Inlet. The blind fault controlling the structure is a Quaternary-active fault, with an estimated slip rate ranging from 0.39 to 2.72 mm/yr, and is included in the PSHA portion of this investigation (Haeussler et al., 2000; Koehler, 2012; Fugro, Report No. 04.10140334-6). Because associated coseismic uplift would likely be broad-scale (over several miles), the generation of large tsunami is less likely to occur. Thus, the source does not present greater hazard to the site than the three selected for numerical analysis.

Alternative submarine landslide scenarios were considered during geomorphic analysis of the 50-m NOAA bathymetric data. Some alternatives were located closer to the Nikiski site, however they were smaller in volume than the modeled landslide and either directed away from or highly oblique to the site. The modeled submarine landslide is significantly larger and directed towards the site. Without modeling the alternative landslides it cannot be concluded with certainty whether these more proximal slides would produce a higher wave despite smaller volumes. However, the magnitude of the increase is unlikely to be significant enough to increase the hazard at the site.

Redoubt volcano is a large stratovolcano located approximately 22 miles to the west of the central Cook Inlet. Since 1788, this volcano has erupted at least six times (Waythomas and Waitt, 1998). Beget et al. (2008) tentatively correlate 3,600 year old tsunami deposits found near Homer to a southward directed summit collapse of the volcano. Additionally, 10,000 to 13,000 years ago a very large debris avalanche from Redoubt volcano traveled down Redoubt Creek (Beget and Nye, 1994; and Waythomas and Waitt, 1998). Waythomas and Waitt (1998) suggest that the debris may have never entered Cook Inlet and, if it did, it may not have displaced enough water to cause a significant tsunami due to the shallow depth offshore. In their hazard assessment of Redoubt volcano, Waythomas and Waitt (1998) rank the overall tsunami hazard posed by the volcano as minor because of the low probability of a large debris flow reaching Cook Inlet. Additionally, Waythomas and Waitt (1998) note that offshore water depths are shallow and Kalgin Island stands as a barrier to the opposite shore of the Cook Inlet if a Redoubt debris avalanche does cause a tsunami.

3.4.4 Numerical Model

For this analysis, the 1964 Great Alaskan Earthquake and a submarine landslide in Cook Inlet were hydrodynamically modeled as tsunami sources. The third tsunami source that is being evaluated as part of this analysis is an Augustine volcano flank collapse. This scenario has been modeled in previous studies (Kienle et al., 1987; Kienle et al., 1996; Waythomas, 2000; Waythomas and Waitt, 1998; Beget and Kowalik, 2006; and Waythomas et al., 2006), and the published results have been evaluated and applied to the Nikiski site. Maximum wave heights and wave heights as a function of time after the event were calculated for three analysis sites along the coast, directly adjacent to the planned onshore LNG facilities. The numerical modeling report prepared by Clayton Hiles and Dr. Roy Walters is presented in Appendix A. The Results section of Appendix A presents figures and results derived from the final model.

Tsunami interaction with the tide can be important in Cook Inlet. Work by Kowalik indicates that at Anchorage, maximum tsunami elevation occurs when the tide is near mean sea level (Kowalik and Proshutinsky (2010)). Concurrent modelling of tides and tsunami was beyond of the scope of this work, but given the above findings, all tsunami simulations were run with a static ambient water level equal to mean sea level. Some testing of this simplification was performed by re-running some of the simulations at highest astronomical tide, 4.23 m (14 ft). We found negligible difference in the maximum tsunami elevation for the 1964 event, and a small (10-20 cm, 0.3-0.6 ft.) increase in tsunami elevation for the landslide scenarios.

Table 3.4 presents the simulated maximum wave heights calculated at the three analysis sites along the shoreline for three tsunami scenarios. The submarine landslide scenario produced maximum wave heights of 16 to 20 feet (5 to 6 meters) (Plate 69) for mean sea level (MSL) conditions. The maximum wave height during highest astronomical tide (HAT) conditions is calculated to be 30 to 33 feet (9 to 10 meters).

An Augustine Volcano flank collapse scenario was not modeled during this analysis, but published results in literature (Kienle et al., 1987; Kienle et al., 1996; Waythomas, 2000; Waythomas and Waitt, 1998; Beget and Kowalik, 2006; and Waythomas et al., 2006) were evaluated and applied to the Nikiski site. Flank collapse of the Augustine volcano is expected to create a maximum wave height of 1 meter or less during mean sea level (MSL) conditions and a maximum tsunami runup of ~16 feet (5 meters) elevation during the highest astronomical tide (HAT).

The simulated results from the 1964 Great Alaskan Earthquake created a maximum wave height of about 2.6 feet (0.8 meter), which at a HAT of 14 feet would rise to an elevation of about 16 feet (Plate 70). No records were available of the observed tsunami height in Nikiski in the 1964 earthquake for comparison to these model results. More details about the model results are provided in Appendix A.

3.4.5 Tsunami Hazard

Model results from three tsunami source event scenarios have been evaluated, and the data suggests that the tsunami hazard at the planned onshore Nikiski site facility is very low. The site is located on a coastal bluff ranging in height from approximately 100 feet (30 meters) up to approximately 125 feet (38 meters), and neither simulated maximum wave heights, nor historical observations of wave heights (NOAA/NGDC), exceeds the bluff height. However, facility structures and lifelines at or near sea level or offshore could be impacted by tsunami waves, which requires detailed hydrodynamic modeling to evaluate.

Historical accounts and modeled scenarios are in agreement that tsunami waves are generally attenuated during their passage from the Gulf of Alaska and southern Cook Inlet into central Cook Inlet due to bathymetry, physiography, shallow water depths, and other factors. Two previous qualitative studies, the Kenai Peninsula Borough All-Hazard Mitigation Plan (KPB, 2014) and the 1978 Nikiski site hazard assessment (Pacific AKLNG Assoc., 1978), provide similar results and conclude that the tsunami hazard of the central Cook Inlet area is moderate.

The results of this analysis are limited by uncertainties including tsunami source parameters, tsunami attenuation, and data resolution. Three sources were selected for modeling based on the current state of knowledge assurmised from 1) a detailed literature review, 2) discussions with local experts (Peter Haeussler (USGS), James Beget (University of Fairbanks, Alaska) and Christopher Waythomas (USGS), and 3) data analysis. The final weighting of tsunami source characterization and significance is subject to change in future based on new information as it becomes available. For this model, the best currently available public-domain data was used to construct the bathymetric and topographic grid and small segments of project-specific bathymetric data.

Table 3.4: Tsunami Modeling Results

Tsunami Source	Maximum Wave Height (MSL)	Maximum Wave Height (HAT)	Exceeds Site Elevation?

Submarine landslide	16-20 feet (5-6 meters)	30-33 feet (9-10 meters)	No
Augustine volcano	<3 feet (1 meter*)	~16 feet (5 meters*)	No
1964 **M** 9.2 Great Alaskan Earthquake	<3 feet (1 meter)	~16 feet (5 meters)	No

**Estimated from published literature*

3.5 Coastal Erosion Hazard

The proposed Nikiski LNG facility is sited at the top of a coastal bluff that rises 100 to 125 feet above mean sea level. The integrity and stability of the bluff face is critical to the project. Previous work and field evidence collected during the 2014 and 2015 geologic field mapping (documented indicate that the bluffs are eroding by a combination of wave erosion which undermines the toe of the slope, followed by shallow landsliding, raveling, and gullying on the face of the bluff (Fugro reports 04.10140094-2, AKLNG document no. USAL-FG-GRZZZ-00-000001-000_0, and 04.10140334-2, AKLNG documents no. USAL-FG-GRZZZ-00-002015-004_0) .

Previous estimates of episodic coastal retreat in the area resulting from storm events range up to a maximum of approximately 50 feet (USACE, 2011). Reger et al (2007) note significant bluff retreat after a powerful storm in October of 2002. Anecdotal information collected by Reger et al (2007) suggests the rates of bluff retreat in the Salamatof area is about 2 feet per year.

Coastal erosion hazard within the study area is assessed by documentation and interpretation of field evidence of erosion processes, comparison of aerial photography from 1980 and 2012 to assess rates of bluff retreat, and examination of LiDAR topographic imagery collected in 2014 and 2015 to identify zones of active erosion. Low altitude oblique aerial photography of the coastal bluffs (Plate 71) provided additional information on the nature and activity of coastal erosion.

3.5.1 Description and Field Observations of Coastal Bluffs

The coastline is characterized by a gently sloping beach of rounded, well-sorted gravel and sand, backed by steep bluffs with heights of 100 to 250 feet within the 5-mile site radius. Within the Onshore LNG Facilities Study Area, the coastal bluffs typically range from 100 to 125 feet in height. Bluff heights rise to the north, with maximum heights reached at the East Foreland (Plate 17). Gravel "storm berms," approximately three to six feet high, discontinuously parallel the bluff approximately nine feet from the base of the bluff, and are interpreted to represent the height of wave run-up during storm events (Plate 72). Small alluvial fan deposits located between the gravel berms and the base of the bluffs suggest the berms provide some natural protection against erosion during high tides and minor storm events (Plate 73). However, the storm berms are breached by larger events, as evidenced by the eroded base of the bluffs behind the berms. The height and position of the berms may vary seasonally and from year to year. Thus the storm berms do not provide consistent protection against strong tidal currents and storm wave erosion.

The coastal bluffs adjacent to the site expose most of the site area stratigraphic units (Table 2.2). At the top of the bluff, an organic mat overlies one- to four-foot thick deposits of loose silt and fine sand composed of loess and tephra. These deposits overlie sands and sandy gravels of the Killey stade outwash deposits, which in turn overlie finer-grained late Moosehorn subestuarine fan-rainout deposits. Typically, colluvial material derived from the Killey outwash deposits mantles the bluffs and obscures the contact with the late Moosehorn age deposits (Plate 71).

Groundwater seepage was observed in many places along the contact between the two deposits. Groundwater seepage was frequently associated with debris flows, minor slumping, and the presence of thicker colluvial deposits, suggesting that groundwater flow along the contact may enhance destabilization of the coastal bluffs (Plate 36). Erosion of the coastal bluffs was observed and documented in multiple locations during field activities. Erosion processes observed included storm water runoff, gullying, wave erosion, vegetation sloughing, raveling, debris flows, shallow slides and slumps.

The bluff face slopes 35 to 40 degrees, and during the 2014 and 2015 field reconnaissance efforts, it was found to be either bare or covered with a veneer of grass and shrubs. Sloughing of the shallow rooted vegetation and the associated root mat was observed discontinuously along the coastal bluffs. Arcuate scarplets in the bluff face typically marked the top of a bare slope of exposed colluvium and the bottom edge of the intact root mat that covered the upper slope. In some places, fragments of vegetated material had collected at the base of the bluffs. Slopes with sloughed vegetation ranged from a small section a few feet wide to continuous stretches 200 feet in extent. Sections of the bluff that have larger exposed colluvial faces from vegetation sloughing showed evidence of further erosion by raveling, gullying, and rilling.

Debris flows were apparent in several locations along the coast (Plate 74). Observed debris flows had head scarps ranging in height from three to six feet, typically in Killey Age glacial outwash deposits, with resultant mass transport deposits mantling the bluff, or forming debris fans at the base of the bluff. Plate 74 shows a debris flow with an alluvial fan deposit approximately five feet thick subsequently eroded by waves. Erosion and removal of material from the debris fan at the base of the flow may promote destabilization of the deposit, and likely result in continued small mass-wasting events. The largest debris flow observed was located at the southern end of the LNG facilities area (Plate 75). Here, the Killey/Moosehorn contact dips slightly, then rises again, allowing groundwater to collect in the low point. The debris flow occurred at that low point, and today a spring emanates from the center of the debris flow scar.

Rotational slumps were observed in a small number of locations along the coastal bluffs, and were often associated with higher observed rates of groundwater seepage at the contact between the Killey outwash deposits and the late Moosehorn subestuarine deposits. Head scarps associated with the slumps were observed up to six feet in height, typically in the Killey gravelly sand deposits.

However, headscarps were also observed in the late Moosehorn clayey silts (Plate 76). Tilted trees noted within one of the slump blocks indicate back-tilting along a rotational slide plane (Plate 76). Slump failures were less common than debris flows, gullying, and ravelling. The slumps were observed to have shallow slide planes that to daylight on the bluff face.

A field traverse of about a half-mile of the top of the bluff was conducted in 2015 to look for evidence of incipient landslide scarps (Plate 77). Most of the traverse was covered with thick forests and undergrowth. The steady retreat of the bluff edge by slope failure was clear from the tilted trees at the crest of the bluff and fallen trees resting on the slope below. Failures appeared to initiate with shallow sliding and raveling of the unconsolidated sediment on the upper slope near the crest of the bluff. This process undercuts the organic root mat and trees, which eventually leads to tilting and ground failure. No ground cracks, tension cracks, or large-scale failures were observed.

Wave erosion at the base of the bluff followed by shallow erosion processes on the bluff face promote long-term retreat of the coastal bluffs. Major storm events are expected to result in accelerated rates of bluff retreat and loss of protective vegetation. No large deep-seated mass-wasting features were observed or documented during the field activities.

LiDAR topographic data collected in 2014 and 2015 for the bluff face within the LNG facilities show many of the geomorphic features discussed above. Plate 78 presents a hillshade image created from the LiDAR data. Notable features, including debris flows, stratigraphic contacts, springs and seeps, revetments, and sea walls are marked on the map.

A number of erosion protection structures were noted during field reconnaissance. In the vicinity of the three long piers, seawalls consisting of a line of steel sheet piles at the base of the bluff protect approximately 1500 feet of coast. These, along with a 250-foot-long gabion structure beneath the second pier, appear to have been effective at significantly slowing the rates of erosion of the top of the bluff. Seepage between the sheet pile section and the gabion section has causes some local erosion (Plate 78, panel A).

3.5.2 Rates of Bluff Retreat

To assess past coastal erosion magnitudes, historical imagery from 1980 was compared to recently obtained 2012 imagery. The analysis focused on mapping the top of the coastal bluff in the 1980 imagery and the 2012 imagery to identify locations of discernible change in the top of the bluff within the project boundary over the last approximately 32 years (Plate 79). Uncertainty related to the geographic registration between the 1980 imagery and the 2012 imagery is estimated to be +/- 5 feet (1.5 meters).

The top of the coastal bluff was mapped in the 1980 imagery based on tonal contrasts in the imagery, which represent changes in vegetation density. Darker red tones at the top of the bluff represent areas with heavy vegetation, while the lighter pinks and reds on the face of the bluff represent areas with relatively minor amounts of vegetation. In locations along the bluff with similar tones of red, changes in texture in the imagery from smooth to rough were used to delineate the top of the bluff. Modified and disturbed areas appear as white in the imagery, likely representing gravel and sandy surfaces. Mapping uncertainty of the top of the coastal bluff is approximately +/- 10 feet (3 meters) in the 1980 imagery where it is well-located, and +/-20 feet (6.1 meters) where it is approximately located.

Tonal contrasts from changes in vegetation density were also used to map the top of the coastal bluff in the 2012 imagery. Darker green tones represent areas of greater vegetation density at the top of the bluff, while lighter green tones and brown tones represent areas of sparse to no vegetation on the bluff face. Changes in texture from rough to smooth provided additional criteria to delineate the top of the coastal bluff in the 2012 imagery. Mapping uncertainty of the top of the coastal bluff is approximately +/- 5 feet (1.5 meters) in the 2012 imagery where it is well-located, and approximately +/- 10 feet (3 meters) where it is approximately located.

The cumulative uncertainty in the location of the top of the coastal bluff based on the mapping and geographic registration of the imagery is approximately +/- 20 feet (6.1 meters) in locations where the top of the bluff is well-located and +/- 35 feet (11 meters) where it is approximately located. The analysis of coastal bluff retreat focused on places where the top of the bluff is well-located in both the 1980 and 2012 imagery. In these locations, differences greater than 20 feet (6.1 meters) in the location of the top of the bluff between the 1980 and 2012 imagery, are positive evidence of measureable coastal erosion (Plate 79).

A comparison of the top of the coastal bluff mapped in the 1980 imagery and the 2012 imagery indicates horizontal variations in its location from 0 feet to approximately 65 feet (19.8 meters). The largest magnitude change in the location of the top of the coastal bluff [approximately 65 feet (+/- 20 feet) or 19.8 meters (+/- 6.1 meters)] occurs at the southern margin of the project boundary (Plate 79). In the 2012 imagery, the top of the bluff has an arcuate shape and the bluff face has lighter tones than the surrounding area. The morphology along the top of the bluff and the lighter tones on the bluff face in the imagery suggest a slump or debris flow likely removed the top of the coastal bluff sometime between 1980 and 2012. Interviews with local residents could help constrain the timing of this occurrence.

Two locations of notable retreat of the coastal bluff occur at the Agrium Fertilizer plant adjacent to the northern margin of the project boundary: a 300-foot (91-meter) long section directly south of the pier structure; and a 500-foot (152-meter) long section that extends north from the northern margin of the site perimeter (Plate 79). In both locations, the top of the coastal bluff has retreated approximately 30 to 40 feet (+/- 20 feet) (9.1 to 12.2 meters +/- 6.1 meters). An engineered revetment structure was constructed between 1980 and 2012 to mitigate the coastal bluff retreat adjacent to the pier. Two additional locations with bluff retreat ranging from approximately 30 to 40 feet (+/- 20 feet) (9.1 to 12.2 meters +/- 6.1 meters) occur south of the large gravel lot (Plate 79).

The coastal erosion assessment indicates that for the majority of the site, horizontal variations in the mapped location of the top of the coastal bluff between 1980 and 2012 are within the cumulative uncertainty (+/- 20 feet or 6.1 meters) of the data. Five locations were noted in the site perimeter where the retreat of the top of the coastal bluff exceeded 20 feet (6.1 meters) (Plate 79). At the southern margin of the project boundary, the top of the coastal bluff has retreated approximately 65 feet (+/- 20 feet) (19.8 +/- 6.1 meters), yielding a maximum retreat rate of 2 feet/yr (+/- 0.5 feet/yr). Additionally, short reaches, 300 and 500 feet (91 and 152 meters) in length, of the top of the coastal bluff adjacent to the Agrium Fertilizer plant have retreated approximately 30 to 40 feet (9.1 to 12.2 meters) .

Although limited by the resolution of the analysis, the rates of coastal erosion near the onshore LNG facilities area based on a comparison of 1980 and 2012 aerial photography are consistent with average rates of 1 to 3 feet of coastal erosion estimated by KPB (2013). However, erosion is an episodic and stochastic process, in which many seasons or years may pass with little to no activity. Conversely, some seasons or years may experience substantial erosion that exceeds rates estimated from historical observations. In addition, the specific locations in which erosion actually occurs is similarly challenging to determine because of the multiple factors driving the process, including the locations of groundwater springs and consequent debris flows, locations of surface water runoff and resulting gullying, or varying intensity of storm wave attacks at the base of the bluffs.

3.5.3 Interpretation of LiDAR Elevation Data of the Coastal Bluff

Detailed LiDAR topographic data were collected for the coastal bluff along the length of the study area in in 2014 and 2015. These data, collected from a vessel in 2014, and from a vehicle on the beach in 2015, were evaluated to identify evidence of mass wasting and erosion processes. Side-scan LiDAR scans a target area from the side, as opposed to from above as is typically the case with LiDAR. Interpretation of the LiDAR data show the presence of debris flows, shallow landslide scarps, stratigraphic contacts, as well as springs and seeps (Plate 78).

Debris flows are recognized by their arcuate head scarps on the bluff and fan-shaped deposits of debris at the base of the bluff, projecting toward the beach. If fresh, the debris-flow deposits are typically smooth and free of vegetation. Scarps are seen as irregular curvilinear and arcuate breaks-in-slope in multiple locations of panel A and panel C in Plate 78. Seeps along the contact between the Killey outwash deposits and the late Moosehorn deposits may provide groundwater that contributes to the occurrence of debris flows. This stratigraphic contact itself can be seen in the LiDAR data as a distinct horizontal break-in-slope midway up the bluff in a few locations (panel B and panel C on Plate 78. Springs and seeps are apparent in multiple locations along the bluffs, defined by narrow channels in and at the base of the bluffs. Spring and seep locations were interpreted from LiDAR topography, field reconnaissance, and interpretation of color aerial photography. The vessel-based LiDAR data confirm and add detail to the assessments of coastal erosion from field observations.

3.5.4 Coastal Erosion Hazard Assessment

A traverse of the coastal bluffs indicates that multiple erosion processes are responsible for continued bluff retreat including: wave erosion, storm water runoff, gullying, raveling, sloughing of vegetation, debris flows, and slumping. Coastal erosion begins with wave erosion at the toe of the bluff, followed by removal of material from the over-steepened slope. No evidence of large, deep-seated, mass-wasting events was observed during the field activities or in the LiDAR topographic data. All slope failures, including slides, slumps, and debris flows, are relatively shallow and involve materials from the bluff face.

Long term measurements of coastal bluff retreat were estimated based on comparison of aerial photographs from 1980 and 2012. Over most of the bluff within the study area, bluff retreat could not be detected to exceed the +/-20 feet cumulative uncertainty in the data. However, five locations showed measured differences ranging from 30 to 65 feet (+/- 20 feet) (9.1 to 19.8 meters +/- 6.1 meters) (Plate 79).

3.6 Volcanic Hazards

The Kenai Peninsula lies across the Cook Inlet from the Aleutian Arc, a string of active volcanoes approximately 1,700 miles long, parallel to the Alaskan-Aleutian Subduction Zone. Many miles away and separated from the Kenai Peninsula by Cook Inlet, the Aleutian arc volcanoes pose no hazard to the LNG site from lava flows, debris avalanches, lahars, pyroclastic flows, or direct blasts. The Aleutian Arc volcanoes do, however, pose a hazard to the site from airborne volcanic ash and pyroclastic debris. Prevailing winds regularly carry ash from these volcanoes east across the inlet to the Kenai Peninsula.

Volcanic ash consists of tiny jagged particles of rock and volcanic glass blasted into the air by a volcano. The ash cloud can travel for hundreds of miles downwind from the volcano, clouding the air and leaving a blanket of ash on the ground. Four active volcanoes -- Augustine, Redoubt, Iliamna, and Mount Spurr -- are sufficiently close to the site (50 to 115 miles) to deposit volcanic ash in the Nikiski area that may impact plant operations (Plate 4).

Historical volcanic ash fall events have been responsible for damage to machinery, human health, and the economy. Ash clouds can prevent travel because of poor visibility, slippery roads, and ash-damaged vehicles. Ash particles are tiny and abrasive, and easily penetrate and damage machinery and electronic devices. Internal combustion engines are vulnerable to stalling as air filters are clogged and bearings and gears are abraded. Cooling water intake structures can be affected. The ash cloud can cause air intake and ventilation systems to clog, causing equipment to overheat. In addition, humans, livestock, and wildlife suffer from breathing ash particles and contamination of forage. Crops covered by ash may fail, although the ash will ultimately enrich the soil for future crops (Brantley and Stauffer, 2000).

Large prehistoric eruptions also resulted in sand-sized pyroclastic debris fallout, as evidenced by by volcaniclastic tephra units in the area. These likely sourced by one of the volcanoes on the east side of Cook Inlet. Distal tephra fallout from eruptions of Redoubt Volcano has been documented in historic time (Table 3.5).

An additional hazard that may result from volcanism is that of a flank collapse into the Cook Inlet, generating a tsunami. Augustine, as it is an island in the Cook Inlet, is the only one of the four nearby active volcanoes capable of such a flank collapse. The hazard to the LNG site from a tsunami generated by an Augustine flank collapse was evaluated and the results presented in section 3.4.

3.6.1 Historical Eruptions and Ash Fall Events

Historical eruptions have been documented at all four of the nearest volcanoes. Primary sources of information are the U. S. Geological Survey volcanic hazard evaluation reports (Waythomas et al., 1997, 1998, 1999, and 2001), the Alaska Volcano Observatory (2016) website documentation of eruptive activity. Seventeen historical eruptions of Augustine, Redoubt, Iliamna, and Mount Spurr have been documented, as listed in Table 3.5. Five historical volcanic ash fall events have been recorded in the Kenai area since 1976 (Table 3.6).

Table 3.5: Historical Volcanic Eruptions

Sources: Waythomas et al. (1997, 1998, 1999, and 2001), and the Alaska Volcano Observatory (2016).

Year	Volcano	Effects
1860s-70s	Iliamna	Reports of historical eruptions in the 1860's and 1870's are poorly documented.
1778	Redoubt	Captain James Cook observed the volcano steaming, but not actually erupting.
1812	Augustine	Small-volume ash emissions, pyroclastic flows?
1819	Redoubt	Ash emission and local fallout.
1883	Augustine	Small-volume ash emissions, pyroclastic flows, Burr Point debris avalanche & small tsunami.
1902	Redoubt	Ash emission and distal tephra fallout.
1933	Redoubt	Ash emission and local fallout.
1935	Augustine	Small-volume ash emissions, pyroclastic flows, dome growth.
1953	Mount Spurr	Volcanian to sub-Plinian pyroclastic eruptions generated relatively large volumes of volcanic ash that fell over parts of south-central Alaska.
1963	Augustine	Small-volume ash emissions, pyroclastic flows.
1964	Augustine	Small-volume ash emissions, pyroclastic flows, dome growth.
1965-1968	Redoubt	Ash emission and distal tephra fallout.
1976	Augustine	Small-volume ash emissions, summit explosions, small pyroclastic flows & lahars, dome growth, ash plumes reaching as high as 10,000 meters.
1986	Augustine	Lava flows and ash emissions, some reaching as high as 12,000 meters, pyroclastic flows & lahars, dome growth. Ash scattered over the Cook Inlet as far as Anchorage.
1989-1990	Redoubt	Ash emission and distal tephra fallout.
1992	Mount Spurr	Volcanian to sub-Plinian pyroclastic eruptions that generated relatively large volumes of volcanic ash that fell over parts of south-central Alaska.
2005-2006	Augustine	Small-volume ash emissions, summit explosions, pyroclastic flows & lahars, ash plumes reaching a height of 14,000 meters.
2009	Redoubt	Ash plumes reaching a height of 19,000 meters, dome growth, pyroclastic flows, lahars, and summit eruptions.

Table 3.6. Historical Ash-Fall Events in the Kenai Area

Sources: Brantley et al., (1990), Schaefer et al, (2012), Waythomas et al. 1997, 1998, 1999, and 2001), and the Alaska Volcano Observatory (2016).

Year	Volcano	Effects	Duration
2009	Redoubt	Up to 2 mm of ash fell in Homer, Anchor Point, and Seldovia. Ash fall over the Kenai Peninsula forced businesses and city offices to close early. Anchorage airport closed and many flights cancelled.	Nineteen major ash-producing events over three weeks
2005-2006	Augustine	Plumes reached altitudes of 14 kilometers above mean sea level and deposited traces of ash on southern Kenai Peninsula communities.	Thirteen ash explosions over 20 days.
1989-1990	Redoubt	Lower Kenai Peninsula was blanketed with ash after an eruption on February 15, 1990. Kenai airport closed.	Twenty three major explosive events between December 1989 and April 1990.
1986	Augustine	Several millimeters of ash fell over parts of the southern Kenai Peninsula. Homer saw an accumulation of about 6 millimeters of ash.	For two days, ash fell over the Cook Inlet region. Dust lingered in the air an additional 3 days as far north as Anchorage .
1976	Augustine	Ash falls took place at Iliamna, Homer, Seldovia, and Anchorage (1.5mm).	Twelve eruptions over three days in January.

The 1989-90 and 2009 eruptions of Redoubt Volcano were well documented. Schaefer (2012) details the 2009 eruptive events and includes photographs of the March 28 ash fall in Nikiski (Plates 80 and 81). Waythomas et al., (1997) report the effects of the ash cloud in Kenai and Anchorage during the 1989-90 eruption:

> "During periods of continuous ash fall-out, the public was advised to remain indoors and wear dust masks. Many schools were closed, and some individuals experienced respiratory problems. The municipal airport at Kenai was closed for several days as a result of ash fallout from the January 8, 1990 eruption. Gas-powered turbines at the Beluga power plant, the primary power supply for Anchorage were shut down in anticipation of the adverse effects of a thick ashfall."

> "Emission of tephra during many of the larger eruptive events, especially in December 1989 and January 1990, caused numerous problems for the airline industry. Hundreds of flights were cancelled… Damage to aircraft was significant…. The total economic impact of the 1998-90 eruptions on the aviation industry was estimated at about 101 million…"

The 1976, 1986, and 2005 and 2006 eruptions of the Augustine Volcano resulted in plumes of volcanic ash reaching heights of as much as 12,000 meters above sea level. Waythomas et al., (1998) describe the effects of the ash cloud in Kenai and Anchorage during the 1976 and1986 eruptions:

> "In anticipation of ashfall during the 1976 and 1986 eruptions, the public was advised to remain indoors, and many schools and businesses were closed. Some individuals experienced respiratory problems, and visibility in some places was reduced to 100 meters or less. On March 28, 1986, the concentration of particulate matter in the air over Anchorage was about 860 micrograms per cubic centimeter (Swanson and Kienle, 1988), just below the threshold for a health emergency."

3.6.2 Earlier Ash Fall Events in the Site Area

Evidence of late Pleistocene to Holocene ash fall events can be seen in soils in Nikiski area, which feature a layer of accumulated *tephra* (volcanic ash) and other loess beneath the organic root mat, resting on the late Pleistocene glacial outwash deposits of the Killey stade (Plate 33). Tephra layers in the soils are typically a few inches thick, but have been documented as thick as several feet, and reflect accumulation over the past approximately 17,500 years.

The ash fall events from the 1953 and 1992 Mount Spurr volcanic eruptions, documented in the city of Anchorage, were not recorded in the Kenai Peninsula. However, fine-grained volcanic-ash deposits of Holocene age originating from Mount Spurr have been identified on the Kenai Peninsula. These ash layers are found within a vertical sequence of unconsolidated sediment and volcanic-ash deposits from other Cook Inlet volcanoes. Specific layers of ash have been correlated by radiocarbon dating and geochemistry to volcanic deposits on the proximal flanks of Mount Spurr and Crater Peak and serve as evidence for relatively large eruptions of the Mount Spurr volcano and Crater Peak during the past 7,000 years (Waythomas et al., 2001).

Airborne ash from Iliamna Volcano has traveled at least as far as the Kenai Peninsula during prehistoric Holocene eruptions. At least two fine-grained volcanic-ash deposits have been identified on the Kenai Peninsula, occurring within a vertical sequence of peat and volcanic- ash deposits from other Cook Inlet volcanoes. These deposits have been radiocarbon dated and geochemically correlated with a pumiceous lapilli tephra found on the proximal flanks of Iliamna Volcano (Waythomas et al., 1999). The first layer consists of pumiceous lapilli tephra and fine ash layer and is evidence for a large plinian eruption from a vent on the northeast upper flank of the volcano about 4,000 yr B.P. The second layer is geochemically similar to the proximal lapilli tephra and is evidence for an older eruption that dates to about 7,000 yr B.P. No associated volcanic deposits have yet been identified on the proximal flanks of the volcano for this second, older event (Waythomas et al., 1998).

Other volcanoes have also deposited ash in the site area. The Lethe tephra is a widespread tephra found in the soils of the Kenai Peninsula. It has been traced to an unknown source near Mount Katmai, located south of Augustine and approximately 200 miles southwest of the site. The Lethe tephra is estimated to have been deposited about 17,800 years cal yr, on landforms of Killey age (Reger et al., 2007). This distinctive stratigraphic marker has been used to correlate glacial events throughout the Cook Inlet area.

3.6.3 Ash-Fall Hazard Assessment

Historical and geologic records show that volcanic ash-fall events are relatively common in the Nikiski area and the Cook Inlet region. Five ash-fall events have been documented in the Kenai area since 1976. In the 50-year life of the LNG plant, it is reasonable to expect that five to ten such events may occur. More extreme events could also result in larger size volcaniclastic debris, particularly in areas proximal to volcanoes bordering Cook Inlet (Plate 4). Ash fall thickness may vary from a fraction of an inch to several inches.

Ash-fall events can hamper plant operations, damage machinery, slow or halt vehicle transportation and aviation, and impact human health. Ash may also affect ship traffic, especially as shipping routes through the Cook Inlet may pass close to volcanic sources.

3.7 Additional hazards

The FERC (2007) guidelines suggest addressing specific geologic features that may affect site stability and foundation design. These features are reviewed below.

1. Subsidence features: Areas of actual or potential surface or subsurface subsidence, uplift, or collapse are not observed at the onshore and marine facilities areas. The area is underlain by Quaternary glacial deposits which are relatively stable. Their surface geomorphology shows no evidence of collapse, subsidence, or uplift features.
2. Loading history: In the onshore LNG facilities area, the upper approximately 60 feet of sediment is the Killey glacial outwash which has never experienced loading from a subsequent glacier. The outwash was deposited as the glacier retreated. The Moosehorn deposits immediately beneath the Killey outwash would have experienced loading by the Killey glacier, as would any Pleistocene deposits in the marine LNG facilities area.
3. Rock features: The Pleistocene glacial deposits beneath the marine and onshore sites are classified as soil rather than rock.
4. Unrelieved residual stresses in bedrock: The site is underlain by soil rather than bedrock.

5. Hazardous soils: Most of the soils underlying the site are glacial or glacially derived deposits of weakly consolidated sand, silt, gravel, and clay. The deposits are horizontally bedded, and individual beds contrast in grain size and sorting characteristics. The soils are not soluble. Perched water is present on top of fine grained beds I the onshore area, and all marine strata are below the water table; therefore, water content is variable. Sand layers are not cohesive. Where saturated they may pose a liquefaction hazard when subjected to earthquake-related ground shaking. The potential for liquefaction at the site is assessed through geotechnical analyses of borehole data. Liquefaction analysis is presented in Fugro report 04.10140334-12 (Table 1.1).

4.0 MARINE GEOLOGIC HAZARDS

Analysis of submarine geologic hazards focuses on those hazards most likely to affect the site. Hazards considered include tectonic deformation, effects of strong ground motions, effects of tidal currents, potential fluid expulsion, submarine slope failures, and potential anthropogenic hazards. Data used to evaluate and analyze these hazards included multibeam high resolution bathymetry, side scan sonar, shallow and deep seismic reflection lines, geotechnical borings, and local and regional mapping.

4.1 Tectonic Deformation Hazard

Offshore tectonic deformation hazards include ground deformation resulting from seafloor faulting, folding, or tilting due to tectonic movement along a fault. The potential for seafloor faulting is discussed in section 4.1.1 and for folding and tilting in section 4.1.2.

4.1.1 Surface Faulting

The evaluation of surface faulting within the marine portion of the 5-mile site radius, shows that the hazard at the site is low. No bathymetric or seismic reflection evidence of faults reaching the seafloor surface was identified. The Pleistocene glacial deposits and Holocene sands and gravels that underlie the seafloor show no evidence of lineaments or linear scarps consistent with a surface faulting origin. In addition, seismic reflectors interpreted to image the Pliocene and Pleistocene strata show no breaks, folding, or stratigraphic thickness changes indicative of either surface faulting or growth of faults at depth. These data provide positive evidence for no surface or subsurface faulting in the marine portion of the 5-mile radius around the site.

4.1.2 Folding and Tilting

The potential for tilting of the region is discussed in section 3.4. The potential for tectonic folding that could cause ground tilting in excess of FERC (2007) guidelines is judged to be very low. Consequently, the risk posed to the proposed marine facilities is also low.

4.2 Effects of Strong Ground Motions

The site area lies within a seismically active region as discussed in section 2.2.1., thus the potential for strong ground motions that may affect the facilities is high. In general, the primary effects will be those associated with shaking and/or ground accelerations. Earthquake-related ground shaking can cause the loss of bearing capacity of seafloor structures or holding capacity of piers due to liquefaction or cyclic degradation of the strength or stiffness of the foundation soils.

Earthquake-related ground displacement and strong ground motions are a significant regional hazard. Strong ground motions and fault displacements are a lesser risk to floating offshore facilities, but a greater risk to onshore or fixed offshore facilities. Secondary hazards to offshore facilities that may result from strong ground motion include mass movement (slumps, landslides, debris flows, turbidity currents) and liquefaction that may affect fixed foundations and facilities.

4.3 Effects of Currents

Cook Inlet has the largest average tidal range in the United States, with a mean of 27.0 feet, (NOAA, 2016a, 2016b). and the fourth highest in the world, behind Bay of Fundy (31.3 feet), Ungava Bay (29.0 feet), and Bristol Channel (28.9 feet) (NOAA, 2016b). In the vicinity of the site area, the tidal range is between 24 and 28 feet (NOAA, 2016a). Tidal currents average 3 to 6 knots (7 mph) for flood currents and can reach a peak of 6 to 8 knots (10 mph) or more for ebb currents (Schumacher, 2005).

The proposed Nikiski LNG facility is sited on the shore of Cook Inlet just south of where the inlet narrows considerably (Plate 3). This morphologic feature, known as the Forelands constriction, between the East Foreland and the West Foreland, acts to concentrate and accelerate tidal flow. This is the primary control over scour, deposition and reworking of sediments within the greater Forelands area.

4.3.1 Scour and Erosion

Strong tidal currents, like any strong current, have abundant energy that can scour and erode the basal seafloor deposits. Dozens of depressions or pits are mapped in the eroded surface of the Pleistocene deposits at the bottom of Cook Inlet where it is not overlain by Holocene gravels or sands. These likely represent scour pits where local turbulent conditions, perhaps caused by the presence of boulders or other seafloor irregularities, have eroded into the Pleistocene deposits and created scour depressions. A less likely origin for these pits is that they have been formed by fluid expulsion (discussed in section 4.4.) The depressions are mapped and presented on Chart 2.

Scour presents a hazard to the marine facilities. If severe and not mitigated by appropriate design and protective measures, it could undermine the pier foundations. The foundations themselves can cause localized current-induced turbulence that could then lead to erosion of foundation support.

4.3.2 Sedimentation

As previously discussed, large quantities of glacially derived fluvial sediment are added to the upper reaches of Cook Inlet during the summer months. Strong tidal currents prevent early deposition of most of the silt and clay, which are transported toward the Forelands morphologic constriction and the vicinity of the site area. Intense tidal flushing removes all but the coarsest sediments. Aggradation of the inlet floor is not occurring in this area. The primary hazard from the seasonal sedimentation and its mobilization through the inlet may be the abrasion of piers or foundations supporting the marine facilities by sand and gravel transported by high energy tidal currents.

4.4 Fluid Expulsion Features

The possibility was considered that the numerous small pits and depressions mapped on the sea floor may be fluid expulsion features formed by natural gas or other fluids. The Cook Inlet basin is known for its oil and natural gas resources, which are extracted from traps in Tertiary strata. Given certain conditions, gas migrating up to the surface could cause pockmarks on the sea floor. These conditions include the presence of unconsolidated sediment on the sea floor.

Sources of shallow gas on continental shelves include free gas migrating along fractures or faults from deeper reservoirs, and gas resulting from biogenic activity or decomposing organic materials buried in shallow sediments. Evidence of methane gas expulsion in sediments includes gas bubbles or plumes in the water column and gas-blanking of gas charged sediments in sub-bottom profiler and seismic survey data. Biologic communities of chemosynthetic organisms that grow up around "cold seeps" may form acoustically reflective hard-grounds (shell beds) detectable with side-scan sonar. Methane seeps are also commonly the site of authigenic carbonate production that leads to formation of localized hard grounds, which can be surrounded by a scour depression in areas affected by strong currents. Potential conduits for gas and water include faults, pipes, mud volcanoes, and mud diapirs. Other geologic expressions of gas expulsion include seafloor subsidence or expansion, pockmarks (primarily in muddy sediments), sediment slumps, and landslides (Paull et al.,, 2015; Hance, 2003)

No data collected as part of the 2014-2015 studies suggest that significant fluid expulsion is occurring within the site area. The shallow and deep seismic reflection data show no bright spots that could represent migrating gas. The areas where the small depressions occur is underlain by eroded Pleistocene deposits. We conclude that the small depressions and pock marks present on the seafloor were likely created from tidal current-induced scour (Chart 2). The seafloor pock marks and depressions are primarily located on the eroded surface of the Pleistocene deposits outside of the immediate vicinity of the proposed marine facilities. Therefore, we consider the risk of shallow gas seeps or fresh water springs affecting the marine facilities to be low.

4.5 Slope Failure

Seafloor slope failures can affect large areas and volumes of soil, and as a group tend to be larger than subaerial landslides. In addition, seafloor slides tend to travel larger distances and occur on flatter slopes than subaerial landslides (Hance, 2003). Previous studies reveal that it is unlikely that most seafloor slope failures are triggered by gravity loads alone; earthquake loading and rapid sedimentation (underconsolidation) are likely triggers of many submarine slope failures (Hance, 2003). In the marine site area, the steepest slopes, thus those most susceptible to slope failure, occur within within one mile of the shore.

High resolution bathymetric data reveals very few submarine slope failure features within a 5-mile radius of the site. One apparent slope failure headscarp is observed approximately 3,800 feet northwest of the proposed marine facilities (Chart 2). This headscarp is about 250 feet wide, 160 feet long and 3 feet deep. No associated slump toe is observed; it has possibly been removed by the action of tidal currents. A second observed feature is an arcuate lineation, concave towards Cook Inlet, approximately 4800 feet northwest of the proposed marine facilities. This is not a fully formed headscarp but may represent an incipient failure plane. These features both occur within Pleistocene glacial deposits and are shown on Chart 2.

In general, sliding or slumping is not occurring on the submarine slopes under the current static gravitational and tidal current regime. Given the rapid removal of sediments being introduced by the Susitna and Knik rivers by the strong tidal currents, rapid sedimentation and loading of the coastal slopes is unlikely. It is unclear whether slides could be induced by earthquake-induced strong ground motions. In general, details of submarine landsliding attributable to seismic events in southeastern Alaska are sparse. A significant number of submarine landslides triggered by the 1964 Good Friday earthquake were documented. These primarily occurred in narrow fjords in steeply dipping (30 degrees or greater) deltaic outwash deposits (Grantz et al., 1964.) No submarine landslides have been extensively documented for more recent large earthquakes in Alaska, such as the 2002 Denali event, or several magnitude 7+ events that have occurred. However, Fugro recommends that quantitative slope stability analyses be performed for the seafloor immediately adjacent to the marine facilities, as well as the coastal bluffs.

4.6 Tsunami and Seiche

Tsunami hazards is judged to be high for the proposed marine LNG facilities. A deterministic tsunami hazard assessment was conducted to determine a range in wave heights for use in design of the facilities. This analysis is described in detail within section 3.3 of this report. The model results show a maximum wave 16 to 20 feet high for a hypothetical submarine landslide event in the main channel of the Cook Inlet. Such a wave could overtop and have a negative impact on the marine facilities.

4.7 Sea Level Changes

Significant sea level rise or fall over the 50-year life of the plant could adversely affect marine terminal operations. Global climate change, tectonic uplift, subsidence, isostatic rebound, changes in wind direction, and other factors may cause changes in sea level.

A study of sea level trends across the United States by NOAA (2012) shows that sea levels in southern Alaska are falling. Rates of sea level fall for the Kenai Peninsula are shown by NOAA (2012) to be 3 to 4 feet per 100 yrs (9-12 mm/ yr). The Nikiski tide gage shows a steady rate of sea level fall of 10.5 +/- 1 mm/yr since about 1973 (NOAA, 2016c). This phenomenon is attributed to a combination of land uplift and changing wind patterns.

Over the 50-year life of the plant, a continuation of this trend would result in a net drop in sea level of (50 yrs x 10.5 mm/yr) 525 mm, or 1.7 feet.

4.8 Anthropogenic Hazards

Anthopogenic hazards in the marine LNG area consist of debris on the sea floor, and various pipelines and cables. Many of these items were visible in the high resolution bathymetric data. They are described below.

4.8.1 Marine Debris

Marine debris observed within the bathymetric data include an arcuate, ~750 foot long sinuous feature located approximately 3,500 feet southeast of the proposed facilities interpreted to be an abandoned salmon gill fishing net and rectangular shaped detritus approximately 6,300 feet southeast of the proposed facilities. The fishing net may or may not be abandoned. If it is abandoned, it could break loose and be transported by tidal current to the marine facilities of the Nikiski marine facilities where it could become entangled. This might pose hazards to shipping, particularly presenting the potential to foul the propellers of ships. The rectangular shaped features located further southeast are approximately 250 feet long and 50 feet wide and 10 feet high. This object may pose a navigation hazard or impact any dredging operations planned for the area.

4.8.2 Pipelines and Cables

Existing and proposed pipelines and cables within the site area are discussed in report USAL-FG-GRZZZ-90-002015-010, “Marine Geophysical Survey Report, Marine LNG Facilities” and are summarized below.

4.8.2.1 Telecommunications Cables

Two segments of an in-service submarine fiber optic telecomm cable are located within the nearshore LNG marine terminal’s approach corridor. The corridor crosses Segments 1 and 2 of the Kodiak Kenai Fiber Link (KKFL).

The Kodiak Kenai Fiber Link (KKFL) is owned by Global Communications Inc. (GCI). The KKFL cable connects Anchorage, Kenai, Homer, Kodiak, Narrow Cape, and Seward and is sometimes referred to as the Alaska United system. The proposed approach channel crosses Segment 1 (Anchorage to Kenai) of the KKFL in a water depth of ±48 feet, approximately 5 miles northwest of the Kenai River mouth. Segment 2 of the KKFL (Kenai to Homer) would be crossed obliquely in water depths from 66 feet on the channel’s eastern edge to 84 feet along its western edge.

4.8.2.2 Power Cables

No known power cables are crossed by nor lay within the LNG marine terminal or the proposed approach channel.

4.8.2.3 Pipelines

No existing pipelines are known to cross the LNG marine terminal or the proposed approach channel. However, a study dated 27 August 2013 has been completed for a Trans-Foreland Pipeline and planning is in progress. The Trans-Foreland Pipeline (TFPL) Project is proposing to construct an 8-inch diameter sales oil pipeline from its existing Kustatan Production Facility on the west side of Cook Inlet to the Kenai Pipeline Company (KPL) Tank Farm on the east side of the inlet. Portions of the pipeline will be installed on the seafloor of Cook Inlet (Cochran, 2013). The current routing of the Trans-Foreland line would cross the proposed approach channel to the LNG Terminal Site just south of the berth area.

5.0 CONCLUSIONS AND RECOMMENDATIONS

Conclusions regarding the potential geologic hazards assessed in this report are presented in this section. The conclusions, or principal findings, are followed by recommendations for further study, especially where such studies have the potential to reduce uncertainty in the hazard assessment. Finally, initial recommendations for hazard mitigation are presented.

5.1 Principal Findings

Principal findings are summarized regarding potential geologic hazards at the onshore and marine Nikiski LNG facilities. Hazards assessed include surface faulting, folding and tilting, effects of strong ground shaking, tsunami inundation, coastal erosion, sea floor erosion and sedimentation, slope failure, and volcanic ash-fall.

5.1.1 Surface Faulting Hazard

The potential for surface faulting is judged to be low at the proposed LNG facilities based on the following lines of evidence:

- No geomorphic evidence of surface faulting was identified within the 5-mile site radius. The Killey stade (17,500 to 18,500 years old) glacial deposits that underlie the ground surface show no evidence of lineaments or linear scarps consistent with a surface faulting origin. All lineaments observed can be attributed to a glacial, or glaciofluvial origin.
- Mapping of the stratigraphic boundary zone between the Killey and Moosehorn stade deposits in the onshore LNG facilities area shows no discernible displacement of bedding consistent with a surface faulting origin. IMASW profiles along a 70,000-foot grid of geophysical lines shows continuous planar bedding in 87% of the line length. Small gaps in the documented planar bedding may be the result of poor resolution of the data.
- Small surface faults documented by previous studies in the bluff face north of the site are interpreted to have resulted from lateral spreading, either as a result of kettle margin failure after melting of the ice block, or failure due to earthquake-related ground shaking. The faults are located adjacent to a kettle depression and many kettles in the site area show clear evidence of shore-parallel slope failures that could have a similar origin. Seismic reflection data show no displacement of Tertiary reflectors beneath these faults, precluding a tectonic origin.
- Interpretation of deep seismic reflection data collected by Fugro in 2015 and archival data from the oil and gas industry, show that faults nearest the site in the Cook Inlet Basin are blind-thrust faults displacing Mesozoic and Tertiary strata. Fault tips do not reach the ground surface. The tip of the blind thrust fault associated with the Middle Ground Shoal anticline is located approximately 4.3 miles west from the onshore site center, at an average depth of approximately 6,750 ft. The tip of the blind thrust fault associated with the Kenai Cannery

Loop monocline is located approximately 4.9 miles east from the onshore site center, at an average depth of about 6,350 feet

- Seismic reflection data provide positive evidence of an absence of tectonic faulting beneath the site. The site lies in a synclinal flat between cored by seismogenic blind-thrust faults. The Tertiary strata beneath the site, imaged by 2015 seismic reflection data, are planar-bedded and gently dipping, with no observed disruption of bedding to a depth of 150 feet.
- The potential for surface faulting is judged to be low within the marine LNG facilities area. Seismic reflection imaging of the Tertiary strata shows continuous planar reflectors underlying the marine facilities area. These data provide positive evidence of the absence of faulting. In addition, no geomorphic features consistent with a surface faulting origin were observed in the bathymetric data.

5.1.2 Folding and Tilting

The potential for tectonic folding that could cause ground tilting in excess of FERC (2007) guidelines is judged to be very low. Tilting documented from the 1964 Great Alaskan earthquake was an order of magnitude lower than permitted by the guidelines. A similar result was computed for hypothetical tilting from an earthquake event on a Cook Inlet style fold within the 5-mile site radius.

Geologic and geomorphic features were assessed for their potential to record long-term tectonic deformation. No positive evidence for tilting was observed.

a. Paleo-shorelines around kettle lakes were found to be a mappable strain marker, but the small size of the lakes, the possible confusion of paloe-shorelines with slump scarps, and the low expected magnitudes of tilting given the likely age of the shorelines, resulted in the uncertainties being comparable to the magnitude of potential tilting.

b. The glacial outwash plains in the 5-mile site radius, although mappable and generally smooth fan-shaped surfaces, are oriented sub-parallel to the known axes of folding. Therefore, longitudinal profiles of the fan surfaces are not effective strain markers for tectonic folding.

c. The Moosehorn-Killey contact, exposed in the coastal bluff face, and imaged in seismic IMASW profiles, was found to be generally planar with some gentle local warping. The warping may be the result of glacial processes.

d. The top-of-Tertiary unconformity, as mapped from marine seismic reflection data, exhibits a gentle tilt to the east-southeast. This tilt may be related to continued growth of the Middle Ground Shoal fold. The magnitude of tilting is relatively low and occurred over a relatively long time period post the erosion of the Tertiary unconformity, therefore does not pose a hazard to the marine facilities.

5.1.3 Effects of Strong Ground Motions

Onshore, strong ground motion associated with the 1964 **M** 9.2 Great Alaskan Earthquake caused extensive ground cracking, water and sand eruptions, settlement, landslides, and deformation of

Pleistocene glacial outwash and moraine deposits in the Kenai Lowland, possibly including areas within the 5-mile site radius. Although no features were documented within the project boundary, the similarity in the geologic materials suggests that such effects could occur. Geotechnical investigations to identify and evaluate pockets of liquefiable or weak sediments, and identify slopes that have the potential to fail during strong ground motions, can enable mitigation of this hazard.

Preliminary evaluation of seismically induced liquefaction and ground failure was performed using borehole and groundwater data from the 2014 geotechnical investigations (Fugro report no. 04.10140094-11). This analysis estimates limited localized liquefaction during the modeled shaking levels. Liquefaction will be re-evaluated with geotechnical data from the 2015 investigations.

In the marine area, there are no historical records of earthquake-induced ground failures, and no evidence of such failures in the high resolution bathymetry of the sea floor. The potential for liquefaction will be evaluated based on geotechnical data, in the Integrated Site Characterization and Engineering Report Marine LNG Facilities (Report 04.10140334-14).

5.1.4 Tsunami Inundation

Model results from three tsunami source event scenarios were evaluated, and the data indicates that the tsunami hazard at the planned Nikiski site is very low. The site is located on a coastal bluff ranging up to approximately 130 feet high, and neither simulated maximum wave heights nor historical observations of wave heights (NOAA/NGDC) exceed the bluff height. Two previous qualitative studies, the Kenai Peninsula Borough All-Hazard Mitigation Plan (KPB, 2014) and the 1978 Nikiski site hazard assessment (Pacific AK LNG Assoc., 1978), also concluded estimated tsunami hazard to be low for the onshore site and other elevated areas of central Cook Inlet near the site.

For the proposed LNG marine facility area the tsunami hazard is considered high. The modeled tsunami wave heights may overtop the marine facilities.

5.1.5 Coastal Erosion

Multiple erosion processes are responsible for continued bluff retreat including: wave erosion, surface water runoff, gullying, raveling, sloughing of vegetation, shallow land sliding, debris flows, and slumping. Coastal erosion begins with wave erosion at the toe of the bluff, followed by removal of material from the over steepened slope by slope processes. No evidence of large deep-seated, mass-wasting events was observed during the field activities or on LiDAR data. All observed slope failures are relatively shallow and involve materials in the bluff face. Overall rates of bluff retreat are moderate, generally not exceeding 20 feet in 32 years (0.62 feet/year). However, small localized areas have experienced as much as 65 feet (+/-20 feet) of bluff retreat in that same time interval [2 feet/year (+/- 0.5)].

5.1.6 Marine Erosion and Sedimentation

The hazards associated with erosion and sediment transport due to the strong tidal currents in the Cook Inlet is judged to be high. The sea floor is an erosional surface cut on Quaternary deposits mantled by a discontinuous cover of shifting sand and gravel. The elevation of the sea floor may fluctuate due to sediment transport and erosion. Sediment transport and current scour may have the ability to erode pilings and other offshore/nearshore foundation structures.

5.1.7 Volcanic Hazards

The LNG onshore and marine facilities are vulnerable to volcanic ash-fall events from active volcanoes located on the west side of the Cook Inlet. Historical and geologic records show that volcanic ash-fall events are relatively common in the Cook Inlet region. Five ash-fall events have been documented in the Kenai area since 1976. In the 50-year life of the LNG plant, it is reasonable to expect that five to ten such events may occur. In larger, more extreme events volcaniclastic debris may also fallout and affect facilities and vessel traffic in portions of Cook Inlet. Ash-fall events caused by volcanic eruptions have the potential to hamper plant operations, damage machinery, slow or halt vehicle, vessel, and aviation transportation, and also negatively impact human health.

5.2 Recommendations

Recommendations are listed below in two categories – recommendations for further studies to either evaluate additional hazards or reduce uncertainty in the current hazard assessments, and recommended actions to mitigate those hazards identified in this report.

5.2.1 Recommendations for further studies

1. While the estimated tsunami run-up heights are relatively low compared to the elevation of the onshore site facility, additional evaluation may be considered to assess the significance of tsunami to coastal bluff erosion and retreat in the vicinity of the onshore facilities.
2. Consider an investigation to constrain the age of the Salamatof Road faults and thereby reduce uncertainty in the hazard of similar faulting in the LNG site. These faults have been shown to be non-tectonic in origin. However, if they were the result of earthquake ground shaking, the possibility of similar future ground displacements within the LNG facilities area should be evaluated. The argument can be made that these late Pleistocene sediments would have been most susceptible to failure during ground shaking shortly after their deposition in the Late Pleistocene, and, due to gradual densification through time, the sediments may no longer be susceptible to this kind of failure.

   The hypothesis that faults such as the Salamatof Road faults are Late Pleistocene in age is based largely on geomorphic arguments regarding the long time required to smooth over fault scarps and fill the intervening graben with sediments. This hypothesis could be confirmed and a stronger argument could be made for a low risk of future failure if geochronologic data could be collected from the graben sediments themselves. This approach has the potential to clearly establish the age of the faulting

Several shallow boreholes may be drilled in the center of the graben to obtain samples of the peat that was deposited in the depression between the faults (Plate 48). The peat can be dated by radiocarbon analysis to help constrainthe age of faulting.

5.2.2 Recommended hazard mitigations

Recommendations for the mitigation of geologic hazards addressed in this report are listed below.

1. No mitigation is recommended of surface fault rupture, folding, or tilting hazards as these hazards are judged to be low.
2. Mitigation of the ground deformation hazard due to strong ground shaking can be addressed through the ongoing geotechnical investigations and seismic engineering analyses. These studies can identify and delineate specific areas of subsurface materials that may be susceptible to liquefaction, settlement or failure, and design appropriate mitigations.
3. No mitigation is needed of tsunami hazards at the onshore LNG facility, as the height of the tsunami wave is predicted to be well below the elevation of the plant. The effects of a tsunami wave on erosion of the coastal bluffs should be considered in the development of mitigation strategies for coastal erosion (see item 4 below).
4. Mitigation of tsunami hazards to the proposed coastal and offshore LNG terminal facilities should be addressed by appropriate engineering design.
5. To mitigate ongoing coastal erosion, we suggest development of potential alternatives to protect or stabilize the bluff from wave erosion or gravitational failure. Such mitigations could include protection at the toe of the bluff (rip rap, sea walls, concrete walls), as well as slope de-watering schemes to control seeps that seem to promote debris flows. Additional mitigations could include controlling surface water runoff at the top of the bluff to minimize the amount and location of water that flows down the bluff face. The development of monitoring plan, to track changes in the face of the coastal bluff over time, would enable any problems to be identified and addressed at an early stage. LiDAR and/or laser scanning of the sea bluffs should be considered as part of the monitoring program.
6. To mitigate the hazard of current scour, seafloor erosion, and sedimentation to the marine facilities, monitoring of the seafloor is recommended. Periodic MBES bathymetry surveys may be performed to monitor changes in the seafloor elevation and topography in the facilities area. The surveys should be designed to detect potential erosion, which may undermine foundations, and sedimentation, which may affect minimum water depths required for safe operation and transit of marine vessels.

7. To mitigate the effects of the bedload carried by strong tidal currents damaging or degrading marine facilities foundations, we recommend appropriate engineering design and periodic monitoring/inspection of the condition of pilings. Conduct regular visual inspections to document erosion or degradation. Evaluation of the condition of the three existing piers in the Nikiski area may provide insights into the severity of this problem.

8. The almost certain occurrence of multiple volcanic ash-fall events during the lifetime of the plant should be considered in the design of the plant and marine terminal facilities, and in the development of operations emergency procedures.

6.0 REFERENCES

Abe, K., 1984, Magnitudes of large shallow earthquakes from 1904 to 1980: Physics of the Earth and Planetary Interiors, v. 27, p. 72–92.

Alaska Earthquake Information Center (AEIC), 2015, Earthquake Catalog, University of Alaska, Fairbanks, AK.

Alaska Earthquake Information Center (AEIC), 2016, M7.1 Iniskin Earthquake Evolving Continent, web page at http://earthquake.alaska.edu/m71-iniskin-earthquake-evolving-content, University of Alaska, Fairbanks, AK, viewed 1/29/2016.

Alaska Oil and Gas Conservation Commission, 1994, 1994 Statistical report: 230 p.

Alaska Volcano Observatory, 2016, website
https://www.avo.alaska.edu/volcanoes/volcact.php?volcname=Augustine
https://www.avo.alaska.edu/volcanoes/volcact.php?volcname=Iliamna
https://www.avo.alaska.edu/volcanoes/volcact.php?volcname=Redoubt
https://www.avo.alaska.edu/volcanoes/volcact.php?volcname=Spurr

Beget J., Gardner, C., Davis, K., 2008, Volcanic tsunami and prehistoric cultural transitions in Cook Inlet, Alaska, Journal of Volcanology and Geothermal Research v176.

Beget, J., and Kowalik, Z., 2006, Confirmation and Calibration of Computer Modeling of Tsunami Produced by Augustine Volcano, Alaska, Science of Tsunami Hazards, v24 p257.

Beget J., and Nye C., 1994, Postglacial eruption history of Redoubt Volcano, Alaska, Journal of Volcanology and Geothermal Research, v62, p31-54.

Bishop, 1982, Undrilled reserves in Cook Inlet oil fields, Alaska, in Wilson, S.T., ed., Transactions of the third Circum-Pacific energy and mineral resources conference: Circum-Pacific Council for Energy and Mineral Resources, v. 3, p. 117-121.

Boss, R.F., Lennon, R.B., and Wilson B.W., 1976, Middle Ground Shoal oil field, Alaska, *in* Braunstein, J., ed., North American oil and gas fields: American Association of Petroleum Geologists Memoir 24, p. 1–22.

Brantley, S.R., 1990, Eruption of Redoubt Volcano, Alaska – December 14, 1989 – August 31, 1990, U.S. Geological Survey Circular 1061, 33 pp.

Brantley, S. R., & Stauffer, P. H. (2000). *Volcanic Ash Fall—a "Hard Rain" of Abrasive Particles*. US Department of the Interior, US Geological Survey Fact Sheet 027-00.

Bruhn, R.L., and Haeussler, P.J., 2006, Deformation driven by subduction and microplate collision: Geodynamics of Cook Inlet Basin, Alaska. Geol. Soc. Amer. Bulletin, v. 118, no. ¾, p. 289-303.

Bucknam, R.C., and Hemphill-Haley, E., and Leopold, E.B., 1992, Abrupt uplift within the last 1,700 years at southern Puget Sound, Washington: Science, v. 258, p. 1611–1614.

Bull, William B., 1964, Alluvial fans: Journal of Geological Education, v. 16, p. 101-106.

Calderwood, K.W., and Fackler, W.C., 1972, Proposed Stratigraphic Nomenclature for the Kenai Group, Cook Inlet Basin, Alaska: A.A.P.G. Bull., v. 56, no. 4, April 1972.

Carver, G., and Plafker, G., 2008, Paleoseismicity and neotectonics of the Aleutian subduction zone – An overview, in Freymueller, J.T., et al., eds., Active Tectonics and Seismic Potential of Alaska: American Geophyiscal Union Geophysical Monograph 179, p. 43-63.

Cochran, S., 2013, Tesoro to Begin Construction of Cook Island Pipeline Next Year, Alaska Public Media, http://www.alaskapublic.org/2013/11/04/tesoro-to-begin-construction-of-cook-inlet-pipeline-next-year/, accessed February 10, 2016.

Dionne, J.C., 1992, Ice-push features: The Canadian Geographer/Le Géographe Canadien, *36*(1), 86-91.

Enos, J., and Maier, B., 2013, Kenai gas field, Cook Inlet, Alaska, *in* D. M. Stone and D. M. Hite, ed., Oil and gas fields of the Cook Inlet Basin, Alaska: AAPG Memoir 104, p. 169-192.

Federal Energy Regulatory Commission (FERC), 2007, Draft seismic design guidelines and data submittal requirements for LNG facilities – Prepared for FERC by Bachman, R., Nyman, D., Bhushan, K., Leyendecker, E.V., and Lister L.

Fisher, M.A., and Magoon, L.B., 1977, Geologic framework of lower Cook Inlet, Alaska: U.S. Geological Survey Open-File Report 77-136, 73 p.

Fisher, M.A., Detterman, R.L., and Magoon, L.B., 1987, Tectonics and petroleum geology of the Cook-Shelikof basin, southern Alaska *in* Scholl, D.W., et al., eds., Geology and resource potential of the continental margin of western North America and adjacent ocean basins, Beaufort Sea to Baja California: Houston, Texas, Circum-Pacific Council for Energy and Mineral Resources Earth Science Series, v. 6, p. 213-228.

Foster, H.L., and Karlstrom, N.V., 1967, Ground Breakage and Associated Effects in the Cook Inlet Area, Alaska, Resulting from the March 27, 1964, Earthquake, U. S. Geological Survey Professional Paper, 543-F.

Fugro-McClelland Marine Geosciences, Inc. (FMMG), 2012a, Geologic Study Potential LNG plant sites, south central Alaska, Report No. 0201-7173-2, prepared for Conoco-Phillips, Inc.

Fugro-McClelland Marine Geosciences, Inc. (FMMG), 2012b, Geologic hazard study, tsunami and surface deformation assessment of potential LNG plant sites, south central Alaska, Phase 1B desktop study – Addendum to report No. 0201-7173-2, prepared for Conoco-Phillips, Inc.

Geomega, Inc., 2006, Chevron Kenai Former Refinery 2006 Site Characterization Report, prepared for Chevron Environmental Management Company, July 11, 2006.

Grantz, A., G. Plafker, and R. Kachadoorian, 1964, Alaska's Good Friday Earthquake March 27, 1964: A Preliminary Geologic Evaluation. U. S. Geol. Survey, Circ. 491. 35 pp.

Haeussler, P. J., Bruhn, R.L. and Pratt, T.L., 2000, Potential seismic hazards and tectonics of upper Cook Inlet basin, Alaska, based on analysis of Pliocene and younger deformation, Geol. Soc. Am. Bull., 112, p 1414-1429.

Haeussler, P. J., Best, T.C., and Waythomas, C.F., 2002, Paleoseismology at high latitudes: Seismic disturbance of late Quaternary deposits along the Castle Mountain fault near Houston, Alaska, Geol. Soc. Am. Bull., 114, 1296-1310, 1 plate.

Haeussler, P.J., 2008, An overview of the neotectonics of interior Alaska—Far-field deformation from the Yakutat Microplate collision, *in* Freymueller, J.T., Haeussler, P.J., Wesson, R.L., and Ekstrom, Goran, eds., 2008, Active tectonics and seismic potential of Alaska: American Geophysical Union, Geophysical Monograph 179, p. 83–108.

Haeussler, P.J., and Saltus, R.W., 2011, Location and Extent of Tertiary Structures in Cook Inlet Basin, Alaska, and Mantle Dynamics that Focus Deformation and Subsidence: USGS Professional Paper 1776-D, 26 p.

Hance, J.J., 2003, Development of a Database and Assessment of seafloor Slope Stability based on Published Literature, Master's Thesis, University of Texas, Austin, 265 pp.

Hartman, D.C., Pessel, G.H., and McGee, D.L., 1972, Preliminary report on stratigraphy of the Kenai group, upper Cook Inlet, Alaska: Alaska Division of Geological Survey Special Report 5, 4 p., 11 sheets, scale 1:500,000. doi:10.14509/2604

Hartman, D.C., Pessel, G.H., and McGee, D.L., 1974, Stratigraphy of the Kenai group, Cook Inlet: Alaska Division of Geological & Geophysical Surveys Alaska Open-File Report 49, 7 p., 11 sheets, scale 1:500,000. doi:10.14509/149

Holdahl S.R., and Sauber, J. (1994). Coseismic Slip in the 1964 Prince William Sound Earthquake: A New Geodetic Inversion Pure Appl. Geophys. 142 (1): 55-82.

Ichinose, G., Somerville, P., Thio, H.K., Graves, R., and O'Connell, D., 2007, Rupture process of the 1964 Prince William Sound, Alaska, earthquake from the combined inversion of seismic, tsunami, and geodetic data. Journal of Geophysical Research, v. 112, B07306.

Johnson, S.Y., Potter, C.J., Armentrout, J.M., Miller, J.J., Finn, C., and Weaver, C.S., 1996, The southern Whidbey Island fault: An active structure in the Puget Lowland, Washington, Geological Society of America Bulletin, v. 108, p. 334-354.

Johnson, J.M., Satake, K., Holdahl S.R., and Sauber, J. 1996. The 1964 Prince William Sound earthquake: Joint inversion of tsunami and geodetic data. Journal of Geophysical Research 101 (BI): 523-532.

Karlstrom, T.N.V., 1964, Quaternary geology of the Kenai Lowland and glacial history of the Cook Inlet region, Alaska: U. S. Geological Survey Professional Paper 443, 69 p., 6 sheets.

Kelly, T.E., 1961, Photogeology—A quick, economical tool for oil hunters: Oil and Gas Journal, November 20, p. 265–272.

Kelly, T.E., 1963, Geology and hydrocarbons in Cook Inlet basin, Alaska, *in* Childs, O.E., and Beebe, W.B., eds., Backbone of the Americas: American Association of Petroleum Geologists Memoir 2, p. 278–296.

Kenai Peninsula Borough (KPB), 2012, Aerial Imagery, RGB and NIR (four-band), horizontal resolution of 2.5 feet.

Kenai Peninsula Borough (KPB), 2013, Draft All-Hazard Mitigation Plan: Section 2.0: Floods and Erosion.

Kenai Peninsula Borough (KPB), 2014, All-Hazard Mitigation Plan: Section 6.0 Tsunami and Seiches.

Kent & Sullivan, 1997, Characterization Report PIRM Extension Area, Tesoro Alaska Refinery Project, prepared for Tesoro Alaska Petroleum Company, Kent & Sullivan Project No. 01-19, November 20, 1997.

Kent & Sullivan, 2000, Response to EPA Comments, Upper Confined Aquifer Corrective Measure Implementation Plan, prepared for Tesoro Alaska Company, Project No. 01-12, January 26, 2000.

Kent & Sullivan, Inc., 2001, B-Aquifer Plume Investigation Report, Characterization Study and Pilot Tests, Tesoro Alaska Refinery, prepared for Tesoro Alaska Company, Project Nos. 01-51 and 01-55, January 4, 2001.

Kenyon, N.H. 1970. Sand ribbons of European tidal seas. Marine Geology 9: p. 25-39.

Kienle, J., Kowalik, Z., and Murty, T.. (1987) Tsunami Generated by Eruptions from Mount St. Augustine Volcano, Alaska Science 236: 1442-1447

Kienle, J., Kowalik, Z., and Troshina, E. (1996) Propagation and runup of tsunami waves generated by Mt. St. Augustine Volcano, Alaska. Science of Tsunami Hazards 14 (3): 191-206.

Kirschner, C.E., and Lyon, C.A., 1973, Stratigraphic and tectonic development of Cook Inlet petroleum province, *in* Pitcher, M.G., ed., Arctic geology: American Association of Petroleum Geologists Memoir 19, p. 396-407.

Koehler, R.D., Farrell, R. E., Burns, P.A.C. and Combellick, R. A., 2012, Quaternary faults and folds in Alaska: A digital database: Alaska Division of Geological & Geophysical Surveys Miscellaneous Publication 141, 31 p., 1 sheet, scale 1:3,700,000.

Kowalik, Z. and Proshutinsky, A., 2010, Tsunami-tide interactions: A Cook Inlet case study, Continental Shelf Research, Vol. 30, p. 633-642.

Lander, J.F., 1996, Tsunamis Affecting Alaska 1737-1996, National Oceanographic and Atmospheric Administration (NOAA), 195 pp.

LePain, D.L, Stanley, R.G., Hemold, K.P., and Shellenbaum, D.P., 2013, Geologic framework and petroleum systems of Cook Inlet Basin, South Central Alaska, *in* Stone, D.M. and Hite, D.M., ed. Oil and Gas Fields of the Cook Inlet Basin, Alaska: AAPG Memoir 104, p. 37-116.

Lim, E., B.W. Eakins, and R. Wigley, 2011, Coastal Relief Model of Southern Alaska: Procedures, Data Sources and Analysis, NOAA Technical Memorandum NESDIS NGDC-43, 22 pp.

Magoon, L.B., Adkinson, W.L., and Egbert, R.M., 1976, Map showing geology, wildcat wells, Tertiary plant fossil localities, K-Ar age dates, and petroleum operations, Cook Inlet area, Alaska: US Geological Survey Miscellaneous Investigations Series Map I-1019, scale 1:250 000.

McElmoyl, C., 2013, Cannery Loop field, Cook Inlet region, Kenai Borough, Alaska, in D. M. Stone and D. M. Hite eds., Oil and gas fields of the Cook Inlet Basin, Alaska: AAPG Memoir 104, p. 193–224.

National Geophysical Data Center / World Data Center (NGDC/WDC) Historical Tsunami Database, Boulder, CO, USA. (Available at http://www.ngdc.noaa.gov/hazard/tsu_db.shtml: data accessed September 2014)

National Oceanic and Atmospheric Administration (NOAA), 2012, Global sea level rise scenarios for the United States National Climate Assessment: NOAA Technical Report OAR CPO-1, 29 p.

National Oceanic and Atmospheric Administration (NOAA), 2016a, Tides and Currents, PORTS ®: 9455760 Nikiski, AK, https://tidesandcurrents.noaa.gov/ports/ports.html?id=9455760&mode=allwater, accessed February 10, 2016.

National Oceanic and Atmospheric Administration (NOAA), 2016b, FAQ – Tide Predictions and Data, http://tidesandcurrents.noaa.gov/faq2.html#26, accessed February 10, 2016.

National Oceanic and Atmospheric Administration (NOAA), 2016c, Mean Sea Level Trend, 9455760, Nikiski, Alaska, http://tidesandcurrents.noaa.gov/sltrends/sltrends_station.shtml?stnid=94557602.

Natural Gas Act (NGA), 15 U.S.C. § 717a (11),2006.

Nichols, G., 1999, Sedimentology and Stratigraphy, Blackwell Science, USA, 355 pp.

Pacific Alaska, LNG Associates, 1978, Western LNG Project Final Environmental Impact Statement, Volume 1, Construction and Operation of an LNG Liquefaction Terminal at Nikiski, Alaska; Federal Energy Regulatory Commission Office of Pipeline and Producer Regulation FERC/EIS-0002F.

Page, R.A., Biswas, N.N., Lahr, J.C., Pulpan, H., 1991, Seismicity of continental Alaska, *in* Slemmons, D.B., Engdahl, E.R., Zoback, M.R., and Blackwell, D.D., eds., Neotectonics of North America: Boulder, Colorado, Geological Society of America, Decade Map Volume 1, p. 47-68.

Paull, C.K., Caress, D.W., Thomas, H., Lundsten, E., Anderson, K., Gwiazda, R., Riedel, M., McGann, M., and Herguera, J.C., 2015, Seafloor geomorphic manifestations of gas venting and shallow subbottom gas hydrate occurrences, Geosphere, Vol. 12, No. 1., doi 10.1130/GES01012.1

Perry, S.E., Garver, J.I., and Ridgway, K.D., 2009, Transport of the Yakutat terrane, Southern Alaska: evidence from sediment petrology and detrital zircon fission-track and U/Pb double dating: Journal of Geology, v. 117, p. 156-173.

Plafker, G., 1969, Tectonics of the March 27, 1964 Alaska earthquake: The Alaska Earthquake Series, U.S. Geological Survey, Professional Paper 543-1, p. 71.

Ratchkovski, N.A., Pujol, J., and Biswas, N.N., 1998, Relocation of shallow earthquakes in southern Alaska using Joint Hypocenter Determination method: Journal of Seismology 2, p. 87-102.

Reger, R.D., Sturmann, A.G., Berg, E.E., and Burns, P.A.C., 2007, A guide to the late Quaternary history of northern and western Kenai Peninsula, Alaska: Division of Geological and Geophysical Surveys Guidebook 8, 120 p., 6 plates.

Reger, R., 2014, Personal communication at informal meetings with Janet Sowers and David Trench on September 9-10, 2014, in Kenai, Alaska.

Reger, R., 2014, Personal communication, Ice-shoved ramparts: unpublished illustration transmitted by e-mail to Janet Sowers on September 11, 2014.

Schaefer, J., Bull, K.F., Cameron, C., Coombs, M., Diefenbach, A.K., Leonard, G., Lopez, T., McNutt, S., Neal, C., Payne, A., Power, J., Schneider, D., Scott, W., Snedigar, S., Thompson, G., Wallace, K., Waythomas, C., Wilson, T., Webley, P., Werner, C., 2012. The 2009 eruption of Redoubt Volcano, Alaska. Alaska Division of Geological & Geophysical Surveys Report of Investigations 2011–5, 45 p.

Schumacher, J.D. (editor), 2005, Cook Inlet Physical Oceanography Workshop Proceedings, Alaska Ocean Observing System (AOOS), 112 pp.

Sharma, G.D., and Burrell, D.C., 1970, Sedimentary Environment and Sediments of Cook Inlet, Alaska, American Association of Petroleum Geologists Bulletin, Vol. 54, No. 4, p. 647-654.

Sharp, R. P., 1988, Living ice: understanding glaciers and glaciation, Chapter 8: Products of glacial deposition: Cambridge University Press, New York, NY,.

Shellenbaum, D.P., Gregersen L.S., and Delaney, P.R., 2010, Top Mesozoic unconformity depth map of the Cook Inlet Basin, Alaska, Alaska Division of Geological and Geophysical Surveys, Report of Investigations 2010-2, Sheet 1 of 1.

Shellenbaum, D. P., 2013, Seismic data acquisition, processing, and interpretation in the Cook Inlet Basin – Local geologic and logistical impacts, *in* D. M. Stone and D. M. Hite, ed. Oil and gas fields of the Cook Inlet Basin, Alaska:

Shennan I., Bruhn, R., Barlow, N., Good, K., and Hocking E., 2014, Late Holocene great earthquakes in the eastern part of the Aleutian megathrust: Quaternary Science Reviews, v. 28, p. 6-13.

Sokolowski, T. 2004. The Great Alaskan Earthquake & Tsunami of 1964. West Coast & Alaska Tsunami Warning Center, Palmer, Alaska.

Stephens, C.D., Page, R.A., Lahr, J.C., and Fogleman, K.A., 1995, Crustal seismicity in the Anchorage region of Alaska: Geological Society of America Abstracts with Programs, v. 27, no. 5, p. 78–79.

Sugiyama, Y., 1995, Geological background of the 1995 Hyogo–Ken Nambu (Kobe) earthquake: Eos (Transactions, American Geophysical Union), v. 76, p. F371.

Suito, H., and Freymueller, J.T. (2009) A viscoelastic and afterslip postseismic deformation model for the 1964 Alaska earthquake. Journal of Geophysical Research 114: B11404. doi:10.1029/2008JB005954.

Suppe, J., and Medwedeff, D. A., 1990, Geometry and kinematics of fault-propagation folding: Eclogae Geol. Helv., v. 83, no. 3, p. 409-454.

Swanson, S. E., and Kienle, J., 1988, The 1986 eruption of Mount St. Augustine: field test of a hazard evaluation: Journal of Geophysical Research, v. 93, n. B5, p. 4500-4520.

U.S. Army Corps of Engineers, 2011, Kenai River Bluff Limited Economic, Cultural and Historic Property Evaluation – February 2011, Report produced by Tetra Tech, Surface Water Group, Seattle, WA.

U.S. Department of Agriculture, 2005, Soil Survey of Western Kenai Peninsula Area, Alaska: Natural Resources Conservation Service, National Cooperative Soil Survey, available at , 618 pages.

U.S. Fish and Wildlife Service, 1950, scanned and georectified black and white aerial photography, obtained in digital GIS format from U.S. Fish and Wildlife Service in Soldotna, Alaska, September 2014.

U.S. Geological Survey (USGS), 1980, Color infrared aerial photography, AR1VEYHF0010108, 1:32,000, obtained from earthexplorer.usgs.gov October 2014.

U.S. Geological Survey (USGS), 1999, National Elevation Dataset (30 meters), EROS Data Center; Data obtained Sept 2014.

U.S. Geological Survey (USGS), 2008, National Elevation Dataset, 1/9 arc second (2.5 meters), LiDAR derived digital elevation model, EROS Data Center, Data obtained Sept 2014 from USGS.

Waythomas, C. F., Dorava, J. M., Miller, T. P., Neal, C. A., and McGimsey, R. G., 1997, Preliminary volcano-hazard assessment for Redoubt Volcano, Alaska: U.S. Geological Survey Open-File Report OF 97-857, 40 p., 1 plate.

Waythomas, C.F., 2000, Reevaluation of tsunami formation by debris avalanche at Augustine Volcano, Alaska, Pure and Applied Geophysics, v157 p1145-1188.

Waythomas, C. F., and Miller, T. P., 1999, Preliminary volcano-hazard assessment for Iliamna Volcano, Alaska: U.S. Geological Survey Open-File Report OF 99-0373, 31p., 1 sheet.

Waythomas, C. F., and Nye, C. J., 2001, Preliminary volcano-hazard assessment for Mount Spurr Volcano, Alaska: U.S. Geological Survey Open-File Report OF 01-0482, 46 p.

Waythomas, C. F., and Waitt, R. B., 1998, Preliminary volcano-hazard assessment for Augustine Volcano, Alaska: U.S. Geological Survey Open-File Report OF 98-0106, 39p., 1 plate.

Waythomas, C. F., Watts, P., and Walder, J.S., 2006, Numerical simulation of tsunami generation by cold volcanic mass flows at Augustine Volcano, Alaska, Natural Hazards Earth Systems, Science, v.6, p.671-685.

Waythomas, C. F., Dorava, J. M., Miller, T. P., Neal, C. A., and McGimsey, R. G., 1997, Preliminary volcano-hazard assessment for Redoubt Volcano, Alaska: U.S. Geological Survey Open-File Report OF 97-857, 40 p., 1 plate, scale unknown.

Wesnousky, S.G., and Scholz, C.H., 1982, Deformation of an island arc: Rates of moment release and crustal shortening in intraplate Japan determined from seismicity and Quaternary fault data: Journal of Geophysical Research, v. 87, p. 6829–6852.

Wesson, R. L., Boyd, O. S., Mueller, C. S., Bufe, C. G., Frankel, A. D., Petersen, M. D., 2007, Revision of time-Independent probabilistic seismic hazard maps for Alaska: US Geological Survey Open-File Report 2007-1043.

Wilson, F.H., Hults, C.P., Schmoll, H.R., Haeussler, P.J., Schmidt, J.M., Yehle, L.A., and Labay, K.A., 2009, Preliminary geologic map of the Cook Inlet region, Alaska, including parts of the Talkeetna, Talkeetna Mountains, Tyonek, Anchorage, Lake Clark, Kenai, Seward, Illiamna, Seldovia, Mount Katmai, and Afognak 1:250,000-scale quadrangles. U.S. Department of the Interior, USGS.

Wilson, F.H., Hults, C.P., Mull, C.G, and Karl, S.M, comps., 2015, Geologic map of Alaska: U.S. Geological Survey Scientific Investigations Map 3340, pamphlet 196 p., 2 sheets, scale 1:1,584,000, http://dx.doi.org/10.3133/sim3340

Zimmerman and Prescott, 2014, AFSC/RACE: Cook Inlet Grid, National Oceanic and Atmosphere Administration (NOAA).

ILLUSTRATIONS

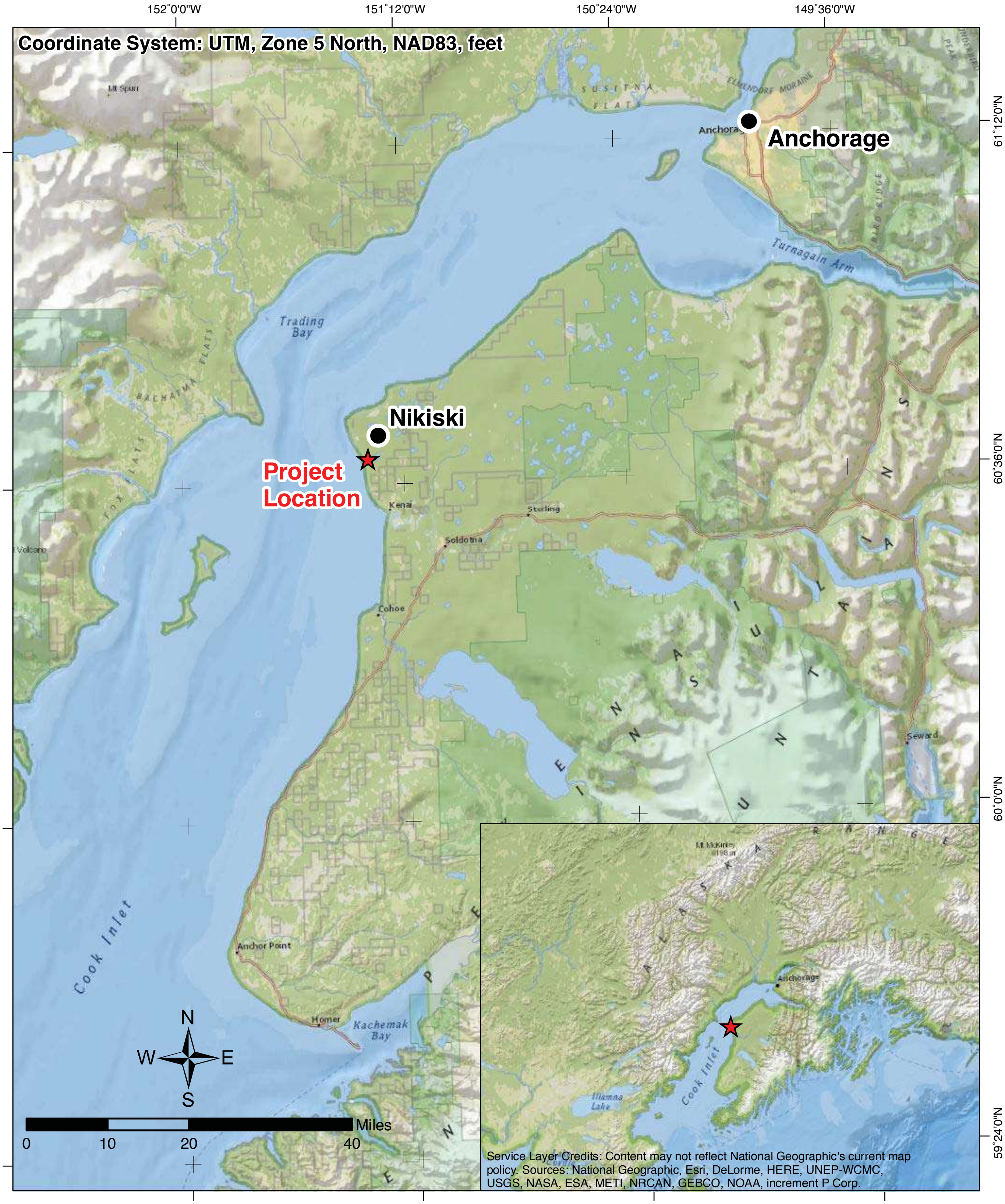

VICINITY MAP
LNG FACILITIES
ALASKA LNG PROJECT
NIKISKI, ALASKA

PLATE 1

R:\04100\2014 Projects\04.10140094 - AKLNG\05_GIS\Outputs\03_PROGRESS\VicinityMap\MXD\20141208_VicinityMap.mxd, 12/7/2015, KimK

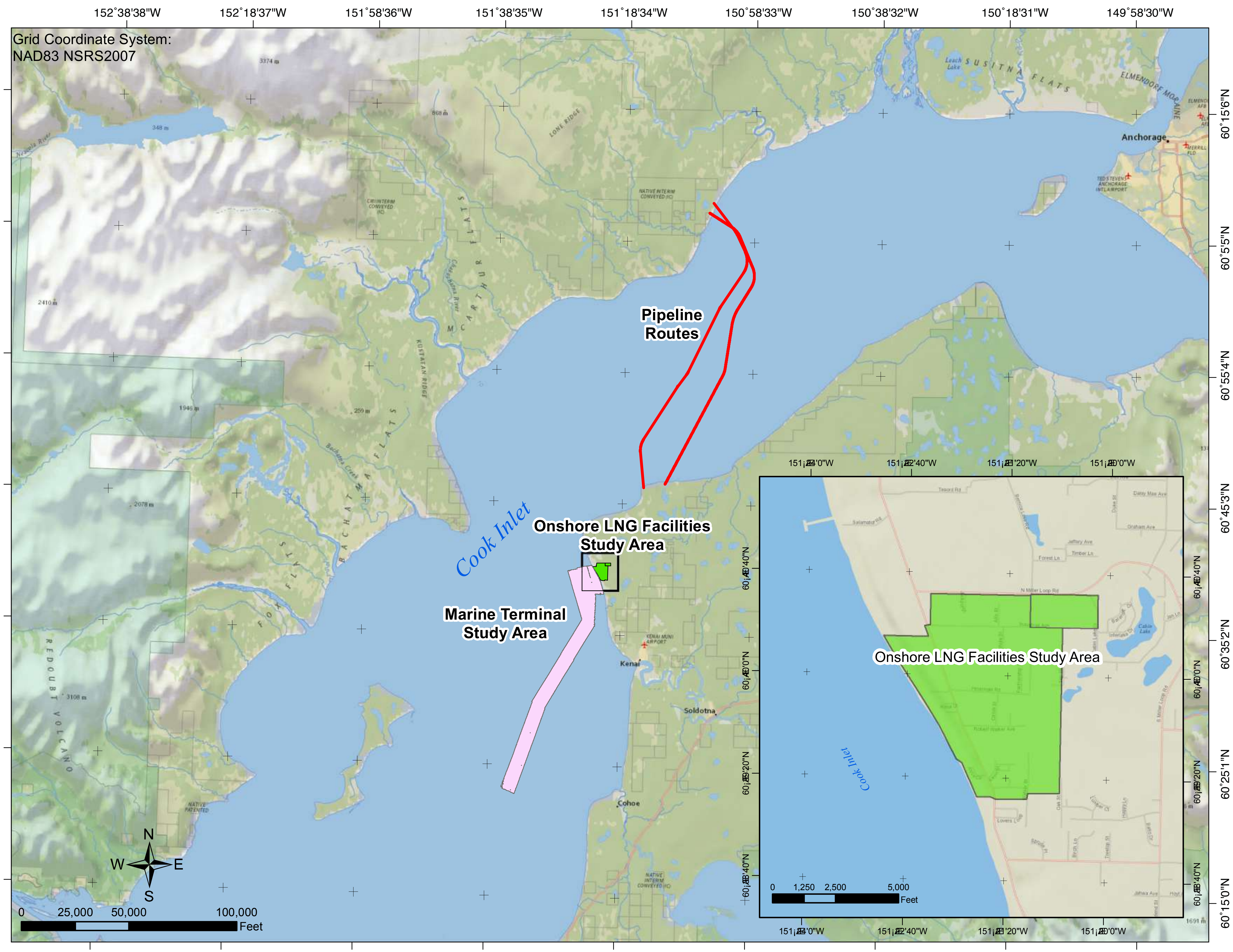

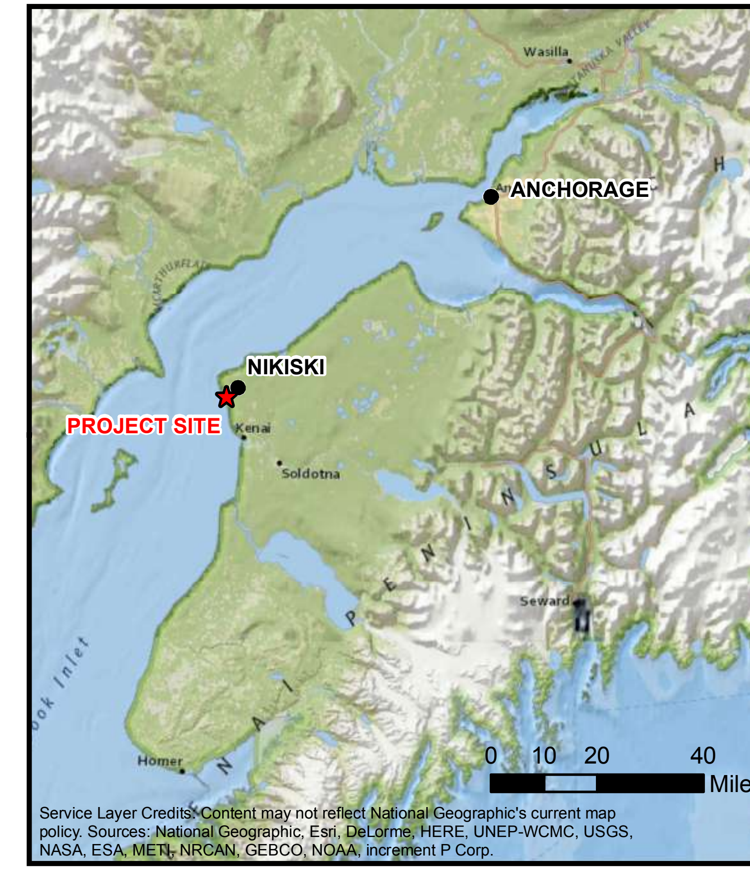

KEY MAP

LEGEND

- Onshore LNG Facilities Study Area
- Marine Terminal Study Area
- Pipeline Routes

NOTE:

1. Onshore LNG Facilities Study Area boundary provided by AKLNG.

OVERALL SITE MAP
LNG FACILITIES
ALASKA LNG PROJECT
NIKISKI, ALASKA

PLATE 2

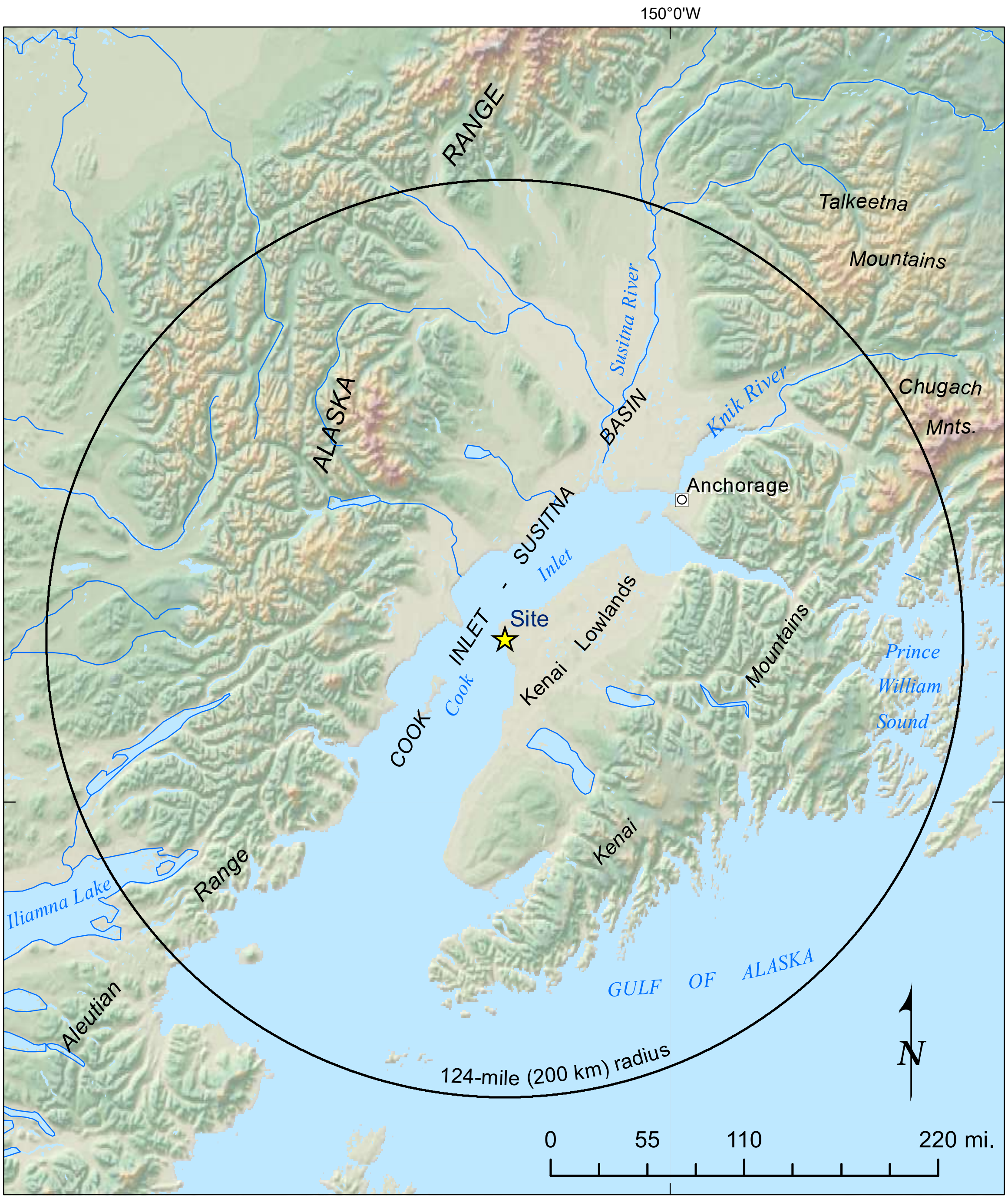

Elevation data from GEBCO

P:\Projects\10_0000\10_140334_AKLNG_PreFEED_Phase2\05_Graphics\10_140334 Geohazards Report\03_D_388_Regional Physiography.mxd; jholmberg; 6/9/2016

REGIONAL PHYSIOGRAPHY

LNG FACILITIES
ALASKA LNG PROJECT
NIKISKI, ALASKA

PLATE 3

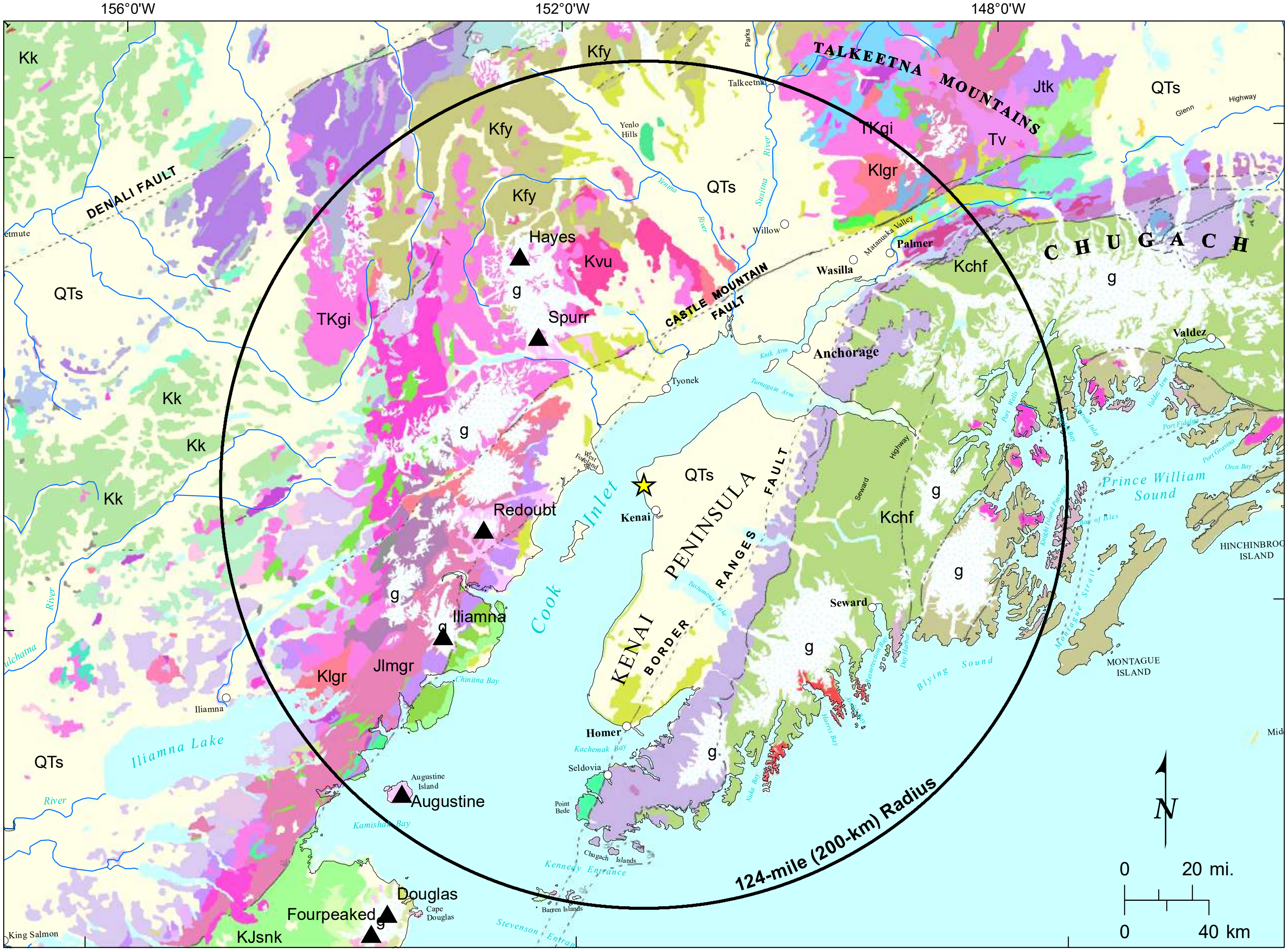

Geology from Wilson et al, 2015 (USGS SIM 3340)

For explanation of units, see Plate 5.

Legend

☆ Site

▲ Volcano

REGIONAL GEOLOGIC MAP

LNG FACILITIES
LNG PROJECT
NIKISKI, ALASKA

PLATE 4

Unit Symbol	Unit Name	Unit Age
bu	Bedrock of unknown type or age or areas not mapped	unknown
DCwbl	Farewell basinal facies carbonate rocks	Devonian or older
DZwp	Farewell platform facies	Upper Devonian, Frasnian to Neoproterozoic
g	Glaciers	Present
JDmc	Mystic structural complex, undivided	Jurassic to Devonian
Jegr	Intermediate to mafic plutonic rocks	Early Jurassic
Jlmgr	Plutonic rocks	Late and Middle Jurassic
JPk	Kakhonak Complex and Tlikakila complex of Carlson and Wallace (1983)	Jurassic, Triassic, and older?
Jsct	Shelikof and Chinitna Formations and Tuxedni Group	Middle Jurassic
Jtk	Talkeetna Formation	Early Jurassic
JTrkp	Limestone and volcanic rocks of the Kenai Peninsula	Early Jurassic and Late Triassic, Norian
JTrmv	Tatina River volcanics of Bundtzen and others (1997a) (Mystic structural complex)	Jurassic and Triassic
JTrsch	Blueschist of southern Alaska	Early Jurassic to Triassic
Kcca	Coquina and calcarenite	Lower Cretaceous
Kchf	Chugach accretionary complex	Cretaceous
Keg	Granodiorite and other plutonic rocks	Early Cretaceous, Aptian to Hauterivian
Kfy	Flysch	Upper and Lower? Cretaceous
KJgn	Gravina-Nuzotin unit	Lower Cretaceous and Upper Jurassic
KJgu	Plutonic rocks and dikes	Cretaceous to Jurassic
KJsnk	Staniukovich and Naknek Formations, Kotsina Conglomerate, and similar rocks of southern Alaska	Lower Cretaceous to Jurassic, Pliensbachian
KJyh	Graywacke of the Yenlo Hills	Cretaceous? and uppermost Jurassic
Kk	Kuskokwim Group, undivided	Upper Cretaceous to upper Lower Cretaceous
Klgr	Intermediate granitic rocks	Late Cretaceous
Kmgr	Granitic rocks of central and southeast Alaska	Cretaceous, Coniacian to Albian
Kmuc	McHugh and Uyak Complexes and similar rocks	Late Cretaceous
Knmt	Nonmarine to shelf sedimentary rocks	Tertiary? and Cretaceous
Kps	Pelitic schist	Late Cretaceous
KPzum	Mafic and ultramafic rocks in southern Alaska	Cretaceous to late Paleozoic
Ksmd	Shallow to moderate depth sedimentary rocks	Upper Cretaceous to upper Lower Cretaceous
KTrvs	Volcanic and sedimentary rocks of southwest Alaska	Cretaceous to Triassic?
Kvu	Volcanic rocks, undivided	Cretaceous
PDms	Sedimentary rocks of the Mystic structural complex	Permian to Devonian
PIPsm	Strelna Metamorphics and related rocks	early Permian to Middle Pennsylvanian
QTgm	Yakataga and Tugidak Formations	Quaternary and uppermost Tertiary
QTs	Unconsolidated and poorly consolidated surficial deposits	Quaternary, Pleistocene, and uppermost Tertiary
QTvi	Young volcanic and shallow intrusive rocks	Quaternary or late Tertiary
SCwbc	Farewell basinal facies clastic rocks	Silurian to upper Cambrian
Tcb	Coal-bearing sedimentary rocks	Tertiary, Pliocene to Eocene?
Tcl	Copper Lake Formation	Tertiary, Eocene to Paleocene
Tehi	Felsic dikes, sills, and small stocks in southern Alaska	Tertiary and older?
Tgb	Gabbroic rocks in southern Alaska	Tertiary
Thi	Hypabyssal intrusions	Tertiary
TKgi	Granitic rocks of southern and interior Alaska	Tertiary, Paleocene to Cretaceous, Maastrichtian
TKm	Mafic intrusive rocks	Tertiary to Late Cretaceous or older
Tknt	Nearshore and nonmarine sedimentary rocks in southern Alaska	Tertiary
TKpr	Flows and pyroclastic rocks	early Tertiary to Late Cretaceous
Tmi	Younger granitic rocks	Tertiary, Pliocene to Miocene
TMzmb	MacLaren metamorphic belt of Smith and Lanphere (1971)	Tertiary to Jurassic or older?
Toeg	Granitic rocks in southern Alaska	Tertiary, Oligocene and Eocene
Togum	Mafic and ultramafic rocks of the Valdez and Orca Groups	Tertiary, Eocene to Paleocene
Togv	Volcanic rocks of the Orca Group and Ghost Rocks Formation	Tertiary, Eocene to Paleocene
Tovs	Sedimentary and volcanic rocks of the Orca Group, undivided	Tertiary, Eocene to Paleocene
Tpgi	Granitic intrusive rocks of the Chugach accretionary complex	Tertiary, Paleocene
TPzi	Undivided dikes and sills	Tertiary to Paleozoic?
Trcs	Calcareous sedimentary rocks	Upper Triassic, middle? Norian and upper Carnian
TrIPms	Skolai and Mankomen Groups, undivided	Triassic to Pennsylvanian
Trmb	Massive basalt and greenstone	Triassic
Trmls	Marble and limestone of Wrangellia	Triassic
Trqd	Quartz diorite and granodiorite	Triassic
Trsf	Shuyak Formation, undivided	Upper Triassic
Tsu	Sedimentary rocks, undivided	Tertiary
Tv	Volcanic rocks, undivided	Tertiary
Tvcs	Volcanic and sedimentary rocks	Tertiary, Oligocene and Eocene
Tvme	Older volcanic rocks, undivided	Tertiary, early Miocene to Eocene
Tvpm	Younger volcanic rocks, undivided	Tertiary, Pliocene and Miocene

\\fwla-wc-file1\project\Projects\10_0000\10_140334_AKLNG_PreFEED_Phase2\05_Graphics\10_140334 Geohazards Report

EXPLANATION OF REGIONAL GEOLOGIC UNITS
LNG FACILITIES
ALASKA LNG PROJECT
NIKISKI, ALASKA

PLATE 5

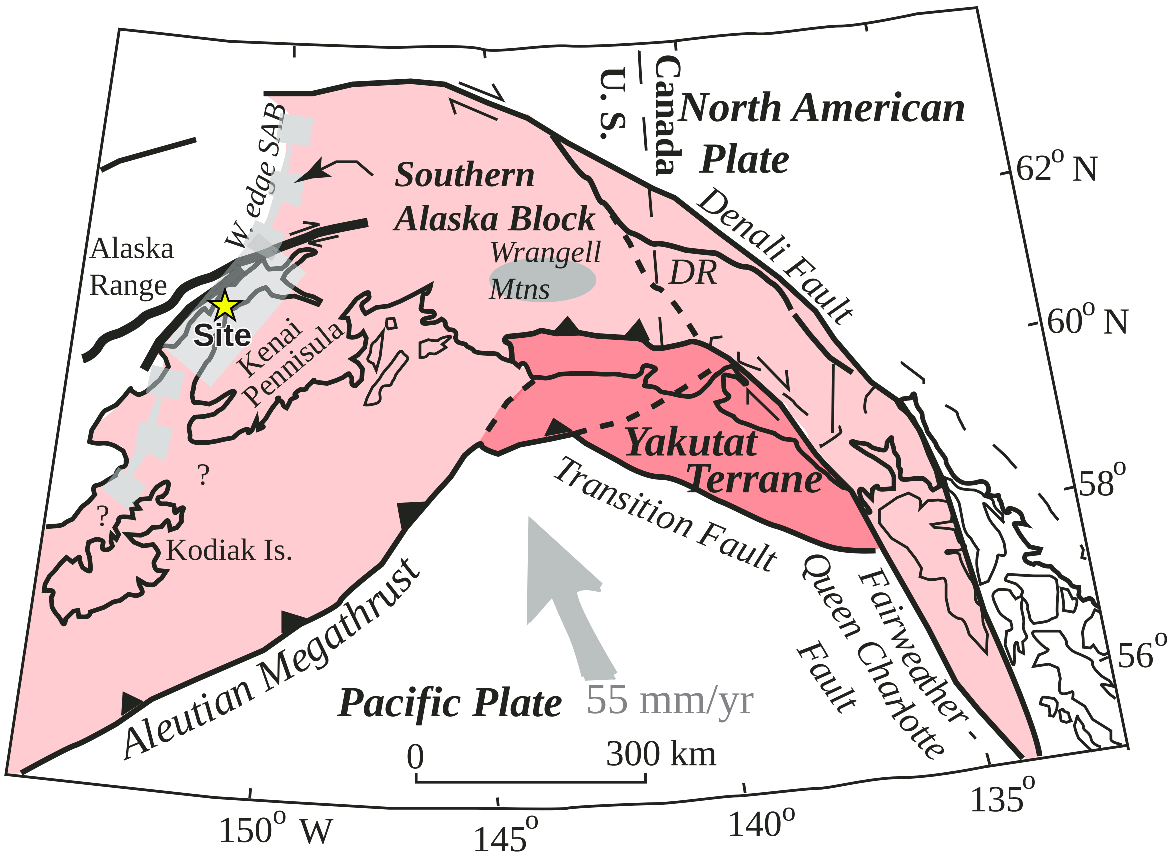

Modified from Bruhn and Haeussler (2012).

TECTONIC PLATES AND MAJOR STRUCTURAL BOUNDARIES OF SOUTHERN ALASKA

LNG FACILITIES
ALASKA LNG PROJECT
NIKISKI, ALASKA

PLATE 6

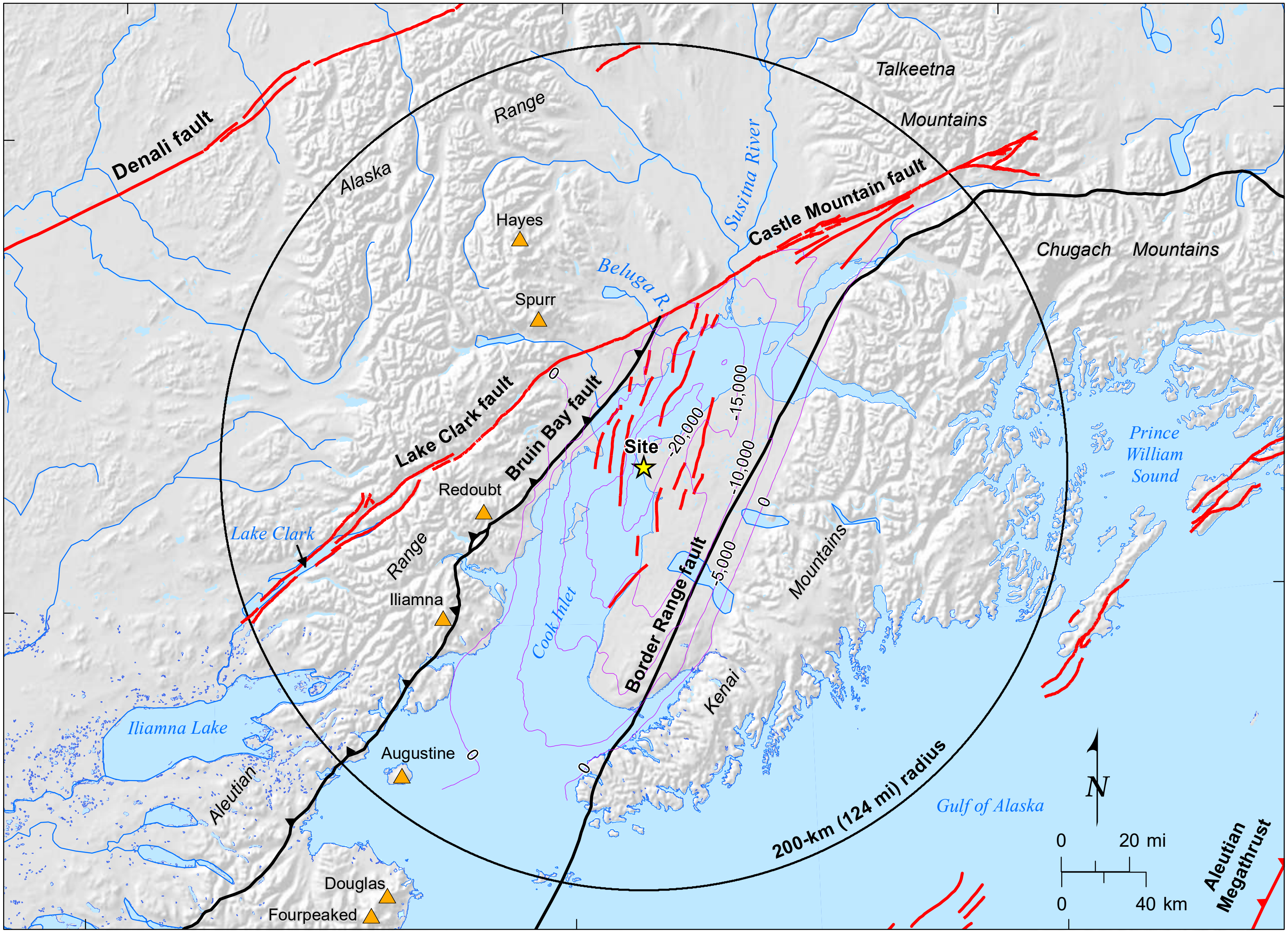

Legend

- Pre-Quaternary fault (Plafker et al., 1994)
- Quaternary-active fault, Koehler et al. (2012)
- Volcano
- 15,000 Depth of Cook Inlet Basin, 5,000-foot contours (modified from Schellenbaum et al., 2010)

REGIONAL TECTONIC MAP
LNG FACILITIES
ALASKA LNG PROJECT
NIKISKI, ALASKA

PLATE 7

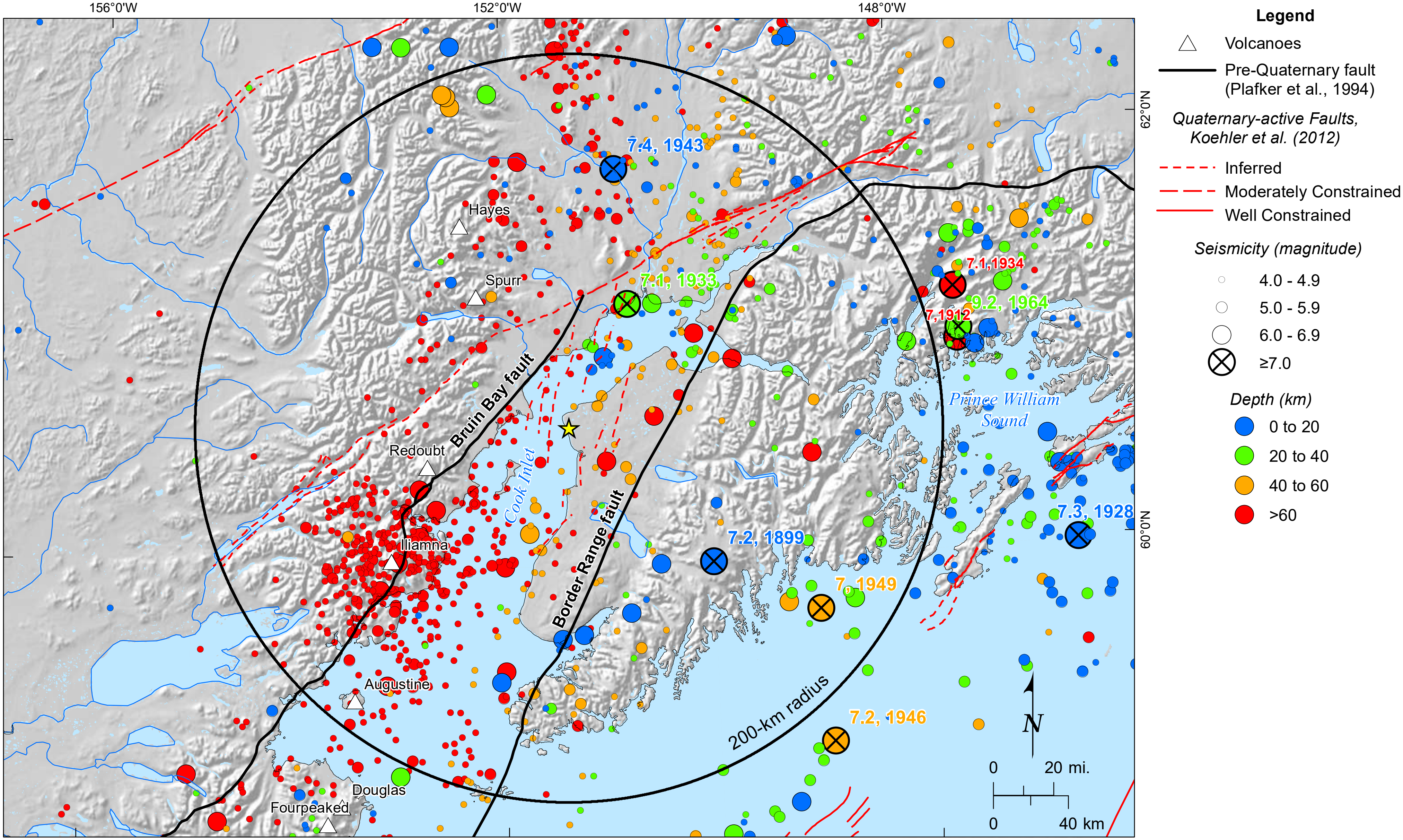

Seismicity from AEIC (1899-2015)

SEISMICITY MAP
LNG FACILITIES
ALASKA LNG PROJECT
NIKISKI, ALASKA

PLATE 8

P:\Projects\10_0000\10_140334_AKLNG_PreFEED_Phase2\05_Graphics\10_140334 Geohazards Report\08_D-19_Regional Seismicity.mxd; jholmberg; 6/8/2016

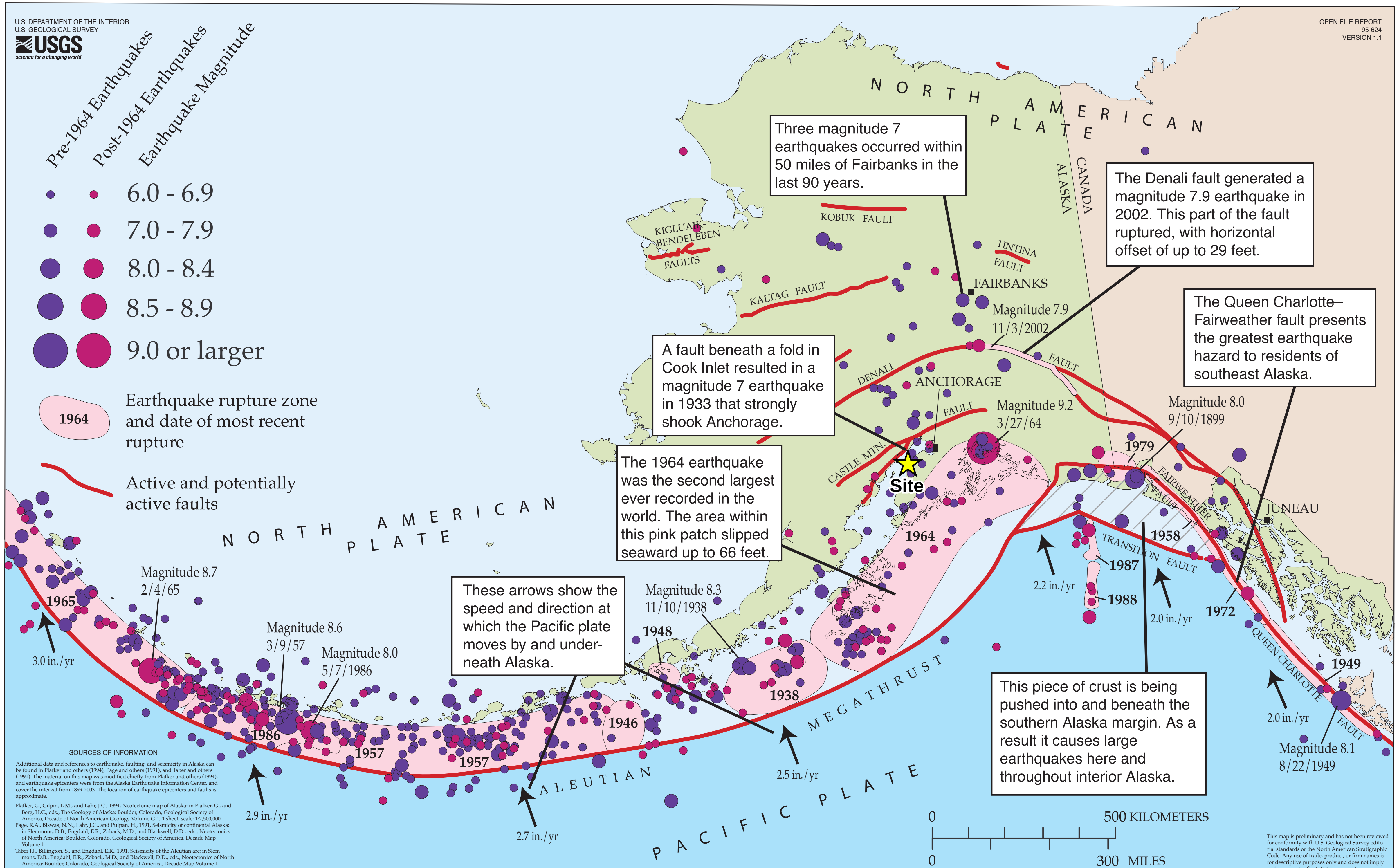

By Peter J. Haeussler and George Plafker, 2004.

Earthquake risk is high in much of the southern half of Alaska, but it is not the same everywhere. This map shows the overall geologic setting in Alaska that produces earthquakes. The Pacific plate (darker blue) is sliding northwestward past southeastern Alaska and then dives beneath the North American plate (light blue, green, and brown) in southern Alaska, the Alaska Peninsula, and the Aleutian Islands. Most earthquakes are produced where these two plates come into contact and slide past each other. Major earthquakes also occur throughout much of interior Alaska as a result of collision of a piece of crust with the southern margin.

EARTHQUAKES IN ALASKA
LNG FACILITIES
ALASKA LNG PROJECT
NIKISKI, ALASKA

PLATE 9

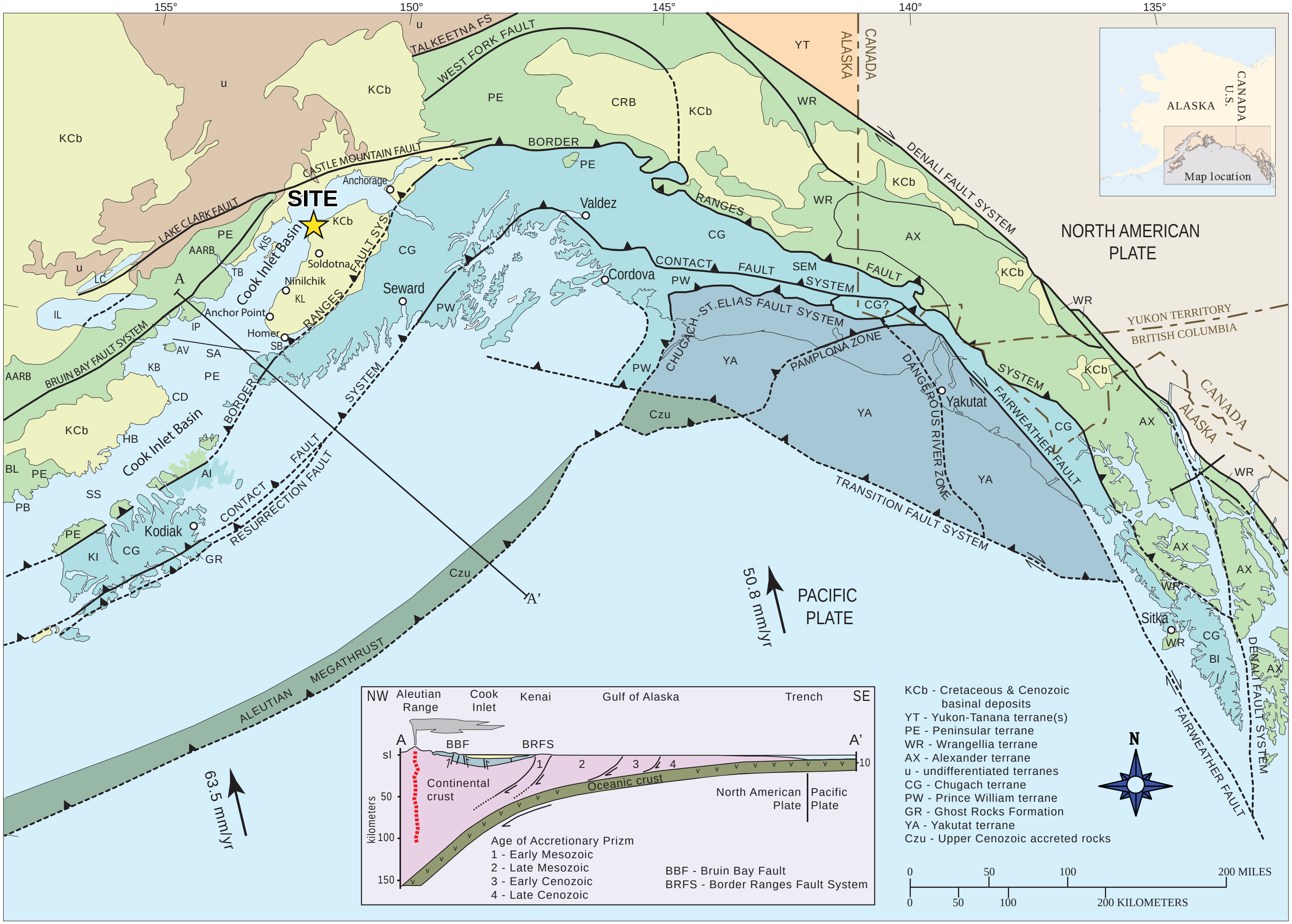

Source: Le Pain et al., 2013.

TECTONIC MAP OF SOUTHERN ALASKA
LNG FACILITIES
ALASKA LNG PROJECT
NIKISKI, ALASKA

PLATE 10

/fwla-wc-file1/project/Projects/10_0000/10_140334_AKLNG_PreFEED_Phase2/05_Graphics/10_140334 Geohazards Report

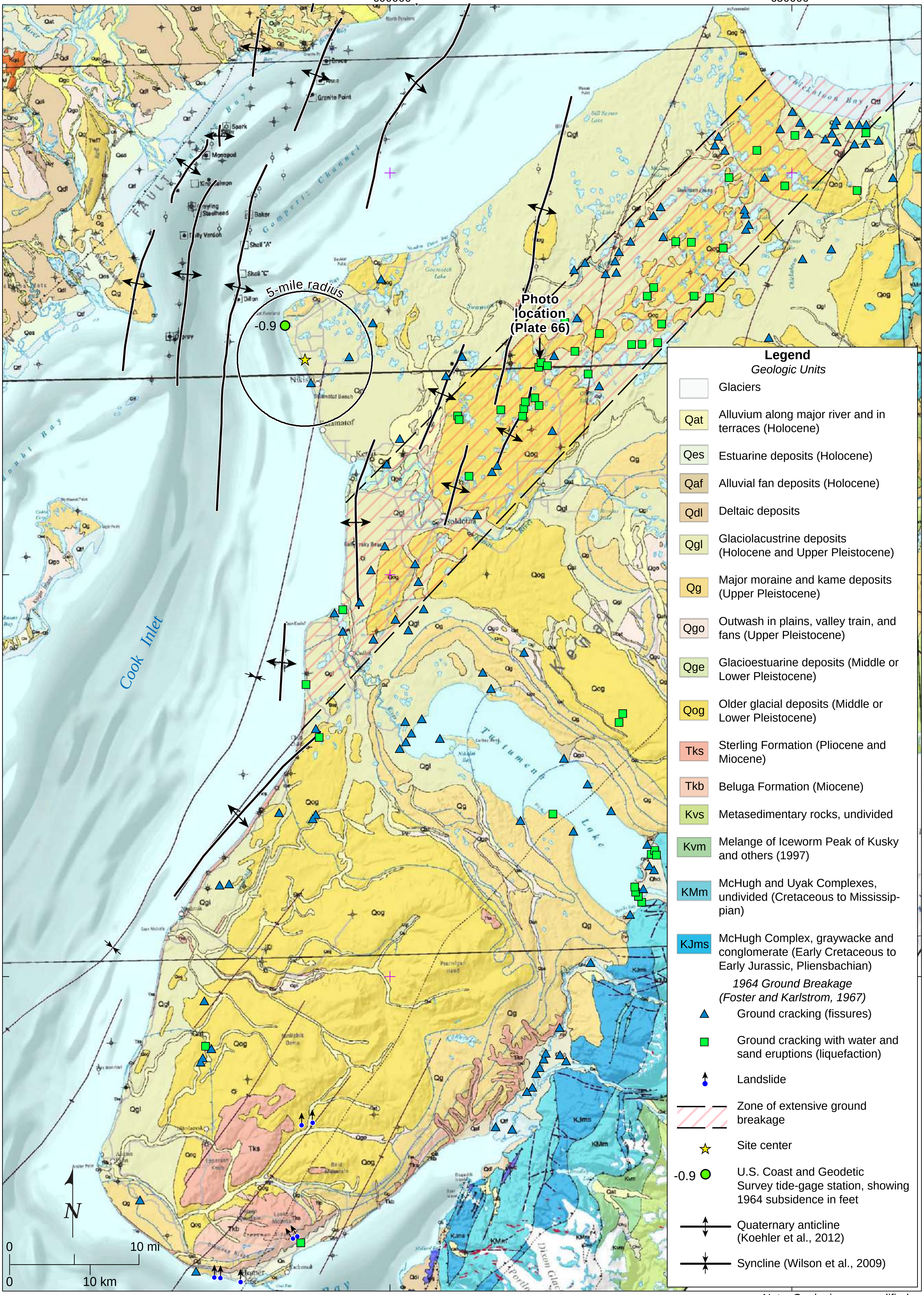

Note: Geologic map modified from Wilson et al., 2009

/fwla-wc-file1/project/Projects/10_0000/10_140334_AKLNG_PreFEED_Phase2/05_Graphics/10_140334 Geohazards Report

GEOLOGIC MAP OF THE KENAI LOWLAND SHOWING GROUND BREAKAGE FROM THE 1964 Mw 9.2 EARTHQUAKE

LNG FACILITIES
ALASKA LNG PROJECT
NIKISKI, ALASKA

PLATE 11

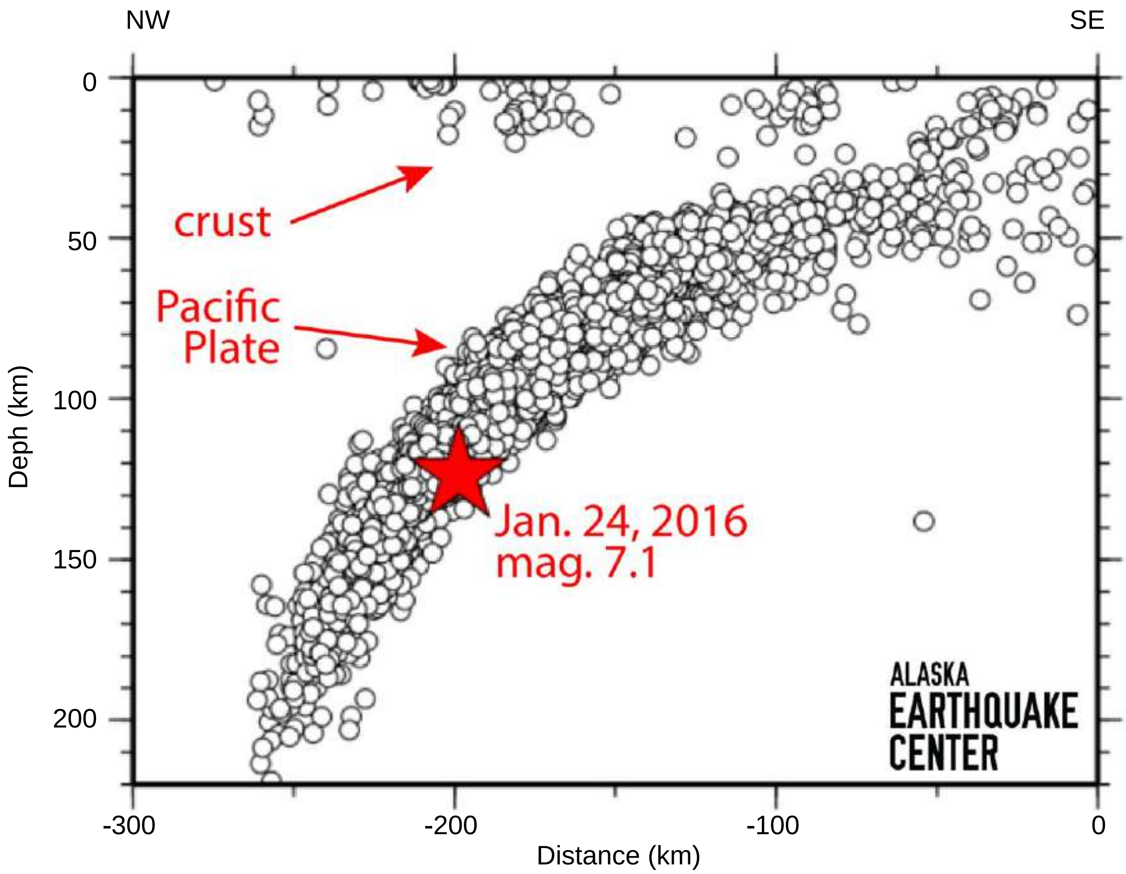

Source: Alaska Earthquake Center, 2016.

\\fwla-wc-file1/project/Projects/10_0000/10_140334_AKLNG_PreFEED_Phase2/05_Graphics/10_140334 Geohazards Report

EARTHQUAKE CROSS SECTION THROUGH THE COOK INLET REGION

LNG FACILITIES
ALASKA LNG PROJECT
NIKISKI, ALASKA

PLATE 12

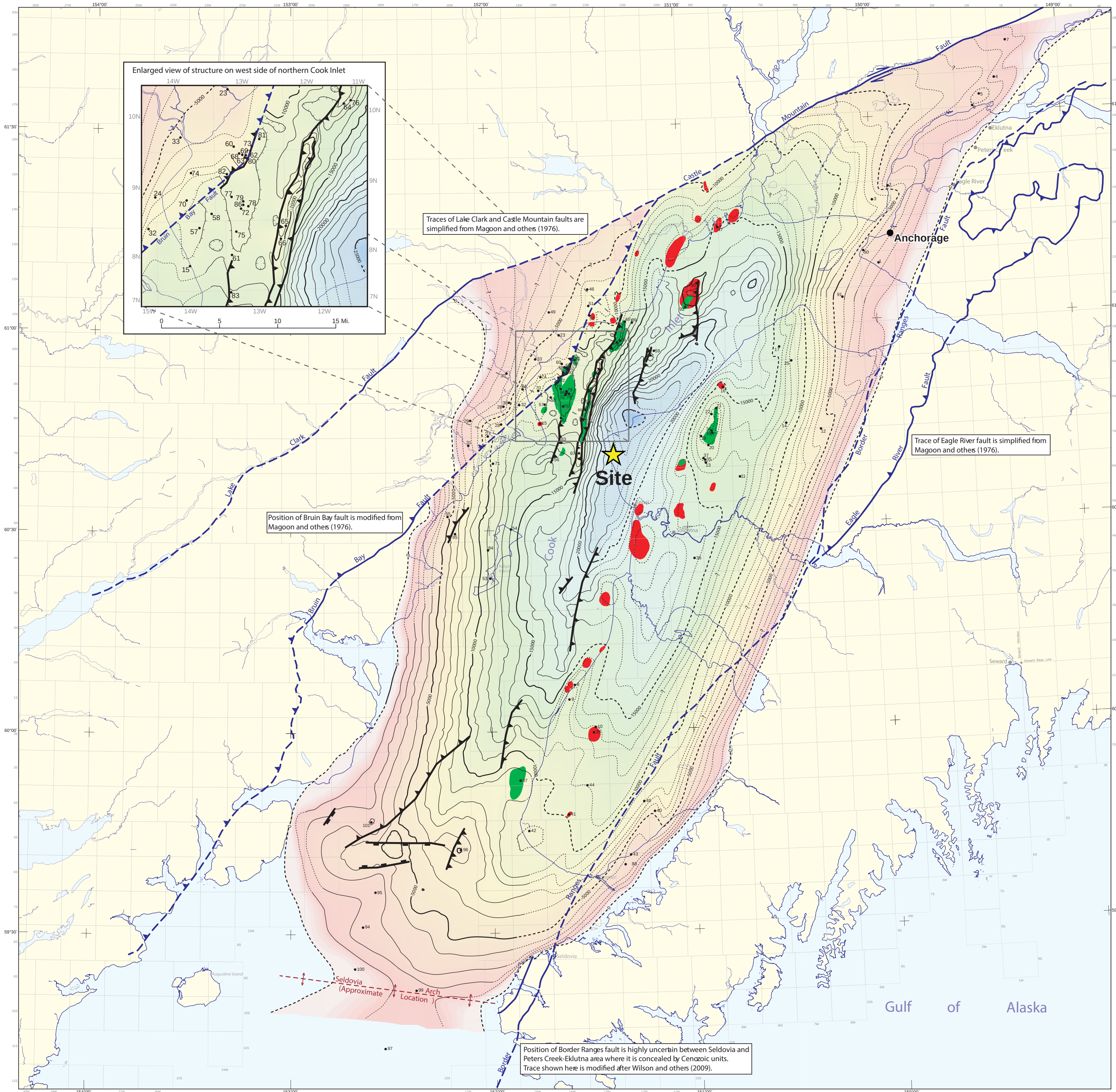

Scale 1: 500,000

10 0 10 20 30 40 50 Miles

10 0 10 20 30 40 50 Kilometers

Map Location

Quadrangle Index

Alaska Department of Natural Resources Division of Oil and Gas

Modified from Shellenbaum et al. (2010)

Legend

Fault - dashed where approximately located

- Strike-slip fault
- Thrust fault - sawteeth on upper plate
- Thrust fault - sawteeth on upper plate (seismic derived)
- Normal fault (seismic derived)

Fold axis - dashed where approximately located

- Anticline
- Syncline
- Anticline
- Syncline

Depth contours - dashed outside of seismic control; queried where inferred or doubtful

- Red line on location map above denotes area of seismic reflection data used in this study
- -5000 Index contour (depth in feet relative to sea level datum)
- Intermediate contour
- •36 Well with base Tertiary penetrations
- Oil accumulation
- Gas accumulation

*Oil and gas accumulations are displayed for reference only. They are typically located within the shallower Tertiary section, not at the mapped surface.

-25000 -19000 -13000 -6500 0

Vertical depth in feet
Datum: Sea Level

TOP MESOZOIC UNCONFORMITY
DEPTH MAP OF THE COOK INLET BASIN
LNG FACILITIES
ALASKA LNG PROJECT
NIKISKI, ALASKA

PLATE 13

\\wla-wc-file1\project\Projects\10_000010_140334_AKLNG_PreFEED_Phase2\05_Graphics\10_140334 Geohazards Report

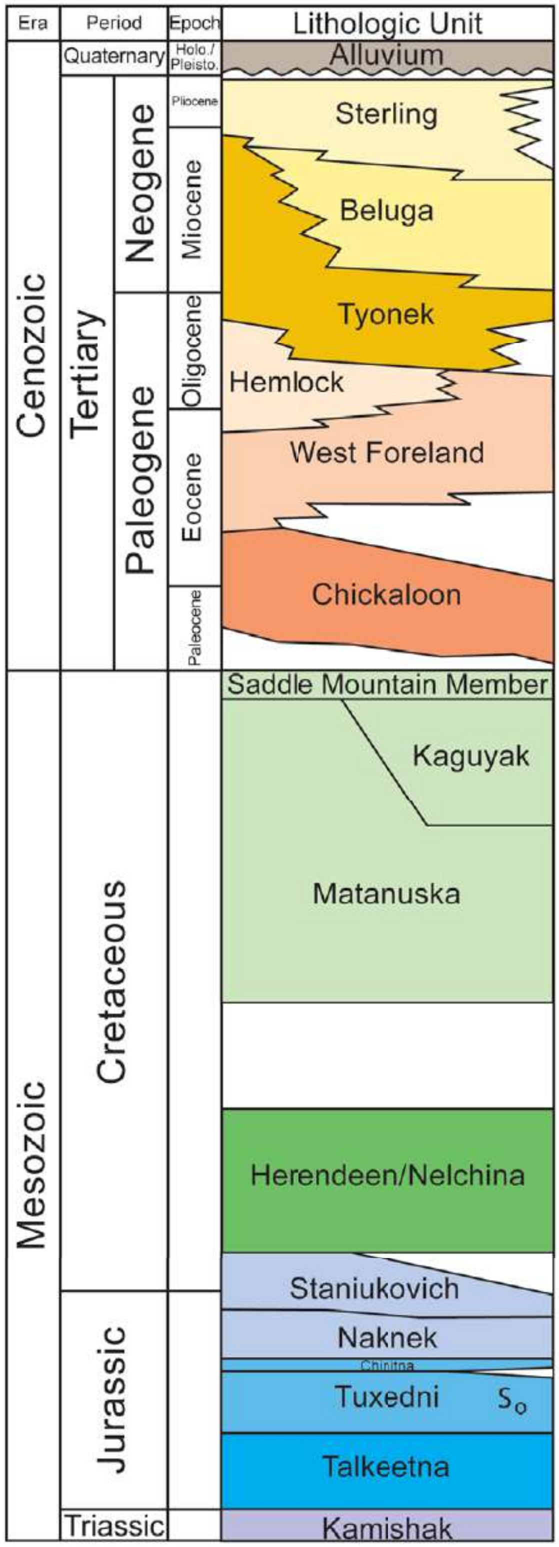

Modified from Enos and Maier, 2013.

STRATIGRAPHIC COLUMN OF COOK INLET BASIN

LNG FACILITIES

ALASKA LNG PROJECT

NIKISKI, ALASKA

PLATE 14

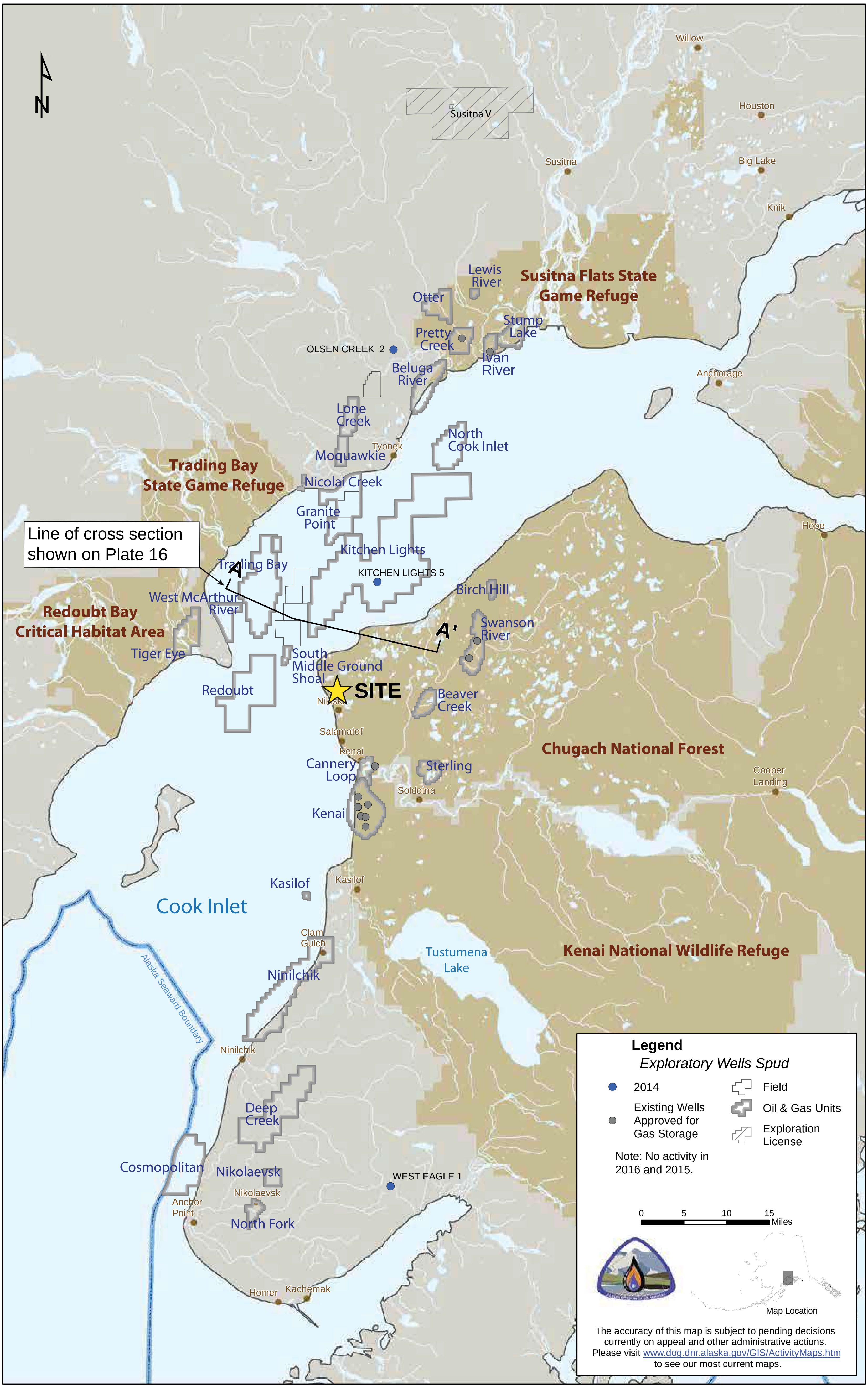

OIL AND GAS FIELDS OF THE COOK INLET BASIN
LNG FACILITIES
ALASKA LNG PROJECT
NIKISKI, ALASKA

PLATE 15

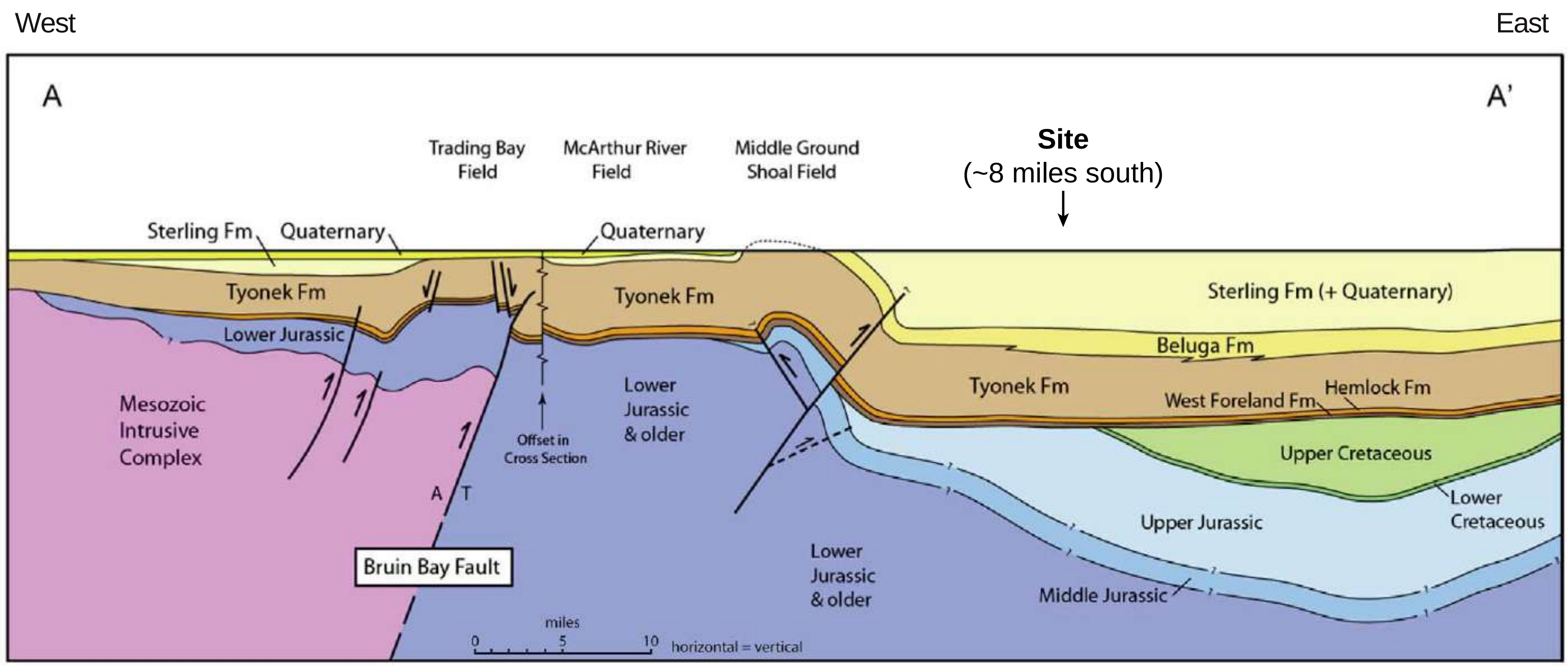

Source: Shellenbaum, 2013.

See Plate 15 for cross-section location.

GENERALIZED CROSS-SECTION
THROUGH THE COOK INLET BASIN
LNG FACILITIES
ALASKA LNG PROJECT
NIKISKI, ALASKA

PLATE 16

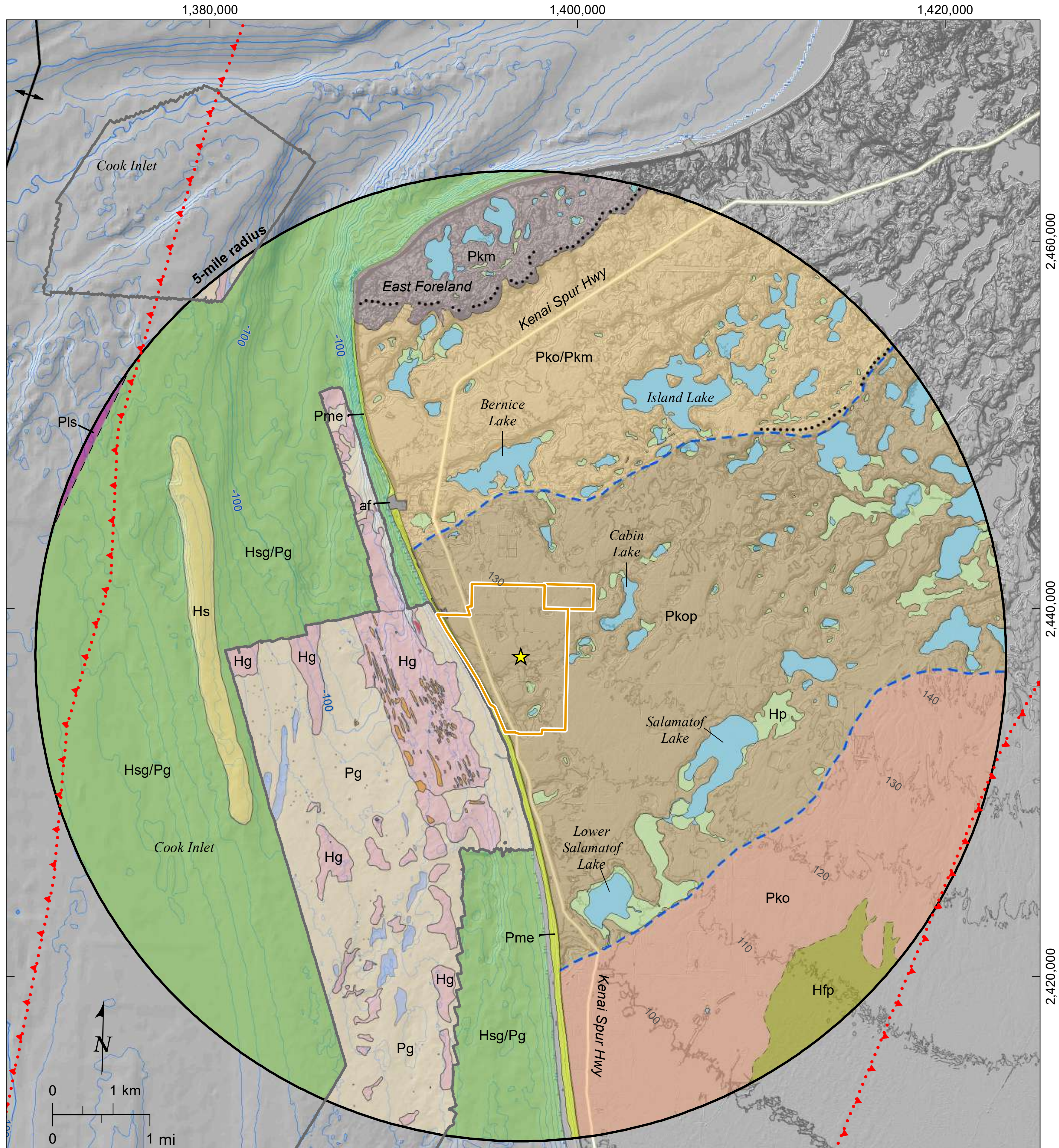

Explanation

☆	Site center
	Onshore LNG Facilities Study Area
	Lake
	Extent of 2014-2015 MBES bathymetry data
100	10-ft contours, onshore
100	10-ft contours, offshore
	Contact, approximate
	Contact, well-located
	Ice margin, approximate
	Moraine crest
	Blind thrust-fault, teeth on upper plate

See Tables 2-1 and 2-2 for unit descriptions.

Geologic Units

Onshore

af	Artificial fill
Hp	Holocene peat and muck deposits
Hfp	Holocene alluvial fan and peat deposits
Pko	Pleistocene glacial outwash deposits, Killey stade
Pkop	Pleistocene glacial outwash deposits, pitted, Killey stade
Pkm	Pleistocene glacial moraine deposits, Killey stade
Pko/Pkm	Undifferentiated Pleistocene glacial outwash and moraine deposits, Killey stade
Pme	Pleistocene glacial subestuarine deposits, Late Moosehorn stade, with thin mantle of modern beach sediments

Marine

Hs	Holocene sand ridge
Hsr	Holocene sand ribbons
Hsw	Holocene sand waves
Hg	Holocene lag gravels
Hs/Pg	Holocene / Pleistocene Undifferentiated Deposits
Pg	Pleistocene glacial deposits
Pls	Pliocene Sterling Formation

Onshore elevation from USGS NED 1/9 arc second, from LiDAR data collected 2008. Bathymetry from NOAA, and Fugro 2015 report no. 04.10140334-5.

Vertical datum NAVD 88.

Confidential
Geologic Hazard Report LNG Facilities
USAL-FG-GRHAZ-00-002015-002 Rev.0
21-Jun-2016

PLATE 17

GEOLOGIC MAP OF THE 5-MILE SITE RADIUS
LNG FACILITIES
ALASKA LNG PROJECT
NIKISKI, ALASKA

FUGRO

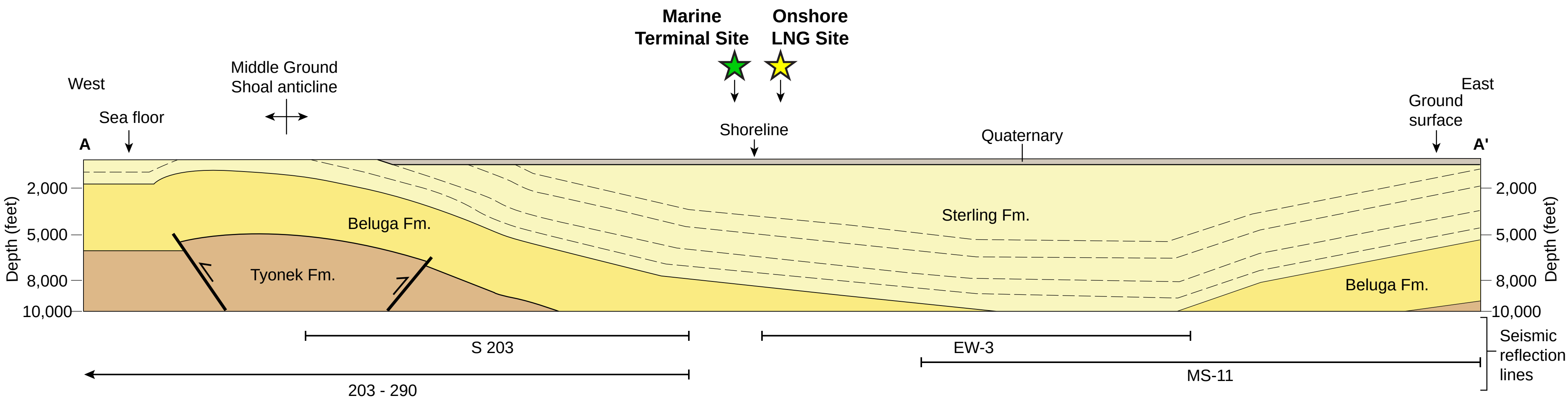

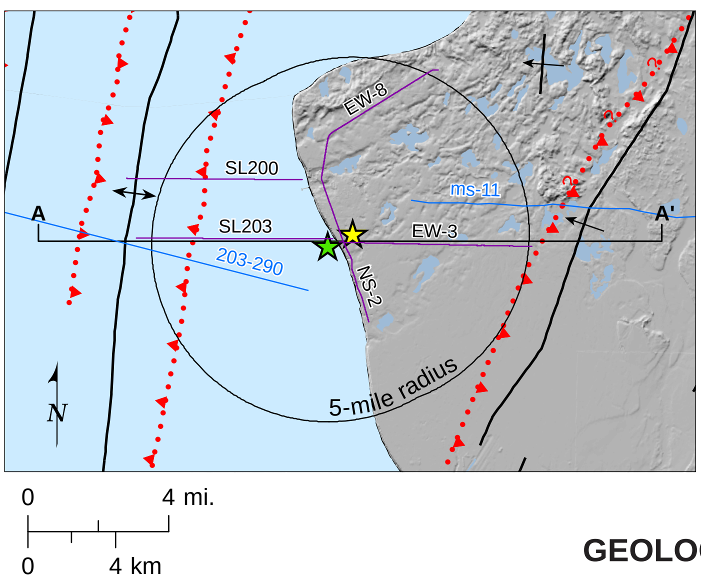

Legend

- Blind thrust fault, teeth on upper plate, queried where uncertain
- Monocline axis
- Anticline axis
- Onshore LNG site center
- Marine terminal site center
- A — A' Structural cross section line

0 2 mi.

0 5,000 10,000 feet

No vertical exaggeration

GEOLOGIC CROSS-SECTION OF THE SITE AREA

LNG FACILITIES

ALASKA LNG PROJECT

NIKISKI, ALASKA

PLATE 18

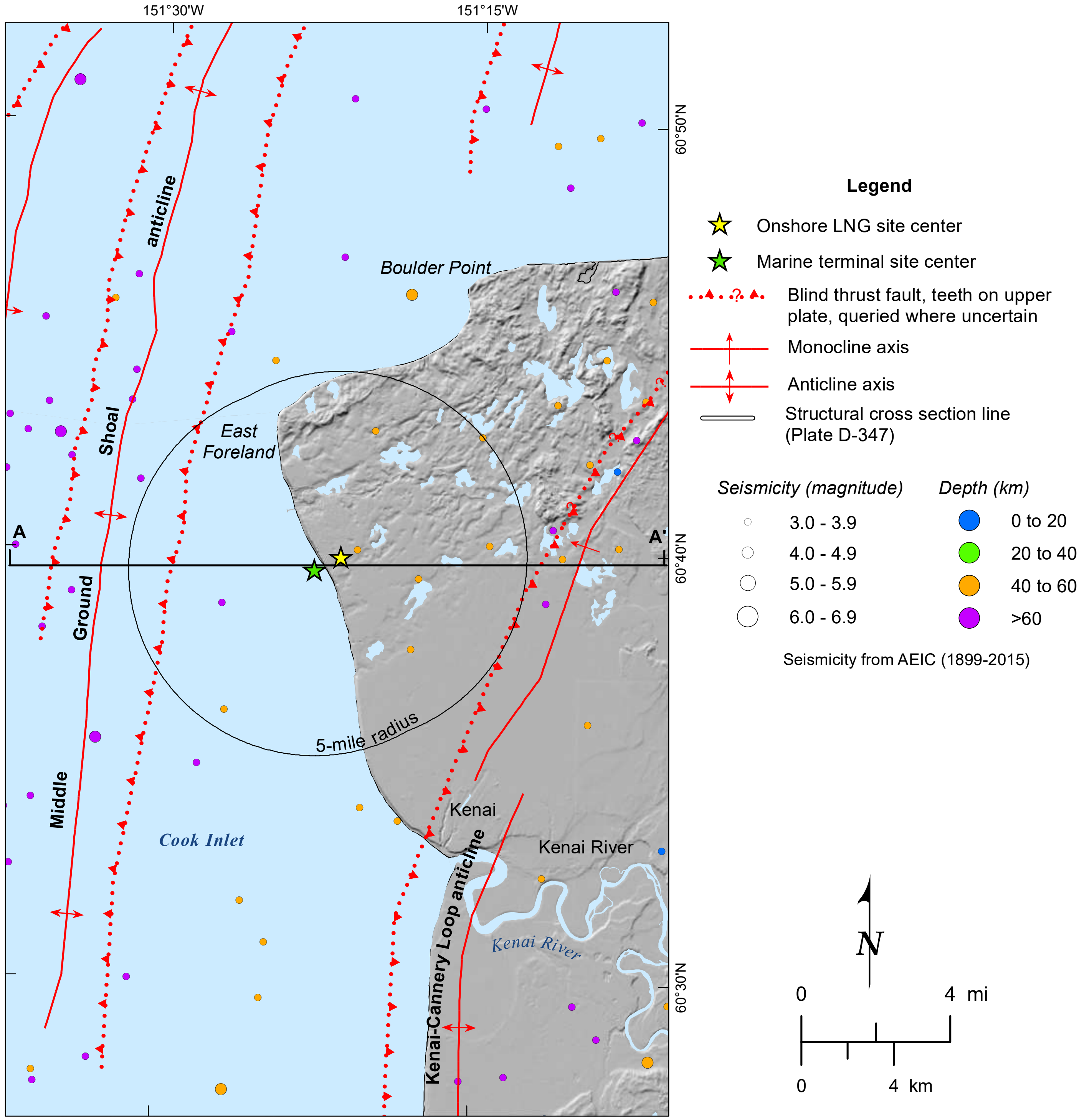

P:\Projects\10_0000\10_140334_AKLNG_PreFEED_Phase2\05_Graphics\10_140334 Geohazards Report\19_D_346_StructuralGeology_Seismicity_020916.mxd; jholmberg; 6/8/2016

STRUCTURAL GEOLOGY AND SEISMICITY OF THE SITE AREA

LNG FACILITIES
ALASKA LNG PROJECT
NIKISKI, ALASKA

PLATE 19

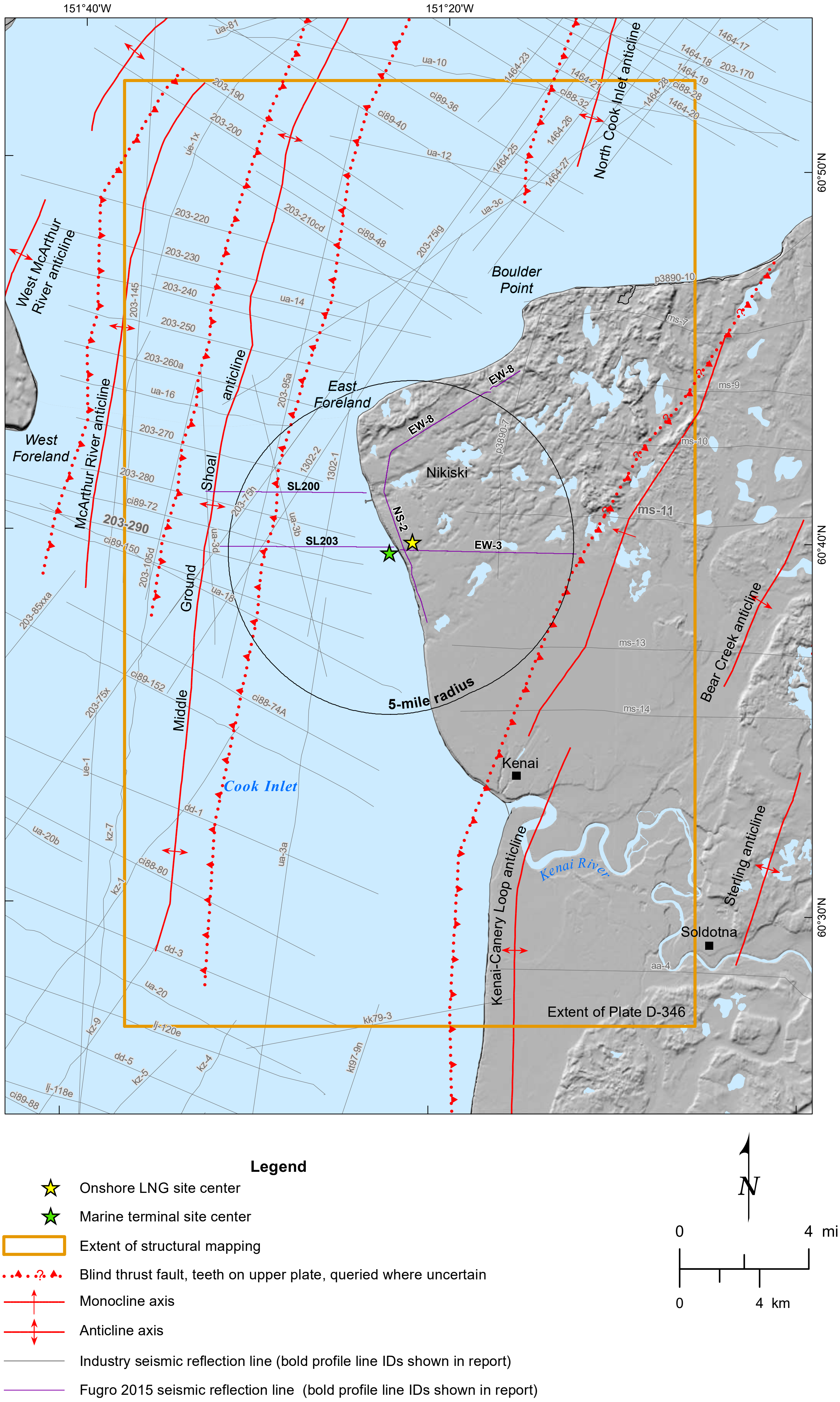

FOLDS AND FAULTS MAPPED FROM SEISMIC REFLECTION DATA
LNG FACILITIES
ALASKA LNG PROJECT
NIKISKI, ALASKA

PLATE 20

P:\Projects\10_0000\10_140334_AKLNG_PreFEED_Phase2\05_Graphics\10_140334 Geohazards Report\20_D_345_FaultsFolds_SeismicLines_021016.mxd; jholmberg; 6/8/2016

Imagery from Kenai Peninsula Borough, 2012.

Legend

NS-2 Deep seismic survey line, with start/end stations

Start station

End station

P:\Projects\10_000\10_140334_AKLNG_PreFEED_Phase2\05_Graphics\10_140334 Geohazards Report\21_D_313_DeepSeismicLines_Location.mxd; jholmberg; 6/8/2016

2015 ONSHORE DEEP SEISMIC SURVEY LINES
LNG FACILITIES
ALASKA LNG PROJECT
NIKISKI, ALASKA

PLATE 21

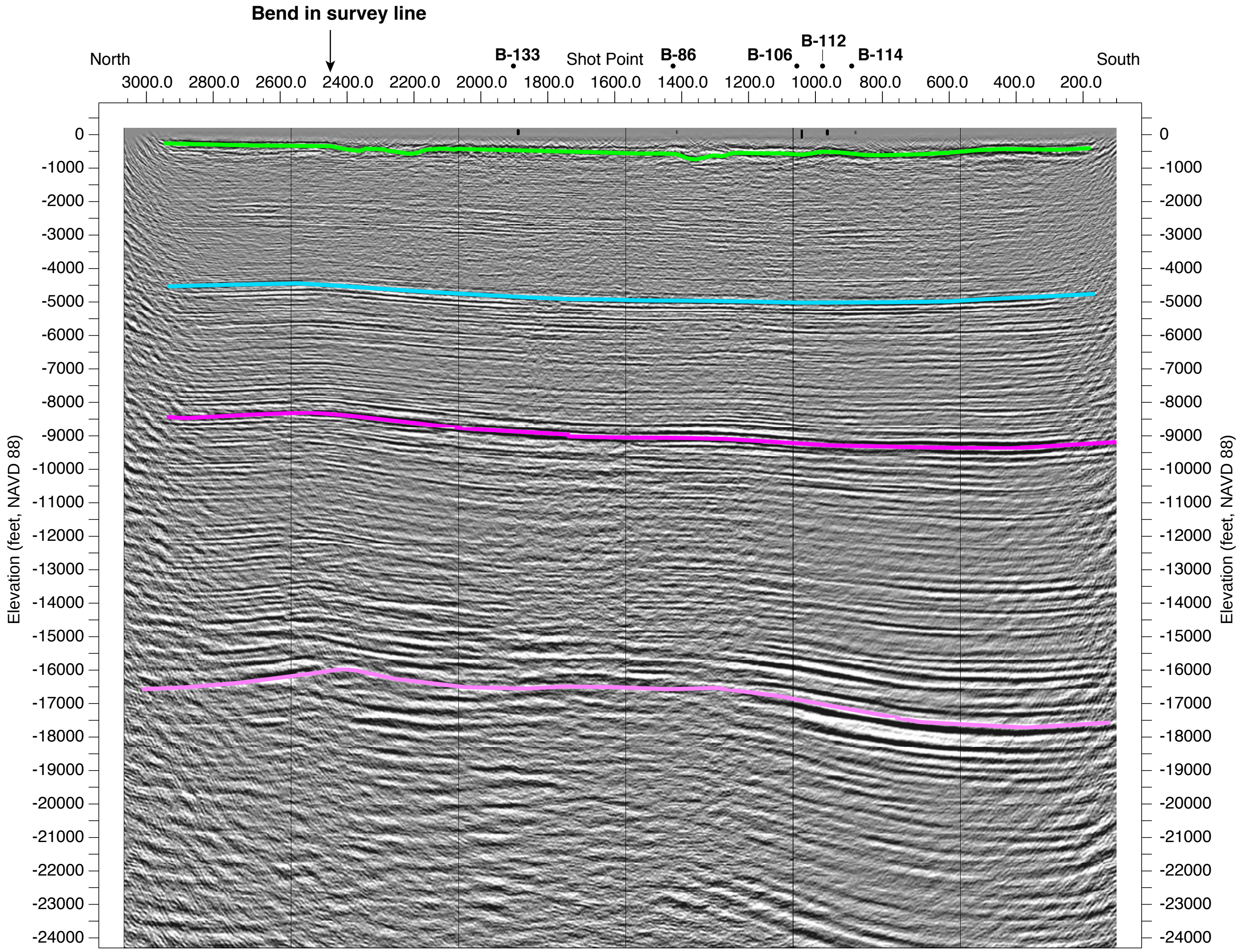

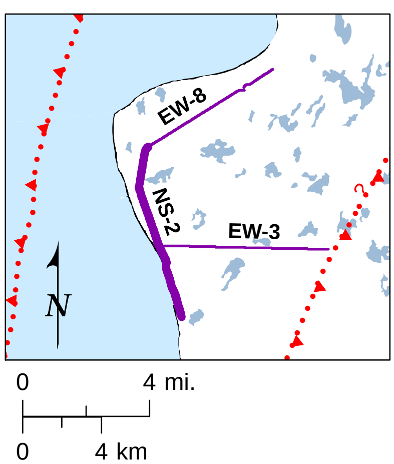

Legend

B-133 • Borehole and number

Unconformity

Arbitrary reflectors

2015 SEISMIC REFLECTION PROFILE LINE
NS-2, DEPTH MIGRATED - INTERPRETED

LNG FACILITIES
ALASKA LNG PROJECT
NIKISKI, ALASKA

PLATE 22

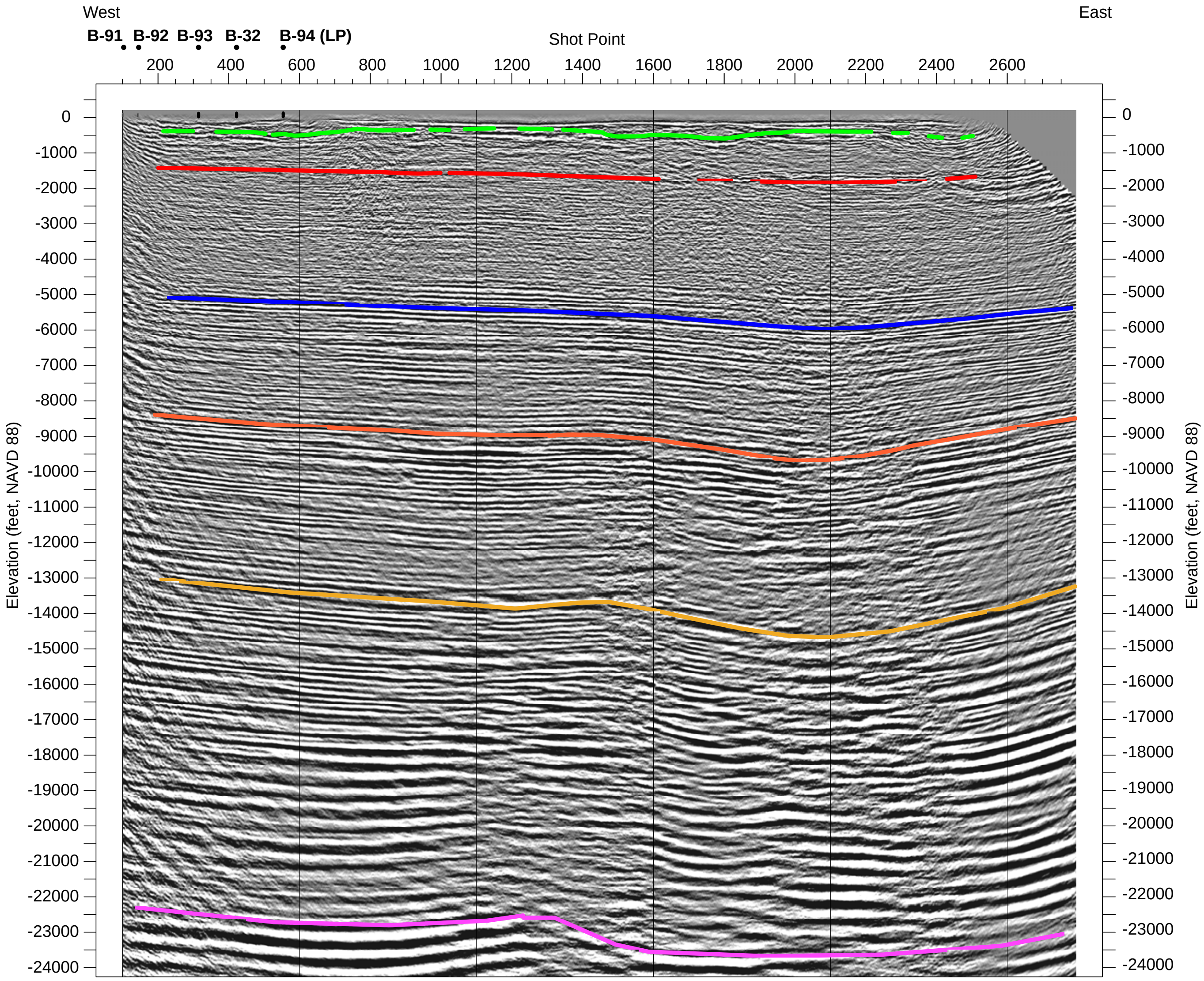

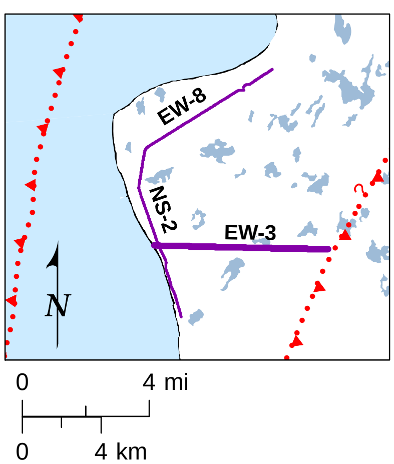

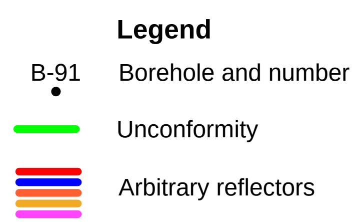

2015 SEISMIC REFLECTION PROFILE LINE EW-3, DEPTH MIGRATED - INTERPRETED

LNG FACILITIES
ALASKA LNG PROJECT
NIKISKI, ALASKA

PLATE 23

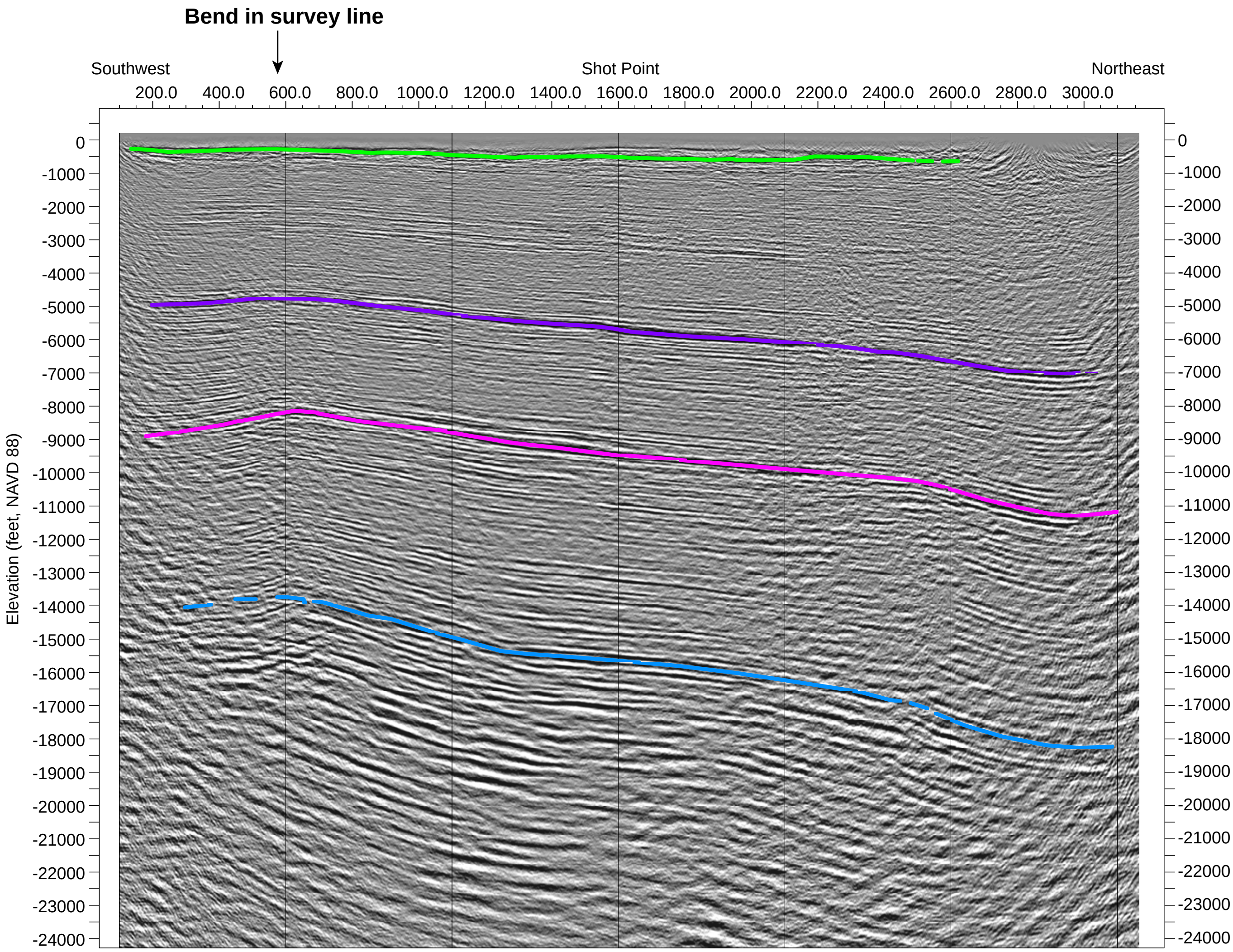

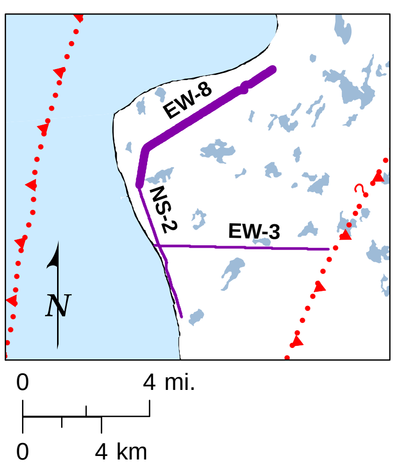

Legend

- Unconformity
- Arbitrary reflectors

/fwla-wc-file1/project/Projects/10_0000/10_140334_AKLNG_PreFEED_Phase2/05_Graphics/10_140334 Geohazards Report

2015 SEISMIC REFLECTION PROFILE LINE
EW-8, DEPTH MIGRATED - INTERPRETED

LNG FACILITIES
ALASKA LNG PROJECT
NIKISKI, ALASKA

PLATE 24

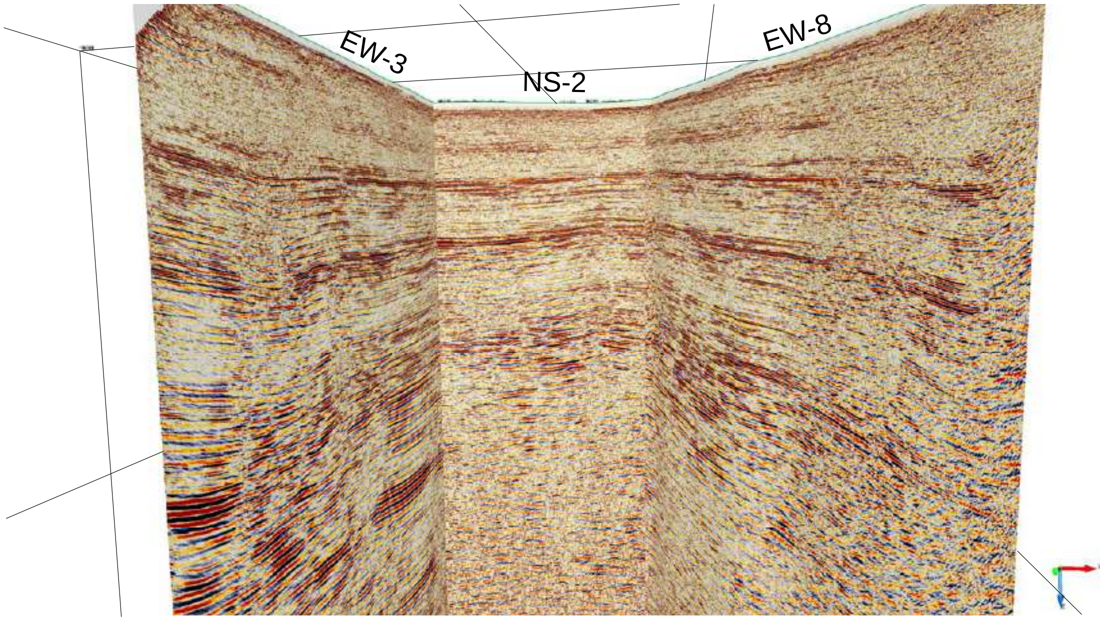

A) 3D view to the west of seismic reflection profile line EW-3, EW-9, and of NS-2, showing planar continuous strata.

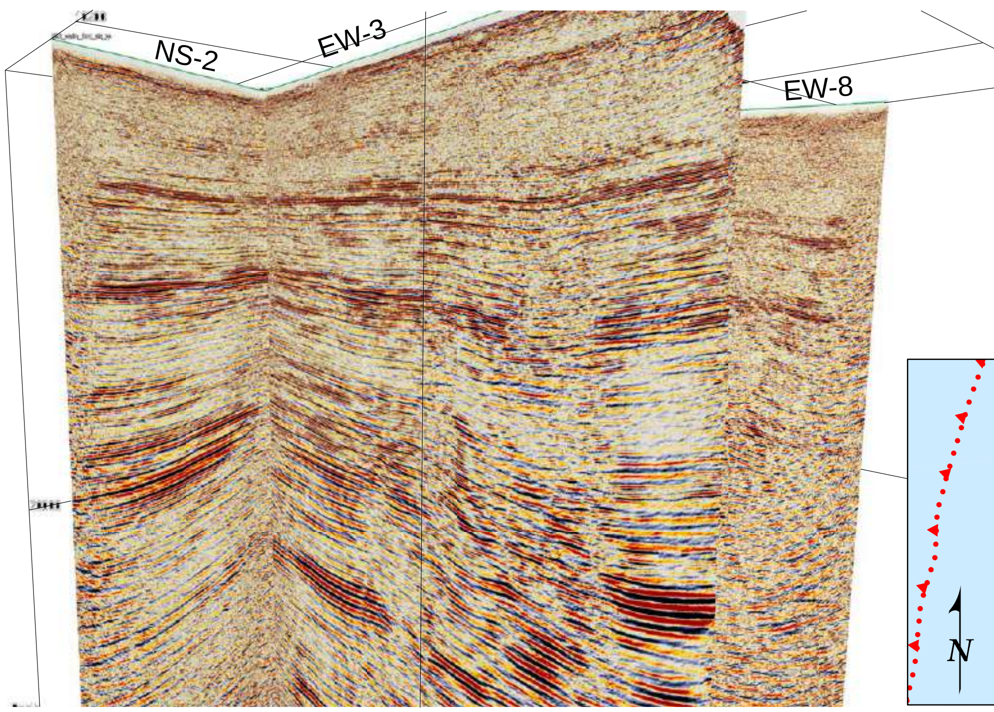

B) 3D view of northwest of seismic reflection profile line EW-3 and the southern end of NS-2, showing planar continuous strata.

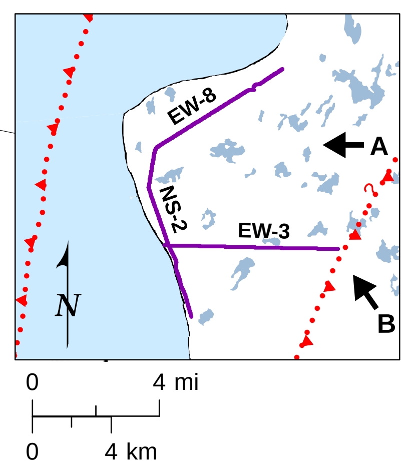

/fwla-wc-file1/project/Projects/10_0000/10_140334_AKLNG_PreFEED_Phase2/05_Graphics/10_140334 Geohazards Report

3D VIEWS OF 2015 ONSHORE SEISMIC REFLECTION DATA
LNG FACILITIES
ALASKA LNG PROJECT
NIKISKI, ALASKA

PLATE 25

Uninterpreted

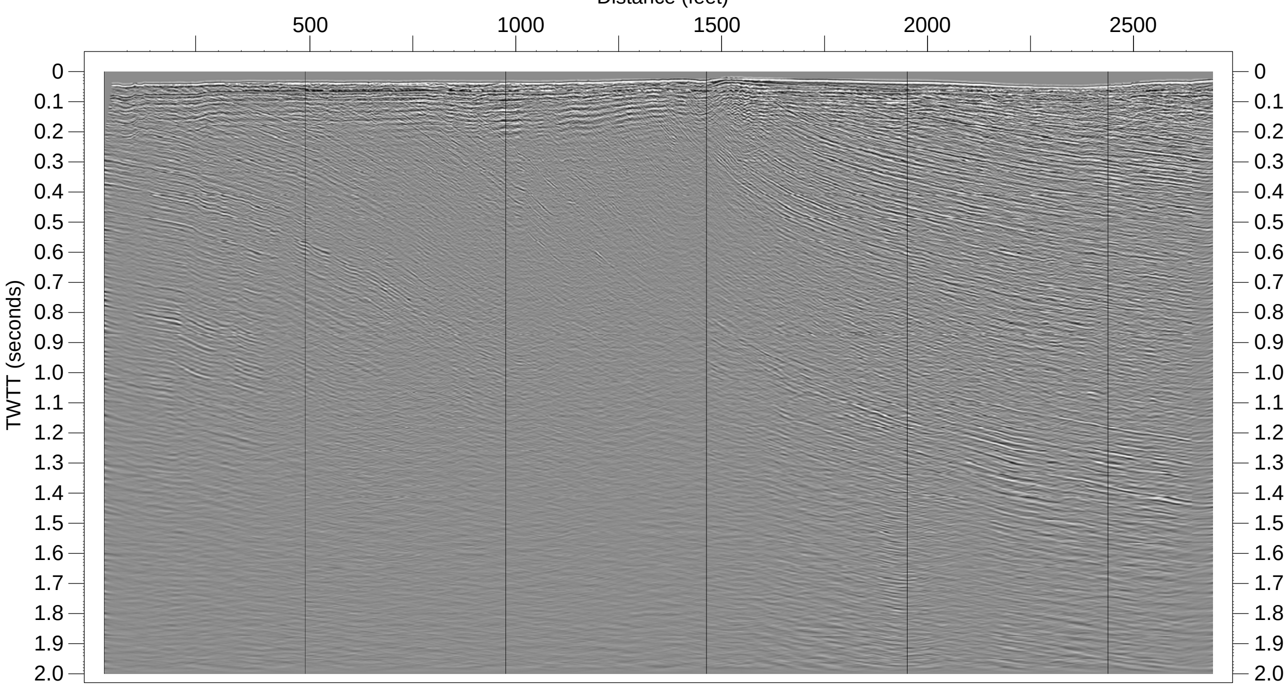

Interpreted

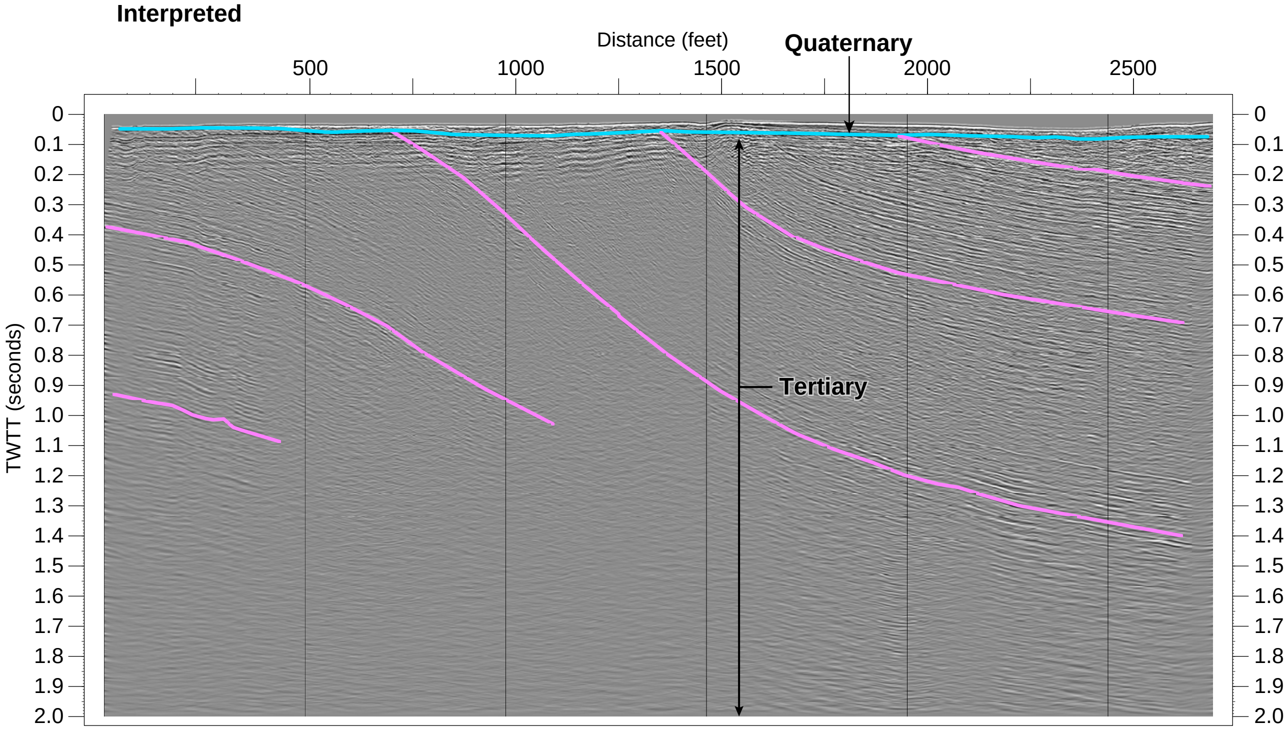

Legend
Tertiary unconformity
Arbitrary reflectors

For location of line see Plate 20.

2015 MARINE SEISMIC REFLECTION PROFILE SL203
LNG FACILITIES
ALASKA LNG PROJECT
NIKISKI, ALASKA

PLATE 26

Uninterpreted

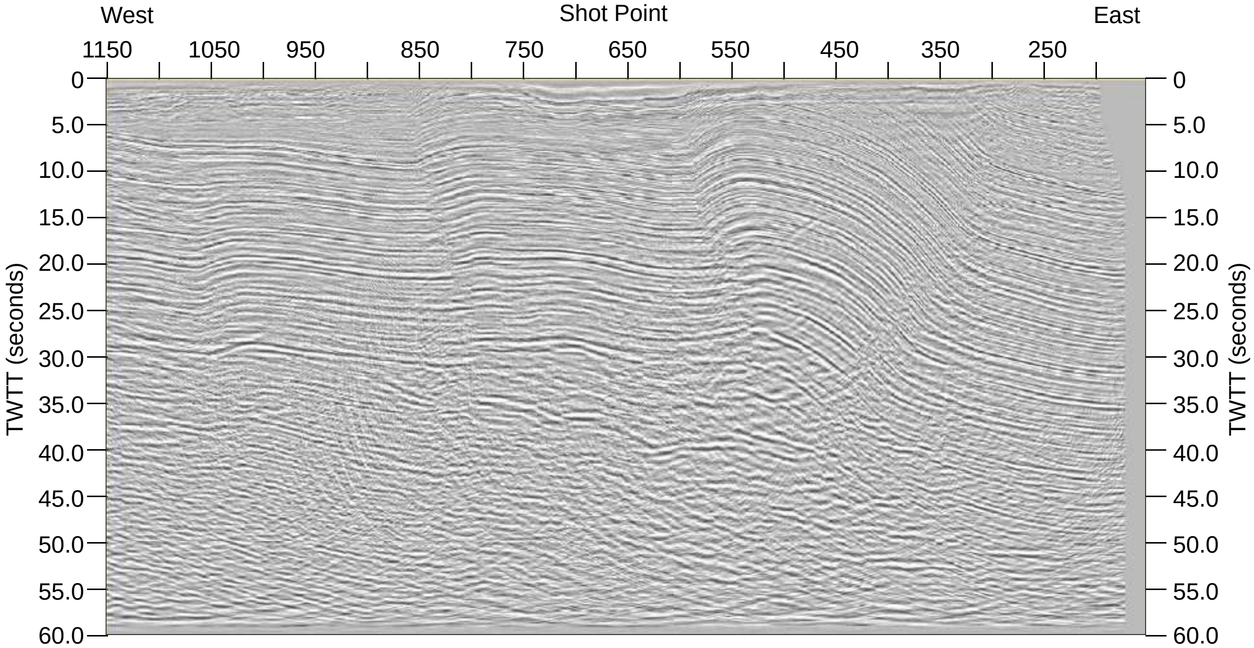

Interpreted

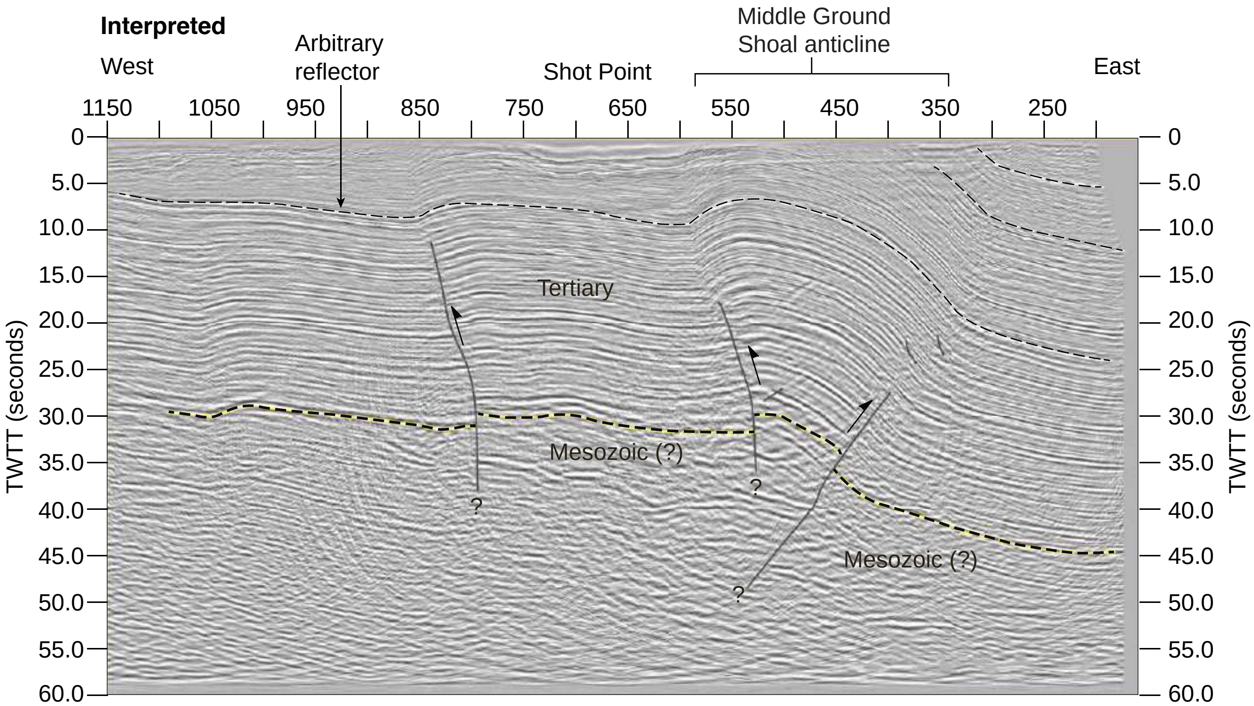

0 7,500 ft.
0 2,500 m

The information contained herein is ConocoPhillips "independent information," as defined in the June 30 2014 Alaska LNG Project Pre-FEED Joint Venture Agreement ("Pre-FEED JVA"), and is provided to Lead Party subject to the Pre-FEED JVA solely for the purpose of geohazard analysis, including probabilistic seismic hazard analysis, to support the Alaska LNG project's FERC filings.

For line location see Plate 20.

SEISMIC REFLECTION LINE 203_290, ILLUSTRATING MIDDLE GROUND SHOAL ANTICLINE

LNG FACILITIES
ALASKA LNG PROJECT
NIKISKI, ALASKA

PLATE 27

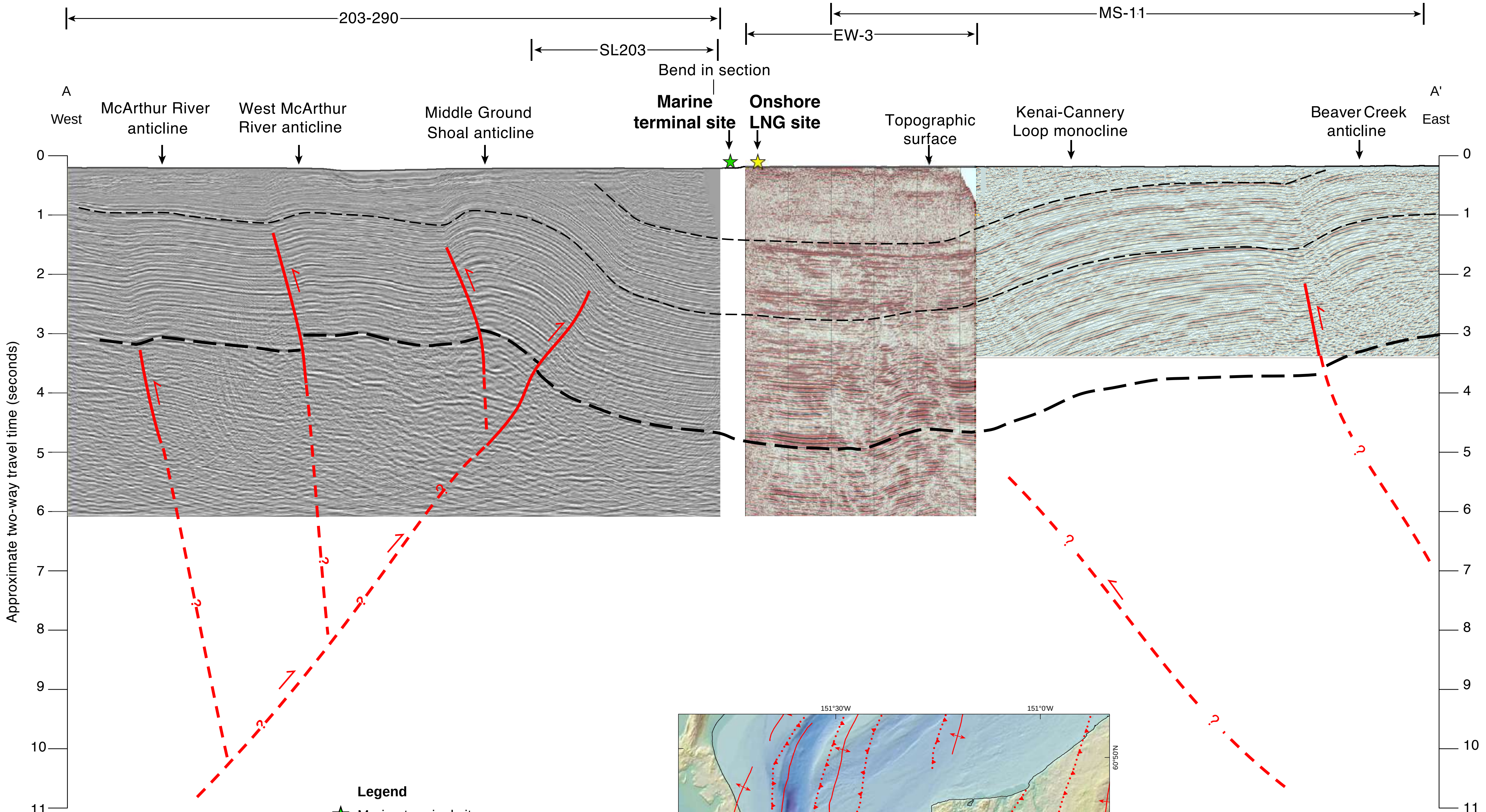

0 10,000 ft.
Horizontal scale

Legend

- Marine terminal site
- Site center
- Structural form line within undifferentiated Tertiary units
- Top of Mesozoic basement
- Faults; dashed where inferred

Notes:
1.For conceptual purposes only.
2. Horizontal and vertical are not to scale.

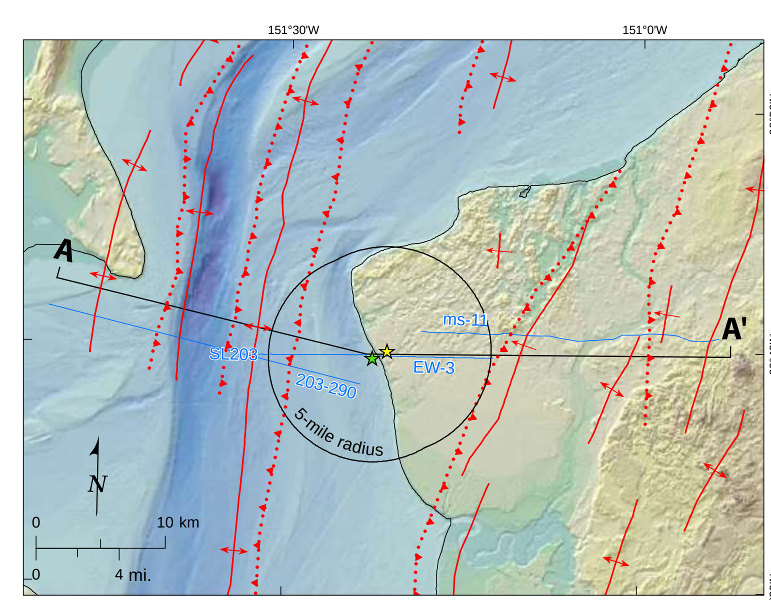

The information contained herein is ConocoPhillips “independent information,” as defined in the June 30 2014 Alaska LNG Project Pre-FEED Joint Venture Agreement (“Pre-FEED JVA”), and is provided to Lead Party subject to the Pre-FEED JVA solely for the purpose of geohazard analysis, including probabilistic seismic hazard analysis, to support the Alaska LNG project’s FERC filings.

CONCEPTUAL CROSS SECTION OF UPPER COOK INLET BASIN AT THE LATITUDE OF THE SITE
LNG FACILITIES
ALASKA LNG PROJECT
NIKISKI, ALASKA

PLATE 28

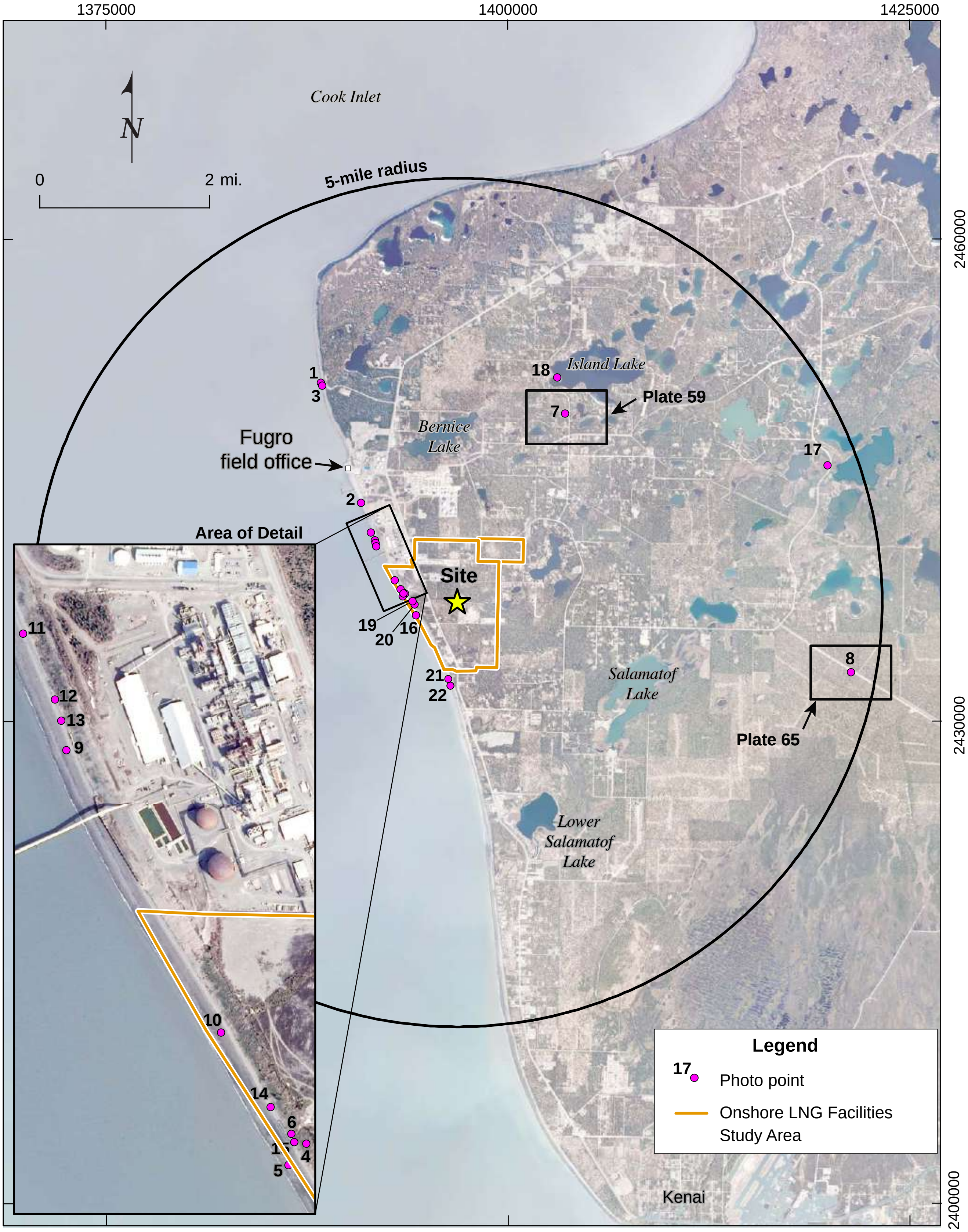

LOCATION OF FIELD PHOTOGRAPHS
LNG FACILITIES
ALASKA LNG PROJECT
NIKISKI, ALASKA

PLATE 29

/fwla-wc-file1/project/Projects/10_0000/10_140334_AKLNG_PreFEED_Phase2/05_Graphics/10_140334 Geohazards Report

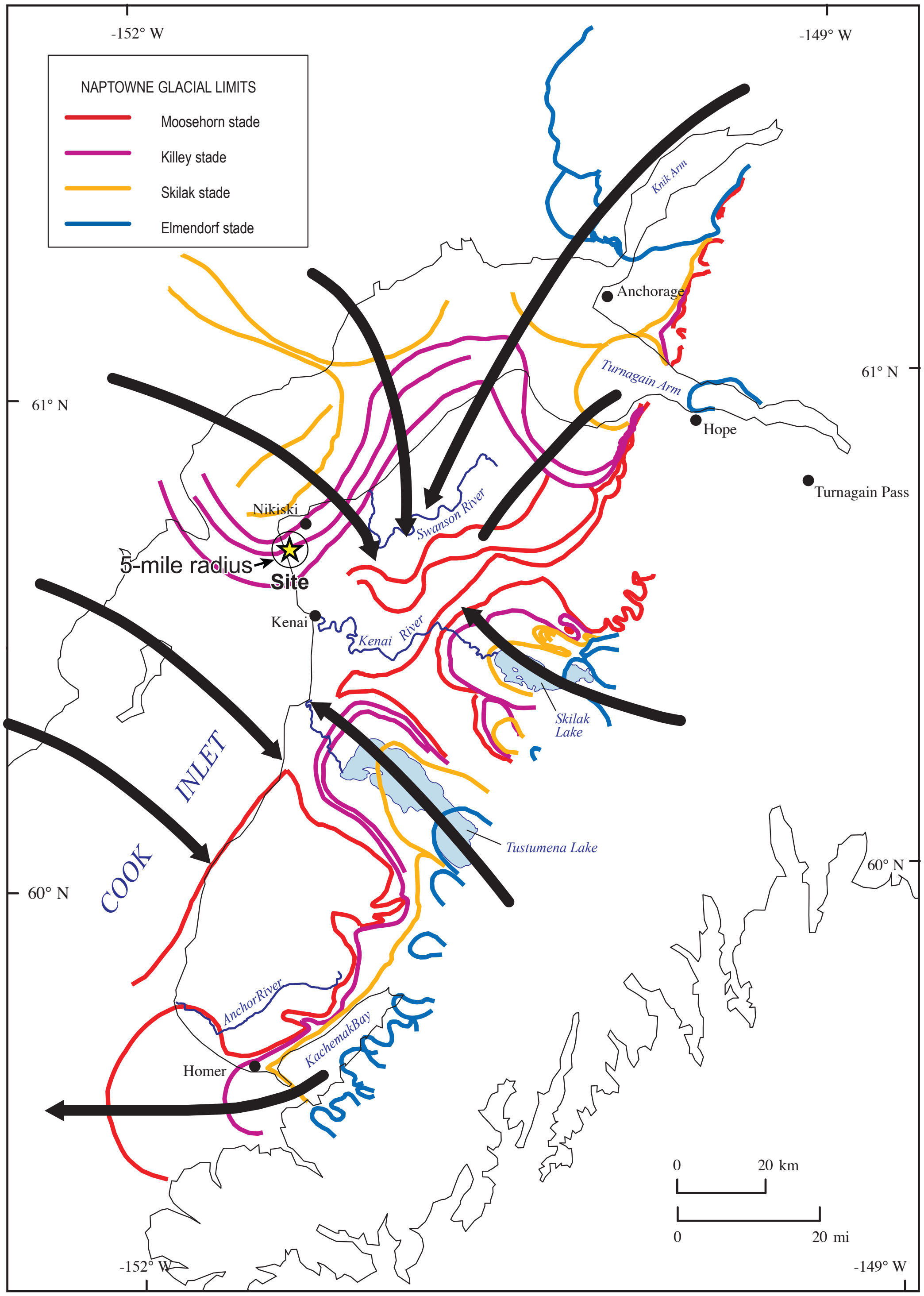

Model of Naptowne glaciation showing principal ice-flow directions (arrows). Modified from Reger et al. (2007)

KENAI PENINSULA LATE PLEISTOCENE GLACIAL ADVANCES
LNG FACILITIES
ALASKA LNG PROJECT
NIKISKI, ALASKA

PLATE 30

/fwla-wc-file1/project/Projects/10_0000/10_140334_AKLNG_PreFEED_Phase2/05_Graphics/10_140334 Geohazards Report

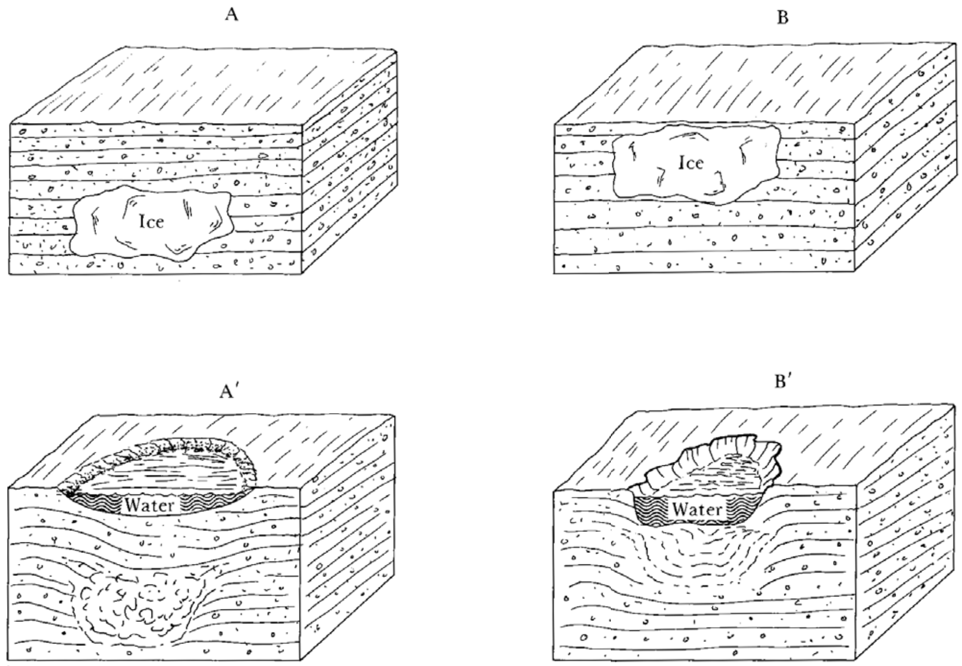

These interpretive sketches illustrate differences in the configuration of kettle holes formed by deeply (A, A') and shallowly (B, B') buried ice masses. Kettle holes with steeper banks and more irregular outline generally indicate shallow or incomplete burial of the ice. From Sharp (1988).

A small kettle hole in outwash debris near the edge of Malaspina Glacier, Alaska, formed the day before yesterday, geologically speaking, by melting of a small completely buried block of glacier ice. From Sharp (1988).

ORIGIN OF KETTLES
LNG FACILITIES
ALASKA LNG PROJECT
NIKISKI, ALASKA

PLATE 31

A)

View of Island Lake. Photo point 18.

B)

Lake surrounded by extensive fen (bog). Photo point 17. See Plate 29 for photo point locations.

/fwla-wc-file1/project/Projects/10_0000/10_140334_AKLNG_PreFEED_Phase2/05_Graphics/10_140334 Geohazards Report

PHOTOGRAPHS OF KETTLE LAKE MORPHOLOGY
LNG FACILITIES
ALASKA LNG PROJECT
NIKISKI, ALASKA

PLATE 32

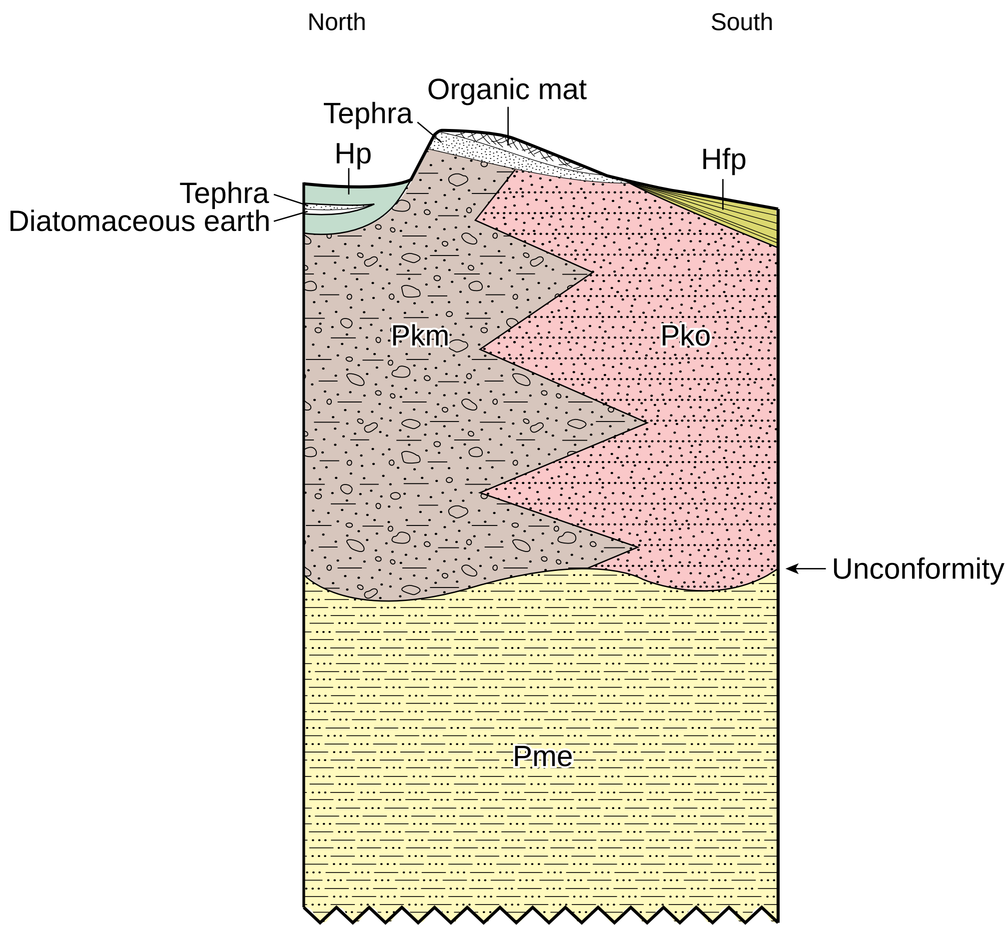

Legend

Hp	Holocene peat and muck deposits
Hfp	Holocene alluvial fan and peat deposits
Pkm	Pleistocene glacial moraine deposits, Killey stade
Pko	Pleistocene fluvial outwash deposits, Killey stade
Pme	Pleistocene glacial subestuarine deposits, Late Moosehorn stade

SCHEMATIC STRATIGRAPHIC COLUMN OF
ONSHORE QUATERNARY UNITS
LNG FACILITIES
ALASKA LNG PROJECT
NIKISKI, ALASKA

PLATE 33

A)

Holocene lake deposits including peat, tephra, and diatomaceous earth. Photo point 1. See Plate 29 for location.

B)

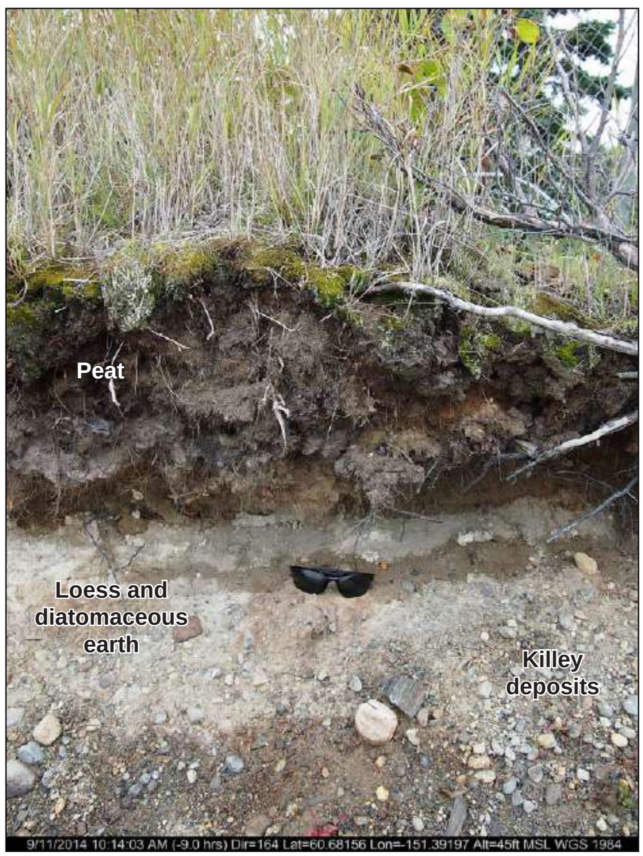

Holocene lake deposits including peat, loess,and diatomaceous earth. Photo point 2. See Plate 29 for location.

PHOTOGRAPHS OF HOLOCENE DEPOSITS

LNG FACILITIES

ALASKA LNG PROJECT

NIKISKI, ALASKA

PLATE 34

fwla-wc-file1/project/Projects/10_0000/10_140334_AKLNG_PreFEED_Phase2/05_Graphics/10_140334 Geohazards Report

A)

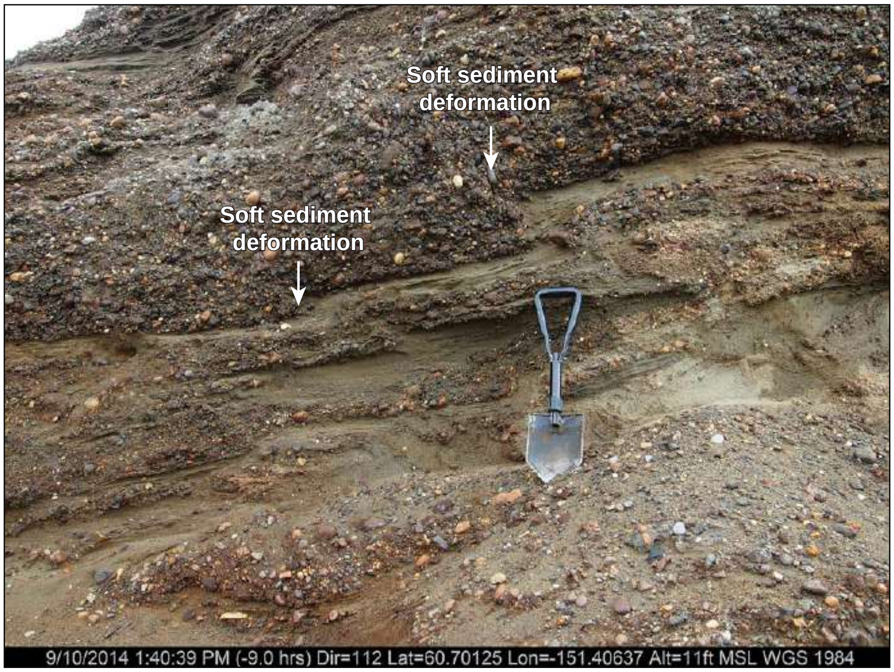

Interbedded medium to coarse sands and silt, overlain by sandy, silty gravel with iron cementation. Photo point 3. See Plate 29 for location.

B)

Interbedded gravels and coarse sand. Photo point 4. See Plate 29 for location.

PHOTOGRAPHS OF KILLEY OUTWASH DEPOSITS
LNG FACILITIES
ALASKA LNG PROJECT
NIKISKI, ALASKA

PLATE 35

A)

Debris flow in Killey deposits, with view of organic mat at the top of the bluff. Photo point 5. See Plate 29 for location.

B)

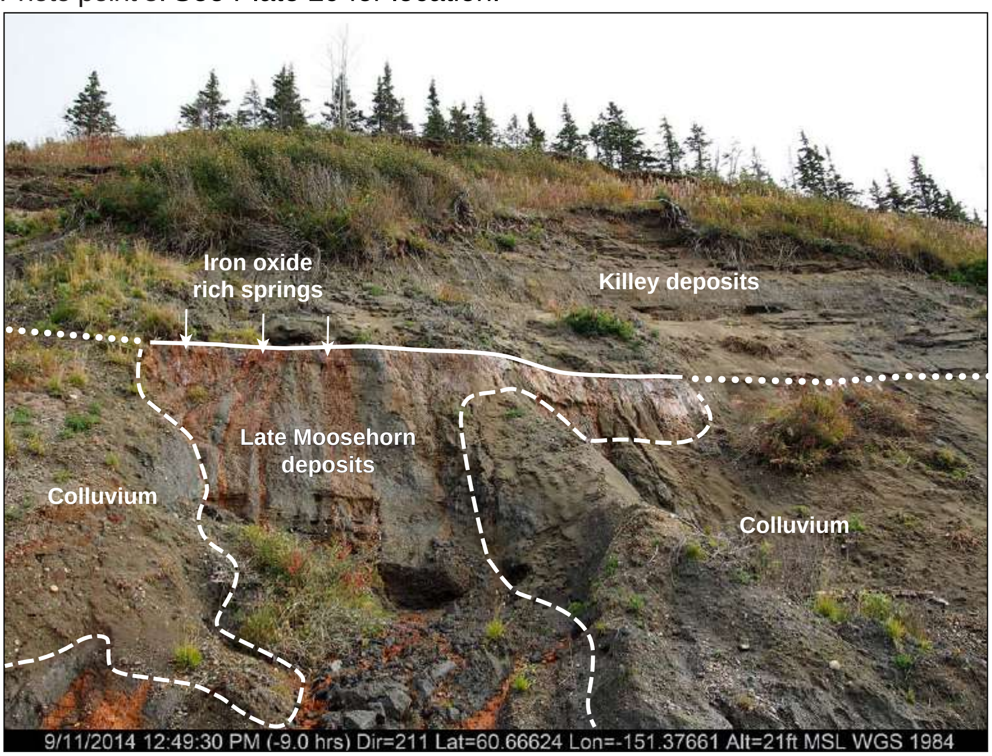

Killey outwash deposits over Late Moosehorn sub-estuarine fan deposits. Iron-rich water seeps out along the contact. Photo point 6. See Plate 29 for location.

PHOTOGRAPHS OF THE CONTACT BETWEEN KILLEY AND MOOSEHORN DEPOSITS EXPOSED IN THE COASTAL BLUFFS

LNG FACILITIES
ALASKA LNG PROJECT
NIKISKI, ALASKA

PLATE 36

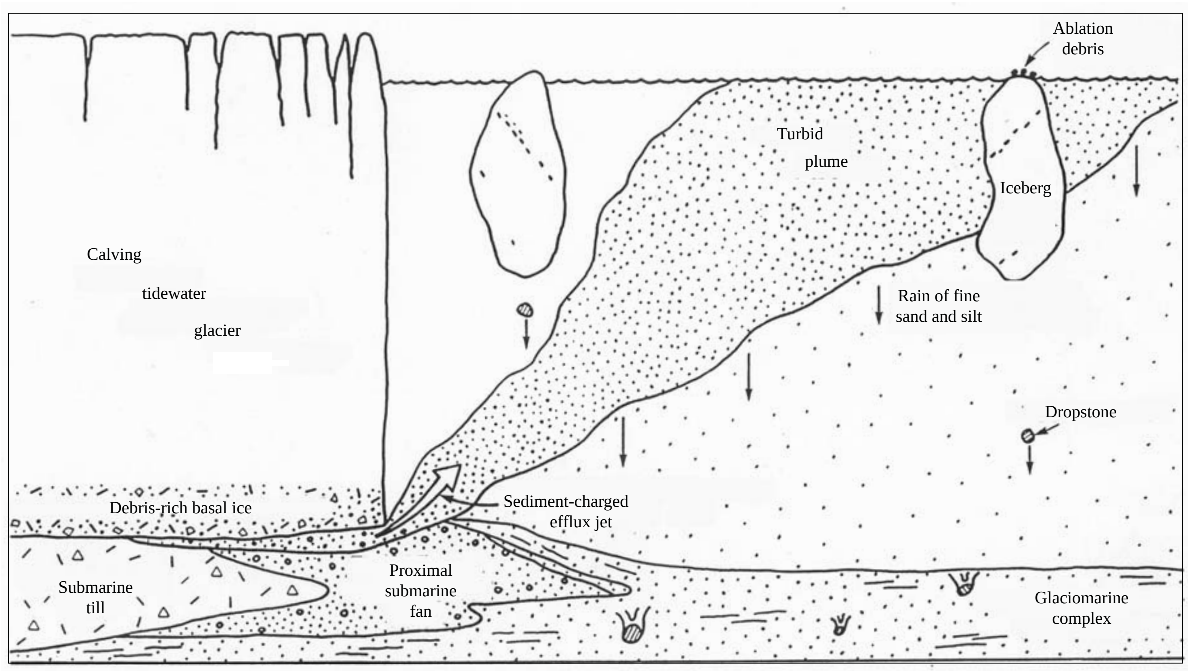

Depositional processes and sediments near a calving tidewater glacier or ice shelf, modified from Eyles and McCabe (1989). Figure and caption from Reger et al. (2007).

fwla-wc-file1/project/Projects/10_0000/10_140334_AKLNG_PreFEED_Phase2/05_Graphics/10_140334 Geohazards Report

DEPOSITIONAL ENVIRONMENT OF LATE MOOSEHORN SUBESTUARINE DEPOSITS

LNG FACILITIES
ALASKA LNG PROJECT
NIKISKI, ALASKA

PLATE 37

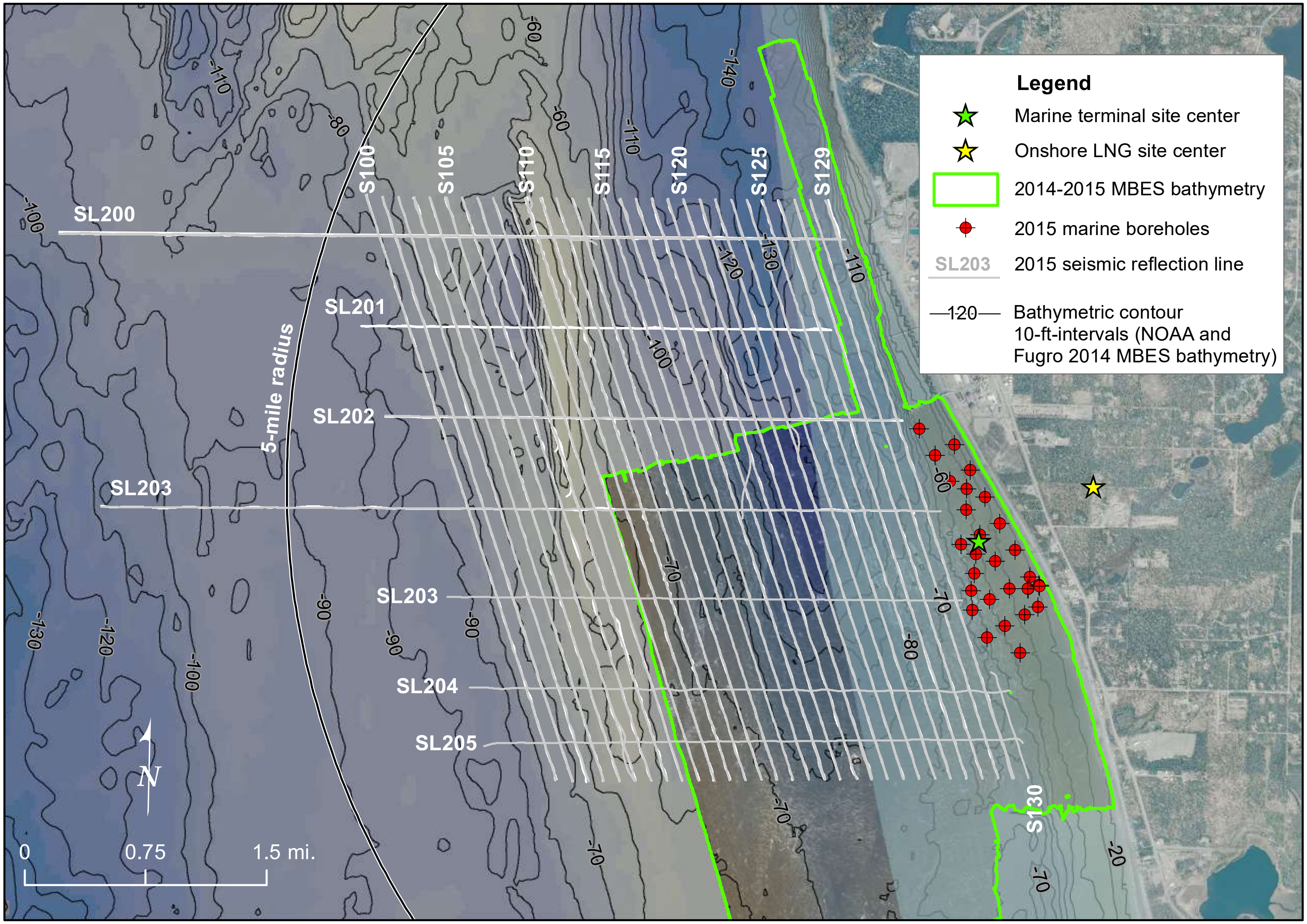

See Plate 4 for detailed nearshore borehole identification map.

GEOPHYSICAL AND GEOTECHNICAL DATA COLLECTION MARINE

LNG FACILITIES
ALASKA LNG PROJECT
NIKISKI, ALASKA

PLATE 38

P:\Projects\10_000010_140334_AKLNG_PreFEED_Phase2\05_Graphics\10_140334 Geohazards Report\38_D_378_Marine_Shot_Line_Map.mxd; jholmberg; 6/8/2016

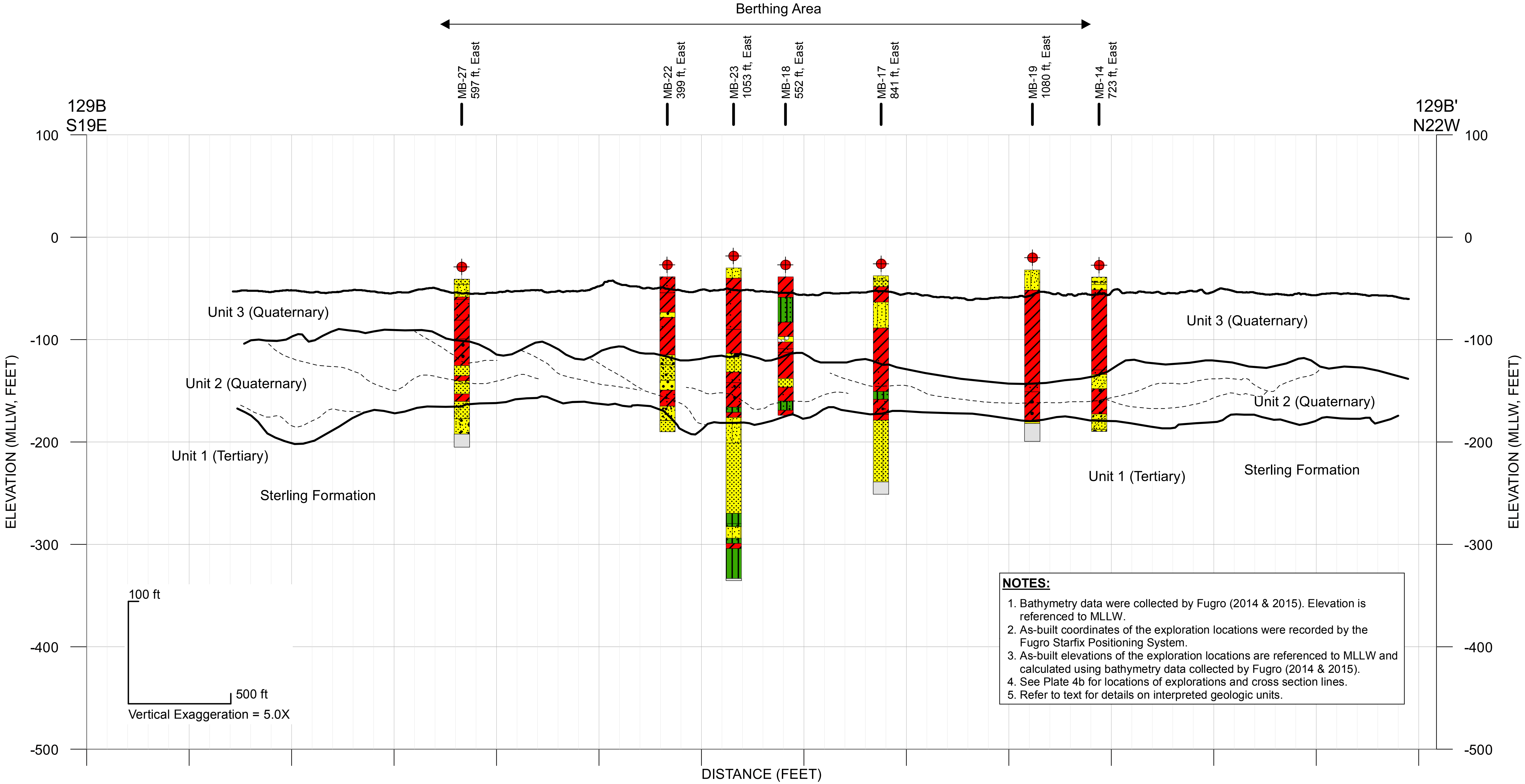

Legend

- Lean CLAY (CL)
- Gravelly Lean CLAY (CL)
- Sandy Lean CLAY (CL)
- Gravelly Lean CLAY with sand (CL)
- Lean Clay with Sand (CL)
- Sandy Silty CLAY (CLML)
- Granite Boulder (COBBLE)
- Clayey Gravel with Sand (GC)
- Gravel (GP)
- Gravel (GW)
- Silt (ML)
- Sandy Silt (ML)
- Silty Sand (SM)
- Sand (SP)
- Sand with Gravel (SP)
- Sand with Clay (SP-SC)
- Sand with Gravel (SW)
- Silty Sand (SM)
- Marine Boring (2015)
- Rat Hole for PS Logging
- Approximate seawater level
- Seafloor (Fugro 2014 & 2015)
- Interpreted Major Unit Boundaries
- Interpreted Burried Channel Boundaries

Notes:
1. Stratigraphy mapped from 2015 seismic reflection line S129.
2. Section B-B' location shown on Plate 40.

MARINE CROSS SECTION B-B' ALONG SEISMIC REFLECTION LINE S129
LNG FACILITIES
ALASKA LNG PROJECT
NIKISKI, ALASKA

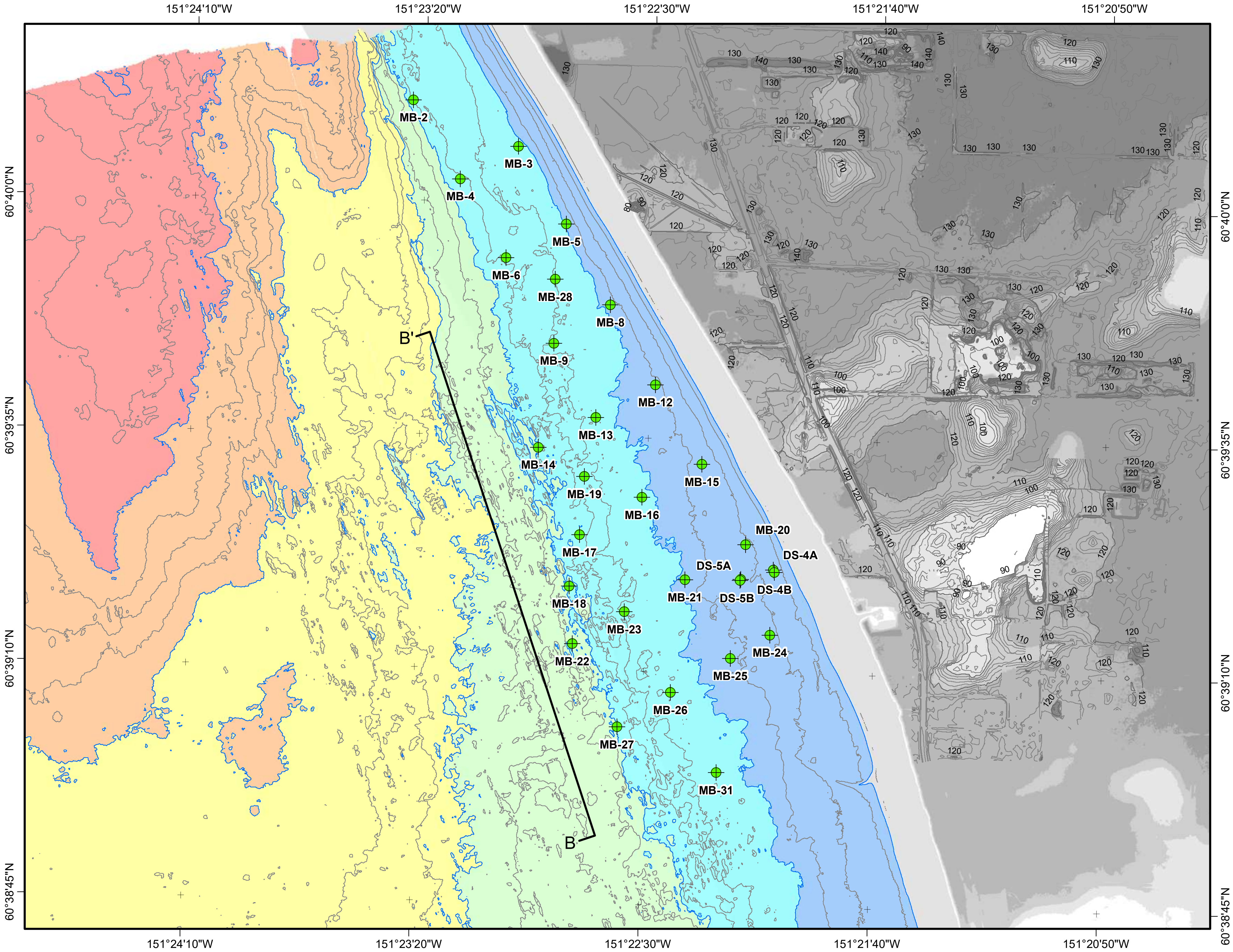

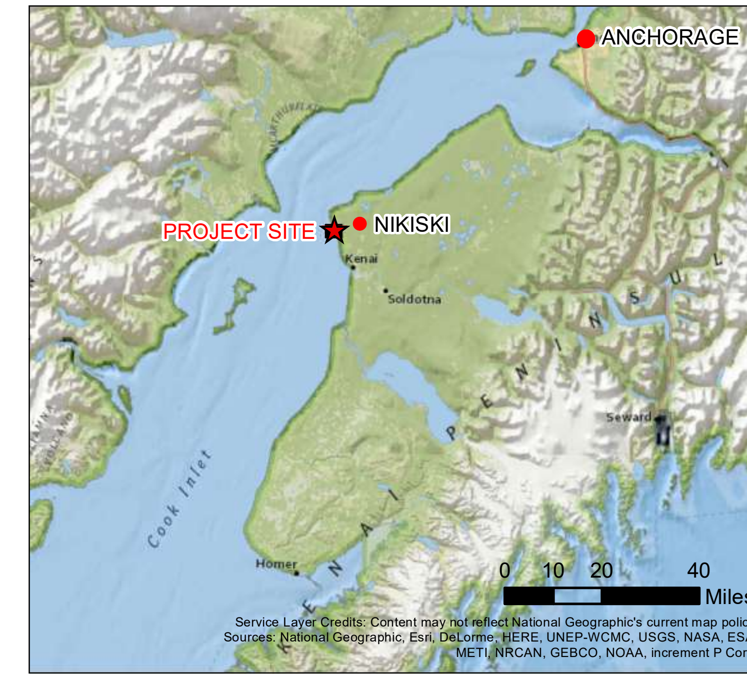

KEY MAP

LEGEND

Completed boring

B B' Cross section B-B'

TOPOGRAPHY (NAVD88, Feet)

Source: LiDAR Digital Elevation Model (DEM), (KPB, 2008) & Contour lines (McLane, 2015)

Major Contour interval is 10 feet

Minor Contour interval is 2 feet

BATHYMETRY (MLLW, Feet)

Source: Multibeam (Fugro, 2014)

Major contour interval is 20 feet.

Minor contour interval is 5 feet.

-123 - 100ft

-99.9 - -80ft

-79.9 - 60ft

-59.9 - -40ft

-39.9 - -20ft

-19.9 - 0ft

NOTES:

1. Topography contour lines provided by McLane Consulting, Inc. (2015).
2. Bathymetry contour lines based on data collected by Fugro (2014 & 2015).
3. As-built coordinates of marine exploration locations was recorded by Fugro Starfix Positioning System.

N W E S

0 1,000 2,000 4,000 Feet

Grid Coordinate System: NAD83 NSRS2007

MARINE BORINGS WITH SITE TOPOGRAPHY

LNG FACILITIES

ALASKA LNG PROJECT

NIKISKI, ALASKA

PLATE 40

R:\04100\2014 Projects\04.10140094 - AKLNG\05_GIS\Outputs\01_REPORTS\2015_05_10_Final_Engineering_Report\MXD\Plate-14_SiteTopographyMap.mxd, 6/8/2016, jholmberg

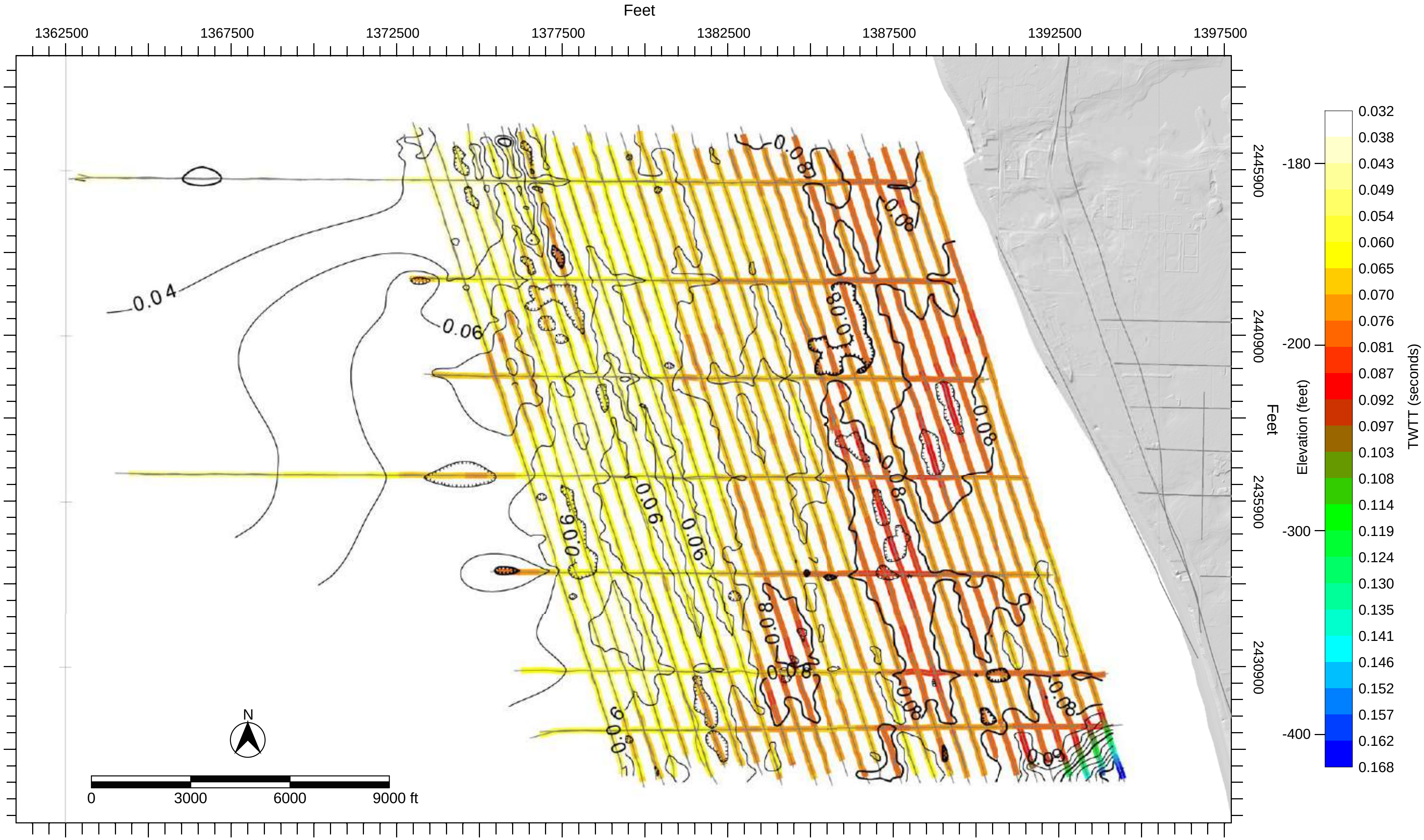

Contours in TWTT

TOP OF THE TERTIARY UNCONFORMITY, MARINE LNG AREA

LNG FACILITIES

ALASKA LNG PROJECT

NIKISKI, ALASKA

PLATE 41

fwla-wc-file1/project/Projects/10_0000/10_140334_AKLNG_PreFEED_Phase2/05_Graphics/10_140334 Geohazards Report

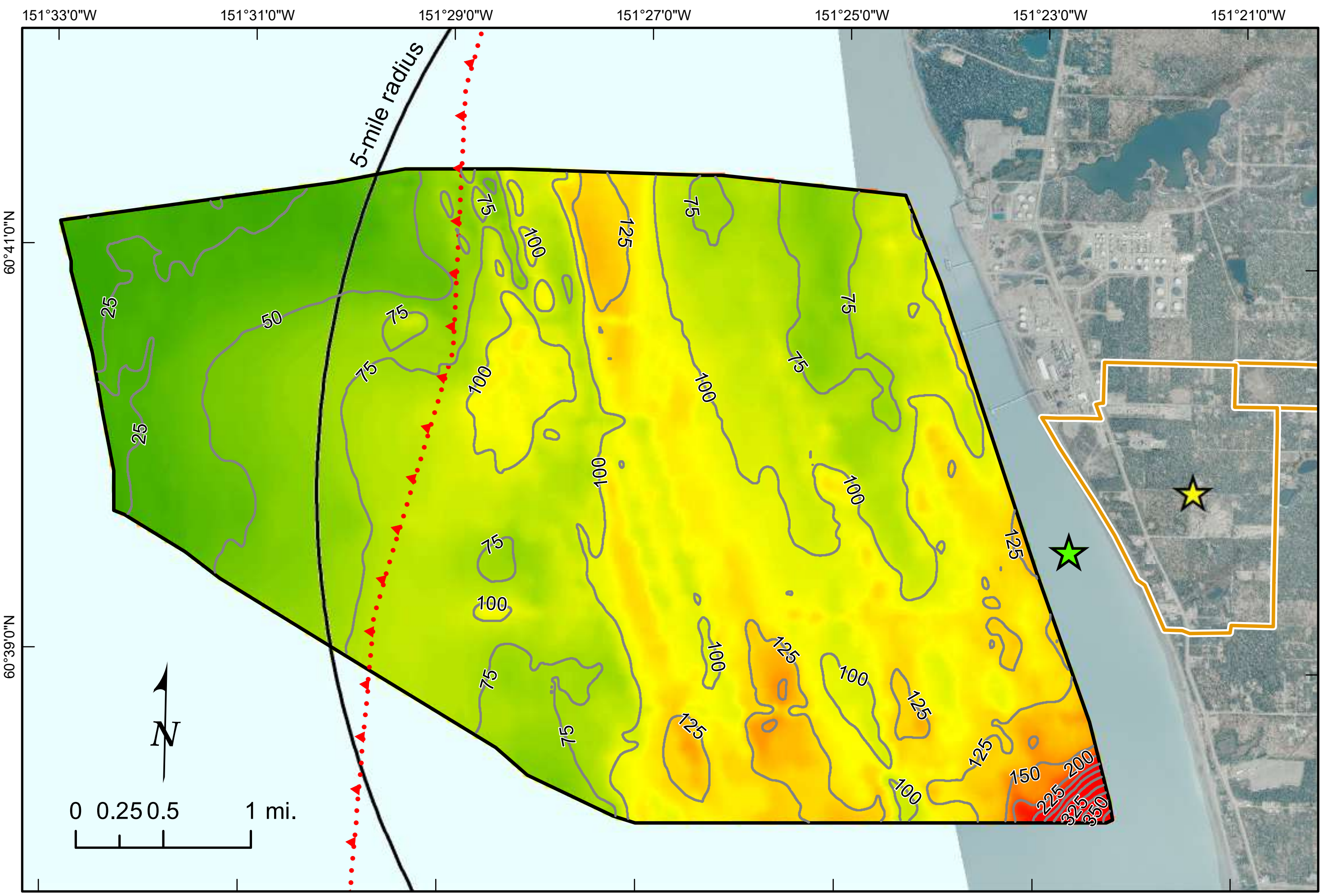

Legend

Onshore LNG site center

Marine terminal site center

Blind thrust fault, teeth on upper plate

Onshore LNG Facilities Study Area

Isopach contour, 25 foot interval

Thickness (feet)

High : 358

Low : 6.0

ISOPACH MAP OF QUATERNARY DEPOSITS, MARINE SITE AREA

LNG FACILITIES

ALASKA LNG PROJECT

NIKISKI, ALASKA

CHART 42

P:\Projects\10_000010_140334_AKLNG_PreFEED_Phase2\05_Graphics\10_140334 Geohazards Report\42_D_391_Marine_Quaternary_Isopach.mxd; jholmberg; 6/20/2016

Uninterpreted

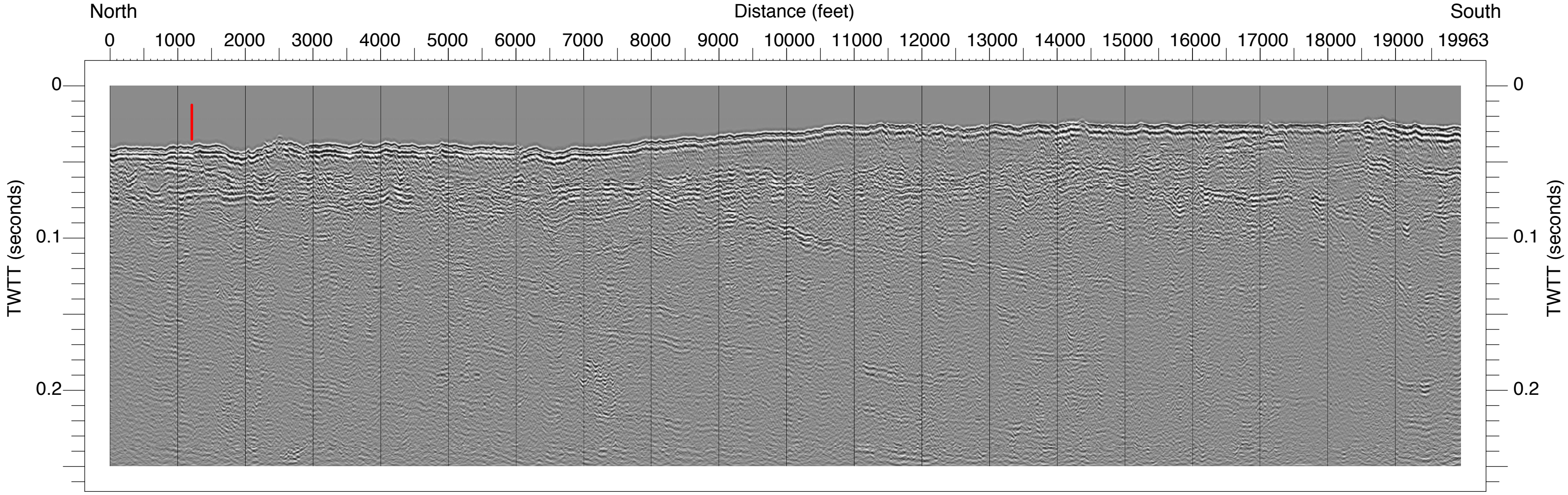

Interpreted

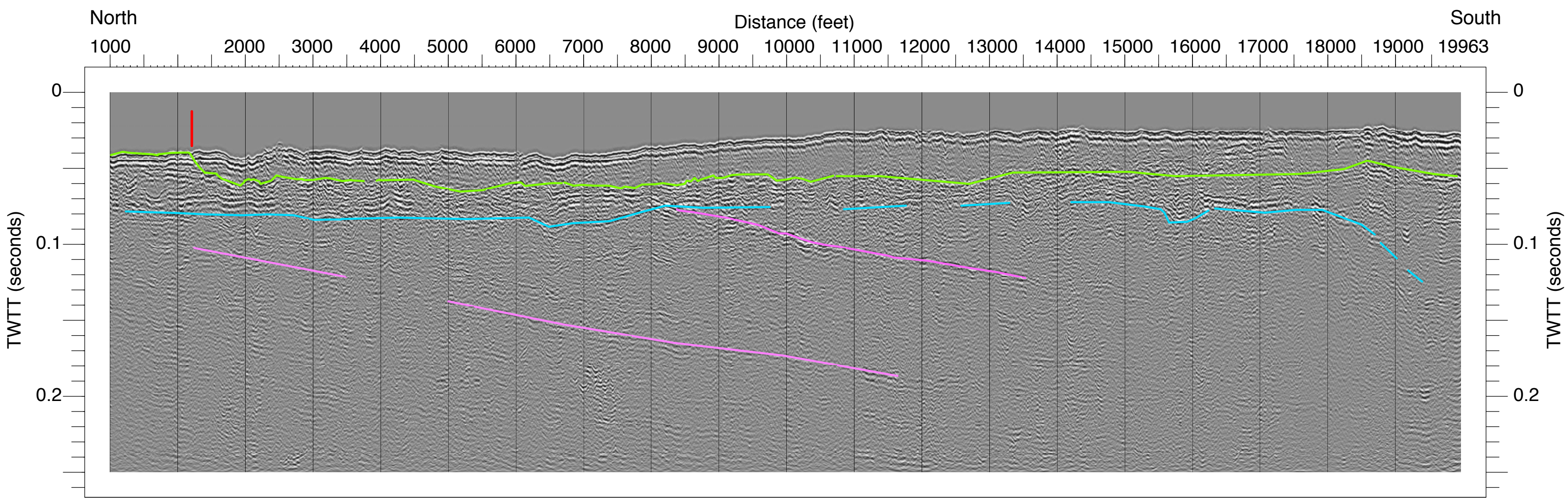

Legend
- Quaternary unconformity
- Tertiary unconformity
- Arbitrary reflectors

2015 SUB-BOTTOM PROFILER BOOMER LINE SB129

LNG FACILITIES
ALASKA LNG PROJECT
NIKISKI, ALASKA

Note: See Plate 38 for line location.

PLATE 43

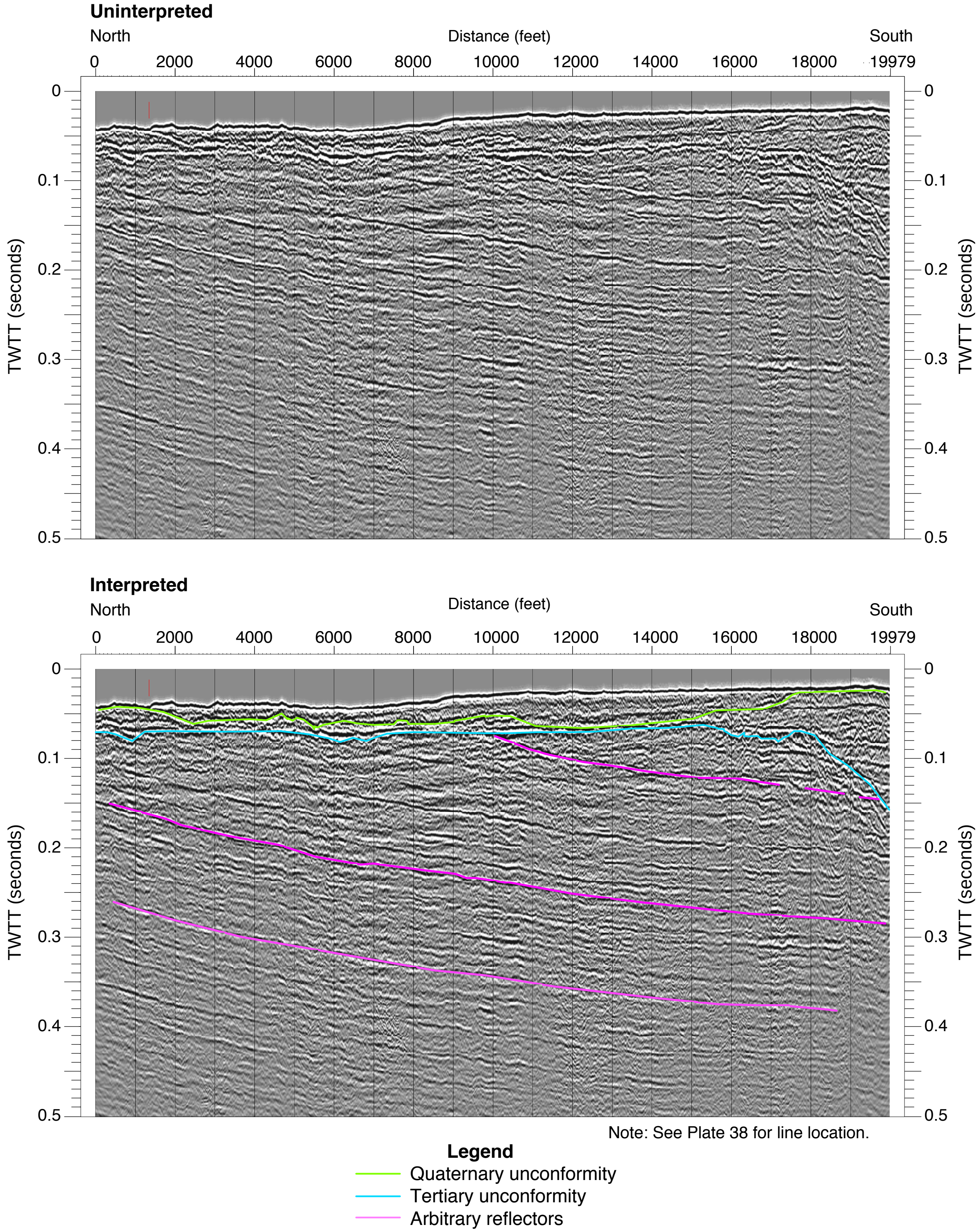

2015 MARINE SEISMIC REFLECTION LINE S-128

LNG FACILITIES

ALASKA LNG PROJECT

NIKISKI, ALASKA

PLATE 44

Uninterpreted

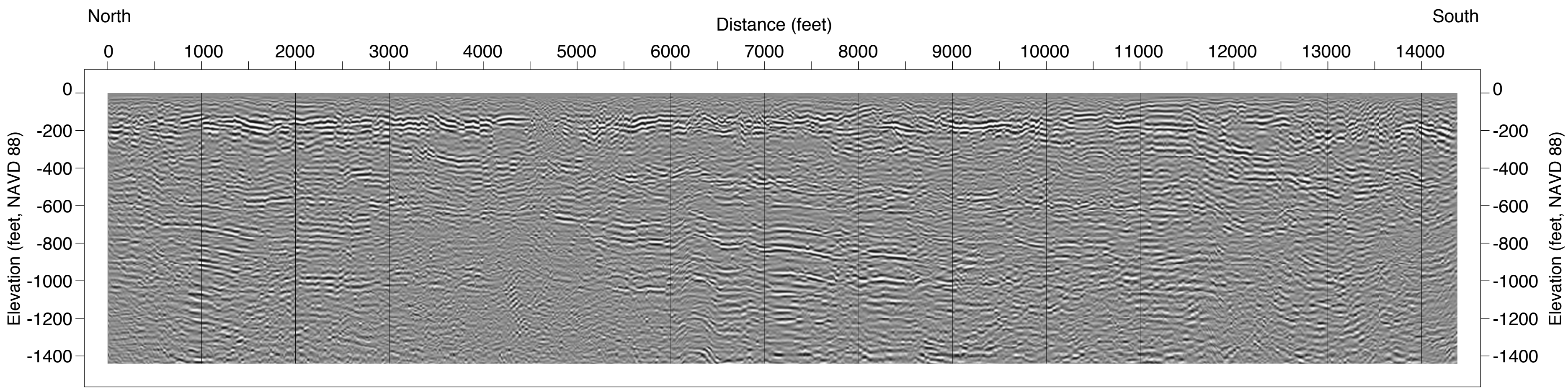

Interpreted

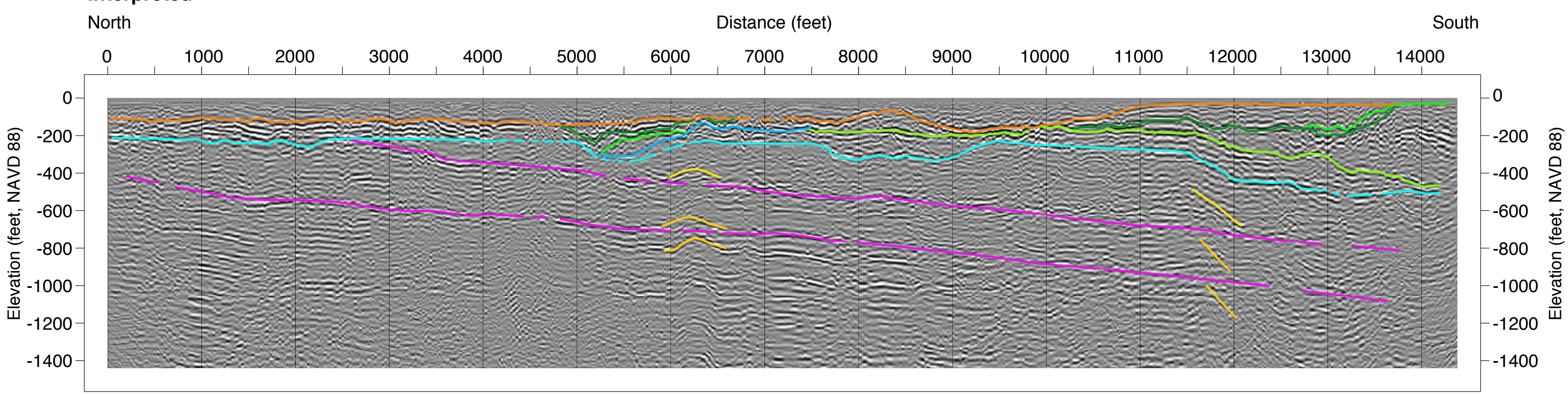

Note: Section location shown on Plate D-29.

Legend

- Shallow glacial contact
- Aggradational glacial packages
- Aggradational glacial packages
- Aggradational glacial packages
- Top Tertiary angular unconformity
- Arbitrary Tertiary bedform lines
- Data artifacts

2015 BEACH SEISMIC REFLECTION PROFILE NS-0

LNG FACILITIES
ALASKA LNG PROJECT
NIKISKI, ALASKA

PLATE 45

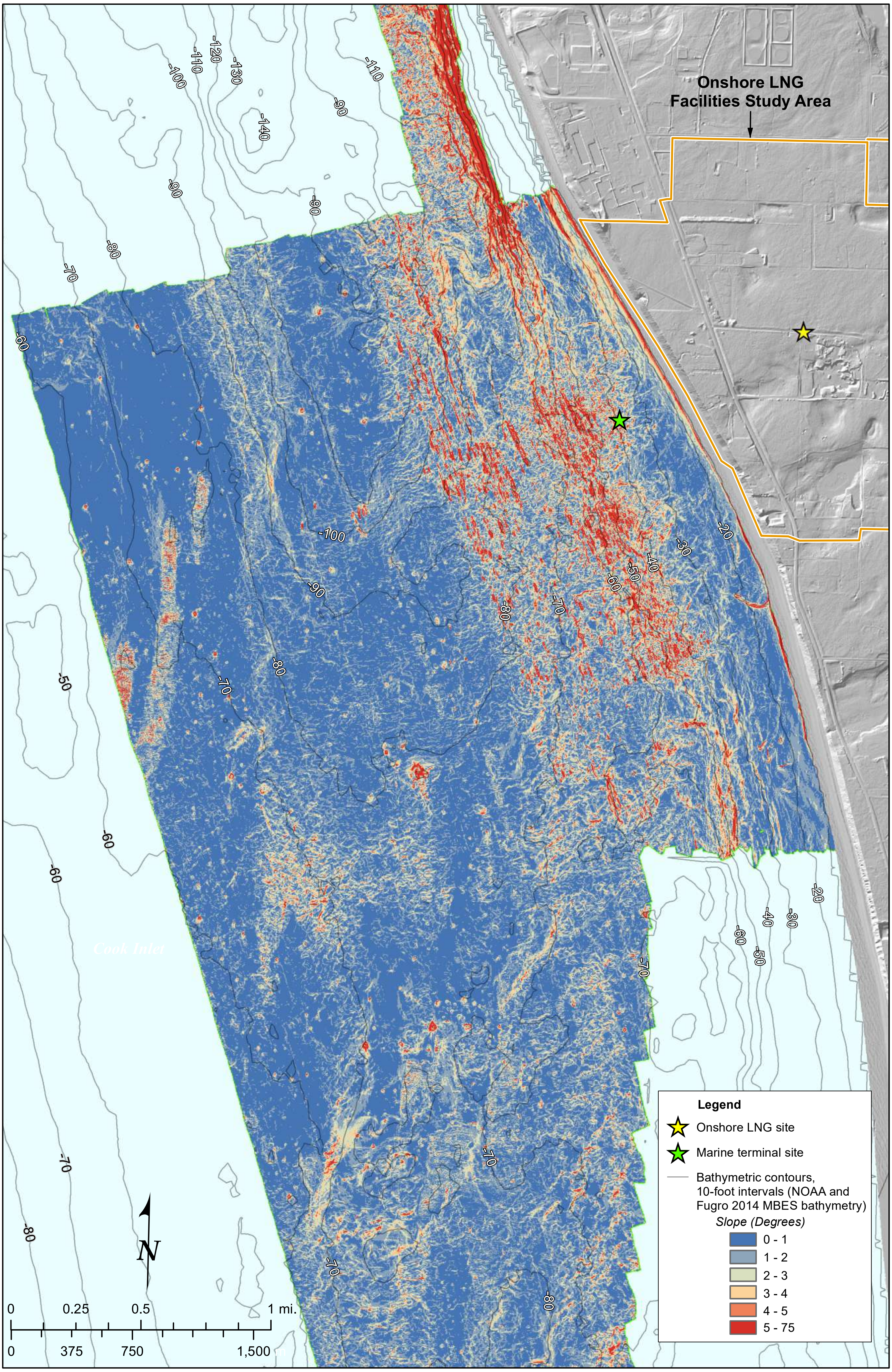

Vertical datum NAVD 88.

SLOPE MAP OF THE MARINE LNG FACILITIES AREA
LNG FACILITIES
ALASKA LNG PROJECT
NIKISKI, ALASKA

PLATE 46

P:\Projects\10_0000\10_140334_AKLNG_PreFEED_Phase2\05_Graphics\10_140334 Geohazards Report\46_D-380_MarineFeatures_Bare_Slope_020516.mxd; jholmberg; 6/20/2016

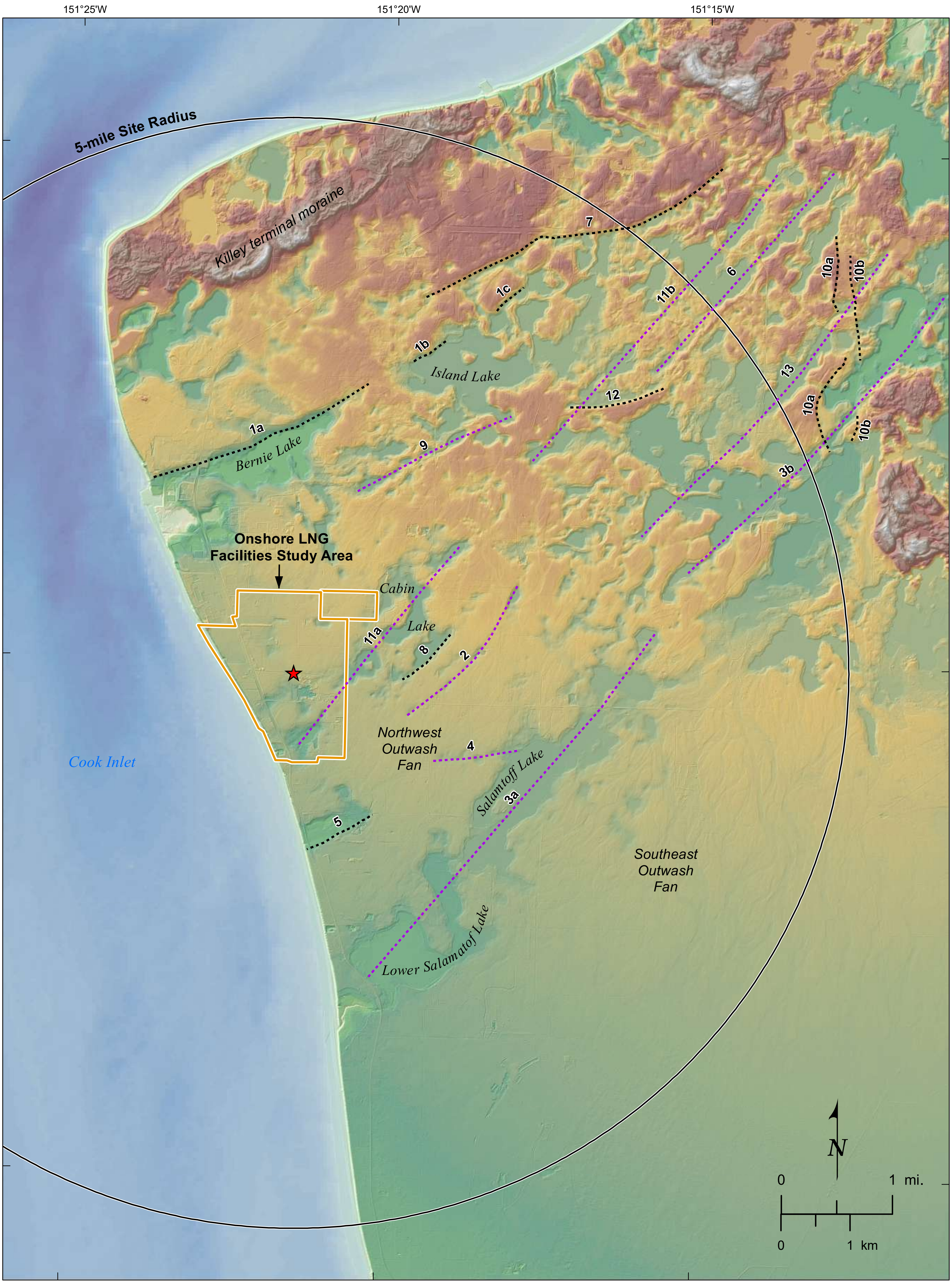

Legend

1 Linear escarpment (with lineament number)

9 Series of aligned features (with lineament number)

LINEAMENT MAP OF THE ONSHORE SITE AREA
LNG FACILITIES
ALASKA LNG PROJECT
NIKISKI, ALASKA

PLATE 47

P:\Projects\10_0000\10_140334_AKLNG_PreFEED_Phase2\05_Graphics\10_140334 Geohazards Report\47_D_351_Lineament_Map.mxd; jholmberg; 6/20/2016